ANALYTICA CHIMICA ACTA

International monthly devoted to all branches of analytical chemistry
Revue mensuelle internationale consacrée à tous les domaines de la chimie analytique
Internationale Monatsschrift fur alle Gebiete der analytischen Chemie

ELSEVIER SCIENTIFIC PUBLISHING COMPANY
AMSTERDAM

Anal. Chim. Acta, Vol. 73, No. 1, 1–228, November 1974
Published monthly

Publication Schedule for 1974

Vol. **68,** No. **1**	January 1974	
Vol. **68,** No. **2**	February 1974	**(completing Vol. 68)**
Vol. **69,** No. **1**	March 1974	
Vol. **69,** No. **2**	April 1974	**(completing Vol. 69)**
Vol. **70,** No. **1**	May 1974	
Vol. **70,** No. **2**	June 1974	**(completing Vol. 70)**
Vol. **71,** No. **1**	July 1974	
Vol. **71,** No. **2**	August 1974	**(completing Vol. 71)**
Vol. **72,** No. **1**	September 1974	
Vol. **72,** No. **2**	October 1974	**(completing Vol. 72)**
Vol. **73,** No. **1**	November 1974	
Vol. **73,** No. **2**	December 1974	**(completing Vol. 73)**

Subscription price: Dfl. 492.00 plus Dfl. 36.00 postage. Subscribers in the U.S.A. and Canada receive their copies by airmail. Additional charges for airmail to other countries are available on request. For advertising rates apply to the publishers.

Subscriptions should be sent to:
Elsevier Scientific Publishing Company, P.O. Box 211, Amsterdam, The Netherlands.

GENERAL INFORMATION

Languages

Papers will be published in English, French or German.

Submission of papers

Papers should be sent to:

PROF. PHILIP W. WEST,
Coates Chemical Laboratories,
College of Chemistry and Physics,
Louisiana State University,
Baton Rouge 3,
La. 70803 (U.S.A.)

or to:

DR. A. M. G. MACDONALD,
Department of Chemistry,
The University,
P.O. Box 363
Birmingham B15 2TT (Great Britain)

Reprints

Fifty reprints will be supplied free of charge. Additional reprints (minimum 100) can be ordered at quoted prices. They must be ordered on order forms which are sent together with the proofs.

PRINTED IN THE NETHERLANDS


Reagents
MERCK
Reagents
for
Instrumental
Analysis

salon du laboratoire 1974

Paris, porte de Versailles

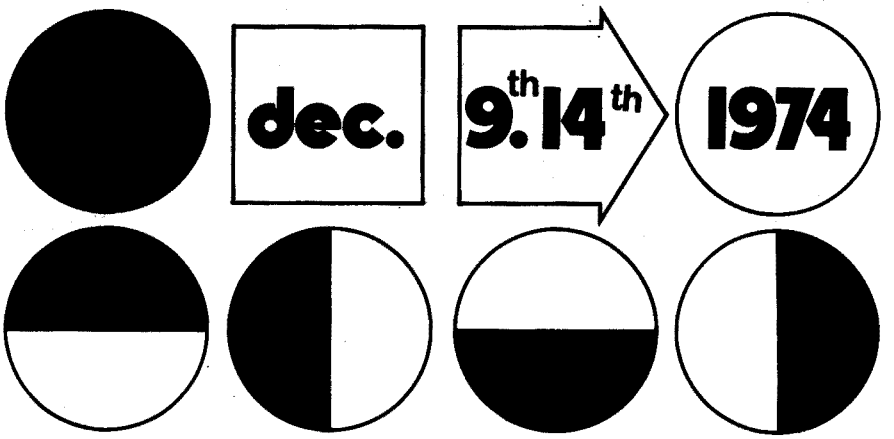

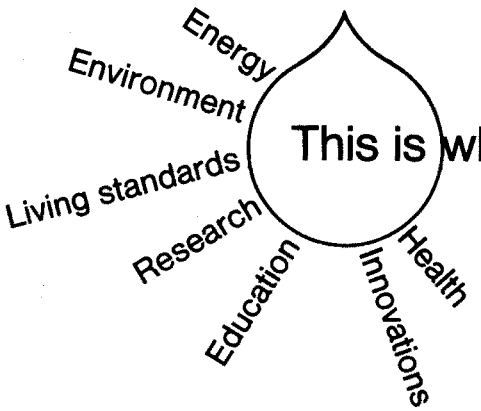

This is why Laboratories exis

The 65th Physics Exhibition is being held along with the Salon du Laboratoire (Laboratory Exhibition); entrance formalities are communal.

The G.A.M.S. (Organisation for the propagation of spectroscopic and physico-chemical methods) will hold its 32nd Congress at the same time and place as the two Exhibitions.

The "Salon du Laboratoire" is organised by the "Association pour le Salon du Laboratoire" 10 avenue Hoche - 75382 PARIS CEDEX 08 - FRANCE - Tel. 622.38.00 ext. 528.

ANALYTICA CHIMICA ACTA
Vol. 73 (1974)

ANALYTICA CHIMICA ACTA

International monthly devoted to all branches of analytical chemistry
Revue mensuelle internationale consacrée à tous les domaines de la chimie analytique
Internationale Monatsschrift für alle Gebiete der analytischen Chemie

ELSEVIER SCIENTIFIC PUBLISHING COMPANY
AMSTERDAM

Anal. Chim. Acta, Vol. 73 (1974)

PRINTED IN THE NETHERLANDS

Analytica Chimica Acta, 73 (1974) 1–32

QUANTITATIVE INORGANIC ANALYSIS BY GAS CHROMATOGRAPHY

A REVIEW

J. A. RODRIGUEZ-VÁZQUEZ*

Department of Chemistry, University of Birmingham, P.O. Box 363, Birmingham B15 2TT (England)

(Received 27th March 1974)

Numerous metallic compounds can be submitted to gas chromatographic analysis: many metal halides, hydrides, carbonyls, nitriles, alkyls, alkoxides, porphyrins (metallocenes) and organometallic compounds have suitable properties of volatility. However, such compounds have also many disadvantages for the application of this technique to the determination of metals: they are usually difficult to prepare in quantitative yield, many are susceptible to hydrolysis and are corrosive, and many lack sufficient thermal stability and volatility.

For satisfactory applications, the compounds used as the analytical form for the inorganic species must meet a number of conditions, and this reduces considerably the number of potentially suitable compounds. First, the analytical form must be volatile; only a few types of metal-containing compounds possess this property. Secondly, the compounds used must be sufficiently thermally stable and resistant to solvolytic effects to be eluted unchanged. In many cases, despite meeting these requirements, the compounds may be degraded at the column temperatures used, owing to non-equilibrium interactions with the column substrates, for which reason the value of preparing inert compounds cannot be overstressed. Thirdly, quantitative reaction of the reagent selected with the inorganic species must be readily achieved and easily reproduced.

From studies of the above-mentioned systems, only the organoderivatives of some complexing agents and a few other compounds meet the essential requirements. Of these, the metal chelates of β-diketones and derivatives, together with the metal halides, have proved to be the most appropriate. Thus, considerable attention has been given during recent years to the application of metal halides[1–27], derivatives of β-diketones[1–3, 7–12, 28–57] and related compounds such as thioketones[58–63] and amino derivatives[64–72] in analysis for metals by gas chromatography.

The early successful gas chromatography of metal β-diketonates greatly contributed to establishing this technique as a useful approach to the problems created by difficult separations or measurements of metal ions at very low concentrations. The general technique provides several advantages such as simplicity, separative ability, high sensitivity and precision, as well as speed and readily

* Present address: Departamento de Química Analítica, Facultad de Ciencias, Universidad de Santiago de Compostela, Santiago de Compostela (Spain).

available equipment, if appropriate reagents can be found. Moreover, it can be used in conjunction with other techniques, such as solvent extraction and mass spectrometry, so that complex problems of separation or measurement can be satisfactorily solved. For example, in combination with solvent extraction, it is possible to eliminate components which otherwise could interfere in the gas chromatographic step simply by choosing the most convenient extraction conditions (pH, use of masking agents, change of solvent, etc.). Furthermore, as the amount of sample needed for a determination is only of the microlitre order, solvent extraction can be used not only for separation but also for concentration. Thus components present at very low levels in large volumes of aqueous solution can be extracted into a few millilitres of a suitable solvent, and, with a possible evaporation step, quite large concentration factors can be achieved.

Such characteristics make gas chromatography a versatile and elegant competitor in the development of viable analytical procedures for the evaluation of inorganic species, provided that preliminary chemical steps are uncomplicated. A further significant advantage is that analyses can be done over a wide range of concentrations from milligrams to picograms, simply by changing the detection system.

Various reviews summarizing much of the work in general and inorganic gas chromatography up to 1972[1–12] have been published, but no in-depth survey of the quantitative analytical methods seems to be available. This paper is intended to cover specifically such methods. The establishment of the technique as an approach for trace analysis has depended largely on extensive work on β-diketone chelates, hence these are discussed first; subsequently, quantitative gas chromatography with metal halides and procedures for the determination of anions are described. But segregation into these categories is not always exact, where one development of procedure has followed logically from another. However, before actual determinations are surveyed, some general remarks about practical aspects such as gas chromatographic columns, detection systems and calibration techniques, seem in order.

Practical gas-chromatographic aspects

Columns. Up to the present time, determinations of metals and anions have been carried out with classical packed columns. Attempts to use capillary columns have proved unsuccessful[4,7].

The choice of the column components—tubing, solid support, liquid phase—is of primary importance for successful quantitative analysis below the microgram level. In the gas chromatography of metallic compounds, non-ideal column phenomena have frequently been encountered[1,32,39,50,53,69], and in some cases such behaviour has tempered the effectiveness of the analytical technique. Anomalous chromatographic behaviour such as the displacement of previously determined complexes by other metal compounds, the need for several injections before peaks of consistent size and shape are obtained, spurious peaks and shoulders, complexation and/or association in the bulk liquid phase, etc., have been reported[32,53]. Thus it is of prime importance to minimize interaction of the compounds to be chromatographed with the column material, solid support and liquid phase, by a correct choice of materials. In most cases, linear partition isotherms over a wide

range of concentration, symmetrical peaks and high column efficiencies can be obtained.

Quite frequently, the use of metallic columns (stainless steel, copper, aluminium) can lead to reactions of the column wall with the compounds examined, or may catalyze the decomposition of the compounds, so that inert materials are necessary. PTFE (Teflon) and borosilicate glass columns have been used in nearly all applications, glass being preferred to PTFE owing to the higher column temperatures possible. The usual length of the columns employed for the described methods is 1–3 m, the internal diameter being 2–4 mm.

The solid support must be chemically inert and have a minimum of adsorption sites. The inertness of the support material can be increased in various ways: silanizing it with reagents such as hexamethyldisilazane or dimethylsilyl-dichloride, treatment with acids or alkalis followed by thorough washing, various forms of heat treatment, etc. The most widely used materials in inorganic analysis are mainly diatomaceous earths properly treated, which give a high quality support with a moderate degree of non-linear adsorption; even so, adsorption on the support can be a problem, particularly at low sample levels. Less used are glass microspheres and PTFE supports; porous polymers, silica gel, alumina and graphite are applied mainly in those determinations involving metal halides and gas–solid chromatography.

Owing to the relatively high temperatures needed in most situations for chromatography of the inorganic compounds, the liquid phase must possess low volatility, high thermal stability and chemical inertness. These requirements eliminate all but a few of the currently available liquid phases, the most commonly employed being high-molecular-weight hydrocarbon greases, *e.g.* Apiezon L, and silicon gums and oils, *e.g.* QF-1, SE-30, E-350; these are non-polar or moderately polar compounds. For reactive substances such as the metal halides, halogenated hydrocarbons such as Kel-F oils are used. The amount of liquid phase in the column varies greatly, depending on the solid support and the compounds being chromatographed. In the case of the above-mentioned substances, solid supports and liquid phases, the degree of impregnation is usually in the low percentage range—about $5 \pm 2\%$.

Detection systems. The potential success of gas chromatography as a means of evaluating trace inorganic species depends particularly on its sensitivity, which should be of at least the same level as other methods in common use for trace analysis. Thus the choice of detector is of primary importance. The three types of detectors commonly utilized in general gas chromatographic work—thermal conductivity, flame ionization and electron capture—have also found wide application in analysis for inorganic ions. Other detectors, *e.g.* flame photometric, mass spectrometric and gas density balance, have been used in a few cases.

The thermal conductivity detector is not destructive but has only a moderate sensitivity—about 10^{-4}–10^{-8} g of metal—and is not selective. It is appropriate for survey studies or when high sensitivity is not required for quantitative work, being relatively unaffected by high concentrations passing through it. In studies with metal halides, it may be necessary to use special corrosion-resistant cells.

Flame ionization detection is at the present time the most widely employed system, its sensitivity being about 1000 times better than that of the thermal

conductivity detector—about 10^{-7}–10^{-10} g of metal. It is inselective and destructive (the latter inconvenience can easily be overcome). Its sensitivity depends on the ion to be determined and on the degree of substitution on carbon atoms in the reagent molecule by atoms such as fluorine; in general, the higher the substitution, the better the sensitivity.

The electron capture detector provides exceptionally high sensitivity—about 1000 times better than with the flame ionization detector—10^{-10}–10^{-13} g of metal. Owing to this characteristic, this detector has been widely employed for detecting and determining fluorinated metal chelates at extremely low concentrations. In contrast to the flame ionization detector, its response increases as the degree of halogenation of the reagent increases, being also a function of the metal present in the compound. It is a non-destructive detector, being more selective than the other two mentioned above. The great sensitivity of this detector has made a considerable contribution to the development of methods for the evaluation of ultratrace quantities of metals by gas chromatography.

Less commonly used are the flame photometric and mass spectrometric detectors, despite their improved selectivity compared to the above-mentioned detection devices. This selectivity can be of considerable importance in situations where complete resolution of mixtures is impossible.

The selectivity of the flame photometric detector is based on the fact that every eluted compound can be detected at an appropriate wavelength of the particular emission spectrum, which is particularly useful if there are overlapping peaks of two metallic compounds: under these conditions the detector allows selective determination of each species[5]. The sensitivity is similar to that of the flame ionization detector but the linear range is narrower. It is specially valuable in the determination of metal halides as it is virtually a corrosion-free device.

Mass spectrometric detection shows a high degree of selectivity and potentially a very high sensitivity, superior to that of the electron-capture detector. When the integrated ion-current technique is used, amounts as low as 10^{-4} g of metal can be detected as the chelate compounds of fluorinated β-diketones[33,39]. The power of resolution allows the determination of elements whose concentrations might vary by several orders of magnitude. However, its application in this field has been very limited, mainly because of the high cost and the unresolved interfacing problems encountered in achieving those very low detection limits.

Very recently, microwave emission detection has been used as a selective system for the detection of various metals eluted as β-diketone chelates[56,57]. Under the given conditions, the device proved to be highly selective with a sensitivity close to that of the electron capture detector, the detector response being dependent on the metal rather than on the chelate as a whole; the limits of detection for acetylacetonates and trifluoroacetylacetonates of the same metal were approximately equal.

Calibration techniques. Of the methods normally utilized to calculate the concentration of an eluted compound present in an unknown, both the direct or absolute method and the internal standard method are commonly employed when dealing with quantititative analysis for inorganic species. With respect to peak size measurements, peak heights and peak areas (obtained by means of electronic integrators or by calculating peak height multiplied by peak width at half height)

are both currently employed. Peak height measurements are preferred when, after the gas chromatographic conditions have been optimized, sharp, well defined peaks are obtained. With respect to accuracy and precision, high standards can be achieved if all the variables of the technique are carefully controlled. When the operator has considerable gas chromatographic practice, precision levels of 2% or even better—1.5% by the internal standard method—can be obtained.

THE DETERMINATION OF METALS AS CHELATES WITH β-DIKETONES AND ANALOGOUS COMPOUNDS

Although gas chromatography has been successfully applied to the analysis of numerous volatile metal compounds such as metal alkyls, carbonyls, alkoxides, halides and various chelates, the β-diketonates have proved to be the most suitable for the separation and determination of metals. Of the great variety of available chelating agents, β-diketones and their derivatives are particularly interesting ligands because they readily react in a quantitative fashion with a considerable number of metallic elements to form compounds which are neither susceptible to hydrolysis nor unduly reactive at the column temperatures required, though many of them undergo some thermal degradation. Moreover, the β-diketonates are easily extracted into various organic solvents. In general, they meet the requirements for a satisfactory gas chromatographic elution, namely volatility, solubility, and thermal and solvolytic stability, with the associated properties of being neutral and monomeric.

The first pioneering work in this field involved eluting from a gas chromatographic column the unchanged acetylacetonates of beryllium(II), aluminium(III) and chromium(III)[74,75], but it was soon realised that excessive temperatures were needed to chromatograph other acetylacetonates; many of them could not be eluted without decomposition at the temperatures necessary. The search for more volatile metal compounds led to an exhaustive study of the fluorinated ligands derived from acetylacetone (HAA), namely trifluoroacetylacetone (HTFA) and hexafluoroacetylacetone (HHFA). These fluorinated chelates needed much lower temperatures for volatilization than the acetylacetonates, this diminishing considerably the danger of thermal degradation. The decrease in the necessary operating column temperatures for elution of the chelates is more noticeable in the case of the hexafluoroacetylacetonates: it is possible to chromatograph some of them at column temperatures only slightly in excess of room temperature. Other higher fluorinated β-diketone ligands as well as some of their metal complexes have been synthesized and investigated similarly[1,28,29,35,36,47]. However, hexafluoroacetylacetone and the more highly fluorinated β-diketone derivatives react with water to form hydroxy compounds, which makes it difficult to prepare the metal chelates in the presence of water. Moreover, many of their metal chelates—and some of the trifluoroacetylacetonates also, especially those of divalent cations—contain coordinated water, for which reason their recoveries from aqueous solutions are very poor; other problems are created by their inadequate thermal stability with strong retention or dehydration on the column, so that the possibilities of their gas chromatographic application are somewhat limited. Nevertheless, these difficulties can sometimes be surmounted as shown in studies

of ternary systems based on metal–β-diketone–neutral donor or organic base, which have been reported by various workers[1, 35, 36, 47, 53, 54, 55]. When a neutral donor or organic base such as tributyl phosphate, dimethylsulphoxide, dimethylformamide, diethylamine, etc., is employed, there is a synergic enhancement of the extraction efficiency; and significant improvements in thermal stability as well as decreased column interactions can be found. The displacement of water from the coordination sphere of the metal chelate by the introduced second ligand, producing an anhydrous and more hydrophobic compound, appears to be mostly responsible for these phenomena. Worthy of mention are the investigations carried out by Banks *et al.*[35, 46, 52, 113] and by Fritz and Burgett[53, 119, 120], who studied the thermal properties of several rare earth–fluorinated β-diketone–neutral donor complexes after their synergic extraction from aqueous solutions into various organic solvents. Fluorinated β-diketones (hexafluoroacetylacetone and decafluoroheptanedione) and neutral donors such as tributyl phosphate, dimethyl sulphoxide and dibutyl sulphoxide were employed. Thermogravimetric analyses indicated that these ternary chelates are volatile and thermally stable, so that their gas chromatographic utilization is feasible. Fritz and Burgett achieved the first rapid preparation of volatile and thermally stable mixed ligand complexes of thorium and uranium, and of the cerium and yttrium groups of the lanthanides, and used these successfully for gas chromatographic separations and determinations at trace level.

Another interesting type of ligand has the common characteristic—β-dicarbonyl group apart—of possessing at least one tert-butyl group attached to a carbonyl group; the other carbonyl function may carry a wide variety of groups, *e.g.*, another tert-butyl group (dipivalylmethane, DPM), a methyl group (acetylpivalylmethane, APM), a trifluoromethyl group (trifluoroacetylpivalylmethane, TPM), a pentafluoroethyl group (pentafluoroethylpivalylmethane, PPM), etc. Several metal chelates have been found to be volatile and stable enough to be submitted to gas chromatography[34, 39, 40–42, 49, 50]. Particularly interesting are the chelates of the alkali metal and alkaline-earth metals[1, 10, 40, 50], although these are hydrated compounds, as shown by elemental and thermogravimetric analyses, and this feature prevents ready volatilization. When the chelates are chromatographed at the column temperatures needed to volatilize them, the coordinated water molecules are removed and polymerization of the compounds occurs. Nevertheless, satisfactory elution can be obtained with the anhydrous compounds although adsorption and displacement effects are evident[50].

All the above-mentioned ligands contain the β-dicarbonyl functional group:

where $R_1, R_2 = CH_3, CF_3, (CH_3)C$, etc. The stabilities of the two tautomeric forms, the carbonyl (I) and the enolate (II), are usually quite similar. In some cases the enol form is more stable, mainly because of significant resonance energy similar to that of carboxylic acids and because of internal hydrogen bonding. In their enolic form (II), the β-diketones have a hydrogen replaceable by a metal and an oxygen donor atom; thus a six-membered chelate ring (III) can be formed, though its

stability is markedly affected by the conjugated double bonds in the enolic structure.

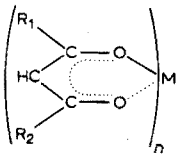

(*n* is the oxidation state of the metal)

(III)

Many metal chelates of these ligands have been prepared and their gas chromatographic characteristics examined, by several workers. The beryllium(II), chromium(III) and aluminium(III) acetylacetonates and their fluorinated derivatives, especially trifluoroacetylacetone, have been particularly well studied, the determination of those metals at trace levels in various matrices being now well established.

However, with the exception of a few complexes of the above-mentioned β-diketones, most of these metal β-diketonates have such chemical and gas chromatographic properties that their application at nanogram levels is unsatisfactory. Particularly with divalent transition metal chelates, the results obtained, except for some copper(II) compounds, have been unsatisfactory; the chelates are too unstable, with tendencies to polymerization, solvation or oxidation. Accordingly, alternative chelate systems, apart from the ternary complexes already mentioned, which might yield improved stability and volatility, have also been investigated.

β-Diketones are interesting in that one or both of the oxygen atoms of the β-dicarbonyl group can be replaced by donor atoms or groups containing donor atoms other than oxygen. Thus attention has recently been given to the potentialities of complexing agents containing sulphur or nitrogen as donor atoms, and the preparation and gas chromatographic characteristics of both unfluorinated and fluorinated monothio-β-diketone and β-ketoamine chelates have been reported. Extensive studies on the synthesis of such ligands and on the preparation and gas chromatography of their complexes, mainly those of copper(II), cobalt(II), nickel(II), palladium(II) and platinum(II), have been reported by Belcher, Stephen, Uden and coworkers[58–60, 63, 65–70].

Thio derivatives of various β-diketones, which contain a mercapto group instead of the enol function of the β-ketoenolate to give a thioenolic grouping, have also been synthesized[58–63]. Infra red, ultraviolet and nuclear magnetic resonance studies of some of these thioketones have shown that the predominant species is the hydrogen-bonded enol or thioenol tautomer, although some enolized tautomer is also present[63]:

(IV) (V)

where $R_1, R_2 = CH_3$, $R_1 = CH_3$, $R_2 = CF_3$, etc.

Various metal chelates of monothio derivatives of β-diketones with divalent transition metal ions have been prepared and subjected to gas chromatography. These studies have mainly centred on nickel, but promising results have been also obtained for other metals. For example, the first recorded chromatogram of platinum(II) was achieved with the bismonothiotrifluoroacetylacetonate complex,

and this ligand also led to the first successful separation of divalent transition metals in the same group of the periodic system—nickel(II), palladium(II) and platinum(II)[59,63].

The thioketone compounds studied need column temperatures between 160 and 250°C for elution. Some of them show excellent gas chromatographic behaviour, which in the case of various fluorinated nickel(II) chelates is as good as that of the beryllium(II) and chromium(III) β-diketonates. An interesting feature of the trifluoro derivative is that beryllium(II), chromium(II) and aluminium(III) do not react with it, so that some separations can be effected before chromatography. These ligands readily form stable, monomeric, volatile, easily extracted bis chelates with various metals that give hydrated or polymeric chelates with β-diketones. As expected, the fluorinated compounds show an increased volatility and lower detection limits for a number of metals, compared to the unfluorinated ligands. However, the thioketonates are not generally as stable or inert with respect to column substrates and support media as some of the β-diketones themselves. Copper(II), lead(II) and cadmium(II) do not form sufficiently stable chelates, and the stabilities of the cobalt(III) and zinc(II) complexes are low. A disadvantage of this kind of compound for g.c. analysis is the relative difficulty in preparing and handling the monothio-β-diketone ligands.

When nitrogen-containing groups are made to react with β-diketones, the ligands obtained can be as follows:

(a)

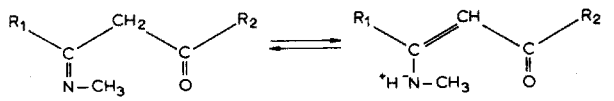

(b)

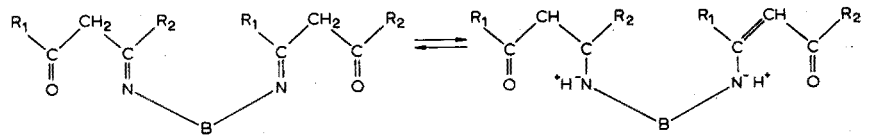

(VI)

where $R_1 = CH_3$, $R_2 = CF_3$, etc; $B = (CH_2)_2$, $(CH_2)_3$, etc.

Thus several β-ketoamine derivatives of acetylacetone and salicylaldehyde have been prepared, and their copper(II) and nickel(II) chelates have been studied by gas chromatography; only the bis(4-aminopent-3-en-2-ono)nickel(II) complex showed sufficient stability for quantitative work[64]. More recently, various other β-ketoamine ligands have been prepared by the reaction of two molecules of β-diketone with one molecule of a diamine—ethylene, -propylene and -butylene[65–72]. Bidentate and tetradentate complexes of copper(II), nickel(II), palladium(II) and platinum(II) can readily be prepared, exhibiting a remarkable solubility in various organic solvents as well as thermal stability and quantitative chromatographic elution to the nanogram level at temperatures up to 300°C. With few exceptions, mainly for the copper chelates, no evidence of decomposition or loss of sample, even at low concentration levels, in the column has been found, despite

the relatively high column temperatures and column material (stainless steel) used. In most cases, these chelates appear to be free of the experimental problems arising from column interaction. These chelates show various interesting features which make them useful for gas chromatographic work; their volatility and thermal stability increase in the order butylene < propylene < ethylene. For various ligands the order of elution in, for example, a non-polar stationary phase is the same for each metal, *i.e.* propylenediamine derivatives are eluted before the ethylenediamine series. As expected, the fluorinated complexes are eluted before their unfluorinated analogues. The separation of a mixture of copper(II), nickel(II), palladium(II) and platinum(II) as their bis-trifluoroacetonepropylenediamine chelates has been achieved, the order of elution being nickel, copper, palladium and platinum; and various nickel chelates of both unfluorinated and fluorinated ligands showed good gas chromatographic characteristics[69].

The ligands are readily prepared and purified, and quantitative reaction with various metals is readily achieved; selective chelation towards divalent metal ions appears to occur. Quantitative prospects for ultratrace determinations of various metals via a β-ketoamine compound seem very promising. The exceptionally good stability of the tetradentate β-ketoamine chelates (VII) is particularly interesting.

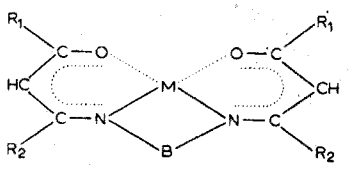

(VII)

where $R_1 = CH_3$, $R_2 = CF_3$, $B = (CH_2)_2$, $(CH_2)_3$, etc.; M = II

Quantitative applications

The application of gas chromatography to the analysis of volatile metal β-diketonates was first suggested as early as 1955[73], only a few years after the establishment of this technique as an invaluable method of separating and analyzing organic compounds. Subsequently, beryllium acetylacetonate was the first metal chelate to be successfully gas-chromatographed[74,75]; later, the determination of beryllium in a beryllium–copper alloy, was achieved with this chelate.

Chromium as chromium(III) acetylacetonate in aqueous solution can also be evaluated[76]. After its formation at pH 9, the complex is extracted into carbon disulphide and an aliquot injected into the gas chromatograph. When peak areas are used, the calibration graph is linear over the range 0.5–1000 p.p.m. of chromium in the aqueous solution; the limit of detection with the flame ionization detector at column temperatures of 145°C is 50 p.p.b. Beryllium(II), aluminium(III) and iron(III) interfere but can be removed by washing the organic layer with aqueous 10% (v/v) hydrochloric acid solution. Hill and Gesser[77] have made a comparative study of the gas chromatographic behaviour of the beryllium, aluminium and chromium complexes of acetylacetone, trifluoroacetylacetone and hexafluoroacetylacetone. They analysed a known solution of the trifluoroacetyl-

acetonates of beryllium, aluminium and chromium; each compound is detected with a flame ionization detector and the amount is evaluated from a calibration graph derived from peak areas, with errors of 1.66, 3.68 and 6.48%, respectively. Carbon tetrachloride serves as solvent, the column temperature being 106°C. Comparable experiments with acetylacetone and hexafluoroacetylacetone gave somewhat similar results.

A mixture of the hexafluoroacetylacetonates of chromium, iron and rhodium has been analysed by Juvet and Durbin[78] who used flame photometric detection; the sensitivity of this detection device towards the complexes was examined. In the determination of chromium, there is a linear relationship between the amount of the element in the range 1–26 μg and the peak area obtained. The relationship deviates from linearity for sample sizes greater than 5 μg of chromium when the amount of the metal is plotted against peak height. Juvet and Durbin explained this on the basis of the increased vaporization time required for larger samples. By extraction of the hexafluoroacetylacetone complex into toluene, amounts of chromium in the range 0.004–100 p.p.m. can be evaluated, and with the use of electron-capture detection as little as $2 \cdot 10^{-12}$ g of metal can be detected[79]; chloroform serves as internal standard.

In a comparison of the response performance of the flame ionization and electron capture detectors towards several metal chelates. Albert[80] utilized the trifluoroacetylacetonate complexes of aluminium, chromium and copper. When electron-capture detection is used, as little as $3.1 \cdot 10^{-15}$ mole of the chromium complex ($1.6 \cdot 10^{-12}$ g of metal), $1.2 \cdot 10^{-13}$ mole of the aluminium complex ($5.9 \cdot 10^{-11}$ g of metal) and $2.0 \cdot 10^{-10}$ mole of the copper complex ($7.4 \cdot 10^{-8}$ g of metal) can be detected. The relative error is −5.6% for 1.7 p.p.m. of the aluminium compound, and −14.0% for 70 p.p.b. of the chromium compound. The calibration graphs are linear in the range 10^{-11}–10^{-9} g of chromium, and 10^{-10}–10^{-8} g of aluminium as their respective chelates.

Beryllium, aluminium, gallium and indium in synthetic mixtures can be determined as their trifluoroacetylacetonates in benzene with an overall relative mean error of 2% for peak area and 2.4% for peak height measurements[81]. The amounts detected with a thermal conductivity detector, corresponding to the lowest point of the calibration graphs (which ranged from 0.075–1.59 μg for beryllium to 12.1–36.4 μg for indium), were 0.075 μg for beryllium, 0.37 μg for aluminium, 2.08 μg for gallium, and 12.1 μg for indium; isothermal conditions were used (115°C for the first three and 120°C for indium). The minimum detectable limit for the beryllium chelate corresponded to 0.04 μg of the metal.

These studies yielded the first satisfactory gas-chromatographic separation of elements—aluminium, gallium and indium—in the same Periodic Group.

Ross *et al.*[82] have studied the trifluoroacetylacetonates of rhodium, aluminium and chromium in synthetic mixtures; the order of elution is aluminium, chromium and rhodium. Quantities of rhodium as small as $2.2 \cdot 10^{-12}$ can be detected, and amounts of aluminium and chromium as low as $6.7 \cdot 10^{-12}$ and $1.2 \cdot 10^{-12}$ g can be measured. Analysis of unknown samples with concentrations ranging from $3.5 \cdot 10^{-11}$ to $1.4 \cdot 10^{-10}$ g of metal are possible; when the internal standard method was used with peak height measurement the average deviation for four runs ranged from 0.0 to ±0.3%. With electron capture detection, the calibration graphs

are usable in the range 10^{-12}–10^{-9} g of metal.

A study of the acetylacetonates and trifluoroacetylacetonates of beryllium, aluminium and scandium has shown that the three metals can be separated as their trifluoroacetylacetonates[83]; scandium can be determined in the presence of beryllium and aluminium. At a column temperature of 185°C, even a few micrograms of scandium can apparently be evaluated with an error of 4%, but few results were reported.

A solvent extraction–gas chromatographic method for the determination of aluminium, gallium and indium in admixture has been developed by Morie and Sweet[84]. The extraction conditions for these three metals with trifluoroacetylacetone into benzene—pH, concentration of metal ion, equilibration time and effect of various ions—have been studied. When an aliquot of the organic phase is injected into the gas chromatograph, the three chelates can be separated and determined; the relative mean errors are 2.3% for 1–4 mg of aluminium, 2.34% for 5–9 mg of gallium, and 5.20% for 10–25 mg of indium, in final volumes of 25 ml. Tartrate, nickel, copper and manganese ions interfere seriously. Morie and Sweet[85] also carried out the simultaneous evaluation of aluminium and iron as their trifluoroacetylacetonates extracted into benzene. The mean relative errors for a series of synthetic samples were 2.86% for 1–3 mg of aluminium and 1.60% for 4–8 mg of iron in final 25-ml volumes. The method has been applied[85] to the determination of iron and aluminium in an NBS nickel–copper alloy, these major constituents being masked with picolinic acid. The calibration graphs are linear in the range 1–4 mg/25 ml for aluminium, and 4–10 mg/25 ml for iron.

Moshier and Schwarberg[86] have determined simultaneously iron, copper and aluminium in NBS alloys. The procedure involves the dissolution of the sample, conversion of the metals to their trifluoroacetylacetonates, solvent extraction, and gas-chromatographic evaluation with thermal conductivity detection. For one alloy, which contained 0.50% aluminium, 2.19% iron and 30.61% copper, the relative mean errors were +3.13, +2.06 and −1.72% for the three metals respectively. For another alloy, which contained 9.59% aluminium, 4.05% iron and 82.25% copper, the errors were −1.39, −0.19 and −0.89% respectively. Other metals present in the NBS samples did not interfere with these determinations.

During the gas chromatographic investigation of several new metal complexes, Sievers *et al.*[87] have developed a simple technique in which the ligand —heptafluorodimethyloctanedione—reacts directly at elevated temperature with the sample, thus eliminating the solvent extraction step for many types of samples. The technique was applied to the analysis of NBS samples of Mesabi iron ore. Iron was determined in several samples, with iron contents of 0.015–0.191 mg, with errors between −17.1 and +6.7%. The calibration graph was linear over the range 0.02–0.2 mg of iron, when thermal conductivity was used for detection.

Cobalt and ruthenium in admixture have been studied as their tri- and hexa-fluoroacetylacetonates by Veening *et al.*[88]. In general, the ruthenium determinations are more satisfactory than those for cobalt, and the responses for the ruthenium chelates are much larger than those for the cobalt chelates. For several concentrations of both metals—$1.81 \cdot 10^{-3}$–$2.96 \cdot 10^{-5}$ g ml^{-1}—in admixture, the relative errors ranged from −8.0 to +4.7%. Electron capture detection was used, and peak areas of both sample and internal standard were measured.

Ultratrace quantities of beryllium as beryllium trifluoroacetylacetonate can be measured by electron capture gas chromatography[89], the minimal detected amount of beryllium being $4 \cdot 10^{-13}$ g. Samples containing beryllium in aqueous solution at several concentrations can be analysed by combining solvent extraction and gas chromatography. After a loss correction factor has been applied (losses occur in the extraction and washing steps), relative errors for beryllium concentrations between $1.12 \cdot 10^{-8}$ and $8.84 \cdot 10^{-10}$ g ml^{-1} vary from 2.5 to 12.1%; without the correction factors, the errors vary between 5.1 and 14.9%. At the concentrations used, none of the fifteen anions and cations tested interfere appreciably. This method has been applied to the determination of beryllium in biological fluids and several other matrices[90–97]. The samples are either directly treated with a benzene solution of the reagent and heated to about 120°C in sealed glass ampoules, or are treated with a benzene solution of the reagent in the presence of EDTA as masking agent, after an ashing and/or digestion process. In some instances, a total sample of 1 ml suffices, and concentrations as low as 1 p.p.b. can be determined; the limit of detection is about 10^{-11} g.

The method has also been used to evaluate beryllium in lunar, terrestrial and meteoritic samples[98,99]. The samples are fused with sodium carbonate and dissolved in hydrochloric acid; after a pH adjustment and treatment with the disodium salt of EDTA, the beryllium chelate is formed by adding a benzene solution of the ligand and extracting into benzene, an aliquot of the extract being submitted to gas chromatographic analysis. With electron capture detection, as little as $4 \cdot 10^{-14}$ g of the element can be detected, and the calibration graph is linear in the interval $0.2–10 \cdot 10^{-12}$ g of beryllium.

Ross and Sievers[100] reported a method for determining small amounts of chromium in NBS low and high carbon steel samples, containing 0.014 and 1.18% chromium. Trifluoroacetylacetone serves as the ligand in the presence of catalytic amounts of nitric acid; the reaction is stimulated with microwave radio-frequency energy. Amounts of chromium between 10^{-10} and 10^{-11} can be determined with a relative mean error of 1.4–1.7%. Chromium has also been determined in biological materials by several workers[101–103]. Ashing or wet digestion of the samples enables the metal to be extracted with a benzene solution of the ligand, the complex subsequently being determined by gas chromatography with electron capture detection. Recoveries of added chromium to the materials studied ranged between 92.5 and 98.0%. By reacting the sample directly with a hexane solution of the ligand in a sealed tube, the ashing or digesting steps can be eliminated, thus simplifying the procedure[104]. Chromium can be evaluated in blood at concentrations of 50 p.p.b.

A modification of the above procedures involves the elimination of serum constituents, which are said to interfere with the formation of the chelate, by coprecipitation of the metal with serum proteins. Comparative studies with methods involving wet and dry ashing or direct extraction, indicated poor recoveries of added chromium, while the introduced modification gave about 75% recovery, the calibration graph being linear in the range 0–40 p.p.b. of chromium when electron capture detection was utilized[105]. The method can be made specific by employing flame photometric detection, which provides sufficient sensitivity for monitoring chromium in human urine samples. The response of this detector is linear in the

range 0–90 p.p.b. of chromium, the sensitivity being 5 p.p.b. Average recoveries of chromium added to urine samples ranged from 79 to 98% (refs. 106, 107).

Lunar samples have been analysed to establish their chromium content, the metal again being chromatographed as the trifluoroacetylacetone chelate[108]. The sample is fused with sodium carbonate followed by dissolution in hydrochloric acid and reaction with the ligand to form the volatile complex; this is then submitted to gas chromatography, electron capture detection being employed. The method requires only 0.6 mg of sample for each determination.

Chromium and beryllium have been determined in biological and environmental matrices by gas chromatography–mass spectrometry[109]. As little as $5 \cdot 10^{-13}$ g of chromium can be detected and concentrations in the sub-p.p.b. range can be evaluated with an accuracy of about 20%. For a concentration of $0.61 \cdot 10^{-12}$ g Cr ml^{-1}, a relative standard deviation of 6.2% is possible. Samples containing beryllium have been analysed by this technique and by conventional gas chromatography with an electron capture detection, the results obtained being in good agreement[109].

The possibility of determining trace amounts of aluminium in biological materials has been examined by Miyazaki and Kaneko[110]. After extraction with a solution of trifluoroacetylacetone into benzene, aluminium can be evaluated at the nanogram level in rat liver, when electron capture detection is used.

A combination of solvent extraction and gas chromatography enables as little as 0.1 p.p.m. of aluminium and chromium in uranium to be determined. Both metals can be extracted from uranyl nitrate solutions with a benzene solution of trifluoroacetylacetone, and the chelates are then submitted to gas chromatographic analysis with electron capture detection[111]. For uranium solutions containing 0.2 p.p.m. of each element, the average results at the 95% confidence level were 0.18 ± 0.03 p.p.m. for aluminium and 0.18 ± 0.06 p.p.m. for chromium. None of the several metals tested at a hundredfold level interfered.

Lee and Burrell[112] have reported the feasibility of determining aluminium in sea water by chelation with trifluoroacetylacetone, extraction into toluene, on-column injection (at a column temperature of 118°C) and electron capture detection. After instrumental conditions had been optimized, picogram amounts of aluminium could be detected.

Separation and determination of uranium and thorium as mixed ligand complexes of hexafluoroacetylacetone and dibutyl sulphoxide have been achieved by Banks *et al.*[113]. Both elements can be determined in the range 1–120 mg ml^{-1} with a relative error of less than 10%, the limits of detection being 0.4 mg ml^{-1} for thorium and 0.6 mg ml^{-1} for uranium.

The determination of cobalt as its heptafluorodimethyloctanedione complex in vitamin B12 and biological materials—liver, blood and urine—by gas chromatography with electron capture detection has been verified[114]. The sample is treated in a pyrex tube with a benzene solution of the chelating agent, the chelate being formed in alkaline medium in the presence of hydrogen peroxide; the tube is sealed and heated in a water bath at 75°C. The organic layer is removed and washed with 0.1 *M* sodium hydroxide solution, in order to eliminate the excess of ligand, and then an aliquot is submitted to gas chromatography. The procedure is very sensitive, the limit of detection being $4.4 \cdot 10^{-11}$ g of metal.

Quantitative prospects for the determination of vanadium as the vanadyl–trifluoroacetylacetonate complex, and nickel and cobalt as mixed ligand complexes of trifluoroacetylacetone and dimethylformamide have been studied by Jacquelot and Thomas[115,116]. Vanadium (10^{-7} g), nickel (10^{-8} g) and cobalt (10^{-8} g) may be evaluated with flame ionization detection.

A procedure for the determination of nickel as the monothiotrifluoroacetylacetonate chelate has been reported[117]. Traces of nickel can be evaluated by a combination of solvent extraction and electron capture detection. The element is extracted at pH 4.4–5.0 by a solution of the thioketone in n-hexane and an aliquot of the extract is submitted to gas chromatography. Amounts of nickel of 1.0 and 0.1 μg ml^{-1} can be evaluated with a relative standard deviation of ± 7.2 and $\pm 15.5\%$, respectively. The limit of detection is $5 \cdot 10^{-11}$ g of nickel and 0.01 p.p.m. of the element can easily be determined. Of the various ions tested, copper, cobalt and mercury interfere and must be removed before analysis. The method has been applied to the determination of nickel in an alloy at the percentage level and at the p.p.m. level in "instant tea" powders and hydrogenated triglycerides.

Under strict experimental conditions, in order to avoid errors from decomposition of the chelates, thorium and uranium can be determined as their heptafluorodimethyloctanedione complexes after extraction into benzene; the optimal pH ranges are 3–7 for thorium, 1.2 ± 0.1 for uranium(IV), and 6–7 for uranium(VI). Flame ionization detection gives a limit of detection of *ca.* 1 μg of metal. The two metal chelates can be readily separated by temperature-programming[118].

The first successful gas chromatographic separation and subsequent determination of the yttrium and cerium groups of rare earths as mixed-ligand complexes has been reported by Burgett and Fritz[119,120]. Lutetium, terbium, ytterbium, gadolinium, dysprosium and holmium are extracted from aqueous solutions with decafluoroheptanedione as ligand and di-n-butyl sulphoxide as neutral donor. Calibration graphs based on peak areas are linear over the range $2 \cdot 10^{-2}$–$1.5 \cdot 10^{-5}$ g of metal, the limit of detection with a flame ionization detector being $2.0 \cdot 10^{-7}$ g of metal for all the elements. Mixtures of the yttrium group elements can be determined with relative errors ranging from -7.97 to $+8.34\%$. Several interferences can be eliminated by extractions based on various mixed-ligand complex systems. The cerium group elements also form complexes with the system employed in the proposed procedure, but are eluted after the yttrium group. Thus by optimizing the instrumental conditions, europium, samarium, praseodymium, neodymium, cerium and lanthanum can be separated and quantatively evaluated after synergic extraction into cyclohexane as their ternary complexes. Calibration curves for individual elements are linear in the range $1.5 \cdot 10^{-5}$–$1.0 \cdot 10^{-7}$ g of metal, peak areas being used; in determinations of single elements, 99.0% recovery and a relative mean deviation of $\pm 2.0\%$ can be achieved. Unknown mixtures of the lanthanides can be analyzed with a 101.2% recovery and a relative mean deviation of $\pm 2.2\%$. When flame ionization detection is used, the limit of detection for all the elements is $2.0 \cdot 10^{-7}$ g of metal. Interferences from various ions tested can be eliminated in the extraction step.

The potential application of gas chromatography of volatile metal chelates to water analysis has been studied by Minear and Palesh[121], aluminium,

chromium, iron and copper trifluoroacetylacetonates and lead–tetramethylheptanedione being examined. Lead proved unsatisfactory, owing to the low extraction efficiency. Aluminium, chromium and copper can be separated and determined in the presence of each other, but iron is eluted simultaneously with copper. After a preconcentration step, aluminium, chromium and copper can be determined, in various natural water samples at the p.p.m. level.

Copper and nickel at low concentrations in aqueous solution can be quantitatively evaluated after extraction into chloroform as their bis(trifluoroacetyl)-acetone–ethylenediimine chelates[70]. The complexes are readily extracted quantitatively into chloroform. With peak area measurements, the calibration graph is linear in the range $7 \cdot 10^{-6}$–$4 \cdot 10^{-9}$ g of metal chelate for both metals. With flame ionization detection the limit of detection is about 10^{-10} g; relative standard deviations are below 5% for most samples. The procedure has been extended to the picogram level by using electron capture detection. Besides the copper and nickel bis(trifluoroacetyl)acetone–ethylendiimine chelates, analogues of the above β-ketoamine and the corresponding bidentate β-ketoamines have also been examined for these metals[122].

Copper, nickel and palladium as their bis(acetylpivalylmethane)–ethylenediimine complexes have been successfully chromatographed at a column temperature of 260°C[123]. With flame ionization detection, as little as 10^{-9} g of each metal can be detected; for peak area measurements, the calibration graphs are linear in the range 10^{-8}–10^{-9} g of each metal. Copper and nickel can be determined in admixtures in ratios of 1:10–10:1, and copper-nickel alloys can be readily analyzed after sample dissolution, adjustment to pH 6–7, and extraction of the chelates into n-hexane. Copper in tap water can also be determined after extraction of the β-ketoamine chelate[123] into n-hexane.

THE DETERMINATION OF METALS AS THEIR HALIDES

Several metal halides are sufficiently volatile to be gas-chromatographed at column temperatures up to 350°C. Very few of these compounds have, however, been employed for actual determinations of metals, mainly because of the experimental difficulties arising from their chemical reactivity. Most metal halides react with the usual liquid phases and with the metallic parts of the flow system at the operating column temperatures. It is therefore necessary to use inert materials for both the stationary phase and the flow system. The ease with which atmospheric moisture hydrolyzes these compounds makes it essential to take special precautions to eliminate all traces of water from the carrier gas, solid support and liquid phase, and to handle and inject the sample in an inert atmosphere. These features make the methods unattractive for routine work.

The metal halides most widely studied by gas chromatography are the metal fluorides—particularly those of some transition elements such as uranium, niobium, tantalum, tungsten, molybdenum and tellurium, which are highly reactive, and the chlorides of some b group elements of the Periodic System, and transition elements such as niobium, tantalum, hafnium, zirconium, titanium, mercury and vanadium. The b group and some transition metal (titanium, mercury and vanadium) chlorides can be eluted from the usual inert stationary phases up to 250°C, but chlorides such as those of niobium, tantalum, hafnium and zirconium

which have higher boiling points than the above, require molten salts as stationary phases or the use of gas–solid chromatography. Although the fluorides are more volatile, the chlorides are more suitable because of their lower degree of reactivity.

Perhaps the first quantitative application of metal chlorides in gas chromatography was made by Phillips and Timms[124] who obtained the silicon–germanium ratio in a mixed silicon–germanium hydride. The hydride is passed over heated gold trichloride which quantitatively converts both elements to their chlorides; these are then separated and determined at a column temperature of 20°C, gas density balance detection being used. The technique has also been successfully applied to the analysis of highly reactive fluorides in plant streams used in atomic energy processes. Thus uranium as uranium hexafluoride can be quantitatively evaluated in a mixture of gases with an overall precision better than $\pm 2\%$ expressed as relative standard deviation, which in favourable circumstances may reach $\pm 1\%$ (ref. 125).

Arsenic and tin as their chlorides can also be separated and determined[126]. Linear relationships exist between peak areas and sample sizes. The analysis of mixtures of tin tetrachloride and arsenic trichloride gives errors less than 6%, greater accuracy being achieved when larger samples—up to 15 mg—are used. The standard deviation for various samples is ± 0.06–$\pm 0.13\%$ for tin tetrachloride and ± 0.06–$\pm 0.19\%$ for arsenic trichloride.

The determination of titanium in oxide mixtures has been described by Sievers *et al.*[127]. The simple, selective and sensitive method involves conversion of the metal to titanium tetrachloride by reaction of the sample with carbon tetrachloride at an elevated temperature in a sealed small capillary tube. After chlorination, the reaction products are introduced directly into the carrier gas stream for gas chromatography. The method was applied to a standard NBS bauxite sample, the titanium content being evaluated with a mean error of 0.03% (certified percentage 2.78% as titanium dioxide; found 2.75%) and a relative error of 1.1%. Electron capture detection was utilized and the (peak area) calibration graph was useful in the range 20–170 μg of titanium dioxide.

Juvet and Fisher[128] have developed a specially designed reactor-injection system to verify an *in situ* fluorine injection technique for the gas chromatographic analysis of metals, alloys and inorganic metal salts, establishing the reaction and elution properties of several elements in various chemical forms. Uranium, sulphur, selenium, tellurium, tungsten, molybdenum and rhenium can be determined as their volatile metal fluorides with relative errors of about 1%. By plotting peak areas against amounts of the elements, useful calibration graphs in the range 0.0–1.5 mg can be obtained; although the linear range extends to at least 5 mg for some elements, reproducibility decreases above 1.5 mg. Thermal conductivity detection is used, the cell being equipped with nickel filaments resistant to corrosion by metal fluorides.

The determination of silicon in iron and steel has been reported by Sie *et al.*[129] who described a method in which chlorine is passed over a weighed sample —1–50 mg—heated at 600–900°C. After purification, the reaction products are injected onto a gas chromatograph equipped with a gas density balance detector. The calibration graph (peak area) is linear and the recovery of silicon tetrachloride is $97 \pm 5\%$ with an accuracy similar to that of wet methods and a sensitivity of

50 p.p.m. of silicon for a 50-mg sample. Other elements normally present do not interfere.

This method has been extended to the determination of silicon in nickel, copper and aluminium alloys, and to tin in non-ferrous alloys[130]. The samples are chlorinated and the volatile chlorides are then separated. Nickel and copper alloys can be analysed with absolute errors of ± 0.02 and -0.07% for silicon, whilst the standard deviation obtained for silicon in an aluminium alloy was 0.026%. A lead–tin alloy with a tin content of 10.2% was found to contain 10.44% of tin with a standard deviation of 0.17%.

The germanium content of coal samples can also be evaluated by gas chromatography[131]. After some preliminary treatment, the sample is chlorinated with hydrogen chloride at 150°C, the germanium tetrachloride formed being absorbed and concentrated on active carbon and submitted to analysis. The sensitivity of the method is 10 p.p.m. for a 0.5-g sample, and 3.3 p.p.m. for a 1.5-g sample, with an average error of about 6%.

Becker *et al.*[132] developed a method for the determination of tin in zirconium–tin alloys in which the sample reacts with chlorine. After removal of the zirconium tetrachloride and the excess of chlorine, the tin tetrachloride is determined by gas chromatography. The limit of detection, under the given operational conditions, is 4 μg of tin, the determination being quantitative for amounts of tin higher than 20–25 μg. The results obtained (1.39% tin) agreed well with those obtained by X-ray fluorescence (1.40%) or polarography (1.37–1.38%).

MISCELLANEOUS METHODS FOR THE DETERMINATION OF METALS

This group includes various procedures which have been developed for the determination of cations, but which do not have a reagent type in common, in contrast to the metal β-diketonates or halides. In most of these methods, the species to be determined is converted in a simple and quantitative fashion by means of some appropriate reagent to a compound which has all the requirements for successful gas chromatography. In some of the methods, the evaluation is achieved indirectly by measurement of the peak corresponding to an evolved or residual gas or to a decomposition product of the injected compound.

Palladium in aqueous solution can be determined after treatment of the solution with perchloric acid and with a 1:1 mixture of propene–propane[133]. Palladium reacts with propene and the residual gas is analysed on a column of activated alumina at 70°C with hydrogen as carrier gas.

Uranium and thorium can be evaluated[134] in sintered specimens by a method which involves formation of the metal hydrides followed by their selective decomposition at 325°C and 600°C, respectively. The hydrogen released is then determined by gas chromatography.

Hogan and Taylor[135] have described a procedure for determining micro-amounts of magnesium metal. The sample is treated with diluted sulphuric acid and the generated hydrogen is injected into the chromatograph (with thermal conductivity detection) to give a peak proportional to the amount of hydrogen evolved and consequently to the amount of free magnesium in the sample. Plotting the height of the peak against micromoles of hydrogen shows a linear response in the range 20–240 micromoles. The method is applicable to any other metal capable

of liberating hydrogen from either dilute acid or alkali.

Aluminium together with aluminium carbide has been determined by indirect gas chromatography; after digestion of the sample with hydrochloric acid, the hydrogen or methane generated is submitted to gas chromatographic analysis[136]. Total and metallic aluminium in thin films can be determined by indirect gas chromatography by measuring the hydrogen evolved after treating the sample with a strong base[137]. With thermal conductivity detection, 60–300 μg of aluminium can be determined. The reproducibility for the total aluminium content is about ±1% and for the metallic aluminium ±3%, the accuracy being ±2% and ±3–4%, respectively.

Ultramicro amounts of selenium have been determined by Nakashima and Tôei[138]. Selenium as selenious acid reacts at pH 0–1 with 4-chloro-*o*-phenylenediamine to form 5-chloropiazselenol which is extracted into toluene; an aliquot of the organic layer is injected into the gas chromatograph (electron capture detection). Calibration graphs based on peak heights are linear up to 0.80 μg of selenium, and the limit of detection is about 0.04 μg. Selenium has also been determined in pure sulphuric acid after conversion to 5-nitropiazselenol[139], which is then extracted into toluene and gas-chromatographed. Peak height measurements provide linear calibration graphs up to 0.15 μg Se ml^{-1} in the solvent. The amount of selenium found in pure commercial sulphuric acid was 10^{-6}–10^{-5}%. As little as 1 ng of selenium may be detected by means of electron capture, for selenium dioxide forms volatile selenous esters which can be detected[140] in amounts down to 10^{-12} g.

Selenium, in pure tellurium metal, has also been evaluated as 5-nitropiazselenol. After treatment of the sample with aqua regia and reaction with 4-nitro-*o*-phenylenediamine, the piazselenol derivative is extracted into toluene for analysis. The amount of selenium in commercially available pure tellurium varied from 10^{-3} to 10^{-4}%. With electron capture detection, about 10 ng of selenium can be detected in a few milligrams of sample. Calibration graphs based on peak height measurements from selenous acid in hydrochloric acid solution and from elemental selenium dissolved in carbon disulphide are parallel and linear in the range 0.0–0.12 μg of selenium. Common ions even in 10^4-fold amounts do not interfere appreciably in the recovery of selenium[141].

The above procedure has also been utilized for the determination of selenium in sea water without a preconcentration step[142]. Amounts of about 2 ng of the element in 1 ml of organic phase can be detected, so that only 50–100 ml of sea water is needed; in the absence of pretreatment, there is no possibility of losses of selenium. Calibration curves based on peak height measurements are parallel for solutions in distilled water, natural sea water, and artificial sea water, and are linear in the range 0.0–0.025 μg of selenium.

Another method for the determination of selenium has recently been reported by Young and Christian[143]. Selenium is made to react at pH 2 with 2,3-diaminonaphthalene to give the corresponding piazselenol compound which is extracted into n-hexane. An aliquot of the hexane layer is analysed with electron capture detection, as little as $5 \cdot 10^{-10}$ g of selenium being detected. The calibration graph is linear in the range 0.1–1.0 μg of selenium. EDTA can be added to eliminate interferences. The method has been applied to the determination of selenium in human blood and urine, averages of 0.38 and 0.007 p.p.m. being found; in river

water the concentration appears to be less than 10^{-2} μg l^{-1}. The results seem to be very reproducible, and their correlation with neutron activation results is excellent.

An indirect method for the determination of ruthenium as a thiosemicarbazide complex in which thin-layer and gas chromatography are combined has been reported by Ballschmiter[144]. The ruthenium complex is formed in 4–6 *M* hydrochloric acid and extracted, along with the excess of ligand into chloroform; ligand and chelate are then separated by thin-layer chromatography. The ruthenium compound is extracted from the plate with a (99 + 1) ethanol–pyridine mixture and submitted to gas chromatography. Ballschmiter states that the complex decomposes reproducibly in the injection port, which is kept at 225°C, and the ligand gives two main peaks. When the first peak height is plotted against the concentration of the whole chelate, the calibration graph is linear in the range 0.2–2.0 ng.

Several chelates of polychlorinated xanthates have been formed and investigated by thin-layer and gas chromatography[145]. At 200°C, the xanthates pyrolyze instantaneously and reproducibly to the corresponding alcohol; this allows the determination of certain metals by gas chromatography with electron capture detection. The method can be applied to the evaluation of nickel in aqueous solution; 10 ng of nickel can be determined with a standard deviation of 0.5 ng, and the reproducibility is not affected by the presence of zinc.

A method for the determination of arsenic has been developed by Schwedt and Rüssel[146]. Arsenic is extracted from a hydrochloric acid medium as the diethyldithiocarbamate, which is then made to react with diphenylmagnesium to form triphenylarsine quantitatively; triphenylarsine is then evaluated with a flame ionization detector. The method has been applied to the determination of arsenic in biological materials, concentrations as low as 2 μg As g^{-1} being determined; the limit of detection is about 0.4 ng of arsenic.

Jones and Nickless[147] developed a method for the determination of mercury as phenylmercury(II) chloride, after reaction of mercury in a weakly acidic medium at near boiling point with sodium benzenesulphinate (Peters reaction). The compound formed is extracted into toluene, and an aliquot of the extract is injected for analysis. With an electron capture detector, the calibration graphs are linear in three ranges of mercury concentration: 5.0–20.0, 0.5–5.0 and 0.05–0.2 μg. No details are given of the detector responses for these ranges. The limit of detection is about $2 \cdot 10^{-10}$ g of phenylmercury(II) chloride.

The quantitative methylation of mercury by means of a trimethylsilyl derivative has also been utilized[148] for the determination of the element in various environmental samples; good agreement with other methods being reported but no details have been published.

The Peters reaction also provides the basis for a procedure for mercury reported by Mushak *et al.*[149]; lithium pentafluorobenzenesulphinate serves as the reagent, pentafluorophenylmercury(II) chloride formed in acidic medium being extracted into xylene and submitted to gas-chromatographic analysis. Inorganic mercury can be evaluated in water, urine and sera. The authors claim that mercury can be determined at the 50 p.p.b. level in waters, the limit of detection with an electron capture detector being 20 p.p.b. Recoveries of added mercury are 70.5% for water, 81.4% for urine and 51.0% for blood serum, and the relative standard

deviations are 6.8, 10.5 and 9.4%, respectively. Linear ranges and interferences have not been reported.

Separation and determination of magnesium and zinc in aluminium-containing alloys with high-temperature gas chromatography have been achieved by Sokolov and Vakin[150], who operated at 1070°C with a diaphragm detector. When pure metals are used as standards and peak areas are weighed, about 0.1% of magnesium can be evaluated. For sample sizes of about 23 mg the relative error ranges from 0.0 to 6.7% for zinc and from 0.0 to 16.8% for magnesium.

Bismuth can be determined by similar techniques at a column temperature of 1250°C[151]. Under the given conditions, the sensitivity is about 0.2% for a 15 mg sample; the calibration graphs obtained by plotting peak height against amounts of pure bismuth are linear in the range 0.2–10 mg. The method can be applied to the analysis of various bismuth alloys containing tin, lead, zinc and cadmium. Zinc and cadmium are eluted almost simultaneously, and the peaks are well separated from that of bismuth. However, lead and tin remain at the start of the column, which must therefore be periodically cleaned.

DETERMINATION OF ANIONS

The extensive research which has been carried out in the development of methods for the gas-chromatographic determination of cations, especially at trace levels has led to many successful procedures which can be applied to the most diverse materials. The availability of ligands such as the β-diketones and their derivatives has greatly contributed to these advances. Unfortunately, the situation is rather different with regard to the determination of anions, for there are no suitable general reagents for anions analogous to the β-diketones for cations.

Some work has been done with trimethylsilyl derivatives which have been investigated in attempts to use them as general reagents for gas chromatography of anions. Although a group of about ten anions does react with the trimethylsilyl derivatives to give the corresponding volatile compounds, which can in fact be separated by chromatography, the only quantitative procedure so far described is one for phosphate. Experimental difficulties appear to be the main explanation for the lack of further developments.

The first application of gas chromatography to analysis for anions as their trimethylsilyl derivatives was probably that described by Lentz, who prepared the silyl derivatives of various silicate compounds to study the silicate structures present in sodium silicate solutions[152]. Some of the compounds formed were identified by gas chromatography with programmed temperature, for it was possible to separate the silyl derivatives of the lower silicate anions and to obtain a partial separation of the higher silicate anions.

Hashizume and Saski[153] have prepared the trimethylsilylorthophosphate derivative by treating ammonium orthophosphate or orthophosphoric acid with a mixture of trimethylchlorosilane (TMCS) and hexamethyldisilazane. The reaction is about 95% complete if phosphate is present as the ammonium salt or as the acid. A pyridine solution of the compound obtained gives a single symmetrical peak when thermal conductivity detection is used. At a column temperature of 100°C, the calibration graph is linear in the range 0.0–25.0 μg when naphthalene is used as internal standard and peak area ratios are plotted against quantities of

phosphorus. The recovery of phosphate from biological samples is 100.3% with a standard deviation of ±1.4%. The results obtained by this method have been compared with spectrophotometric results; agreement is good and excellent precision and accuracy are claimed[154,155].

Butts and Rainez[156,157] have reported the formation of the trimethylsilyl derivatives of several anions—borate, carbonate, oxalate, phosphite, sulphate, arsenite, phosphate, vanadate, arsenate and sulphamate. These are obtained by reaction of their ammonium salts with bistrimethylsilylfluoroacetamide (BSTFA) in dimethylformamide as solvent, in order to increase their solubility. Each silyl derivative gave a single peak when gas chromatographed (with flame photometric or flame ionization detection), either singly or in mixtures; the peak contents were identified by mass spectrometry. The authors pointed out that the silyl derivatives are not formed when the anions are present as their sodium or potassium salts, and overcame this difficulty by passing the solution through an ion exchanger in the ammonium form. The method offers good prospects for quantitative work as shown by Matthews *et al.*[158], who described a procedure for the determination of traces of phosphate in aqueous solution. After isolation and concentration of phosphate by a single solvent-extraction step with a quaternary ammonium salt in toluene–octanol, the extracted phosphate is silylated directly in the organic phase, an aliquot of which is submitted to gas chromatography. As little as 100 p.p.b. of phosphate can be determined with a precision of 7–10% when a flame photometric detector is used; the calibration graphs based on peak areas are linear in the range 0.2–1.1 p.p.m. of phosphate in the aqueous solution.

A modification of the above method in which the reaction between phosphate in aqueous solution and the silylating agent (BSTFA–1% TMCS) takes place in a heated precolumn after the elimination of water, has been reported by Wiese and Hanson[159]. The reaction products are analyzed by means of temperature programming and thermal conductivity detection. The method is useful for 10–100 μg of phosphate, and under the given conditions, the error is ±2.7%.

This procedure of determining phosphate as its silyl derivative has been employed for the evaluation of phosphate in fruit juices and wines[160,161], the values obtained with flame ionization detection being only slightly higher than those obtained by spectrophotometric measurement of molybdenum blue[160].

In a continuation of Lentz's work, the trimethylsilyl derivatives of various silicon anions have been resolved by gas–liquid chromatography at column temperatures below 290°C, with temperature programming and flame ionization detection[162]. The corresponding peaks for each of the silyl derivatives can be obtained and the resolution of higher anions has been considerably improved. Their structures were elucidated in the eluate by high-resolution mass spectrometry.

Sulphate and sulphonic acid groups have been determined[163] after their reduction to hydrogen sulphide, which is chromatographed at a column temperature of 90°C with hydrogen as carrier gas and carbon dioxide as internal standard. The calibration graph based on peak area ratios is linear from 0.44 to 4.40 mg of sulphur. The method is applicable to various soluble and insoluble sulphates, persulphates and aromatic sulphonic acids; thiosulphates, sulphites and hydrogensulphites are first converted to sulphates. Acetate, nitrate and chloride interfere, so that it is necessary first to separate sulphate as barium sulphate.

A method for the indirect determination of sulphate in glycosaminoglycans has been developed by Srinivasan *et al.*[164]. Sulphate is converted to n-butylammonium sulphate by passing sodium sulphate solution through an ion exchanger in the acidic form and reacting the acid produced with n-butylamine. The excess of amine is then volatilized and sulphate is evaluated after gas chromatography of the n-butylamine liberated by adding sodium hydroxide solution; a column temperature of 145°C and flame ionization detection are used. With n-amyl alcohol as internal standard and peak area ratios, the calibration graph is linear in the range 0.0–4.0 mg ml^{-1} based on amine concentrations, with a standard deviation of about 7%. In terms of sulphate concentration, the calibration graph is linear in the range 0–80 μg. The values obtained by this method for total sulphates in glycosaminoglycans were in good agreement with the results of the spectrophotometric benzidine method; in the analysis of heparin an absolute standard deviation of 1.6% was achieved.

Carbonate has been determined in rocks and minerals by gas chromatography after treatment of the sample with hydrochloric or phosphoric acids[165,166]. The evolved carbon dioxide can be measured with a thermal conductivity detector; as little as 0.2 p.p.m. can be detected and the precision of the method is better than 1%. Sodium carbonate (0.13–1.3 mg) in admixture with sodium hydroxide can be determined after treating the sample with sulphuric acid[167].

Birk *et al.*[168] have developed a rapid procedure for the determination of sulphide, sulphite and carbonate in salts on the basis that these anions form gaseous products in acidic medium. The evolved gases are determined by injecting an aliquot of the gaseous mixture into the gas chromatograph. The standard deviations for both sulphide and sulphite are about 6% and about 2% for carbonate. With thermal conductivity detection, the calibration graphs are linear in the ranges 2–18 mg of sulphite and 1–10 mg of sulphide, both as their respective salts. At low concentrations, sulphide recovery was high and sulphite recovery was low, whilst an average of 100.2% recovery was obtained for carbonate.

These same anions have also been evaluated after decomposition of their salts with 60% phosphoric acid in an acidifying device connected to the column inlet[169]. Calibration graphs based on peak areas are linear up to 10% salt concentrations; precision studies for about 2% concentrations show relative mean deviations of 0.37% for sulphide and sulphite, and 0.25% for carbonate at a column temperature of 100°C; the deviation for carbonate increases to 0.55% at 130°C. Under the given conditions carbonate can be detected at the 0.01% level, and the other salts at the 0.02% level.

Oxalic acid has been determined in urine at a column temperature of 190°C after its extraction from strong acidic medium with tributylphosphate and methylation of the extracts with a mixture of methanol and diazomethane; the organic phase is then chromatographed with flame ionization detection[170]. Calibration graphs based on peak heights show good linearity between 0.05 and 2.0 μg of methyloxalate; but recovery of added oxalate is only 60–80%. This method has been employed by Mee and Stanley[171] for the determination of oxalic acid in biological materials. After addition of methanol in hydrochloric acid medium, followed by ultrasonic mixing and extraction, quantitative analysis can be readily achieved by comparing samples against standards. The calibration graph based on peak areas

is linear in the range 0.0–25.0 μg of oxalic acid, at a column temperature of 105°C with a flame ionization detector. Recovery of added oxalic acid to urine ranges from 92 to 95%.

Bock and Semmler[172] have developed a method for the determination of fluoride after its conversion to a silane derivative by reaction with triethylsilanol in a hydrochloric acid medium, the compound formed being extracted into tetrachloroethylene. The extraction conditions have been studied in detail, and it has been shown that the extraction is highly selective, although zirconium and high concentrations of silica, thorium and vanadium seriously interfere. Thermal conductivity, flame ionization, electron capture and mass spectrometric detection systems were employed, the best results being obtained with flame ionization. With cyclohexane as internal standard and peak height ratio measurements, calibration graphs are linear in two ranges of concentration: 3.8–38.0 μg F ml^{-1} and 0.4–3.8 μg F. ml^{-1}. The relative standard deviation for 0.95 μg F ml^{-1} is ±6% and as little as 0.1 μg F ml^{-1} can be detected. The method has been applied to the determination of fluoride in water and inorganic salts. Fluoride in biological materials has also been evaluated by this method, amounts of about 1 μg being determined with suitable accuracy[173].

Fluoride in biological materials has been determined[174] after conversion to trimethylfluorosilane by reaction in acidic medium with TMCS. The product is extracted into benzene, and an aliquot of the organic layer is chromatographed at a column temperature of 75°C with isopentane as internal standard and flame ionization detection. A serum sample containing 0.035 μg F ml^{-1} was analysed with an absolute standard deviation of ±0.0012 μg[174]. The method has been employed by Cropper and Putnam[175] for the determination of fluoride in dental creams. The procedure is very similar to that of Fresen *et al.*[174], but n-pentane serves as internal standard. Peak height ratios are calculated and the fluoride content is obtained by using a response factor, for which the standard deviation is ±0.8%. The mean recovery of added fluoride is 100.5% and there is good agreement between the gas chromatographic results and results obtained by a colorimetric method. Total fluoride at the 0.1% level in dental cream samples can be evaluated with a relative standard deviation of 0.001% (ref. 175).

Bock and Strecker[176] have studied the separation of traces of fluoride from aqueous solutions and their subsequent determination by gas chromatography, after extraction with triethylchlorosilane in *m*-xylene or with tetraphenylantimony hydroxide in dichloromethane. Extraction conditions for both systems were thoroughly investigated. For the former method, 0.2–8.0 μg F ml^{-1} can be determined with a relative standard deviation of 6.4%, with cyclohexane as internal standard and peak height ratio measurement after flame ionization detection. Recoveries depend on the volume of acidifying agent—2.5 *M* hydrochloric acid—decreasing from 100% to 88% as the volume increases from 25 to 500 ml. As little as 0.05 μg F ml^{-1} can be determined, but variable blanks (0.5–1.5 μg of fluoride) prevent the evaluation of less than *ca.* 3 μg of fluoride. Several coprecipitation reactions with various carriers—calcium carbonate, lanthanum hydroxide, hydroxyapatite—were investigated, the last being most suitable.

An attempt has been made to determine fluoride ions in aqueous solution in which a displacement reaction and gas chromatography are used[177]. If fluoride

displaced the ligand from a metal chelate by forming a more stable fluoride–metal complex, it should be possible to determine the amount of ligand liberated or the reduction in the amount of the chelate itself. Volatile beryllium and aluminium complexes of β-diketones have been tested, but the complexes were too easily hydrolysed for satisfactory results. The insolubility of fluoride salts in non-aqueous systems is another limiting factor.

Rüssel[178] has determined chloride, bromide and iodide, after converting them to halogen-alcohols, by reaction in acidic medium with 1,2-olefin oxides. As the addition of sulphuric or phosphoric acids produces the corresponding glycol, the halide ions must be converted to their corresponding acids by passage of the solutions through a strongly acidic ion exchanger. Ethylene oxide is then passed into the ice-cooled eluate, and an aliquot of the solution is injected into the chromatograph. In this way, measurable peaks can be obtained at concentrations as low as $0.5 \cdot 10^{-4}$ *M* hydrochloric acid, with flame ionization detection. Conversion to the halogen-alcohols ranged from 95 to 99%; this was investigated by comparing peak areas of both samples and standards.

MacGee and Allen[179] have reported the successful application of Hoffman's degradation procedure to the gas-chromatographic determination of halides. The halides are converted by ion exchange to their tetraalkylammonium salts, and an aliquot of the eluate is injected into a pyrolyzer, the salts being decomposed to the trialkylamine and the corresponding alkyl halide. The degradation products are separated from each other at a column temperature of 125°C, and thermal conductivity detection is used. This approach appears viable for the determination of low amounts of halides in aqueous solution, but no further results have been published.

Recently, Matthews *et al.*[180] have described another procedure for the determination of aqueous halides at low concentrations. Chloride, bromide and iodide are extracted from aqueous solutions with tetraheptylammonium carbonate in 10% toluene–undecanol solution, the extraction efficiency ranging from 90 to 100%. The extracted compounds are analysed by on-column injection and undergo thermal degradation to 1-haloheptane and triheptylamine at temperatures above 150°C. Derivatization efficiencies are 63% for chloride, 58% for bromide and 69% for iodide. Based on peak areas, linear calibrations are obtained for 0–20 μg Cl ml^{-1}, 3–35 μg Br ml^{-1}, and 4–55 μg I ml^{-1}, referred to the aqueous solution. Both flame ionization and electron capture detection systems have been used, but the latter becomes unresponsive because of the effect of some degradation products. A gas chromatography–mass spectrometry system was also employed in order to identify the derivative peaks by comparing them with those of pure 1-haloheptanes.

Oxidizing agents such as iodate can be determined through the iodine liberated in acidic solution in their presence[181]. The iodine is then extracted into carbon tetrachloride and an aliquot of the organic layer is injected. With a thermal conductivity detector, the relationship between peak area and iodine concentration is linear over the range 25–125 μg. A single extraction with carbon tetrachloride suffices to recover 96% of the theoretical amount of iodine liberated. The limit of detection is restricted by the relatively low sensitivity of the thermal conductivity detector.

Iodine has been quantitatively evaluated by employing electron capture

detection after reaction with acetone and extraction of the iodoacetone formed into n-hexane[182]. The response of the detector is linear up to 1 μg I ml^{-1} and the relative standard deviation is 8% for concentrations above 0.14 μg ml^{-1}. Milligram amounts of chloride or bromide and microamounts of iodide do not interfere. Amplification of the amount of the reaction product and the determination of both iodine and iodide can be accomplished by addition of potassium iodate. However, when derivatization of iodine is carried out with 2-butanone, 2-pentanone or 3-pentanone, the products obtained show a greater response to electron capture detection and are extracted more completely than the product of the iodine reaction with propanone[183]. These findings permit an extension of the range of iodine concentrations which can be determined. The detector response (per cent of full scale) is a linear function of the initial aqueous concentration of iodine in the range 0–0.6 μg ml^{-1}, although the slope of the curve varies notably with the ketone used. Unfortunately, a decrease in detector response prevents experimental extension to the lowest possible limit of the range of iodine concentrations that could be determined by this method.

The bromide content of blood has been evaluated by a similar technique[184]. After elimination of proteins, bromide is oxidized to bromine in acidic medium, and reacted with cyclohexene to give 1,2-dibromocyclohexane which is extracted into cyclohexane. An aliquot of the extract is chromatographed (flame ionization detection) with programmed temperature of 70 to 170°C; 1,6-dibromohexane is used as internal standard and peak height ratios are plotted. Calibration graphs are linear in the range 0.1–1.0 μg Br ml^{-1}. An average recovery of added bromide to blood of 100.8% was obtained. Oxalate, fluoride, heparin and chloride at the normal levels found in blood do not interfere. The results obtained for several samples agree well with those found by x-ray fluorescence spectrometry.

A method for the determination of trace levels of chloride has been reported[185]. The halide ion is treated with phenylmercury(II) nitrate in a perchloric acid medium at pH about 1.5, and the phenylmercury(II) chloride formed is extracted into chloroform. With flame ionization detection and injection of large samples, it is possible to detect as little as $2.3 \cdot 10^{-10}$ g of chloride. Calibration graphs obtained by plotting peak heights or areas are linear in the ranges 5–100 and 0.4–7.0 μg Cl ml^{-1}, respectively. Aqueous solutions containing 0.008 p.p.m. of chloride can be determined with a relative mean error of 25.0% (peak height) or 21.3% (peak area). With electron capture detection, a tenfold increase in sensitivity can be achieved and about $3 \cdot 10^{-11}$ g of chloride can be detected[186].

Nota and Palombari[187] have reported a simple method for the determination of trace amounts of cyanide and/or thiocyanate in aqueous solution. Cyanide or thiocyanate are converted to cyanogen bromide by treating the sample with bromine, and cyanogen bromide is then measured by gas–solid chromatography with electron capture detection, at levels as low as 10^{-8} g of the corresponding anion. Calibration graphs based on peak heights are linear in the range 0.0–0.5 p.p.m. of cyanide and 0.0–1.2 p.p.m. of thiocyanate. The sensitivity can be improved by extraction of cyanogen bromide into diisopropylether before injection; about 1 p.p.b. of cyanogen bromide can then be detected. Complex cyanides do not interfere, but can be determined by converting them to the simple cyanide. Thiocyanate might be evaluated by eliminating cyanide with formaldehyde, the amount of the anion present being determined by difference.

TABLE I

INORGANIC SPECIES DETERMINED BY GAS CHROMATOGRAPHY

Species	*Detection Limit (g)*	*Ref.*	*Species*	*Detection Limit (g)*	*Ref.*	*Species*	*Detection Limit (g)*	*Ref.*
Al[a,d]	$6.7 \cdot 10^{-12}$	82	Pd[a,d]	$1.5 \cdot 10^{-10}$	69	Zn[d]	—	150
As[c,d]	$4 \cdot 10^{-10}$	146	Re[c,g]	$1 \cdot 10^{-4}$	128	Br^{-}[g]	$1 \cdot 10^{-7}$	184
Be[a]	$1 \cdot 10^{-14}$	99	Rh[a]	$2.2 \cdot 10^{-12}$	82	$C_2O_4^{2-}$	$5 \cdot 10^{-8}$	170
Bi[d]	$2 \cdot 10^{-3}$	151	Ru[a,d,g]	$1 \cdot 10^{-8}$	88	Cl^{-}	$3 \cdot 10^{-9}$	186
Ce[b,e]	$2 \cdot 10^{-7}$	120	S[c,g]	$1 \cdot 10^{-4}$	128	CN^{-}	$1 \cdot 10^{-9}$	187
Co[a,b]	$4.4 \cdot 10^{-11}$	114	Sc[a]	$1 \cdot 10^{-6}$	83	CO_3^{2-}	$1 \cdot 10^{-7}$	169
Cr[a]	$5 \cdot 10^{-13}$	109	Se[c,d]	$5 \cdot 10^{-10}$	143	F^{-}	$1 \cdot 10^{-10}$	172
Cu[a]	$1 \cdot 10^{-10}$	70	Si[c]	$5 \cdot 10^{-5}$	129	I_2[g]	$1.4 \cdot 10^{-10}$	182
Fe[a,g]	$2 \cdot 10^{-5}$	87	Sn[c]	$4 \cdot 10^{-6}$	132	I^{-}[g]	$1 \cdot 10^{-9}$	177
Ga[a,g]	$2.1 \cdot 10^{-6}$	81	Te[c,g]	$1 \cdot 10^{-4}$	128	IO_3^{-}[g]	$1 \cdot 10^{-6}$	181
Ge[c]	$3.0 \cdot 10^{-6}$	131	Th[a,b,d]	$6 \cdot 10^{-7}$	113	PO_4^{3-}	$1 \cdot 10^{-10}$	158
Hg	$1.1 \cdot 10^{-10}$	147	Ti[c,g]	$2 \cdot 10^{-5}$	127	S^{2-}	$1 \cdot 10^{-7}$	169
In[a,g]	$1.2 \cdot 10^{-5}$	81	U[a,b,c,d]	$4 \cdot 10^{-7}$	113	SCN^{-}	$1 \cdot 10^{-9}$	187
Mg[d,g]	$2 \cdot 10^{-5}$	134	V[a]	$1 \cdot 10^{-7}$	115	SO_3^{2-}	$1 \cdot 10^{-7}$	169
Mo[c,g]	$1 \cdot 10^{-4}$	128	W[c,g]	$1 \cdot 10^{-4}$	128	SO_4^{2-}[g]	$8 \cdot 10^{-7}$	164
Ni[a,b,d]	$5 \cdot 10^{-11}$	117	Y[b,f]	$1 \cdot 10^{-7}$	119			

[a] Determined as β-diketone or derivative.
[b] Determined as ternary system.
[c] Determined as halide.
[d] Miscellaneous procedure.
[e] Cerium group lanthanides—europium, samarium, praseodymium, neodymium, cerium, lanthanum.
[f] Yttrium group lanthanides—yttrium, ytterbium, dysprosium, gadolinium, holmium, lutetium, terbium.
[g] Limit of detection taken as the lowest point in the calibration graph.

CONCLUSIONS

Gas chromatography is being increasingly employed in quantitative inorganic analysis; many methods have already been developed for the determination of numerous cations and anions in solution. Some 58 species in different concentration ranges and under various forms (Table I) have so far been determined by this technique. The literature on actual applications is at present small, but with further studies of the various ligand systems which have already been described, and with further development of new chelating agents for cations, as well as reagents for anions, the prospects for useful trace methods seem good.

Of the proposed quantitative procedures, those concerned with the assay of beryllium, chromium, aluminium, nickel, selenium, phosphate, fluoride and chloride have been utilized quite extensively for determinations at trace level in substances as varied as biological material[90–97, 101–107, 143, 155, 173] (blood, urine, human tissue) and extraterrestrial samples such as lunar and meteoritic rock[98, 99]. The gas chromatographic method for beryllium is at the present time the most sensitive for this element, and by a combination of solvent extraction, masking and gas chromatography, interferences of other elements are minimal. The determinations of nickel, chromium and aluminium also show useful selectivity and sensitivity. The determination of nickel provides a good example of the possibilities of overcoming interferences: some are eliminated in the preliminary solvent extraction step (*e.g.* copper) and others in the gas chromatography (*e.g.* iron). The determination of selenium by gas-chromatographic procedures has a sensitivity comparable with the most widely employed methods for its evaluation (fluorimetry and neutron activation) and is considerably superior to them in terms of cost and time. The use of flame photometric detection conveys high selectivity and sensitivity to the procedure developed for phosphate; the utilization of flame ionization detection gives results comparable to the molybdenum blue method. Fluoride can be selectively determined at very low levels. The direct chloride method is subject to fewer interferences than the currently used indirect spectrophotometric method, and is more sensitive as well as faster.

Various applications which have been described in the literature are summarized in Table II. However, the relative value of the gas-chromatographic methods reported in this review with respect to established procedures based on other techniques remains to be evaluated. But the gas-chromatographic methods are in general fast, simple and sensitive, and require only relatively inexpensive equipment which is already available in most laboratories.

Comparison with other techniques

Provided that the preliminary chemical steps are not complicated, new analytical methods which are to be superior to, or competitive with, existing approaches must possess several features of which simplicity and reproducibility are probably the most essential. In addition to these characteristics, gas chromatography has other advantages, such as high sensitivity and powers of separation. In comparison with other techniques offering high sensitivity, such as atomic absorption or fluorescence spectrometry, gas chromatography has certain advantages, although its breadth of application is currently by no means so great.

TABLE II

SOME APPLICATIONS OF GAS CHROMATOGRAPHY TO THE DETERMINATIONS OF VARIOUS IONS

Specie(s) to be analysed	*Matrix*	*Ref.*
Al	Biological, environm. materials	110, 112
As	Biological materials	146
Be	Biolog., environm., extraterr. samples	89–99
Co	Biological materials	114
Cr	Alloys, biolog., extraterr. samples	100–108
Cr, Al	In uranium salts	111
Cr, Be	Biolog., environm. materials	109
Cu	Tap water	123
Cu, Ni	Alloy, coin	123
Fe	Alloy	87
Fe, Al	Alloy	88
Fe, Cu, Al	Alloy	86
Fe, Cu, Cr, Al	Environmental samples	121
Ge	In coal	131
Hg	Biolog., environm. materials	148, 149
Ni	Alloy, biolog. materials	117
Se	Biolog., environm. samples	142, 143
Si	Alloys, iron and steel	129, 130
Sn	Alloys	130, 132
Ti	NBS sample	127
Br^-	Biological material	184
$C_2O_4^{2-}$	Biological material	170, 171
Cl^-	Drinking water	188, 189
CO_3^{2-}	NBS samples, minerals, rocks	165–169
F^-	Biolog. mat., salts, water samples	172–175
PO_4^{3-}	Biological materials	154, 155, 160, 161
SO_4^{2-}	Biological materials	164

Linear calibration graphs can be achieved over wider ranges, and day-to-day shifting of the calibration curves is usually less. If suitable reagents and dual detection systems are available, the simultaneous determination of p.p.b. of one constituent and percentage amounts of another in a matrix becomes feasible. In respect to the final volume of sample needed for an analysis, only the non-flame devices[190] of atomic absorption or atomic fluorescence spectrometry can compete with gas chromatography, a few microlitres being sufficient. The separation ability of gas chromatography combined with the use of selective detectors such as the flame photometric or microwave emission devices makes it possible to envisage simultaneous determinations of several species, which is the ultimate goal of inorganic gas chromatography.

It would seem that these potential and actual advantages should ensure a more widespread exploitation of this technique of inorganic analysis especially in ecological and environmental studies where sensitivity and selectivity are of crucial importance.

The author thanks Prof. R. Belcher for his interest and encouragement and Drs. A. M. G. Macdonald, W. I. Stephen and P. C. Uden for their helpful discussions and comments on this paper. A fellowship award in the European Science Exchange Programme between the Royal Society and the Consejo Superior de Investigaciones Cientificas is gratefully acknowledged.

SUMMARY

In the past decade, the application of gas chromatography to the analysis of inorganic species and organometallic compounds has been studied extensively. This particular field of gas chromatography is expanding rapidly, and much attention is devoted to the development of quantitative methods of analysis. The literature on quantitative procedures for inorganic species is reviewed.

REFERENCES

1 R. W. Moshier and R. E. Sievers, *Gas Chromatography of Metal Chelates*, Pergamon, Oxford, 1965.
2 R. S. Juvet Jr. and F. Zado in J. C. Giddings and R. A. Keller (Eds.), *Advances in Chromatography*, Vol. I, Marcel Dekker, New York, 1966, pp. 249–307.
3 C. Pommier, *Rev. Chim. Miner.*, 3 (1966) 401.
4 R. S. Juvet Jr. and S. Dal Nogare, *Anal. Chem.*, 40 (5) (1968) 33R.
5 R. S. Juvet Jr. and S. P. Cram, *Anal. Chem.*, 42 (5) (1970) 14R.
6 B. I. Anvaer and Y. S. Drugov, *Zh. Anal. Khim.*, 26 (1971) 1180.
7 C. Pommier and G. Guiochon, *La Chromatographie en phase gazeuse en Chimie Inorganique*, Gauthier–Villars, Paris, 1971.
8 R. S. Juvet Jr. and S. P. Cram, *Anal. Chem.*, 44 (5) (1972) 230R.
9 D. N. Sokolov, *Zh. Anal. Khim.*, 27 (1972) 993.
10 W. I. Stephen, *Proc. Soc. Anal. Chem.*, 9 (1972) 137.
11 L. Gascó and T. H. Risby, *Energ. Nucl.*, 78 (1972) 421.
12 P. Jacquelot and G. Thomas, *Bull. Soc. Chim. Fr.*, 4 (1973) 1261.
13 J. Wilkie, A. Losse and H. Sackman, *J. Chromatogr.*, 18 (1965) 482.
14 S. T. Sie, J. P. A. Bleumer and G. W. A. Rijnders, *Separ. Sci.*, 1 (1966) 41.
15 E. Rudzitis, *Anal. Chem.*, 39 (1967) 1187.
16 W. S. Pappas and J. G. Million, *Anal. Chem.*, 40 (1968) 2176.
17 T. S. Zvarova and I. Zvara, *J. Chromatogr.*, 44 (1969) 604.
18 O. Pitak, *Chromatographia*, 2 (1969) 304.
19 O. Pitak, *Chromatographia*, 2 (1969) 463.
20 O. Pitak, *Chromatographia*, 3 (1970) 29.
21 G. Parissakis, D. Vranti-Piscon and J. Z. Kontoyannakos, *Chromatographia*, 3 (1970) 541.
22 V. V. Brazhnikov and K. I. Sakodynsky, *Zh. Prikl. Khim. (Leningrad)*, 43 (1970) 2247.
23 T. S. Zvarova and I. Zvara, *Joint Inst. Nucl. Invest. Rep.*, 1970, from *Chem. Abstr.*, 75 (1971) 53570r.
24 G. Parissakis, D. Vranti-Piscon and J. Kontoyannakos, *Z. Anal. Chem.*, 254 (1971) 188.
25 D. Vranti-Piscon, I. Kontoyannakos and G. Parissakis, *J. Chromatogr. Sci.*, 9 (1971) 499.
26 V. V. Brazhnikov and K. I. Sakodynsky, *J. Chromatogr.*, 66 (1972) 361.
27 I. Toyama and K. Otozai, *Z. Anal. Chem.*, 262 (1972) 346.
28 K. I. Eisentraut and R. E. Sievers, *J. Amer. Chem. Soc.*, 87 (1965) 5254.
29 C. S. Springer Jr., D. W. Meek and R. E. Sievers, *Inorg. Chem.*, 6 (1967) 1105.
30 J. R. Stokely Jr., *U.S. At. Energy Comm. TID-23663; Chem. Abstr.*, 68 (1968) 8966n.
31 T. Shigematsu, M. Matsui and K. Utsunomiya, *Bull. Inst. Chem. Res., Kyoto Univ.*, 46 (1968) 256.
32 P. C. Uden and C. R. Jenkins, *Talanta*, 16 (1969) 893.
33 B. R. Kowalski, T. L. Isenhour and R. E. Sievers, *Anal. Chem.*, 41 (1969) 998.
34 T. Shigematsu, M. Matsui and H. Utsunomiya, *Bull. Chem. Soc. Jap.*, 42 (1969) 1278.
35 W. C. Butts and C. V. Banks, *Anal. Chem.*, 42 (1970) 133.

36 R. Fontaine, B. Santoni, C. Pommier and G. Guichon, *Chromatographia*, 3 (1970) 532.
37 N. M. Karayannis and A. H. Corwin, *J. Chromatogr. Sci.*, 8 (1970) 251.
38 S. P. Cram and T. R. Booher, *159th ACS National Meeting, Houston, Texas, February 22–27, 1970.*
39 R. Belcher, J. R. Majer, W. I. Stephen, I. J. Thomson and P. C. Uden, *Anal. Chim. Acta*, 50 (1970) 423.
40 J. E. Schwarberg, R. E. Sievers and R. W. Moshier, *Anal. Chem.*, 42 (1970) 1828.
41 R. Belcher, C. R. Jenkins, W. I. Stephen and P. C. Uden, *Talanta*, 17 (1970) 455.
42 K. Tanikawa, H. Ochi and K. Arakawa, *Jap. Anal.*, 19 (1970) 1669.
43 T. Fujinaga, T. Kuwamoto and S. Murai, *Talanta*, 18 (1971) 432.
44 M. Z. Gurevich, T. M. Sas, B. D. Stepin and V. V. Zelantsov, *Russian J. of Inorg. Chem.*, 16 (1971) 927.
45 A. Kito, Y. Miyake, H. Kobayashi and K. Ueno, *Jap. Anal.*, 20 (1971) 1363.
46 P. Jacquelot and G. Thomas, *J. Chromatogr.*, 66 (1972) 121.
47 J. W. Mitchell and C. V. Banks, *Anal. Chim. Acta*, 57 (1971) 415.
48 K. Utsunomiya and T. Shigematsu, *Anal. Chim. Acta*, 58 (1972) 411.
49 K. Utsunomiya, *Anal. Chim. Acta*, 59 (1972) 147.
50 R. Belcher, C. R. Cranley, J. R. Majer, W. I. Stephen and P. C. Uden, *Anal. Chim. Acta*, 60 (1972) 109.
51 P. Jacquelot, J. P. Meille and G. Thomas, *Anal. Chim. Acta*, 60 (1972) 335.
52 R. F. Sieck and C. V. Banks, *Anal. Chem.*, 44 (1972) 2307.
53 C. A. Burgett and J. S. Fritz, *J. Chromatogr.*, 77 (1973) 265.
54 J. W. O'Laughlin and T. P. O'Brien, *166th ACS National Meeting*, Chicago, Ill., August 27–31, 1973.
55 C. A. Burgett, *J. Chromatogr. Sci.*, 11 (1973) 611.
56 H. Kawaguchi, T. Sakamoto and A. Mizuike, *Talanta*, 20 (1973) 321.
57 R. M. Dagnall, T. S. West and P. Whitehead, *Analyst (London)*, 98 (1973) 647.
58 W. I. Stephen, I. J. Thomson and P. C. Uden, *Chem. Commun.*, (1969) 269.
59 R. Belcher, W. I. Stephen, I. J. Thomson and P. C. Uden, *Chem. Commun.*, (1970) 1019.
60 R. Belcher, W. I. Stephen, I. J. Thomson and P. C. Uden, *J. Inorg. Nucl. Chem.*, 33 (1971) 1851.
61 E. Bayer and H. Müller, *Tetrahedron Lett.*, 6 (1971) 533.
62 E. Bayer, H. Müller and R. E. Sievers, *Anal. Chem.*, 43 (1971) 2012.
63 R. Belcher, W. I. Stephen, I. J. Thomson and P. C. Uden, *J. Inorg. Nucl. Chem.*, 34 (1972) 1017.
64 M. Miyazaki, T. Imanari, T. Kumugi and Z. Tamura, *Chem. Pharm. Bull.*, 14 (1966) 117.
65 R. Belcher, M. Pravica, W. I. Stephen and P. C. Uden, *Chem. Commun.*, (1971) 41.
66 P. C. Uden, K. Blessel and D. E. Henderson, *163rd ACS National Meeting*, Boston, Mass., April, 1972.
67 A. Khalique, M. Sc. Thesis, University of Birmingham, 1972.
68 P. C. Uden and K. Blessel, *Inorg. Chem.*, 12 (1973) 352.
69 R. Belcher, K. Blessel, T. Cardwell, M. Pravica, W. I. Stephen and P. C. Uden, *J. Inorg. Nucl. Chem.*, 35 (1973) 1127.
70 R. Belcher, D. E. Henderson, A. Kamalizad, R. J. Martin, W. I. Stephen and P. C. Uden, *Anal. Chem.*, 45 (1973) 1197.
71 R. Belcher, A. Khalique and W. I. Stephen, unpublished work.
72 P. C. Uden, D. E. Henderson and A. Kamalizad, *166th ACS National Meeting*, Chicago, Ill., August 27–31, 1973.
73 M. Lederer, *Nature (London)*, 176 (1955) 462.
74 A. A. Duswalt, *Diss. Abstr.*, 20 (1959) 52.
75 W. J. Biermann and H. Gesser, *Anal. Chem.*, 32 (1960) 1525.
76 W. W. Brandt and J. E. Heveran, *142nd ACS National Meeting*, Atlantic City, N.J., September, 1962.
77 R. D. Hill and H. Gesser, *J. Gas Chromatogr.*, 1 (10) (1963) 11.
78 R. S. Juvet and R. P. Durbin, *J. Gas Chromatogr.*, 1 (12) (1963) 14.
79 W. D. Ross and G. Wheeler Jr., *Anal. Chem.*, 36 (1964) 266.
80 D. K. Albert, *Anal. Chem.*, 36 (1964) 2034.
81 J. E. Schwarberg, R. W. Moshier and J. H. Walsh, *Talanta*, 11 (1964) 1213.
82 W. D. Ross, R. E. Sievers and G. Wheeler Jr., *Anal. Chem.*, 37 (1965) 598.
83 T. Fujinaga, T. Kuwamoto and Y. Ono, *Nippon Kagaku Zasshi*, 86 (1965) 1294.
84 G. P. Morie and T. R. Sweet, *Anal. Chem.*, 37 (1965) 1552.
85 G. P. Morie and T. R. Sweet, *Anal. Chim. Acta*, 34 (1966) 314.

86 R. W. Moshier and J. E. Schwarberg, *Talanta*, 13 (1966) 445.
87 R. E. Sievers, J. W. Connolly and W. D. Ross, *J. Gas Chromatogr.*, 5 (1967) 241.
88 H. Veening, W. E. Bachmann and D. M. Wilkinson, *J. Gas Chromatogr.*, 5 (1967) 249.
89 W. D. Ross and R. E. Sievers, *Talanta*, 15 (1968) 87.
90 M. L. Taylor, E. L. Arnold and R. E. Sievers, *Anal. Lett.*, 1 (1968) 735.
91 M. H. Noweir and J. Cholak, *Envir. Sci. Technol.*, 3 (1969) 927.
92 J. K. Foreman, T. A. Gough and E. A. Walker, *Analyst*, 95 (1970) 797.
93 M. L. Taylor and E. L. Arnold, *Anal. Chem.*, 43 (1971) 1328.
94 W. D. Ross and R. E. Sievers, *Environ. Sci. Technol.*, 6 (1972) 155.
95 G. Kaiser, E. Grallath, P. Tschöpel and G. Tölg, *Z. Anal. Chem.*, 259 (1972) 257.
96 Y. S. Drugov, G. V. Murav'eva, K. M. Grinberg, G. N. Nesterenko and D. N. Sokolov, *Zavod. Lab.*, 38 (1972) 1305.
97 M. S. Black and R. E. Sievers, *Anal. Chem.*, 45 (1973) 1773.
98 K. J. Eisentraut, D. G. Johnson, M. F. Richardson and R. E. Sievers, *161st ACS National Meeting*, Los Angeles, Calif., March–April, 1971.
99 K. J. Eisentraut, D. J. Griest and R. E. Sievers, *Anal. Chem.*, 43 (1971) 2003.
100 W. D. Ross and R. E. Sievers, *Anal. Chem.*, 41 (1969) 1109.
101 J. Savory, P. Mushak and F. W. Sunderman Jr., *J. Chromatogr. Sci.*, 7 (1969) 674.
102 J. Savory, P. Mushak, F. W. Sunderman Jr., R. H. Estes and N. O. Roszel, *Anal. Chem.*, 42 (1970) 294.
103 G. H. Booth Jr. and W. J. Darby, *Anal. Chem.*, 43 (1971) 831.
104 L. C. Hansen, W. G. Scribner, T. W. Gilbert and R. E. Sievers, *Anal. Chem.*, 43 (1971) 349.
105 J. Savory, M. T. Gleen and J. A. Ahlstrom, *J. Chromatogr. Sci.*, 10 (1972) 247.
106 W. D. Ross and M. T. Shafik, *161st ACS National Meeting*, Los Angeles, Calif., March–April, 1971.
107 R. Ross and T. Shafik, *J. Chromatogr. Sci.*, 11 (1973) 46.
108 W. R. Wolf and R. E. Sievers, *161st ACS National Meeting*, Los Angeles, Calif., March–April, 1971.
109 W. R. Wolf, M. L. Taylor, B. M. Hughes, T. O. Tiernan and R. E. Sievers, *Anal. Chem.*, 44 (1972) 616.
110 M. Miyazaki and H. Kaneko, *Chem. Pharm. Bull.*, 18 (1970) 1933.
111 C. Genty, C. Honin, P. Malherbe and R. Schott, *Anal. Chem.*, 43 (1971) 235.
112 M. L. Lee and D. C. Burrell, *Anal. Chim. Acta*, 66 (1973) 245.
113 R. F. Sieck, J. J. Richard, K. Iversen and C. V. Banks, *Anal. Chem.*, 43 (1971) 913.
114 W. D. Ross, W. G. Scribner and R. E. Sievers in N. Sock (Ed.), *Gas Chromatography*, Institute of Petroleum, London, 1970.
115 P. Jacquelot and G. Thomas, *Bull. Soc. Chim.*, (1970) 3167.
116 P. Jacquelot and G. Thomas, *Bull. Soc. Chim.*, (1971) 702.
117 R. S. Barratt, R. Belcher, W. I. Stephen and P. C. Uden, *Anal. Chim. Acta*, 59 (1972) 59.
118 R. Fontaine, B. Santoni, C. Pommier and G. Guichon, *Anal. Chim. Acta*, 62 (1972) 337.
119 C. A. Burgett and J. S. Fritz, *Anal. Chem.*, 44 (1972) 1738.
120 C. A. Burgett and J. S. Fritz, *Talanta*, 20 (1973) 363.
121 R. A. Minear and C. M. Palesh, *165th ACS National Meeting*, Dallas, Texas, April, 1973.
122 P. C. Uden, D. H. Henderson and A. Kamalizad, *166th ACS National Meeting*, Chicago, Ill., August, 1973.
123 R. Belcher, A. Khalique and W. I. Stephen, unpublished work.
124 C. S. G. Phillips and P. L. Timms, *Anal. Chem.*, 35 (1963) 505.
125 A. G. Hamlin, G. Iveson and T. R. Phillips, *Anal. Chem.*, 35 (1963) 2037.
126 J. E. Denison and H. Freud, *Anal. Chem.*, 37 (1965) 1766.
127 R. E. Sievers, G. Wheeler Jr. and W. D. Ross, *Anal. Chem.*, 38 (1966) 306.
128 R. S. Juvet Jr. and R. L. Fisher, *Anal. Chem.*, 38 (1966) 1860.
129 S. T. Sie, J. P. A. Bleumer and G. W. A. Rijnders, *Separ. Sci.*, 2 (1967) 645.
130 S. T. Sie, J. P. A. Bleumer and G. W. A. Rijnders, *Separ. Sci.*, 3 (1968) 165.
131 M. L. Sazonov, T. E. Alymova, M. S. Selenkina and A. A. Zhuhovitskii, *Khim. Tverd. Topl.*, 3 (1968) 64.
132 J. H. Becker, J. Chevallier and J. Spitz, *Z. Anal. Chem.*, 247 (1969) 301.
133 T. Koga and T. Hara, *Bull. Chem. Soc. Jap.*, 39 (1966) 1353.
134 E. A. Schaefer and J. O. Hibbits, *Nucl. Sci. Abstr.*, 20 (1966) 2280.
135 V. D. Hogan and F. R. Taylor, *Anal. Chem.*, 40 (1968) 1387.

136 A. B. Nersesyants, E. L. Zaklarov and Z. A. Bystrova, *Zavod. Lab.*, 36 (1970) 1043.
137 H. Neidhard and F. Scholl, *Mikrochim. Acta*, (1970) 1264.
138 S. Nakashima and K. Tôei, *Talanta*, 15 (1968) 1475.
139 Y. Shimoishi and K. Tôei, *Talanta*, 17 (1970) 165.
140 G. Tölg, *Angew. Chem., Int. Ed. Eng.*, 10 (1971) 661.
141 Y. Shimoishi, *Bull. Chem. Soc. Jap.*, 44 (1971) 3370.
142 Y. Shimoishi, *Anal. Chim. Acta*, 64 (1973) 465.
143 J. W. Young and G. D. Christian, *Anal. Chim. Acta*, 65 (1973) 127.
144 K. Ballschmiter, *J. Chromatogr. Sci.*, 8 (1970) 496.
145 I. Schuphan, K. Ballschmiter and G. Tölg, *Z. Anal. Chem.*, 255 (1971) 116.
146 G. Schwedt and H. A. Rüssel, *Chromatographia*, 5 (1972) 242.
147 P. Jones and G. Nickless, *J. Chromatogr.*, 76 (1973) 285.
148 P. Jones and G. Nickless, *Proc. Soc. Anal. Chem.*, 10 (1973) 270.
149 P. Mushak, F. E. Tibbets, P. Zarnegar and G. B. Fisher, *J. Chromatogr.*, 87 (1973) 215.
150 D. N. Sokolov and N. A. Vakin, *J. Chromatogr. Sci.*, 10 (1972) 417.
151 D. N. Sokolov and N. A. Vakin, *Zavod. Lab.*, 39 (1973) 274.
152 C. W. Lentz, *Inorg. Chem.*, 3 (1964) 574.
153 T. Hashizume and Y. Saski, *Anal. Biochem.*, 15 (1966) 199.
154 T. Hashizume and Y. Saski, *Anal. Biochem.*, 21 (1967) 316.
155 T. Hashizume and Y. Saski, *Anal. Biochem.*, 24 (1968) 232.
156 W. C. Butts, *Anal. Lett.*, 3 (1970) 29.
157 W. C. Butts and W. T. Rainez Jr., *Anal. Chem.*, 43 (1971) 538.
158 D. R. Matthews, W. D. Shults, M. R. Guerin and J. A. Dean, *Anal. Chem.*, 43 (1971) 1582.
159 P. M. Wiese and R. H. Hanson, *Anal. Chem.*, 44 (1972) 2393.
160 J. J. Ryan and J. A. Dupont, *J. Agr. Food Chem.*, 21 (1973) 45.
161 H. T. Chan Jr., E. Chenchin and P. Vonnahme, *J. Agr. Food Chem.*, 21 (1973) 208.
162 F. F. H. Wu, J. Götz, W. D. Janneson and C. R. Masson, *J. Chromatogr.*, 48 (1970) 515.
163 S. Ito and T. Hara, *J. Chem. Soc. Jap., Pure Chem. Sect.*, 90 (1969) 1027.
164 S. R. Srinivasan, B. Radhakrisnamurthy, E. R. Dalferes Jr. and G. S. Berenson, *Anal. Biochem.*, 35 (1970) 398.
165 F. G. Carpenter, *Anal. Chem.*, 34 (1962) 66.
166 P. G. Jeffery and P. J. Kipping, *Analyst (London)*, 87 (1962) 379.
167 E. Schoenberger and S. Bahmueller, *Stud. Univ. Babes-Bolyai, Ser. Chem.*, 15 (1970) 135.
168 J. R. Birk, C. M. Larsen and R. G. Wilbourn, *Anal. Chem.*, 42 (1970) 273.
169 K. L. McDonald, *Anal. Chem.*, 44 (1972) 1298.
170 G. Charransol and P. Desgrez, *J. Chromatogr.*, 48 (1970) 530.
171 J. M. L. Mee and R. W. Stanley, *J. Chromatogr.*, 76 (1973) 242.
172 R. Bock and H. J. Semmler, *Z. Anal. Chem.*, 230 (1967) 161.
173 H. A. Rüssel, *Z. Anal. Chem.*, 252 (1970) 143.
174 J. A. Fresen, F. H. Cox and M. J. Witter, *Pharm. Weekbl.*, 103 (1968) 909.
175 E. Cropper and N. A. Putnam, *J. Soc. Cosmet. Chem.*, 21 (1970) 533.
176 R. Bock and S. Strecker, *Z. Anal. Chem.*, 266 (1973) 110.
177 R. S. Barratt, private communication.
178 H. A. Rüssel, Angew. Chem., *Int. Ed. Eng.*, 9 (1970) 374.
179 J. MacGee and K. G. Allen, *Anal. Chem.*, 42 (1970) 1672.
180 D. R. Matthews, W. D. Shults and J. A. Dean, *Anal. Lett.*, 6 (1973) 513.
181 S. N. Pennington, *J. Chromatogr.*, 36 (1968) 400.
182 R. A. Hasty, *Mikrochim. Acta*, (1971) 348.
183 R. A. Hasty, *Mikrochim. Acta*, (1973) 621.
184 A. W. Archer, *Analyst (London)*, 97 (19[illegible] 128.
185 R. Belcher, J. R. Majer, J. A. Rodriguez Vazquez, W. I. Stephen and P. C. Uden, *Anal. Chim. Acta*, 57 (1971) 73.
186 R. Belcher, J. A. Rodriguez-Vazquez and W. I. Stephen, unpublished work.
187 G. Nota and R. Palombari, *J. Chromatogr.*, 84 (1973) 37.
188 R. Belcher, J. A. Rodriguez-Vazquez and W. I. Stephen, *Anal. Chim. Acta*, 61 (1972) 223.
189 R. Belcher, A. Nadjafi, J. A. Rodriguez-Vazquez and W. I. Stephen, *Analyst (London)*, 97 (1972) 998.
190 See, *e.g.* G. F. Kirkbright, *Analyst (London)*, 96 (1971) 609.

Analytica Chimica Acta, 73 (1974) 33–38

SUB-MICROGRAM PER GRAM CONCENTRATIONS OF MERCURY IN ORCHARD LEAVES DETERMINED BY ISOTOPE DILUTION AND SPARK-SOURCE MASS SPECTROMETRY

ROBERT ALVAREZ

Institute for Materials Research, National Bureau of Standards, Washington, D.C. 20234 (U.S.A.)

(Received 8th April 1974)

The difficulty of reliably determining sub-microgram per gram ($\mu g\ g^{-1}$) concentrations of mercury in biological materials has been reported[1,2]. In 1967, an interlaboratory comparison was made of elemental determinations in a kale powder by different analytical techniques[1]. For mercury, the neutron activation results from two laboratories could be pooled to give a value of $0.150 \pm 0.008\ \mu g\ g^{-1}$ for the mean concentration and standard deviation but the colorimetric value reported by a single laboratory was $0.0122 \pm 0.0024\ \mu g\ g^{-1}$. In 1971, recent analytical methods for mercury developed in Scandinavia and in the United States were reviewed under the principal headings of neutron activation, atomic absorption, and gas chromatography[2]. Reliable chemical analyses having a sensitivity of at least $0.1\ \mu g\ g^{-1}$ and an accuracy, if possible, to within $\pm 10\%$ were cited as desirable for regulatory purposes.

The availability of biological Standard Reference Materials with certified values for trace amounts of mercury would enable an analyst to verify the accuracy of existing methods in his laboratory and aid him to develop new procedures. As a first step in this certification, an analytical program was undertaken by the National Bureau of Standards to provide a reliable value for the mercury content of the ground Orchard Leaves, SRM 1571[3]. Three independent analytical methods were used: atomic absorption spectrometry, neutron activation, and stable-isotope dilution with the spark source mass spectrograph (i.d.–s.s.m.s.). The last method is the object of this investigation.

In previous applications of i.d.–s.s.m.s. methods to standardization problems at NBS[4,5,6], the trace elements being determined were not appreciably volatile under the experimental conditions employed. For these determinations, relatively simple procedures and apparatus sufficed to avoid losing the trace elements and added enriched isotope spikes before equilibration. Once this prerequisite has been achieved, trace element losses do not invalidate the results because only isotope ratios are measured. The volatility of mercury required a more complex procedure and apparatus to ensure its retention before equilibration and determination.

EXPERIMENTAL

Reagents and special solutions

Deionized water was prepared by flowing distilled water from the laboratory distribution system through a mixed-bed, ion-exchange resin column. High-purity

nitric and perchloric acids, which had been prepared previously for other trace element determinations by double distillation of the reagent-grade acids in a sub-boiling quartz still were used[7].

Isotopically enriched mercury(II) oxide, containing 81.53 at.% ^{201}Hg and 11.10 at.% ^{202}Hg for the isotopes of interest, was obtained from the Oak Ridge National Laboratory. Isotopically enriched mercury containing 99.11 at.% ^{198}Hg, <0.003 at.% ^{201}Hg, and 0.004 at.% ^{202} Hg was obtained from Atomic Energy of Canada Limited for use as a carrier. Solutions of these materials were prepared by weighing 5 mg of the element or equivalent to $\pm$0.01 mg, dissolving in 1 ml of 4 *M* nitric acid, and diluting to volume with water in 5-ml volumetric flasks.

A natural mercury solution was prepared by weighing 100 mg of high-purity mercury (99.99+%) to $\pm$0.05 mg, dissolving in 4 ml of 4 *M* nitric acid, and diluting to volume with water in a 50-ml volumetric flask.

Apparatus for wet-ashing of sample

The apparatus used in this study (Fig. 1) is similar to that described by Bethge[8] for wet-ashing organic matter. The borosilicate glass components, assembled with standard taper 24/40 joints, consist of a 250-ml flask, a reflux collector, a 300-mm water-cooled (West) condenser, and a bubbler. For the present application, the modified apparatus also serves for chemically and isotopically equilibrating the mercury of the sample with the enriched isotope spikes without losses. The joints

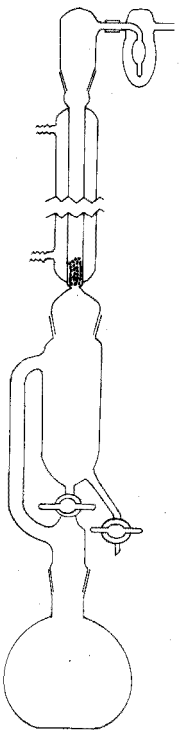

Fig. 1. Apparatus for wet-ashing sample.

are provided with polytetrafluorethylene (PTFE) sleeves for better sealing of the components. The lower portion of the condenser tube is indented immediately above the inner joint to support an 80-mm height of 4-mm diam. quartz Raschig rings[9]. Connected to the top of the condenser is an inner joint sealed at the top and having a side tube. A bubbler containing 4 *M* nitric acid is attached to this side tube with a short section of PTFE tubing. This arrangement prevents mercury vapor that may be present in the laboratory environment from being drawn into the system during the cooling periods. The flask and side tube of the reflux collector are electrically heated with a heating mantle and insulated resistance wire respectively. Variable transformers are used to regulate the voltage to the heaters.

Electrolysis cell

The electrolysis cell consists of a 30-ml beaker with a PTFE cover from which are suspended a 0.51-mm diam. platinum wire anode and two 0.9-mm diam. gold wire cathodes in a tubular holder. The beaker is made of a translucent fluorinated copolymer. The wires had been examined previously by spark source mass spectrometry and found to be of high purity. The portion of the 7-cm length of platinum wire that dips into the solution is coiled into a small loop. The cathode wires, *ca.* 10 cm in length, are forced through undersize holes in a PTFE plug, which fits tightly into a 6-mm diam. PTFE tube. Approximately 2 mm of each wire projects through the plug for exposure to the solution being electrolyzed. A PTFE-encapsulated stirring bar is used for magnetically stirring the solution.

Mass spectrograph and microphotometer

The double-focussing Mattauch–Herzog design spark-source mass spectrograph and the microphotometer with its analog computer have been described previously[4, 5].

Procedure

Determine the moisture content by drying 1-g samples of the orchard leaves material in an oven at 90°C for 24 h. Weigh a 5-g sample to the nearest mg, transfer to a 250-ml flask, and spike with a solution containing 0.370 μg ^{201}Hg and 50 μg ^{198}Hg as a carrier. At the same time, mix an aliquot with a known volume of the natural mercury solution for future verification of the ^{201}Hg concentration in the spiking solution. The ^{201}Hg addition to the sample should be calculated to yield an altered isotope ratio of almost unity, which is desirable to minimize the effect of photographic emulsion calibration errors. After a preliminary spiking, the experimental procedure must be followed to determine the approximate mercury content. The general isotope dilution equation was used in these calculations[4, 5].

After assembling the apparatus with water flowing through the condenser, and adding 20 ml of 8 *M* nitric acid to the sample through the condenser, heat the flask gently until the initial reaction subsides. Add 20 ml of nitric acid–perchloric acid (1 + 1) through the condenser, and heat the flask and side tube of the reflux collector to accumulate the acid condensate in the collector. When the organic material in the flask has been oxidized, allow the acid in the collector to flow back into the cooled flask. Add several portions of water through the con-

denser, swirl the collector, and allow the water to flow into the flask. Then remove the collector and attach the flask to the condenser. After draining the condenser water, heat the flask to distil the acid through the condenser until 1–2 ml of perchloric acid remains. Add *ca.* 5 ml of water in small portions through the condenser to the cooled flask. Transfer the solution to the electrolysis cell and electrolyze while stirring for *ca.* 16 h at an applied voltage of 2.2 V.

Spark the gold wire-cathodes in the mass spectrograph and prepare a graded series of exposures.

The ion-sensitive photographic plates (Ilford Q-2) were processed with the bleach and internal image developer MK-7 described by Cavard[10]. They were placed in the dichromate bleach for 4 min, rinsed in water for 0.5 min, developed for 7 min, fixed for 1 min, and washed for 15 min. The intensity-areas of ^{201}Hg and ^{202}Hg on the photographic plate were measured and the altered isotopic ratios were determined. The mercury concentrations were calculated from these ratios and other data, by means of the general isotope dilution equation.

For evaluation of the method blank, the entire analytical procedure was performed with the same quantities of acids and 100 mg of bovine liver, NBS-SRM 1577[3]. The liver sample, which has a mercury content approximately ten times lower than that of the orchard leaves, was used in simulating the spiking operation.

The solution that had been set aside for confirming the concentration of ^{201}Hg in the spiking solution was electrolyzed after adding a solution containing 50 μg of high-purity copper. The conditions for electrolysis were the same as described in the experimental procedure for the sample.

Losses of mercury in the mass spectrograph

Because of the low source-pressures that are routinely obtained in the mass spectrograph, the possibility of electrodeposited mercury on gold wire cathodes being lost through volatilization was investigated. A solution of mercury and copper, both present in approximately the same amounts as found in a 5-g sample of orchard leaves, was spiked with radioactive ^{203}Hg and electrolyzed with gold wire cathodes as in the chemical procedure. The wires were loaded into the mass spectrograph, which was evacuated for the same period used in a normal analysis. The unsparked wires were removed from the instrument, counted, and found to have greater than 95% of the original activity. These results indicated that no significant mercury loss occurred from the electrodes while they were in the evacuated instrument.

Recovery of mercury in the chemical procedure

A 5-g sample was spiked with radioactive ^{203}Hg and a solution containing 50 μg of natural mercury – the amount of ^{198}Hg carrier added in the procedure. After assembling the apparatus, the analytical procedure was followed to the point of oxidizing the sample and allowing the accumulated acid in the reflux collector to flow back into the flask. The nitric acid from the bubbler was counted with a single-channel scintillation γ-counter. No activity above background was found, indicating that ionic mercury was not lost through the bubbler during oxidation.

At this stage in the actual analytical procedure, the mercury would have been

equilibrated and losses would not invalidate the results. The trace experiment was then continued. After evaporation of the acid through the condenser and addition of water to the flask, the activity of the solution in the flask was counted. The results indicated that over 90% of the mercury remained in the flask at this stage.

RESULTS AND DISCUSSION

In the procedure, separation of most of the acid from the equilibrated mercury, although time-consuming, does not require much attention. If necessary, the time for this step could be decreased by leaving the apparatus in Fig. 1 assembled after the wet-oxidation step, heating the flask, and collecting 20 ml of the distillate through the stopcock at the side of the collector. However, by using radioactive mercury, it was found that further distillation resulted in appreciable loss of mercury; approximately 65% of the total mercury has been lost when 1–2 ml of perchloric acid remained in the flask. Therefore, when 20 ml of distillate has been removed, the distillation should be continued through the packed condenser as before.

The individual mercury concentrations are listed in Table I in the order they were determined. They were corrected for the moisture content and the method blank, 0.004 μg. The second and third determinations were made by spiking

TABLE I

MERCURY CONTENT OF ORCHARD LEAVES, SRM 1571, DETERMINED BY ISOTOPE DILUTION AND SPARK-SOURCE MASS SPECTROMETRY

Determination	*Concentration in μg g^{-1} (p.p.m.)*
1	0.133
2	0.131
3	0.144
4	0.134
5	0.142
6	0.160
	Average concentration 0.141
	95% Confidence limits ±0.009

TABLE II

COMPARISON OF MERCURY RESULTS BY ISOTOPE DILUTION WITH OTHER ANALYTICAL METHODS FOR ORCHARD LEAVES, SRM 1571

Average concentration and 95% confidence limits in μg g^{-1}	*Number of determinations*	*Method*	*Lab*
0.141±0.009	6	Isotopic dilution	NBS
0.160±0.012	15	Atomic absorption	NBS
0.155±0.006	11	Neutron activation	NBS
0.145±0.014	5	Neutron activation	A
0.148±0.010	4	Neutron activation	B

the solutions from the wet-oxidation step to determine whether this change would affect the equilibration and results. These determinations were compatible with the other results obtained by spiking the samples.

The Dixon Criterion[11] was used to reject an aberrant value, 0.199 $\mu g\ g^{-1}$, which may have been caused by contamination; its inclusion would have resulted in an average concentration and 95% confidence limits of $0.149 \pm 0.018\ \mu g\ g^{-1}$ instead of $0.141 \pm 0.009\ \mu g\ g^{-1}$ listed in Table II. Independent results obtained by atomic absorption and neutron activation are also shown in this table. A consideration of methods and data led to a certified value of $0.155 \pm 0.015\ \mu g\ g^{-1}$ for the mercury content of the Orchard Leaves, SRM 1571.

The author gratefully acknowledges the assistance rendered by P. J. Paulsen in performing the mass spectrographic measurements and by H. L. Rook in evaluating possible losses of mercury in the mass spectrograph.

SUMMARY

A stable isotope dilution procedure in conjunction with the spark source mass spectrograph was developed for determining sub-$\mu g\ g^{-1}$ concentrations of mercury in orchard leaves. A 5-g sample was spiked with a solution of mercury, isotopically enriched in ^{201}Hg and ^{198}Hg. The ^{198}Hg served as a carrier. After wet-ashing the sample with nitric and perchloric acids under reflux and distilling most of the acid, the isotopically equilibrated mercury was electrodeposited onto high-purity gold wires for sparking in the mass spectrograph. The concentration was calculated from the altered isotope ratio, $^{201}Hg/^{202}Hg$, and other data. The results were compared with those obtained by atomic absorption spectrometry and neutron activation, leading to a certified value of $0.155 \pm 0.015\ \mu g\ g^{-1}$ for the mercury content of Orchard Leaves, SRM 1571 of the National Bureau of Standards.

REFERENCES

1 H. J. M. Bowen, *Analyst (London)*, 92 (1967) 124.
2 A. Weissler, *Environ. Res.*, 4 (1971) 53.
3 *Catalog of Standard Reference Materials, NBS Special Publication 260*, April 1973, Office of Standard Reference Materials, National Bureau of Standards, Washington, D.C. 20234, April 1973. (Available from the Superintendent of Documents, U.S. Government Printing Office, Washington, D.C. 20402.)
4 R. Alvarez, P. J. Paulsen and D. E. Kelleher, *Anal. Chem.*, 41 (1969) 955.
5 P. J. Paulsen, R. Alvarez and D. E. Kelleher, *Spectrochim. Acta, Part B*, 24 (1969) 535.
6 P. J. Paulsen, R. Alvarez and C. W. Mueller, *Anal. Chem.*, 42 (1970) 673.
7 E. C. Kuehner, R. Alvarez, P. J. Paulsen and T. J. Murphy, *Anal. Chem.*, 44 (1972) 2050.
8 P. O. Bethge, *Anal. Chim. Acta*, 10 (1954) 317.
9 R. K. Munns and D. C. Holland, *J. Ass. Offic. Anal. Chem.*, 54 (1971) 202.
10 A. Cavard in E. Kendrick (Ed.), *Advances in Mass Spectrometry*, The Institute of Petroleum, London, 1968, pp. 419–429.
11 M. G. Natrella, *Experimental Statistics, National Bureau of Standards Handbook 91*, Washington, D.C., 1963, Section 17-3.

Analytica Chimica Acta, 73 (1974) 39–48

CONTRÔLE DE LA PURETÉ D'ÉCHANTILLONS DE NIOBIUM ET DE TANTALE PAR SPECTROMÉTRIE GAMMA DIRECTE APRÈS IRRADIATION AU MOYEN DE PROTONS DE 10 MeV

J. N. BARRANDON, P. BENABEN, J. L. DEBRUN et M. VALLADON

Groupe d'Application des Réactions Nucléaires à l'Analyse Chimique, Service du Cyclotron, Centre National de la Recherche Scientifique 45045 Orléans Cedex (France)

(Reçu le 19 avril 1974)

Du fait de leur utilisation dans l'industrie nucléaire, le génie chimique et l'électronique, le niobium et le tantale sont deux métaux très importants dans l'industrie moderne et il est nécessaire de disposer de méthodes permettant d'effectuer leur analyse et de contrôler leur pureté. En effet, la concentration en impuretés (surtout interstitielles) a une influence sur les propriétés mécaniques de ces métaux ainsi que sur d'autres propriétés comme la supraconductivité du niobium. Actuellement, les impuretés majeures, outre l'oxygène, l'azote et le carbone, sont les métaux réfractaires qui les suivent au cours de beaucoup de leurs processus de purification. Rappelons aussi que Nb et Ta sont toujours associés dans leurs minerais (niobiotantalates), et qu'en conséquence le niobium contient du tantale et réciproquement.

Il ne sera pas question ici du dosage des éléments O, C et N, qui peut d'ailleurs être aisément réalisé par activation, mais qui relève d'autres modes d'irradiation utilisant les hélions-3 et les photons.

Il est bien connu que l'analyse par activation neutronique classique, nécessite des séparations chimiques très élaborées dans le cas du tantale, du fait de la forte radioactivité induite à partir de cet élément[1]. Le niobium par contre, possède des caractéristiques nucléaires favorables et plusieurs auteurs décrivent le dosage dans ce métal, d'une ou de plusieurs impuretés sans séparations chimiques et directement après activation dans les neutrons thermiques[2]; il s'agissait cependant du dosage d'un petit nombre d'impuretés à la fois. Nous proposons ici une méthode d'activation qui permet de doser simultanément et directement deux impuretés métalliques majeures de Ta et de Nb, tout en déterminant en même temps les niveaux maxima de concentration d'une trentaine d'autres éléments non décelables dans nos conditions expérimentales. Il s'agit de l'activation au moyen de protons de 10 MeV, méthode que nous avons déjà employée avec succès pour l'analyse d'autres métaux tels que Ag, Al, Au, Co, Ir et Rh[3–6]; les réactions utilisées sont les réactions (p, n). Signalons l'utilisation dès 1962 par Tomita et Saisho[7], de l'activation par les protons pour le dosage du niobium dans le tantale; il s'agissait d'irradiations à 14,5 MeV et il était procédé à une séparation chimique de ^{93m}Mo obtenu à partir de ^{93}Nb.

PARTIE EXPÉRIMENTALE

Irradiations

Nous avons utilisé le cyclotron à énergie variable du Service Hospitalier

F. Joliot à Orsay. Les protons accélérés ont une énergie initiale de 11 MeV qui est réduite à 10 MeV après la traversée de diverses feuilles minces métalliques, ainsi que le montre la Fig. 1. Le titane constitue la fenêtre par laquelle les protons quittent le vide du cyclotron; la feuille de havar (alliage constitué principalement de Fe, Co, Ni, Cr, W) sert de moniteur de flux grâce à la réaction $^{56}Fe(p, n)^{56}Co$; l'aluminium empêche un contact direct entre le moniteur et l'échantillon.

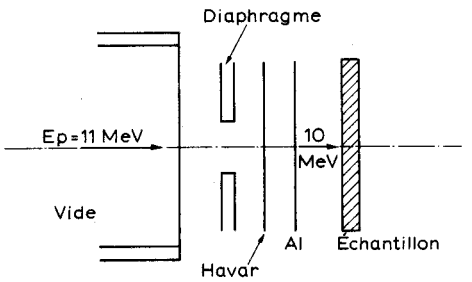

Fig. 1. Irradiations.

Tantale et niobium ont été irradiés à une intensité de l'ordre de 1,5 μA et les temps d'irradiations ont varié de 30 à 60 min.

Mesures radioactives

Les échantillons sont très légèrement décapés après irradiation, de façon à éliminer les contaminations de surface sans introduire d'erreur mesurable dans le dosage. Ils sont ensuite enveloppés dans une feuille d'une vingtaine de microns d'aluminium et prêts à être comptés. Les mesures sont effectuées à l'aide d'une chaîne de spectrométrie γ comprenant les éléments suivants:

(a) Détecteur Ge(Li): ce détecteur possède une résolution de 2,7 KeV ainsi qu'un rapport pic sur Compton de 34 et une efficacité de 22%, ceci étant relatif à la raie à 1332,5 KeV de ^{60}Co et l'efficacité étant mesurée en comparaison avec celle d'un cristal NaI (Tl) de 75×75 mm.

(b) Analyseur: 4000 canaux avec sortie de résultats sur bande magnétique ou imprimante rapide.

Précautions à prendre lors des mesures

L'activation au moyen de particules chargées pose un problème un peu particulier car, du fait de la pénétration limitée des particules (200 et 300 μm dans Ta et Nb respectivement) et de l'épaisseur des échantillons qui atteint couramment plusieurs millimètres, il existe une "face irradiée" et une "face non irradiée". Pour éviter des erreurs systématiques dûes à l'absorption des rayons-γ et à des géométries de comptage légèrement différentes, il convient de repérer la face irradiée (par exemple) et de compter les étalons épais (nous utilisons la méthode de la section efficace moyenne[8]) et les échantillons, la face irradiée tournée vers le détecteur. Etant donné que les profondeurs de pénétration vont de 620 μm pour Al à 200 μm pour Ta et que ce sont deux cas extrêmes, on peut alors considérer que les conditions de géométrie sont les mêmes d'autant plus que la surface irradiée est faible (*ca.* 0,5 cm^2) et que les dimensions de notre détecteur Ge(Li) sont importantes. En outre,

le parcours activable est encore plus faible que le parcours réel des particules, et en travaillant à 10 MeV la majorité de l'activité se trouve concentrée dans les 130 premiers μm pour Ta ou les 400 premiers μm pour Al.

L'activité diminue très vite au fur et à mesure que les particules pénètrent dans l'échantillon, les maxima des courbes de section efficace des réactions (p, n) se trouvant en général situés entre 10 et 15 MeV. Le fait que l'activation s'étende sur une assez faible profondeur et soit surtout concentrée vers la surface explique que nous ayons constaté qu'aucune correction d'absorption n'était nécessaire, compte-tenu des autres causes d'erreurs, pour les énergies-γ supérieures ou égales à 150 KeV et pour la grande majorité des matrices. Pour certaines matrices très absorbantes comme Au et Pb des erreurs systématiques de quelques pour cent existent même jusqu'à 200–250 KeV et doivent être corrigées.

D'autres problèmes se posent pour les mesures.

Tantale. Une forte radioactivité provenant principalement des réactions $^{16}O(p, \alpha)^{13}N$, $^{13}C(p, n)^{13}N$ et $^{14}N(p, \alpha)^{11}C$ se manifeste sous la forme d'un pic-γ à 511 KeV très important, car ^{13}N et ^{11}C sont des émetteurs β^+ et les trois éléments ci-dessus s'activent fortement et sont présents à des teneurs de plusieurs parties par million et même plus. Il est nécessaire d'attendre environ 1 h avant l'effectuer des mesures valables, ou alors il faut éloigner l'échantillon du détecteur et se limiter à l'exploitation d'éventuelles raies-γ d'énergie nettement supérieure à 511 KeV; ceci implique un étalonnage pour la nouvelle position de comptage employée, ainsi qu'une perte de sensibilité. Il est certain que la spectrométrie-γ d'échantillons de tantale plus purs en C, N et O pourrait être faite immédiatement après irradiation et en plaçant ces échantillons directement sur le détecteur.

Niobium. Il est nécessaire d'attendre la décroissance de ^{93m}Mo produit par la réaction $^{93}Nb(p, n)^{93m}Mo$. Nous avons en effet mesuré qu'on obtenait $4{,}4 \cdot 10^8$ désintégrations par min en irradiant du niobium avec des protons de 10 MeV durant 1 h à un courant de 1 μA, et la réaction $^{93}Nb(p, n)^{93m}Mo$ est donc par ailleurs tout à fait intéressante pour doser le niobium[7,9]. Cependant la période de ^{93m}Mo n'est que de 6,9 h et la spectrométrie-γ directe de l'échantillon peut être effectuée dans d'excellentes conditions après plusieurs jours d'attente. De ce fait, plusieurs éléments ne donnant naissance qu'à des radioisotopes de périodes plus courtes ou proches de celle de ^{93m}Mo, ne peuvent pas être dosés (ex.: Ni, Ag).

Méthode de calcul

Les spectres sont enregistrés sur bande magnétique et sont traités automatiquement au moyen du programme Sampo[10] modifié dans notre laboratoire. Les teneurs sont calculées par la méthode de Ricci et Hahn[8] et à l'aide des tables donnant les parcours des particules dans la matière[11]. La formule donnant la teneur x en parties par million est:

$$x = \frac{(A_{\text{échantillon}})}{(A_{\text{étalon}})} \cdot \frac{(R_{\text{étalon}})}{(R_{\text{échantillon}})}$$

où R est le parcours, A l'activité, et où les activités sont mesurées dans des conditions identiques après des irradiations identiques, $A_{\text{étalon}}$ étant relative à 1 p.p.m. d'étalon. Nous avions au cours d'expériences antérieures[3] mesuré les activités spécifiques $(A_{\text{étalon}})$ relatives à l'irradiation d'une trentaine d'éléments dans les protons, et ceci nous

avait permis de doser ces éléments dans divers échantillons[4]. Ces expériences ont été reprises et complétées et nous possédons maintenant les valeurs de plus de 130 activités spécifiques correspondant à l'irradiation d'environ 55 éléments[12]. Ces valeurs ainsi qu'une bibliothèque de raies-γ seront prochainement combinées avec le programme Sampo de manière à effectuer une analyse entièrement automatique.

RÉSULTATS ET DISCUSSION

Tantale

Le métal analysé est un produit industriel de la firme Hoboken (Reframet). Nous avons volontairement limité le nombre d'éléments recherchés, en éliminant en particulier les terres rares: de ce fait les tableux I et III contiennent des résultats pour 34 éléments seulement. Seuls Nb et Mo ont été décelés et dosés; on peut voir sur la Fig. 2 les 3 pics de ^{93m}Mo provenant du niobium et des pics correspondant à ^{94}Tc, ^{95}Tc et ^{96}Tc. On aperçoit sur le spectre, les pics de ^{182}Ta qui est produit à partir de la matrice de tantale par capture des neutrons secondaires créés par les réactions (p, n). Nous avions déjà noté ce phénomène lors de l'analyse d'échantillons de Ag, Al et Co (ref. 4) où les neutrons secondaires produisent des réactions (n, p) et (n, α) en plus des (n, γ). La figure 2 correspond à une mesure effectuée après plusieurs heures de refroidissement et la diminution déjà très importante du pic à 511 KeV permet de bien apercevoir les pics de basse énergie des radioisotopes provenant de Mo et de Nb, et permet d'observer les pics de basse énergie de ^{182}Ta.

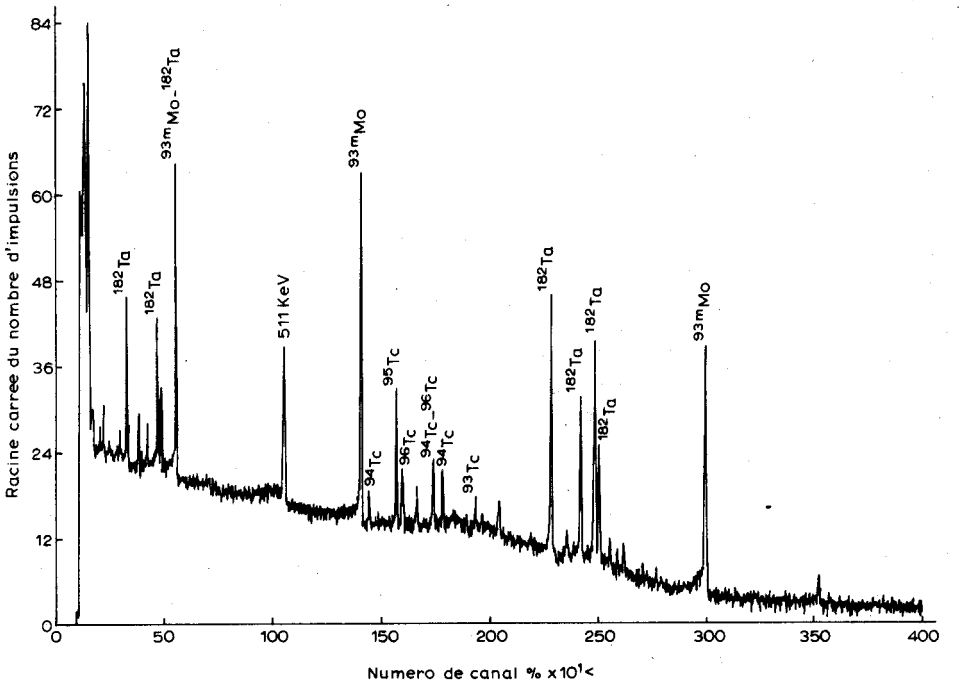

Fig. 2. Spectre du tantale. Comptage 5 h, refroidissement 3,4 h.

Remarquons sur le Tableau I, que malgré la présence de ^{182}Ta, de 40 p.p.m. de niobium et de 2 p.p.m. de molybdène, 26 limites sont inférieures ou égales à 1 p.p.m. Ces limites sont élevées pour la plupart des éléments lourds (Ba, Re, Ir, Au, Hg...), car ils s'activent moins que les éléments légers à 10 MeV étant donné l'existence de la barrière de Coulomb, ceci est valable en règle générale.

TABLEAU I

LIMITES EXPÉRIMENTALES[a] OBTENUES POUR LE DOSAGE D'IMPURETÉS DANS Ta ET Nb

(Irradiation de 1 h à 1.5 μA)

Elément dosé par réaction (p, n)	*Tantale*		*Niobium*	
	Radioisotopes utilisés	*Limite supérieure de concentration en p.p.m. (en poids)*	*Radioisotopes utilisés*	*Limite supérieure de concentration en p.p.m. (en poids)*
Li	^{7}Be	$\leqslant$ 0,15	^{7}Be	$\leqslant$ 0,02
Ca	^{44}Sc	$\leqslant$ 0,05	^{48}Sc	$\leqslant$ 65
Ti	^{48}V	$\leqslant$ 0,07	^{48}V	$\leqslant$ 0,01
V	^{51}Cr	$\leqslant$ 0,3	^{51}Cr	$\leqslant$ 0,05
Cr	^{52m}Mn	$\leqslant$ 0,01	^{52}Mn	$\leqslant$ 0,2
Fe	^{56}Co	$\leqslant$ 0,4	^{56}Co	$\leqslant$ 0,2
Ni	^{60}Cu	$\leqslant$ 0,04	—	—
Cu	^{63}Zn	$\leqslant$ 0,05	^{65}Zn	$\leqslant$ 2
Zn	^{66}Ga	$\leqslant$ 0,09	^{67}Ga	$\leqslant$ 1,5
Ga	^{69}Ge	$\leqslant$ 0,03	^{69}Ge	$\leqslant$ 0,15
Ge	^{72}As	$\leqslant$ 0,1	^{72}As	$\leqslant$ 0,04
As	^{75}Se	$\leqslant$ 0,4	^{75}Se	$\leqslant$ 0,02
Se	^{80}Br	$\leqslant$ 0,07	^{82}Br	$\leqslant$ 0,4
Br	^{79}Kr	$\leqslant$ 0,1	^{79}Kr	$\leqslant$ 0,5
Rb	^{87m}Sr	$\leqslant$ 0,08	—	—
Sr	^{86}Y	$\leqslant$ 0,2	^{86}Y	$\leqslant$ 0,04
Zr	^{90}Nb	$\leqslant$ 0,04	^{96}Nb	$\leqslant$ 3,8
Ru	^{99m}Rh	$\leqslant$ 0,5	^{100}Rh	$\leqslant$ 1,5
Pd	^{104}Ag	$\leqslant$ 0,1	^{105}Ag	$\leqslant$ 0,2
Ag	^{107}Cd	$\leqslant$ 11	—	—
Cd	^{113m}In	$\leqslant$ 0,3	^{111}In	$\leqslant$ 0,3
Sn	^{117}Sb	$\leqslant$ 0,3	^{122}Sb	$\leqslant$ 1,5
Sb	^{121}Te	$\leqslant$ 0,9	^{121}Te	$\leqslant$ 1
Te	^{130}I	< 0,7	^{124}I	< 0,6
I	^{127}Xe	$\leqslant$ 0,3	^{127}Xe	$\leqslant$ 0,05
Ba	^{135}La	$\leqslant$ 25	—	—
W	^{184}Re	$\leqslant$ 8	—	—
Re	^{185}Os	$\leqslant$ 4,5	^{185}Os	$\leqslant$ 0,6
Ir	^{191}Pt	$\leqslant$ 4,5	^{191}Pt	$\leqslant$ 20
Pt	^{194}Au	$\leqslant$ 0,6	^{194}Au	$\leqslant$ 2,5
Au	^{197m}Hg	$\leqslant$ 10	^{197m}Hg	$\leqslant$ 70
Hg	^{198}Tl	$\leqslant$ 1,5	^{200}Tl	$\leqslant$ 2
Tl	^{203}Pb	$\leqslant$ 0,6	^{203}Pb	$\leqslant$ 2,5
Pb	^{206}Bi	$\leqslant$ 2	^{206}Bi	$\leqslant$ 5

[a] La limite de détection expérimentale est calculée en prenant 3 fois la racine du total des impulsions de la portion de spectre située dans la bande d'énergie où le pic-γ recherché devrait être présent.

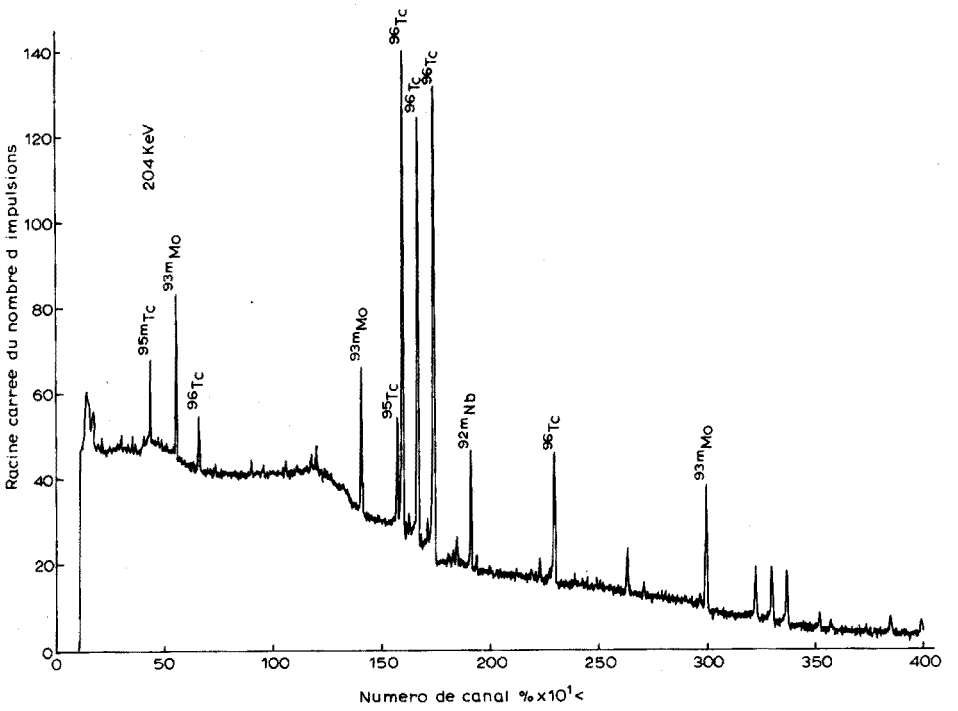

Fig. 3. Spectre du niobium. Comptage 20 h, refroidissement 5 jours.

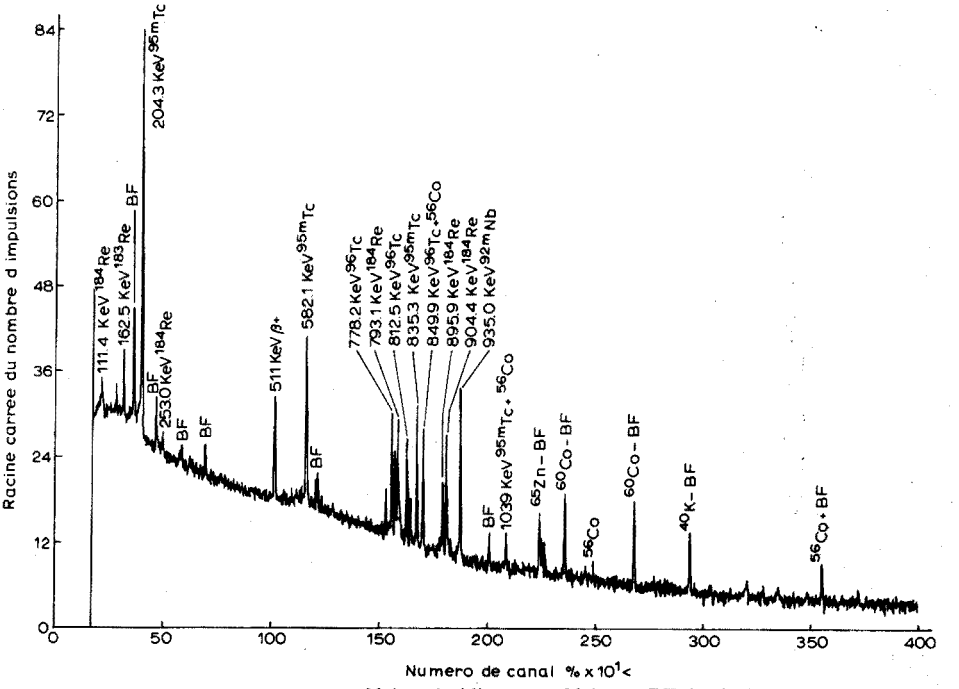

Fig. 4. Spectre du niobium. Comptage 92 h, refroidissement 32 jours. BF, bruit de fond.

Il est raisonnable de penser que beaucoup des impuretés recherchées ont une concentration très faible dans le tantale étant donné son mode de purification à haute température et leur faible abondance dans les minerais de départ. Notons que la méthode n'est pas assez sensible pour doser ici le tungstène qui doit cependant être présent dans l'échantillon au niveau de la partie par million.

Niobium

Le métal provient aussi de la firme Hoboken (Reframet). Seuls Mo et W ont été décelés et dosés. Ils sont présents en quantité importante (70 p.p.m.). La présence de fer est fortement probable car tous les pics de ^{56}Co sont présents; néanmoins étant donné la présence d'interférences sur les pics à 846,7 KeV, 1037,5 KeV et 1237,6 KeV, une certitude de la présence du fer nécessite ici de suivre la décroissance de ces pics, ce que nous n'avons pas fait. Du fait de la forte concentration en molybdène et du temps nécessaire à la décroissance de ^{93m}Mo, 16 limites de détection seulement sont inférieures à la partie par million contre 26 dans le tantale. Remarquons sur la Fig. 3 les importants pics de ^{95}Tc et ^{96}Tc, ainsi que les trois pics caractéristiques de ^{93m}Mo. Sur la Fig. 4 on peut voir les pics de ^{183}Re et ^{184}Re, les radioisotopes provenant du tungstène; notons aussi les pics de ^{95m}Tc et ^{96}Tc provenant du molybdène. Le pic à 935 KeV est dû à ^{92m}Nb obtenu soit par les réactions ^{93}Nb(p, pn)^{92m}Nb et ^{93}Nb(p, d)^{92m}Nb, soit par la réaction ^{93}Nb(n, 2n)-^{92m}Nb.

On pourrait penser que dans le cas du niobium, l'analyse par activation neutronique possède des performances bien supérieures à celles de l'activation protonique: nous avons vérifié qu'il n'en était rien en irradiant avec des neutrons thermiques, un échantillon de niobium provenant du même lot que celui qui avait été irradié dans des protons. En effet, il s'avère qu'en plus de tungstène qui s'active déjà fortement, le niobium contient beaucoup de tantale (150 p.p.m. dans notre cas). Les limites de détection des autres impuretés sont fortement rehaussées par la présence de W et Ta. On peut cependant voir dans le Tableau II que certaines impuretés seront dosées avec beaucoup plus de sensibilité avec les neutrons (Na, Au, Hg) alors qu'il vaut mieux utiliser les protons pour d'autres (Cr, Ge, Zr, Cd). Les quelques exemples rassemblés dans le Tableau II montrent qu'en réalité les deux méthodes sont ici complémentaires. Notons enfin que le molybdène est difficile à doser par activation neutronique à cause de la forte radioactivité obtenue à partir du tungstène et du tantale, qui eux sont dosés dans d'excellentes conditions. Inversément, l'activation protonique est à recommander pour le dosage du molybdène, alors que ses performances sont médiocres dans le cas du tungstène (à 10 MeV) et qu'elle ne permet pas de doser le tantale.

Influence de l'énergie d'irradiation

Les dosages ont été effectués à 10 MeV car nos mesures d'activités spécifiques ont été faites à cette énergie. Nous avions au départ choisi 10 MeV car c'est une énergie qui permet de doser beaucoup d'éléments par spectrométrie-γ directe, dans plusieurs matrices différentes, avec une bonne sensibilité et sans interférences. Une énergie plus élevée aurait réduit considérablement le nombre de ces matrices car les réactions (p, pn) commencent à être visibles vers 10 MeV et deviennent très importantes audelà de 10 MeV. En conséquence une activité forte et le plus souvent durable

TABLEAU II

COMPARAISON DES SENSIBILITÉS OBTENUES PAR ACTIVATION NEUTRONIQUE ET PAR ACTIVATION PROTONIQUE, POUR LE DOSAGE DE QUELQUES ÉLÉMENTS DANS LE NIOBIUM

(Présence de 150 p.p.m. de tantale dans le niobium; résultats en p.p.m.-poids.)

Eléments	*Neutrons thermiques 30 min, $4 \cdot 10^2$ n cm^{-2} s^{-1}*	*Protons de 11 MeV, 1 h, 1,5 μA*
Na	< 0,003	Non dosable
Cr	< 21	< 0,25
Zn	< 2	< 1,5
Ga	< 0,1	< 0,15
Ge	< 8	< 0,04
Zr	< 54	< 3,8
Cd	< 15	< 0,3
Sb	< 0,08	< 1
Hf	< 0,25	—
Au	< 0,006	< 70
Hg	< 0,03	< 2,2

aurait été induite à partir des matrices étudiées, interdisant tout dosage direct (ex: $^{59}Co(p, pn)^{58}Co^* - {}^{93}Nb(p, pn)^{92}Nb^*$). Inversement, plus l'énergie est basse, plus les sensibilités sont mauvaises, l'activité obtenue étant de plus en plus faible.

Il est certain que dans le cas du tantale l'énergie des protons pourrait être plus élevée, car ce métal s'active très peu, même à 15 MeV; les sensibilités seraient alors meilleures, surtout pour les éléments lourds[13]. Des interférences par réactions (p, pn) et (p, α) seraient alors à craindre pour certains éléments légers. Pour le niobium, l'énergie choisie est optimale puisque la réaction $^{93}Nb(p, pn)^{92m}Nb^*$ (ou (p, d)) n'est vraiment sensible qu'à partir de 10 MeV[9]. On peut d'ailleurs remarquer sur la Fig. 4 que le pic à 935 KeV de ^{92m}Nb est du même ordre d'importance que les pics dûs aux impuretés alors que ce radioisotope provient de la matrice elle-même.

Précision, justesse et sélectivité des dosages

Dans le Tableau III, les résultats pour les éléments détectés et dosés sont accompagnés de la déviation standard sur 6 dosages. Cette déviation standard est d'environ 4% pour 40 p.p.m. de Nb et de 7% pour 2 p.p.m. de Mo dans le tantale. Elle est de 3,3% pour 72 p.p.m. de Mo et de 8% pour 72 p.p.m. de W dans le niobium.

Nous n'avons pas de données en ce qui concerne la justesse de la méthode appliquée au tantale et au niobium; elle n'aurait pu être testée qu'en effectuant des intercomparaisons avec d'autres méthodes analytiques ou en utilisant des étalons certifiés. Le seul recoupement effectué l'a été pour le niobium lors de la détermination des quelques limites regroupées dans le Tableau II. Les teneurs en W et Mo mesurées par activation neutronique sont 20% inférieures à celles mesurées par activation protonique. Cette différence est plus importante que celle qui a pu être observée dans d'autres cas où des comparaisons ont pu être faites avec d'autres méthodes.

En ce qui concerne la sélectivité, deux facteurs entrent en jeu: les interférences nucléaires et les interférences dues à l'existence de raies-γ identiques pour

LEAU III

URETÉS DÉTECTÉES DANS Nb ET Ta, ET ÉVALUATION DES LIMITES DE DÉTECTION EXPÉRI-NTALES CORRESPONDANTES

Tantale			*Niobium*		
Radio-isotopes utilisés	*Teneur[a] en p.p.m.-poids*	*Limite de détection expéri-mentale[b] en p.p.m.-poids*	*Radio-isotopes utilisés*	*Teneur[a] en p.p.m.-poids*	*Limite de détection expéri-mentale[b] en p.p.m.-poids*
^{93m}Mo	38,7 ± 1,6	0,4			
^{94}Tc ^{95}Tc ^{96}Tc	2,1 ± 0,14	0,07	^{95}Tc ^{96}Tc	71,5 ± 2,4	0,2
			^{183}Re ^{184}Re	72 ± 6	1,7

eur moyenne et déviation standard sur 6 dosages.
culée en prolongeant sous les pics détectés, le bruit de fond qui existe de part et d'autre, et en prenant 3 fois la ine de la somme des impulsions dans la bande d'énergie correspondante.

des radioisotopes différents. Nous avons vérifié[3,12] qu'à 10 MeV il n'existe qu'une seule possibilité de réactions nucléaires concurrentes: il s'agit de ^{7}Li(p, n)^{7}Be et ^{10}B(p, α)^{7}Be. Le dosage du lithium est donc le seul qui ne soit pas sélectif puisque dans ce cas ^{7}Be est le seul radioisotope vraiment utilisable. Dans tous les autres cas où une réaction (p, α) interfère avec une réaction (p, n), il est possible de trouver une autre (p, n) sélective. Enfin, aucune réaction (p, pn) ou (p, d) ne peut fausser un dosage de façon mesurable, à moins que les rapports des impuretés sur lesquelles se font les réactions (p, n) et (p, pn) ne soient dans un rapport de 10^5 à 10^6. Par exemple, ^{92m}Nb produit par (p, pn) + (p, d) (peut être aussi par ^{93}Nb(n, 2n)^{92m}Nb) sur ^{93}Nb qui est la matrice, a une activité qui correspond à 9 p.p.m. de zirconium par ^{92}Zr(p, n)^{92m}Nb. En fait dans la plupart des cas, cette interférence n'est même pas gênante car il existe d'autres (p, n) utilisables: pour le zirconium par exemple on peut utiliser ^{90}Zr(p, n)^{90}Nb ou ^{96}Zr(p, n)^{96}Nb.

Quant aux interférences dûes à des coïncidences de raies-γ, il existe de nombreuses possibilités de les éliminer en effectuant des recoupements grâce aux autres raies-γ et aux périodes radioactives. Le dosage du molybdène par exemple est effectué sur 3 radioisotopes et 8 raies-γ. L'analyse par activation protonique à 10 MeV est donc très sélective.

CONCLUSIONS

L'activation protonique appliquée à l'analyse d'échantillons de tantale et de niobium est une méthode permettant de contrôler très facilement et très sûrement la pureté de ces métaux en ce qui concerne de nombreux éléments. Il est possible d'améliorer les résultats obtenus, du point de vue des sensibilités expérimentales, en utilisant des courants plus intenses et des temps d'irradiation plus longs car les impuretés principales Nb et Mo (W s'active assez peu) conduisent à des radio-isotopes de périodes relativement courtes. Dans le cas du tantale, les sensibilités pourront également être améliorées en augmentant l'énergie d'irradiation.

Pour le niobium, l'analyse protonique doit être complétée par une analyse neutronique par exemple, de façon à doser aussi le tantale qui est présent à grandes concentrations dans ce métal (150 p.p.m. dans notre cas).

Il existe peu de méthodes analytiques utilisables pour le dosage de traces et qui puissent être mises en oeuvre sans séparations chimiques, pour de nombreux éléments simultanément. Celles qui existent posent de difficiles problèmes d'étalonnage (spectrométrie d'émission et spectrométrie de masse), et de reproductibilité (spectrométrie de masse). Elles sont par ailleurs limitées en sensibilité pour certains éléments, de même que l'activation protonique l'est à 10 MeV pour la plupart des éléments lourds.

Si nous considérons les grandes sensibilités obtenues pour beaucoup d'éléments, la sélectivité et la facilité de mise en oeuvre, il semble que l'activation protonique soit particulièrement intéressante dans le cas de l'analyse du tantale et du niobium.

RÉSUMÉ

Nous avons analysé des échantillons de tantale et de niobium par activation au moyen de protons de 10 MeV et spectrométrie-γ directe après irradiation. Dans les conditions opératoires nous avons détecté et dosé Nb et Mo dans le tantale ainsi que Mo et W dans le niobium. Pour une trentaine d'autres éléments qui n'ont pas été détectés, nous avons établi des limites supérieures de concentration qui sont en majorité inférieures à la partie par million et qui atteignent même 1/10 et 1/100 de partie par million.

SUMMARY

Non-destructive analysis of samples of niobium and tantalum has been achieved by activation with 10-MeV protons and γ-ray spectrometry. Niobium and molybdenum have been detected and determined in tantalum, as well as molybdenum and tungsten in niobium. Upper limits of concentration have been established for over thirty other undetected elements; most of these limits are below the p.p.m. level, and some reach the p.p.b. level.

REFERENCES

1 G. Auboin, F. Dugain et J. Laverlochere, *Bull. Soc. Chim. Fr.*, 2 (1965) 547.
2 J. F. Emery, W. T. Mullins, L. C. Bate et J. W. Leddiccotte, *TID—7629*, (Oct. 1961) 239; F. Dugain et J. Laverlochere, *Anal. Chem.*, 37 (1965) 998.
3 J. L. Barrandon, J. L. Debrun et A. Kohn, *J. Radioanal. Chem.*, 16 (1973) 617.
4 J. L. Debrun et J. N. Barrandon, *J. Radioanal. Chem.*, 17 (1973) 291.
5 J. N. Barrandon, J. L. Debrun et M. Hours, Communication au Congrès International sur *L'application des Méthodes Nucléaires dans le domaine de l'art et l'archéologie*, Rome–Venise, 24–29 mai, 1973.
6 J. N. Barrandon, J. L. Debrun, P. Benaben et C. Rouxel, *Annales du Laboratoire de Recherche des Musées de France*, 1973, pp. 59–63.
7 I. Tomita et H. Saisho, *Nature (London)*, 195 (1962) 1189.
8 E. Ricci et R. L. Hahn, *Anal. Chem.*, 37 (1965) 742.
9 J. L. Debrun, J. N. Barrandon et Ph. Albert, *Ann. Chim. (Paris)*, (1970) T. 5, 357.
10 J. T. Routti et S. G. Prussin, *Nucl. Instr. Methods*, 72 (1969) 125.
11 C. S. Williamson, J. P. Bougeot et J. Picard, *Rapport C.E.A. R 3042*, 1966.
12 J. N. Barrandon, J. L. Debrun et P. Benaben, *Nucl. Inst. Meth.*, (soumis).
13 W. Krivan, D. L. Swindle et E. A. Schweikert, *Anal. Chem.*, (soumis).

Analytica Chimica Acta, 73 (1974) 49–52

THE DETERMINATION OF TRACES OF LEAD(II) BY SOLID-STATE LUMINESCENCE

D. E. RYAN, J. HOLZBECHER and H. ROLLIER

Trace Analysis Research Centre, Life Sciences Building, Dalhousie University, Halifax, Nova Scotia (Canada)

(Received 12th March 1974)

Solid-state luminescence of inorganic phosphors makes possible the determination of traces of heavy and paramagnetic metal ions which are not easily determined by solution fluorescence. Some of the factors involved have been discussed in a recent preliminary report[1] and the determination of bismuth(III) has also been described[2]. The present paper outlines the determination of lead in the range 5–2,000 ng ml^{-1}, after dissolution of practical samples, by co-precipitation with calcium oxalate, ignition to CaO:Pb phosphor, and measurement of its luminescence at 530 nm.

EXPERIMENTAL

Apparatus, reagents, solutions

All fluorimetric measurements were made with a Farrand VIS-UV Chromatogram Analyzer and with a Turner Model 111 Fluorimeter fitted with Camag TCL Scanner. The sample cell was a blackened aluminium sheet with drilled holes (diam. 5 mm) covered with a thin glass plate. The holes were packed with a sample powder which was held in place by masking tape.

A stock solution containing 1,000 μg Pb ml^{-1} was prepared from lead nitrate (Baker) and was standardized by EDTA titration with xylenol orange indicator[3]. Solutions of the desired concentrations were prepared by dilution of this stock solution. The calcium chloride (Baker) solution contained 50 g of the dihydrate per liter. The ammonium oxalate (Baker) was a solution of 50 g of monohydrate per liter. The "synthetic blood" solution contained major cations in concentrations given by Bowen[4].

Procedure

To 100 ml of solution containing 0.5–200 μg of lead, add 5 ml of (1+1) nitric acid followed by 5 ml of calcium chloride solution and 1 ml of ammonium oxalate solution*. Heat to 80°C, add a few drops of methyl red indicator, and precipitate by dropwise addition of (1+1) ammonia solution until the colour

* For analysis of practical samples in which relatively high concentrations of calcium may be expected, an excess of calcium is used for precipitation instead of the excess of oxalate employed in previous procedures[1,2].

changes from red to yellow (stir rapidly with a magnetic stirrer during precipitation). Allow to cool to room temperature (about 1 h) and filter through filter crucibles. Wash with distilled water and dry the precipitates at 200°C for 1 h. Transfer to microcrucibles and ignite at 850–900°C for 15 min; allow to cool to room temperature in a desiccator. Grind and mix the powders in an agate mortar, pack the cell and measure the luminescence. Settings of the Farrand instrument for highest sensitivity: λ_{ex}—350 nm, λ_{em}—530 nm, entrance slit removed, emission filter 8, aperture 0.75, photomultiplier RCA 1P21 with the slit removed, gain 10.0. For the Turner fluorimeter use excitation filter 7-60 and emission filter 8.

RESULTS AND DISCUSSION

The fluorescence intensity is a linear function of lead concentration from 0.5 to 200.0 μg. For higher lead concentrations there is no substantial increase in fluorescence intensity. A typical straight line for 2–50 μg of lead is shown in Fig. 1A; a calibration curve for lower lead concentrations (0.5–2.0 μg) is depicted in Fig. 1B.

The relative standard deviation of six determinations of 0.1 μg ml^{-1} was *ca.* 9%.

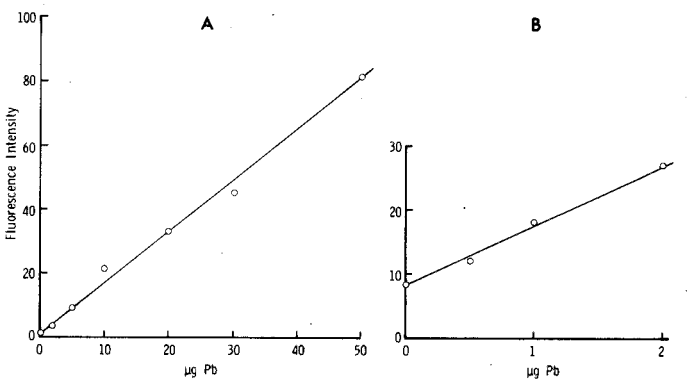

Fig. 1. Calibration curves for lead. (A) Photomultiplier slit inserted; (B) photomultiplier slit removed.

Factors affecting fluorescence

The optimal ignition temperature is 850–900°C for the time period of 15 min. Higher temperatures and longer periods of time cause lower fluorescence readings because of the lead volatilization, while lower temperatures or shorter time periods result in greyish coloured powders (carbon) and, therefore, lower fluorescence intensities[1]. The ignition loss of precipitate corresponds to complete conversion of calcium oxalate to calcium oxide[2].

The fluorescence intensity of ignited samples exposed to the atmosphere decreases with time, because of water adsorption and conversion to calcium hydroxide. When the CaO:Pb phosphor is left exposed overnight or longer, there is a complete loss of luminescence (*i.e.*, no difference from blank); re-ignition of the exposed sample for 5 min, however, restores the luminescence completely. When stored in a desiccator or in the sample cell, there is virtually no decrease in luminescence overnight.

Lead (10 μg in 100 ml of water) was successfully determined in the presence of a 100-fold weight excess of Al(III), Cr(III), Mg(II), Hg(II) or Zn(II); a ten-fold excess of Fe(III) and equivalent amounts of Cd(II), Cu(II) and Ag(I) were also without interference, but 10 μg of Co(II), Mn(II) and Ni(II) interfered seriously. Bismuth(III) was the only element of those tested to give fluorescence[2]; equivalent amounts did not interfere and when measurement was made at a longer emission wavelength (600 nm). bismuth could be tolerated at a ten-fold excess (the sensitivity of lead determination, however, was decreased by a factor of two).

APPLICATIONS

The method has been successfully applied to the direct determination of lead in leaves and in synthetic blood. Lead can also be determined in matrices containing interferences after separation by solvent extraction.

Leaves

Lead was determined in leaves after both dry and wet ashing procedures with excellent results. In the dry ashing procedure, the ground dry leaves were placed into platinum crucibles and ashed at 500°C in a muffle furnace for 4 h. The ash was dissolved in 5 ml of (1+1) nitric acid and the solution was then filtered through a filter crucible to remove any undissolved residue; the filtrate was diluted to 100 ml with water and the usual precipitation procedure was performed. The recovery of lead was checked by standard addition to 0.2 g of leaf samples which contained no measurable amounts of lead. The same results were obtained for leaf standards and for leaf samples with added lead; no lead was, therefore, lost during ashing and the leaf matrix was without interference.

The wet digestion was done by a modified Middleton and Stuckey method[5] in which no sulphuric acid is used. The sample was heated on a hot-plate with 10 ml of (1+1) nitric acid at 320°C (the temperature was checked with anhydrous sodium acetate, m.p. 324°C), evaporated to dryness and baked for 5 min. After cooling, 2 ml of 70% nitric acid was added and the solution was evaporated once again. This was twice repeated and the last organic residue was finally destroyed with 2 ml of 70% nitric acid and 1 ml of 60% perchloric acid. The colorless residue obtained was then dissolved in 5 ml of (1+1) nitric acid, the solution was diluted to 100 ml and the usual calcium oxalate precipitation was performed. Leaf samples known to contain lead were analyzed by standard addition and the lead content in ashed samples was also determined by atomic absorption. Two different leaf samples were found to contain 43 and 1,060 μg g^{-1} of lead; respective values obtained by atomic absorption were 43 and *ca.* 1,000 μg g^{-1}. Results obtained for another leaf sample, after both dry and wet ashing, were 284 μg g^{-1} and 281 μg g^{-1}, respectively. Errors arising from inhomogeneity of samples are minimized by ashing large sample sizes (*ca.* 0.5 g) and using aliquots after dissolution of the residue.

Synthetic blood

A 0.1 ml sample of synthetic blood (equal to 1 ml of blood) containing 1,990 μg Na, 1,690 μg K, 62 μg Ca, 41 μg Mg, 475 μg Fe(III), 13 μg Zn and

1 μg Cu was diluted to 100 ml with water. For additions of 0.5, 1.0 and 1.5 μg of lead, 0.4, 0.9 and 1.4 μg were found, respectively, with the Farrand instrument.

Larger samples (1 ml of synthetic blood) are required with the Turner instrument because of its lower sensitivity; higher concentrations of interfering ions, especially iron(III), are introduced, so that there is some coloration of the precipitate. By a re-precipitation procedure, however, satisfactory results are obtained. The initial calcium oxalate precipitate is dissolved with 5 ml of (1+1) nitric acid and, after dilution to 100 ml with water and addition of 5 ml of ammonium oxalate solution, the calcium oxalate is re-precipitated with ammonia.

Extraction

The extraction of lead into carbon tetrachloride with dithizone at pH 9.0–9.5 in the presence of ammonia, citrate, cyanide and hydroxylamine with subsequent re-extraction into dilute nitric acid eliminates a large number of interferences[6]. Virtually no difference in fluorescence intensity was found between samples (containing 0–10 μg of lead) carried through a simplified extraction procedure and then co-precipitated, and those subjected only to the regular co-precipitation procedure. In the simplified procedure the lead was twice extracted into the organic phase and twice back-extracted into the aqueous phase without any additional washing.

The method should find many more applications, apart from those described above, where high sensitivity is required (*e.g.*, water- or air-pollution analyses). Reliable dry and wet ashing procedures allow a simple determination of lead in biological materials.

This work was supported by a grant from the National Research Council of Canada.

SUMMARY

Microgram amounts of lead(II) are selectively determined by solid-state luminescence (λ_{ex}—350 nm, λ_{em}—530 nm) of CaO:Pb phosphor after co-precipitation with calcium oxalate and ignition at 850–900°C. Trace quantities of lead have been directly determined in leaves, after dry and wet ashing, and in synthetic blood.

REFERENCES

1 D. E. Ryan, R. J. Prime, J. Holzbecher and R. E. Young, *Anal. Lett.*, 6 (1973) 721.
2 D. E. Ryan, H. Rollier and J. Holzbecher, *Can. J. Chem.*, 52 (1974) 1942.
3 G. Schwarzenbach and H. Flaschka, *Complexometric Titrations*, Methuen, London, 1969, p. 299.
4 H. J. M. Bowen, *Trace Elements in Biochemistry*, Academic Press, London, 1966.
5 G. Middleton and R. E. Stuckey, *Analyst (London)*, 79 (1954) 138.
6 I. M. Kolthoff and P. J. Elving, *Treatise on Analytical Chemistry, Part II*, Vol. 6, Interscience, New York, 1964, p. 159.

Analytica Chimica Acta, 73 (1974) 53–59

NON-DESTRUCTIVE DETERMINATION OF SILICON IN ALUMINIUM–SILICON ALLOYS BY NEUTRON ACTIVATION ANALYSIS WITH A ^{227}Ac–Be ISOTOPE NEUTRON SOURCE

L. ALAERTS*, J. P. OP DE BEECK and J. HOSTE

Institute for Nuclear Sciences, Rijksuniversiteit Gent, Proeftuinstraat 86, B-9000 Gent (Belgium)

(Received 18th April 1974)

During the production of aluminium standard reference electrodes for spectrographic analysis with known concentrations of metals, difficulties arise with the homogeneity of the distribution of the metals, if silicon is present in concentrations of the order of 10%. A precise and fast method for the silicon determination is therefore very desirable.

The simultaneous determination of silicon and aluminium in ferrosilicon, containing *ca.* 75% Si and 1.5–3.5% Al, by double irradiation with an ^{227}Ac–Be isotopic neutron source, has already been described[1]; each pellet was irradiated twice at two different fast-to-thermal neutron flux ratios and after correction for the manganese activity induced by the reactions ^{56}Fe(n,p)^{56}Mn and ^{55}Mn(n,γ)^{56}Mn, it was possible to calculate the fraction of the activity due to, respectively, silicon and aluminium from the ^{28}Si(n,p)^{28}Al, ^{27}Al(n,γ)^{28}Al, and ^{27}Al(n,p)^{27}Mg reactions.

If the same method is used for the determination of silicon in binary Al–Si alloys containing 85–99% Al and 0.5–13.5% Si, it can readily be calculated that the precision is quite poor. In this work it will be shown that with a single irradiation under a cadmium shield at an irradiation position coinciding with the maximum of the fast flux gradient and after elimination of the ^{27}Mg activity by an adequate discriminator baseline setting in the counting equipment, silicon can be determined in Al–Si alloys with a precision better than 0.1% absolute.

Principle of the method

In Table I typical compositions for some Al–Si alloys are given. If such samples are exposed to a flux of both fast and thermal neutrons, several nuclear reactions give rise to measurable activities. The relevant data are listed in Table II. Among these reactions, the first is the one selected for the silicon determination, whereas reactions 4 and 5 are the main sources of interference which to a large extent are the limiting factor for the final precision. The (n,γ) reactions 4, 8, 9 and 10 can be practically completely suppressed by shielding the sample with a 1-mm cadmium cover and irradiating at the top of the fast flux gradient. By using a discriminator baseline setting corresponding to a cut-off below 1400 keV, all activity from reactions 2, 3 and 5 is eliminated, whereas activities from reactions 6 and 7 are greatly reduced. The remaining ^{24}Na activity is taken into account,

* Aspirant of the N.F.W.O.

TABLE I

CONCENTRATIONS IN PERCENT OF THE MOST IMPORTANT ELEMENTS PRESENT IN Al–Si ALLOYS

Sample	*Si*	*Fe*	*Cu*	*Mn*	*Mg*	*Zn*	*Ti*	*Cr*	*Ni*	*V*	*Ca*
Al–Si 1340	13.4	0.91	0.10	0.57	0.75	0.156	0.60	0.53			0.12
B. 05	13.0	0.15	0.01	0.015	0.01	0.05	0.02				
A. 05	10.8	0.35	0.02	0.35	0.006	0.07	0.01				
Al–Si 1000	10.0	0.29	0.035	0.22	0.22	0.054	0.007	0.009			0.035
Ac-800	7.95	0.14	0.010	0.054	0.45	0.097	0.15				
Ac 600/4	6.3	0.67	0.11	0.65	0.80	0.125	0.10	0.07	0.045		
Ac 450/1	4.65	0.42	0.030	0.39	0.44	0.032	0.025				
R 68/Ac 100	0.975	0.23	0.005	0.31	0.80	0.091					
6083/1	0.99	0.62	4.91	1.25	1.64	0.096	0.094	0.094	0.10		
R Al 50	0.50	0.54	0.040	0.038	0.033	0.079	0.048	0.036	0.040	0.046	

TABLE II

RELEVANT NUCLEAR REACTIONS

Reaction	*Abundance parent isotope (%)*	*Cross-section (mb)*[3,4]	*Half-life*[3]	*γ-Energies (keV)*[5]
1 $^{28}Si(n,p)^{28}Al$	92.21	2.0	2.240 min	1778.8
2 $^{29}Si(n,p)^{29}Al$	4.7	0.6	6.52 min	1273.3
3 $^{30}Si(n,\alpha)^{27}Mg$	3.09	0.1	9.45 min	843.8; 1014.4
4 $^{27}Al(n,\gamma)^{28}Al$	100	231	2.240 min	1778.8
5 $^{27}Al(n,p)^{27}Mg$	100	4.3	9.45 min	843.8; 1014.4
6 $^{27}Al(n,\alpha)^{24}Na$	100	0.65	15.02 h	1368.5; 2754.0
7 $^{56}Fe(n,p)^{56}Mn$	91.7	0.9	2.582 h	846.8; 1811.0;
8 $^{55}Mn(n,\gamma)^{56}Mn$	100	13300	2.582 h	2112.8
9 $^{63}Cu(n,\gamma)^{64}Cu$	69.1	4400	12.74 h	511.0; 1345.7
10 $^{65}Cu(n,\gamma)^{66}Cu$	30.9	2170	5.10 min	1039.0; 833.0; 1332.5

whereas the remaining ^{56}Mn activity is negligible. As a result, the total measured activity consists mainly of ^{28}Al activity from the silicon fraction of the sample, the remainder being ^{28}Al and a small amount of ^{24}Na activity solely from the aluminium fraction.

The specific activities from silicon and aluminium are determined once and for all for the given irradiation and counting conditions with the aid of high-purity elemental silicon and aluminium. However, as both silicon and aluminium give rise to the same isotope ^{28}Al, an iterative calculation procedure is required. The iteration converges rapidly even when a large fraction of the isotope arises from aluminium.

EXPERIMENTAL

The neutron source and counting equipment

For all irradiations, an annular ^{227}Ac–Be isotopic neutron source with a total neutron output of 10^8 ns^{-1} was used. The characteristics of this irradiation facility have been described elsewhere[2].

All measurements were carried out with a 7.5 × 7.5 cm NaI(Tl) detector with a well of 3.3 cm diameter and 4.3 cm depth. The detector assembly was coupled to a Canberra model 1418 Amplifier and a model 1431 single-channel analyser, used in the integral counting mode. Counts were collected with a N.E. 4613 scaler. The automatic irradiation, waiting and counting cycle-time was controlled by three N.E. 4624 timers. At the end of the counting cycle the results were printed out automatically on a Teletype printer.

Sample preparation

Cylindrical samples of 6 mm height and 18 mm diameter were machined out of the available Al–Si alloy rods. No special mechanical cleaning or chemical etching was required before irradiation.

As standards, discs having exactly the same dimensions as the unknown

samples, were machined from respectively a high-purity silicon semiconductor monocrystal, and high-purity (99.99%) aluminium metal.

Irradiation and counting

Figure 1 shows the polyethylene rabbit used for irradiating the cylindrical samples as well as its position in the fast flux of the ^{227}Ac–Be isotope neutron source. The rabbit was internally lined with two layers of 0.5-mm cadmium foil. The samples were supported at the bottom by an aluminium disc and at the top by a steel spring to keep them secured at the correct irradiation position. No hydrogen-containing material was allowed inside the cadmium lining, in order to avoid any thermalization of epithermal neutrons.

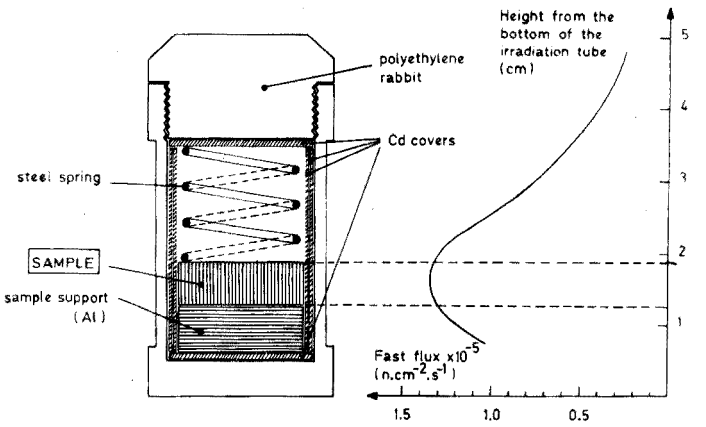

Fig. 1. Construction of the polyethylene rabbit and its position in the fast flux of the ^{227}Ac–Be isotope neutron source.

Each sample was irradiated for 200 s in this position and then transferred to a glass counting vial. A counting time of 300 s was started exactly 40 s after the end of the irradiation. The second sample was irradiated while the first was being counted.

Under the given irradiation and measuring conditions, the specific activity for silicon was 21101 counts $(300\ s)^{-1}\ g^{-1}$, and for aluminium 762 counts $(300\ s)^{-1}\ g^{-1}$ including *ca.* 90 counts from ^{24}Na.

Calculation procedure

Before analysis of the samples, the specific activities of pure silicon and aluminium were accurately determined once and for all for the rigorously controlled irradiation and counting conditions.

From the comparison of the measured total specific activity of the samples with the specific activity of the silicon standard, one obtains an initial estimate of the silicon content:

$$C_{\mathrm{Si},1} = \frac{SA_{\mathrm{S},1}}{SA_{\mathrm{Si}}} 100 \qquad (1)$$

where SA_S is the specific activity of silicon in the sample, and SA_{Si} the specific activity of silicon in the standard.

Subtracting $C_{Si.1}$ from 100 gives a first estimate of the aluminium concentration:

$$C_{Al.1} = 100 - C_{Si.1} \tag{2}$$

By comparison with the specific activity of the aluminium standard this yields a first estimate of the activity from the aluminium fraction in the sample, which can be used to correct $SA_{S.1}$:

$$SA_{S.2} = (SA_{S.1} - SA_{Al}) \frac{C_{Al.1}}{100} \tag{3}$$

where SA_{Al} is the specific activity obtained from a pure standard.

The new estimate $SA_{S.2}$ can be substituted in eqn. (1) and the sequence of eqns. (1), (2) and (3) can be reiterated until:

$$(SA_{S.n} - SA_{S.n-1})/SA_{S.n} \leqslant 0.001 \tag{4}$$

For the samples analysed in this work 4 iterations were sufficient to fulfil condition 4.

The method assumes, of course, that the aluminium and silicon fractions in the samples really add up to 100%. If this is not so eqn. (2) has to be replaced by

$$C_{Al,n} = (100 - D) - C_{Si,n} \tag{5}$$

where D is the total concentration of elements not including Si and Al. The error caused by neglecting D is discussed below.

RESULTS AND DISCUSSION

From each sample three discs were analysed. Table III gives the results for ten different standard reference electrodes for spectrographic analysis. The standard

TABLE III

RESULTS

Sample code	*% Si given*	*% Si found*	*Sr*	*Error of mean*
Al–Si 1340	13.4	13.49 ± 0.09[a]	0.7	+0.09
B.05	13.0	13.02 ± 0.08	0.6	+0.02
A.05	10.8	10.51 ± 0.07	0.7	+0.29
Al–Si 1000	10.0	10.26 ± 0.09	0.9	+0.26
Ac 800	7.95	8.07 ± 0.04	0.5	+0.13
Ac 600/4	6.3	6.47 ± 0.09	1.4	+0.17
Ac 450/1	4.63	4.77 ± 0.12	2.5	+0.14
R 68/Ac 100	0.975	1.04 ± 0.05	4.8	+0.07
6083/1	0.99	1.06 ± 0.06	5.7	+0.07
R Al 50	0.50	0.62 ± 0.05	8.1	+0.12

[a] Standard deviation on mean (70% confidence level) for 3 determinations.

deviation on the mean, taking into account Student's t-factor for 70% confidence level, is indicated. In the fourth and fifth columns the relative standard deviation and the difference between given values and activation results are given.

As can be seen, the precision of the results as well as their agreement with the given values is very satisfactory. Again, as for ferrosilicon[1], there is a tendency for systematically slightly higher n.a.a. results to occur. It may, however, be noted that in gravimetric silicon determinations a tendency for systematically low results is known to occur[6]. In Fig. 2 the experimental precision of the proposed method is plotted against the silicon content and compared with the precision that can be obtained with the Fe–Si method. The new technique improves the precision on the silicon determination by a factor of *ca.* 4 compared to the Fe–Si technique.

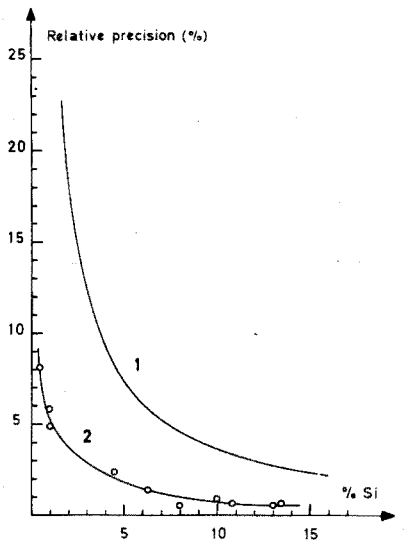

Fig. 2. Precision on a silicon determination. Curve 1, using the Fe–Si technique; Curve 2, experimental precision of the method proposed in this work.

The amount of all other metals (normally 0–2.5%) present in the samples gives a small systematic error if it is not known *a priori*. For the samples analysed in this work, the maximum error amounts to *ca.* 0.1% absolute. For one sample (6083/1), containing 8.7% of other metals, a negative error of 0.3% absolute, arising from overestimation of the aluminium correction would have occurred, if it had not been corrected for. It can be concluded that the method is fast, simple, precise and accurate for the determination of silicon in binary Al–Si alloys. The relative precision ranges from 0.6% to 8.1% for silicon contents between 13.5% and 0.5%. The analyses of three samples of the same alloy can be performed within 21 min.

Thanks are due to the National Fonds voor Wetenschappelijk Onderzoek for partial financial support, and to Dr. U. Mannweiler (Alusuisse) and Dr. Kraft (Metallgesellschaft) for providing the Al–Si standard reference electrodes.

SUMMARY

A method has been developed for the accurate determination of silicon in binary Al–Si alloys by instrumental neutron activation analysis with the aid of an ^{227}Ac–Be isotope neutron source. Discs, weighing *ca.* 4 g, are irradiated at the maximum of the fast flux gradient in a rabbit lined internally with two layers of cadmium foil. Each irradiation is followed by an integral mode counting with discriminator baseline setting at 1400 keV. Standards consist of discs from high-purity semiconductor silicon and aluminium (99.99%) metal. An iterative calculation procedure yields results with a relative precision from 0.6 to 8.1% for silicon contents between 13.5 and 0.5%. Triplicate analysis requires 21 min.

REFERENCES

1 L. Alaerts, J. P. Op de Beeck and J. Hoste, *Anal. Chim. Acta*, in press.
2 L. Alaerts, J. P. Op de Beeck and J. Hoste, *Anal. Chim. Acta*, 69 (1974) 1.
3 N. E. Holden and F. W. Walker, *Chart of the Nuclides*, General Electric Company, Schenectady, N.Y., 1972.
4 J. C. Roy and J. J. Hawton, *AECL-1181 (CRC-1003)*, 1960.
5 R. Dams and F. Adams, *J. Radioanal. Chem.*, 7 (1971) 127.
6 I. M. Kolthoff and P. J. Elving, *Treatise on Analytical Chemistry, Part II*, Vol. 2, Wiley, New York, 1962, p. 156.

Analytica Chimica Acta, 73 (1974) 61–72

DETERMINATION OF ALUMINIUM IN SILICATE ROCKS BY 14-MeV NEUTRON ACTIVATION ANALYSIS

K. HUYSMANS, R. GIJBELS* and J. HOSTE

Institute for Nuclear Sciences, Rijksuniversiteit Gent, Proeftuinstraat 86, B-9000 Gent (Belgium)

(Received 18th April 1974)

Aluminium is the third most abundant element in the earth's crust. Table I shows the estimated abundances, after Ahrens[1], of the elements which constitute the earth's crust, together with the nuclear reactions usually employed for their determination in 14-MeV neutron activation analysis. Eight elements are found in the percent concentration range. Of these, oxygen and silicon can most easily be determined with 14-MeV neutrons, whereas aluminium and iron can be determined after longer neutron irradiation. The determination of calcium, sodium, potassium and magnesium is difficult, except for the latter in ultrabasic rocks. Since the determination of oxygen and silicon[2] in rocks with 14-MeV neutrons is convenient, it is attractive to use the same technique for the determination of aluminium. Moreover, the use of a multichannel analyser allows, in principle, the simultaneous determination of other major elements, such as iron and sometimes magnesium. However, with a multichannel analyser, serious dead-time problems may arise, owing to the relatively long analysis time per pulse, compared with a single channel analyser. Four methods for dead-time correction have already been discussed and compared in detail elsewhere[3].

Nuclear data

Irradiation of aluminium with fast neutrons gives rise to several nuclear reactions, which are summarized in Table II, together with the most important interfering reactions. Two nuclear reactions on aluminium can be considered for quantitative analysis: the $^{27}Al(n,p)^{27}Mg$ and the $^{27}Al(n,\alpha)^{24}Na$ reactions, the former reaction being generally used[4]. Disadvantages of the use of ^{24}Na are that a long irradiation time is needed, that the same sample cannot be used for rapid successive irradiations, and that the interference from the $^{24}Mg(n,p)^{24}Na$ reaction may be considerable. In the present work, the aluminium determination is based on the measurement of ^{27}Mg. Although the γ-peak at 0.84 MeV is more intense than that at 1.01 MeV, the former peak can contain contributions from iron via the $^{56}Fe(n,p)^{56}Mn$ reaction (0.8469-MeV peak). These two peaks (0.844 MeV and 0.8469 MeV) can obviously not be resolved by a NaI(Tl) scintillator and are difficult to resolve even with a Ge(Li) detector.

* Present address: Universitaire Instelling Antwerpen, Department of Chemistry, B-2610 Wilrijk, Belgium.

TABLE I

ESTIMATED % ABUNDANCES OF MAJOR ELEMENTS IN EARTH'S CRUST AND NUCLEAR REACTIONS USUALLY EMPLOYED IN 14 MeV NEUTRON ACTIVATION ANALYSIS

Element	*Abundance (%)*	*Nuclear reaction*	*Threshold energy (MeV)*	*Cross-section (10^{-27} cm^2)*	*Half-life*	*γ-Transition energies (MeV)*
O	46.29	$^{16}O(n,p)^{16}N$	10.2	40 (90)	7.11 s	6.130; 7.119
Si	28.2	$^{28}Si(n,p)^{28}Al$	4.0	250 (400)	2.24 min	1.7789
Al	8.2	$^{27}Al(n,p)^{27}Mg$	1.9	80	9.45 min	0.17; 0.844; 1.0141
		$^{27}Al(n,\alpha)^{24}Na$	3.3	120	15.02 h	1.3684; 2.7536
Fe	5.6	$^{56}Fe(n,p)^{56}Mn$	3.0	115	2.582 h	0.8469; 1.8107; 2.1128
Ca	4.2					
Na	2.4	$^{23}Na(n,p)^{23}Ne$	3.8	30 (10)	37.6 s	0.44; 1.64
		$^{23}Na(n,\alpha)^{20}F$	4.1	220 (30)	11.1 s	1.633
K	2.1	$^{39}K(n,2n)^{38}K$	13.4	6	7.63 min	0.511 (β^+); 2.17; 3.94
Mg	1.95	$^{24}Mg(n,p)^{24}Na$	4.9	200	15.02 h	1.3684; 2.7536
Ti	0.570	$^{46}Ti(n,2n)^{45}Ti$	13.6	30	3.078 h	0.511 (β^+)
P	0.105	$^{31}P(n,\alpha)^{28}Al$	2.0	140	2.24 min	1.7789
		$^{31}P(n,2n)^{30}P$	12.8	10	2.50 min	0.511 (β^+); 2.23
Mn	0.095	$^{55}Mn(n,\alpha)^{52}V$	0.6	35	3.755 min	1.4342
		$^{55}Mn(n,\gamma)^{56}Mn$	—	0.76	2.582 h	0.8469; 1.8107; 2.1128
F	0.063	$^{19}F(n,p)^{19}O$	4.2	15 (135)	26.9 s	0.20; 1.36
		$^{19}F(n,\alpha)^{16}N$	1.6	57	7.11 s	6.130; 7.119
		$^{19}F(n,2n)^{18}F$	11.0	55	109.8 min	0.511 (β^+)
S	0.026	$^{34}S(n,p)^{34}P$	4.5	85	12.4 s	2.128; 4.000
Cr	0.010	$^{52}Cr(n,p)^{52}V$	3.2	100	3.755 min	1.4342
Ni	0.008	$^{58}Ni(n,2n)^{57}Ni$	12.0	35	36.0 h	0.127; 0.511 (β^+); 1.378
		$^{60}Ni(n,p)^{60m}Co$	2.1	9	10.48 min	0.0586; 1.3325
Co	0.003	$^{59}Co(n,\alpha)^{56}Mn$	−0.4	31	2.582 h	0.8469; 1.8107; 2.1128
Others	0.176					

TABLE II

NUCLEAR REACTIONS ON ALUMINIUM AND INTERFERING REACTIONS

Element	*Reaction*	*Isotopic abundance (%)*	*Cross-section (mb)*	*Half-life*	*γ-Transition energy (keV) and relative abundance (%)*
Al	$^{27}Al(n,p)^{27}Mg$	100	80	9.45 min	170; 844.0 (70); 1014.1 (30)
	$^{27}Al(n,\alpha)^{24}Na$	100	120	15.02 h	1368.4 (47); 2753.6 (52)
	$^{27}Al(n,\gamma)^{28}Al$	100	0.53	2.24 min	1778.9 (100)
Si	$^{28}Si(n,p)^{28}Al$	92.21	250 (400)	2.24 min	1778.9 (100)
	$^{29}Si(n,p)^{29}Al$	4.70	100 (35)	6.52 min	1273.3 (100)
	$^{30}Si(n,\alpha)^{27}Mg$	3.09	45 (125)	9.45 min	170; 844.0 (70); 1014.1 (30)
Mg	$^{24}Mg(n,p)^{24}Na$	78.70	200	15.02 h	1368.4 (47); 2753.6 (52)
	$^{26}Mg(n,\gamma)^{27}Mg$	11.17	0.2	9.45 min	170; 844.0 (70); 1014.1 (30)
Fe	$^{56}Fe(n,p)^{56}Mn$	91.66	115	2.582 h	846.9 (70); 1810.7 (20); 2112.8 (10)

EXPERIMENTAL

Apparatus

The neutron generator was a Sames Type J accelerator (150 kV, 2.5 mA) with a 100 MHz–60 W radiofrequency ion-source. The 14-MeV neutrons were produced by the $^{3}H(d,n)^{4}He$ reaction from a 90-Ci rotating water-cooled tritium target (Nukem Type RTE-1). The neutron production was controlled by means of a pneumatically operated removable tantalum screen. The pneumatic transfer system consisted of a pair of aluminium tubes with rectangular cross-section (26.5 × 9.5 mm). Possible contamination of the rabbits, by scouring off the aluminium of the transfer tubes, appeared to be negligible; the cooling time after irradiation allowed careful cleaning of the rabbits. The entire activation and counting process was controlled automatically. The neutron generator, transfer system and counting equipment have been described in detail elsewhere[5,6].

Irradiated samples were counted with a 7.62 × 7.62 cm NaI(Tl) detector, connected to a NE-5281 preamplifier and a NE-4603 amplifier. The double delay-line differentiated output of the amplifier was fed to the converter of an Intertechnique SA 40B 400-channel analyser. The resolution of the system was *ca.* 8%. Neutron monitoring was performed by means of a low-geometry BF_3 counter, surrounded by about 8 cm of paraffin. The NaI(Tl) detector was shielded with lead, a copper foil, a cadmium sheet and also with a 10-cm paraffin cover[7]. This was necessary because the background activity increased slightly during a working day, owing to activation of the detector ($^{127}I\ (n,\gamma)^{128}I$, $T_{\frac{1}{2}} = 25$ min) by the small neutron flux penetrating the counting room (a few neutrons $cm^{-2}\ s^{-1}$).

Dead-time correction

Bartošek *et al.*[8,9] developed a simple automatic, electronic dead-time correction system, which is valid for all kinds of mixtures of short-lived radionuclides and requires no subsequent calculation. In this method, the total dead-time during the whole measurement is kept constant by the creation of additional dead-time at the end of very short counting intervals in the live-time mode. The total counting time T_c (selected with the multichannel analyser clock) is subdivided into a number (n) of very short intervals T_N (10 ms). T_N consists of a measuring time T_{AN} ($T_{AN} < T_N$) and the imposed dead-time T_{DI}. Whenever a pulse is analysed during T_{AN}, the normal live-time correction will extend the measurement. The increase of T_{AN} requires an equal decrease of T_{DI}, in such a way, that the total dead-time remains constant. The interval T_N is so small that decay or change of the pulse rate have no influence. Any multichannel analyser can easily be adapted with this "dead-time stabilizer". The "dead-time" and the "blockade" plugs of the "dead-time stabilizer" unit must simply be connected with the corresponding plugs of the multichannel analyser. To avoid unnecessary counting losses, arising from the imposed dead-time, a range of imposed dead-times from 5% to 60% can be selected, which allows a setting just above the dead-time at the beginning of the measurement.

Preparation of samples and standards

Four U.S.G.S. standard rocks[10], two silicate rock standards from the Geological Survey of Japan and four standard rocks of the South African Bureau

of Standards were analysed for their aluminium content. In addition, two refractory standards 1.68 and 1.69[11], with much higher aluminium contents (20.22% and 31.78%) were included. Each sample was dried at 110°C for at least 30 h. The sample holders were cylindrical polyethylene boxes (5 mm internal height, 12.7 mm diameter, 0.63 cm^3 volume) carefully selected for equal dimensions. Owing to the differences in density between the samples, different weights of the samples were needed to fill the boxes completely. Two sample holders were packed from each of the standard materials available. These sample holders were placed in polyethylene cylindrical "rabbits" (9 mm thickness, 26 mm diameter) fitting the pneumatic system[2]. Aluminium standards were prepared by mixing suitable amounts of silica and alumina, covering the aluminium range of the studied standard rocks. Silica (Quarz feinkörnig, E. Merck) and alumina (Johnson Matthey) were ignited at 1000°C, mixed and homogenized by tumbling for 30 h. Packing of the standards was done in the same way as the samples. To check the composition of the mixtures, they were analysed for aluminium against aluminium metal (refined 99.99%) as standard. In the same series, pure aluminium from a different origin (Schering-Kahlbaum, A. G., Berlin) and two types of alumina (Degussit and Pechiney) were included. Each sample was analyzed ten times. The results are given in Table III for the 0.84-MeV and the 1.01-MeV peaks of ^{27}Mg; as can be seen, the results are practically the same for the two MeV peaks, and the results agree well with the expected composition. All results were not only corrected for dead-time variations but also for neutron and gamma attenuation (see below). When necessary, a correction for silicon was made. The relative standard deviation includes counting statistics and an additional instrumental error[2] (0.7–1.0%).

ABLE III

LUMINIUM DETERMINATION IN STANDARDS

mple	*Expected Al content (%)*	*Al content found (%)*	
		0.84-MeV peak	*1.01-MeV peak*
l (I)	100	100[a]	100[a]
l (II)	100	(10)[b] 100.97 ± 1.23 (1.22)[c]	(10)[b] 100.47 ± 1.21 (1.20)[c]
l (II)	100	(8) 100.06 ± 1.26 (1.26)	(8) 100.25 ± 1.27 (1.27)
l_2O_3 (I)	52.92	(10) 53.45 ± 0.99 (1.85)	(10) 53.65 ± 1.20 (2.24)
l_2O_3 (II)	52.92	(10) 52.95 ± 0.95 (1.79)	(10) 52.90 ± 1.00 (1.89)
$l_2O_3 + SiO_2$	5.24	(10) 5.20 ± 0.19 (3.65)	(10) 5.23 ± 0.27 (5.16)
$l_2O_3 + SiO_2$	7.97	(10) 8.17 ± 0.29 (3.55)	(10) 8.22 ± 0.27 (3.28)
$l_2O_3 + SiO_2$	10.59	(9) 10.39 ± 0.35 (3.37)	(9) 10.44 ± 0.21 (2.01)

Al (I) was taken as the reference material.
Number of analyses.
The standard deviation was calculated on a single determination; the relative standard deviation is given in rackets.

Irradiation procedure

An irradiation capsule or transfer "rabbit" was loaded in the pneumatic transport system. After transfer to the irradiation site, the sample was irradiated during 100 s at a beam intensity of 300 μA. During the irradiation the neutron flux was monitored by means of the BF_3-counter. At the end of the irradiation

the sample was automatically returned to the counting room and allowed to cool for 10 min. During this time the sample was positioned on a sample holder fitting the NaI-detector. After 10 min, the first counting with the multichannel analyser in real time (clock time) was started for 5 min. A constant dead-time of 25% was imposed with the dead-time stabiliser. This first count gives the silicon determination required for the correction of the silicon interference; the dominant activity is due to ^{28}Al (Fig. 1A). After a delay of 5 min the multichannel analyser was started again for 10 min in real time, for the measurement of the 1.01-MeV peak of ^{27}Mg. (Fig. 1B). The dead time was again kept constant at 25%.

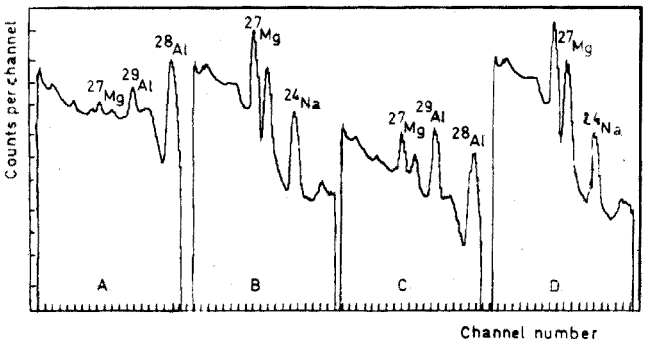

Fig. 1. NaI(Tl) spectra of fast neutron-irradiated aluminium (4.3 g) and silicon (4.0 g). Irradiation time: 100 s at 80 μA. Time after irradiation – 10 min: first counting time (5 min), Si-sample (Fig. 1A), Al-sample (Fig. 1D); 20 min: second counting time (10 min), Si-sample (Fig. 1C), Al-sample (Fig. 1B).

Interferences

The most serious interference encountered in the determination of aluminium in silicate rocks is the ^{30}Si$(n,\alpha)^{27}$Mg reaction (Fig. 1C). A correction can be applied if the silicon content is known; this can be obtained from the same irradiation by measuring the samples after 10 min of cooling. In principle, it would be better to choose a shorter cooling time, but this would require a change in the imposed dead-time for the next measurement. The determination of the silicon correction factor was carried out as follows. A semiconductor-grade silicon disk and pure aluminium (99.99%) were irradiated five times in the same way as the samples. The net peak area was calculated by the method of Sterlinski[12] (see *Calculation of results*). The results showed that 100% Si gave an apparent aluminium content of $3.06 \pm 0.13\%$ at the 0.84-MeV peak, and $3.96 \pm 0.26\%$ at the 1.01-MeV peak, *i.e.* a significant difference for the two peaks. Similar irradiations with silica and alumina gave for the 1.01-MeV peak a silicon correction factor of $3.83 \pm 0.18\%$, in agreement with the data obtained from pure silicon and aluminium.

In order to explain this systematic difference in the correction factors, decay curve analyses were done for the 0.84- and 1.01-MeV peaks on samples of pure magnesium and magnesium oxide, irradiated for 10 min in the nuclear reactor Thetis, at a thermal neutron flux of *ca.* 10^{10} n cm^{-2} s^{-1} and a fast fission flux of about 10^8 n cm^{-2} s^{-1}. Si, SiO_2, Al and Al_2O_3 samples were irradiated with 14-MeV neutrons as described above. Results are given in Table IV. The half-lives obtained agree well with the accepted values ($T_{\frac{1}{2}} = 9.45$ min), except for

TABLE IV

DECAY CURVE ANALYSIS OF ^{27}Mg[a]

^{27}Mg from $^{30}Si(n,\alpha)$			*^{27}Mg from $^{27}Al(n,p)$*			*^{27}Mg from $^{26}Mg(n,\gamma)$*		
Sample	*0.84-MeV peak*	*1.01-MeV peak*	*Sample*	*0.84-MeV peak*	*1.01-MeV peak*	*Sample*	*0.84-MeV peak*	*1.01-MeV peak*
SiO_2	9.27	8.55	Al_2O_3	9.30	9.28	Mg	–	9.35
Si	9.42	8.25	Al_2O_3	9.43	9.37	Mg	—	9.41
Si	8.91	8.74	Al	9.47	9.54	MgO	9.43	9.37
Si	9.74	8.71	Al	9.34	9.41	MgO	9.52	9.51
Si	9.57	8.10						

[a] $T_{\frac{1}{2}}$ in min.

the 1.01-MeV peak of ^{27}Mg originating from fast neutron-irradiated silicon. The decay curve analysis program gave two components, but the program could not resolve them, probably because of the similar half-lives. As can be seen in Fig. 1C ^{29}Si(n,p)^{29}Al has a prominent peak at 1.27 MeV ($T_{\frac{1}{2}} = 6.52$ min). Since the Compton edge of the ^{29}Al peak (1.06 MeV) coincides with the 1.01-MeV peak of ^{27}Mg, a smaller apparent half-life is found. Although the silicon correction factor becomes higher, no systematic error is introduced, because both components originate from silicon and a standardized analytical procedure is followed. The same argument is valid for other possible interferences originating from silicon (^{28}Al-Compton region). The ^{26}Mg(n,γ)^{27}Mg interference is generally considered to be negligible, owing to the low magnesium content of ordinary rocks (Table I). Moreover, 14-MeV neutrons have very small cross-sections for (n,γ) reactions. Irradiation of pure magnesium and pure aluminium gave an apparent content of 0.54% Al in 100% Mg. Thus this interference was not taken into account for the samples studied.

Neutron and gamma-ray attenuation

The effect of neutron and γ-ray attenuation has been studied in detail by Nargolwalla *et al.*[13,14] and by Vandecasteele *et al.*[15]. Neutron and γ-ray attenuation can be expressed as a semi-empirical exponential absorption given by

$$C_x/C_s = \exp[-(\Delta\Sigma + \Delta\mu)d] \tag{1}$$

where C_x and C_s are the correction factors for the sample and standard, respectively; $\Delta\Sigma$ is the difference in total removal cross-section between sample and standard, $\Delta\mu$ the difference in total γ-ray linear attenuation coefficient between sample and standard and d the effective sample or standard thickness, (0.205 cm).

Attenuation differences are negligible for rock powders having the same apparent density as the standards. Because of systematic differences in density, corrections were calculated from the mean composition of samples NIM-L; NIM-N; NIM-P; NIM-D and JB-1, taking into account the bulk composition and the known weights. The d-value was determined from the neutron flux measurements of Van Grieken *et al.*[16].

Calculation of results

The net peak area was calculated as described by Sterlinski[12]:

$$S_n = na_0 + \sum_{i=1}^{n-1} (n-2i+1/2)(a_{-i}+a_i) - (n-1/2)(a_{-n}+a_n) \tag{2}$$

where S_n is the net peak area, a_0 the number of counts in channel zero (channel of the peak with the maximum number of counts), n the number of channels around the center of the peak, and a_i the number of counts in channel i.

This technique was preferred to Covell's method[17], as in this case the precision of the net peak area is determined by the two outer channels a_n and a_{-n}; if counting statistics are poor, these two channels contribute severely in the obtained precision.

If the multichannel analyser is stable and if the counting rate is not too high, the variance on the accumulated counts is given by:

TABLE V

DETERMINATION OF ALUMINIUM IN U.S.G.S. STANDARD ROCKS

Sample	*% Al present*	*14-MeV results (%Al)*[a]	*14-MeV results (% Al)*[b]
GSP-1	8.00	(7) 7.95±0.18 (2.26)[c] (6) 7.94±0.22 (2.77) } (13)[d] 7.94±0.19[e] (2.39)	(7) 7.92±0.20 (2.53) (6) 7.94±0.21 (2.64) } (13) 7.93±0.19 (2.40)
AGV-1	9.00	(7) 9.10±0.21 (2.31) (6) 8.97±0.16 (1.78) } (13) 9.04±0.19 (2.10)	(7) 9.09±0.23 (2.53) (6) 8.99±0.16 (1.78) } (13) 9.04±0.20 (2.21)
BCR-1	7.23	(7) 7.16±0.30 (4.19) (6) 7.12±0.15 (2.11) } (13) 7.14±0.23 (3.22)	(7) 7.16±0.30 (4.19) (6) 7.13±0.18 (2.52) } (13) 7.15±0.24 (3.36)
G-2	8.12	(7) 8.05±0.20 (2.48) (5) 7.93±0.15 (1.89) } (12) 8.00±0.18 (2.25)	(7) 8.02±0.22 (2.74) (5) 7.92±0.17 (2.15) } (12) 7.98±0.20 (2.51)
1.68	20.22	(7) 20.45±0.43 (2.10) (5) 20.04±0.35 (1.75) } (12) 20.28±0.44 (2.17)	(7) 20.47±0.45 (2.20) (5) 20.05±0.36 (1.80) } (12) 20.30±0.45 (2.22)

[a] Corrected for silicon content from first counting time.

[b] Corrected for known silicon content.

[c] For explanation of layout, see footnotes to Table III.

[d] Weighted mean, $\mu = \dfrac{\sum_i x_i/s_i^2}{\sum_i 1/s_i^2}$

[e] Variance of mean, $s\mu^2 = 1/\sum_i s_i^2$.

TABLE VI

DETERMINATION OF ALUMINIUM IN STANDARD ROCK SAMPLES FROM THE GEOLOGICAL SURVEY OF JAPAN, AND FROM THE SOUTH AFRICAN BUREAU OF STANDARDS

Sample	*% Al present*	*% Al present (correct. for H_2O)*[a]	*Uncorrected 14-MeV results (% Al) (Mean)*	*Neutron and gamma attn. factor*	*Si interference*	*Corrected 14-MeV results (% Al)*[b]
JB-1	7.68	7.76	8.692	1.0056	0.95	(5) 7.79±0.30 (3.85) } 7.76±0.12 (1.55)
			8.635	1.0072	0.95	(6) 7.75±0.13 (1.68) }
JG-1	7.52	7.53	8.810	1.0030	1.32	(6) 7.52±0.27 (3.59) } 7.69±0.16 (2.08)
			9.068	1.0035	1.32	(6) 7.78±0.19 (2.44) }
NIM-N	8.81		9.602	1.0057	0.95	(6) 8.71±0.28 (3.21) } 8.71±0.16 (1.84)
			9.584	1.0077	0.95	(5) 8.71±0.19 (2.18) }
NIM-S	9.17		9.957	1.0023	1.16	(6) 8.82±0.27 (3.06) } 9.04±0.19 (2.10)
			10.403	1.0023	1.16	(6) 9.27±0.28 (3.02) }
NIM-L	7.37		8.127	1.0050	0.96	(6) 7.21±0.38 (5.27) } 7.21±0.28 (3.88)
			8.143	1.0047	0.96	(6) 7.22±0.40 (5.54) }
NIM-G	6.39		7.572	1.0028	1.38	(6) 6.21±0.14 (2.25) } 6.19±0.11 (1.78)
			7.525	1.0027	1.38	(6) 6.17±0.18 (2.92) }
1.69	31.78		31.927	1.0080	0.67	(6) 31.51±0.56 (1.78) } 31.72±0.28 (0.88)
			32.215	1.0076	0.67	(6) 31.79±0.33 (1.04) }
1.68	20.22		21.317	1.0039	1.00	(6) 20.40±0.39 (1.91) } 20.33±0.32 (1.57)
			21.086	1.0045	1.00	(5) 20.18±0.57 (2.82) }

[a] % Al calculated, corrected for water content.
[b] For explanation of layout, see Table V.

$$V_{SN} = n^2 a_0 + \sum_{i=1}^{n-1} (n-2i+1/2)^2(a_{-i}+a_i)+(n-1/2)^2(a_{-n}+a_n) \quad (3)$$

A FORTRAN 4 program (COMS) was used for the calculation of the net peak area. The program searches for the center of the peak and calculates the net peak area (S_n) for increasing values of n. For each value of n, the corresponding variance V_{SN} is calculated. For the calculation of the eventual results, the value of n with minimal relative variance was adopted (*e.g.* with the center of the peak in channel 100, n equals 9 or 10). A similar procedure was followed by Ehmann and Morgan[18].

RESULTS AND DISCUSSION

Results for the determination of aluminium in four U.S.G.S. standard rocks using the refractory material 1.69 as a standard, are given in Table V. In the third column, the results are corrected by taking the silicon content as derived from the first counting time; the last column shows the same results corrected for the "known" silicon content of the samples. As can be seen, the results are not significantly different, because counting statistics during the first count (1.78-MeV peak of ^{28}Al from silicon) are quite good. Thus the limiting factor in the aluminium determination arises from the silicon interference in the 1.01-MeV region and is similar in both cases. For each sample and each method, two sets of results with corresponding coefficients of variation are given, as well as the weighted means of these two results and the variance of the weighted mean.

Results for the determination of aluminium in Japanese and South African standard rocks are given in Table VI; mixtures of silica and alumina were used as standards. The mean standard deviation on a single determination is 2.8% at the 6–10% aluminium level (omitting NIM-L standard deviations), which corresponds to twice the counting statistics (1.5%) for standard and sample, and an instrumental error of about 1%.

For a haplogranite sample (16.19% Al_2O_3), analysed by 11 selected laboratories, Fairbairn and Schairer[19] report a relative standard deviation of 1.6%, and this may be considered typical of the present attainable accuracy for a classical determination at the 15% Al_2O_3 level on an interlaboratory basis.

Although the precision and accuracy of the aluminium determination with 14-MeV neutrons seem to be of the same order of magnitude (or slightly worse) as the classical determination, the method has the advantage of being fast and non-destructive. Especially in combination with a simultaneous fast neutron determination of other major elements (O, Si, Fe), 14-MeV activation is a valuable analytical tool for determining aluminium in rocks if the content is not below 5%.

SUMMARY

Aluminium has been determined in various standard rocks by 14-MeV neutron activation analysis. The induced ^{27}Mg activity (1.01-MeV photopeak) was counted with a multichannel analyser, equipped with Bartošek's dead-time stabilizer system. Aluminium standards were prepared by mixing silica and alumina. Correction

was made for the interfering reaction $^{30}Si(n,\alpha)^{27}Mg$ by counting the 1.78-MeV peak, 10 min after irradiation. The mean coefficient of variation on a single determination was 2.8% at the 6–10% aluminium level.

REFERENCES

1 L. H. Ahrens, *Distribution of the Elements in Our Planet*, McGraw-Hill, New York, 1965.
2 K. Huysmans, R. Gijbels and J. Hoste, *Talanta*, 20 (1973) 843.
3 K. Huysmans, R. Gijbels and J. Hoste, *J. Radioanal. Chem.*, 20 (1974) 51.
4 R. Van Grieken and J. Hoste, *Annotated Bibliography on 14 MeV Neutron Activation Analysis*, C.E.C. Eurisotop 65 Series, Bibliographies-8, Brussels, 1972.
5 J. Hoste, D. De Soete and A. Speecke, *Euratom Report EUR-3565e*, 1967.
6 R. Gijbels, A. Speecke and J. Hoste, *Anal. Chim. Acta*, 43 (1968) 183.
7 R. Van Grieken and R. Dams, *Anal. Chim. Acta*, 63 (1973) 369.
8 J. Bartošek, F. Adams and J. Hoste, *Nucl. Instru. Methods*, 103 (1972) 45.
9 J. Bartošek, G. Windels and J. Hoste, *Nucl. Instru. Methods*, 103 (1972) 43.
10 F. J. Flanagan, *Geochim. Cosmochim. Acta*, 33 (1969) 81.
11 Certificate, Groupement des Utilisateurs de Matériaux Réfractaires, Brussels, Belgium.
12 S. Sterlinski, *Anal. Chem.*, 40 (1968) 1995.
13 S. S. Nargolwalla, M. R. Crambes and J. R. De Voe, *Anal. Chem.*, 40 (1968) 666.
14 S. S. Nargolwalla, M. R. Crambes and J. E. Suddueth, *Anal. Chim. Acta*, 49 (1970) 425.
15 C. Vandecasteele, R. Van Grieken, R. Gijbels and A. Speecke, *Anal. Chim. Acta*, 64 (1973) 187; 65 (1973) 1.
16 R. Van Grieken, A. Speecke and J. Hoste, *J. Radioanal. Chem.*, 10 (1972) 95.
17 D. F. Covell, *Anal. Chem.*, 31 (1959) 1785.
18 W. D. Ehmann and J. W. Morgan, *Proc. Sec. Oak Ridge Conf. on the Use of Small Accelerators for Teaching and Research*, March 23–25, 1970, p. 205.
19 H. W. Fairbairn and J. F. Schairer, *Amer. Mineral.*, 37 (1952) 744.

Analytica Chimica Acta, 73 (1974) 73–80

THE DETERMINATION OF LEAD IN BLOOD BY ATOMIC FLUORESCENCE FLAME SPECTROMETRY

H. G. C. HUMAN and E. NORVAL

National Physical Research Laboratory, Council for Scientific and Industrial Research, P.O. Box 395, Pretoria 0001 (South Africa)

(Received 8th May 1974)

The determination of the lead concentration of whole blood remains the most important test for measuring the extent of an individual's absorption of lead from his environment. As this test is frequently used for routine screening, the method should be capable of determining lead in the blood of normal subjects at concentrations of about 0.2 p.p.m. Since a very small change in the amount of lead may represent an increased absorption of the metal and since the danger of contamination is ever-present, a sensitive method is required which combines minimal handling of samples with good precision and accuracy.

Delves[1] extended the detection limit of flame atomic absorption spectrometry by using precision-made nickel crucibles placed in the flame and employing a pre-oxidation step. Hauser *et al.*[2] employed a tantalum sampling boat and low-temperature ashing. Flameless atomic absorption techniques have been employed frequently[2–6]. However, these methods all require extraction of the lead[3], or a partial pre-oxidation of the organic matter[5], or a background correction system[4, 6]. Amos *et al.*[7] determined lead in blood by atomic fluorescence spectrometry using a carbon rod. Samples were preheated to remove most of the organic material at a temperature just below that at which lead vaporizes. Table I summarizes the techniques mentioned and gives the detection limits obtained.

The method described in this paper employs flame atomic fluorescence and is sufficiently sensitive for samples to be diluted to an extent where the sample can be nebulized directly and also where the red blood cells are completely haemolized, resulting in a homogeneous liquid. Because of the great measure of dilution, sample volume is not a consideration and possible matrix interferences are eliminated. Two types of interference remain which can, however, be easily eliminated.

EXPERIMENTAL

Primary source

A boosted-output hollow-cathode lamp of the improved type described by Lowe[8] was employed as the primary irradiating source for the atomic fluorescence measurements. The anode and cathode of the supplementary discharge circuit in this version are situated on opposite sides of an open-ended cathode so that the auxiliary discharge has to traverse the cathode. A demountable lamp with flow-

TABLE I

DETECTION LIMITS OBTAINED FOR THE DETERMINATION OF LEAD IN BLOOD BY DIFFERENT METHODS

Method	*Detection limit in μg ml⁻¹ (3 × standard deviation)*	*Ref.*
Atomic absorption, 'Delves Cup', sample dried and ashed with H_2O_2 in nickel crucible	0.018	1
Flameless atomic absorption, tantalum boat, sample dried and ashed in low temperature asher	0.002	2
Flameless atomic absorption, tantalum strip, chelation with APDC, extraction with MIBK	0.0018	3
Flameless atomic absorption, tantalum ribbon, sample dilution, background correction	0.06	4
Flameless atomic absorption, special graphite tube, sample dried in tube, digested with H_2O_2	0.05	5
Flameless atomic absorption, carbon rod, 0.5 μl heparinized blood with 0.3 and 0.2 μl xylene on either side of the sample, injected into the rod	0.03	6
Atomic fluorescence using the carbon rod, sample dilution	0.005	7
Present work—atomic flame fluorescence	0.0012	—

through gas system (argon) and watercooled cathode, also described by Lowe[9], was employed (Fig. 1).

The hollow cathode was prepared by melting lead into a copper cup with inner and outer diameters of 10 and 12 mm, respectively. A central hole of 8-mm diameter was drilled through the lead and the ends of the cylinder were turned on a lathe so that the lead hollow cathode thus obtained had a length of 10 mm, an

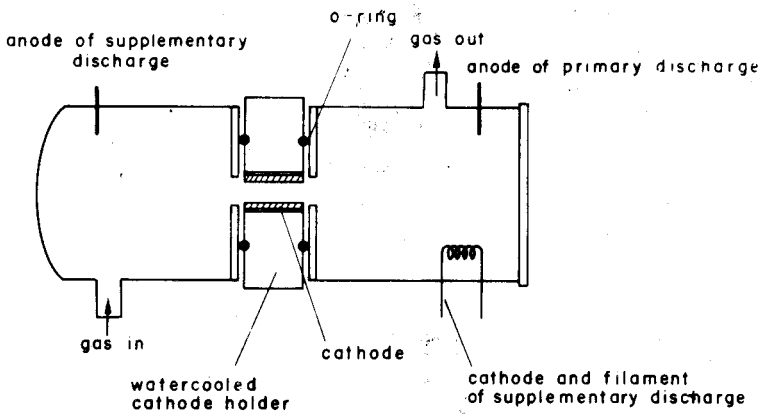

Fig. 1. Schematic diagram of hollow-cathode lamp with auxiliary discharge as in Lowe's design[8,9].

inner diameter of 8 mm, and a wall thickness of 1 mm. It was contained in a copper body also with a length of 10 mm, an external diameter of 12 mm and a wall thickness of 1 mm. The copper body was machined accurately to press-fit in the water-cooled brass cathode holder.

With a hollow cathode (primary) discharge current of 40 mA (peak value of current modulated at 285 Hz), the supplementary discharge enhances the line intensities as shown in Table II. The optimal argon pressure in the lamp was *ca.* 100 Pa.

TABLE II

INTENSITY ENHANCEMENT OF 3 LEAD LINES BY SUPPLEMENTARY DISCHARGE

Line (nm)	*Intensity enhancement factor*
405.8	25
283.3	137
217.0	78

Monochromator and optics

A Jarrell–Ash 0.25-m monochromator with an effective aperture ratio of f/3.5 was used. This instrument has two gratings, one blazed at 300.0 nm with 2400 lines per mm and the other blazed at 500.0 nm with 1200 lines per mm (providing dispersions of 1.65 nm mm^{-1} and 33 nm mm^{-1}, respectively). With the hydrogen–oxygen–argon flame used as atom reservoir (see below) the optimal entrance and exit slit widths were 500 μm, providing a band pass of 0.8 nm with the higher dispersion grating. The main cause of noise under these experimental conditions was shot noise, from the background emission of the flame while the blood sample was being aspirated. At a narrower band pass of 0.5 nm (150 μm slit, low dispersion grating), the aperture of the monochromator proved to be insufficient so that when the photomultiplier voltage was increased sufficiently to obtain a reasonable signal, the dark-current noise was equal to the flame noise, and the total noise resulted in a poorer signal-to-noise ratio.

The output from the photomultiplier (RCA IP28) was fed into a lock-in amplifier (Keithley 840 Autoloc) and the output of this was connected to a strip-chart recorder.

The hollow cathode was imaged in the flame by a 50-mm diameter, 50-mm focal length quartz lens. No improvement in signal-to-noise ratio could be obtained by the use of a spherical mirror to refocus the transmitted radiation back into the flame; light reflection from the environment caused a large background signal and created unacceptable associated noise. A section of the flame 15 mm above the burner was focussed onto the horizontal monochromator slit of 10 mm height by means of a 50-mm diameter, 75-mm focal length quartz lens filling the monochromator collimator completely with its image.

Burner and flame

A circular flame of 20 mm diameter was formed on a Meker-type burner.

An argon–hydrogen–oxygen flame was selected, being the most suitable for lead fluorescence measurements[10,11]. The burner was equipped to separate the primary and secondary reaction zones of the flame by means of a gas sheath which prevented the entrainment of atmospheric air. With argon used as the sheathing gas, a considerable reduction of background emission was achieved, as well as slight enhancement of the fluorescence signal. A cool fuel-rich flame (argon, 6.5 l min^{-1}; oxygen, 0.8 l min^{-1}; hydrogen, 3.5 l min^{-1}) yielded the best signal-to-noise ratio. A standard commercial EEL nebulizer was used, and no problem with clogging was experienced when the diluted blood solutions were used.

The temperature of the flame was measured by the sodium line reversal method[12]. The temperature of the tungsten strip lamp used as a comparison source was measured with an optical pyrometer. The temperature of the unseparated flame was found to be 1780°K and that of the separated flame 1650°K, both measured at the actual flame zone utilized for the fluorescence measurements (with an estimated error of ± 20°K).

The emission spectrum of the flame in the region of the analytical lead 405.8-nm line for a 20× diluted blood sample consisted of a continuum of unknown origin and the 404.4–404.7-nm potassium doublet. When the separating gas was introduced, the continuum was reduced by a factor of 5 and the line emission by a factor of only 2.7. It was therefore advisable to use a spectral slit sufficiently narrow to exclude the potassium line emission from the measurements.

RESULTS

Limit of detection and working range

The limit of detection (defined as the concentration giving a signal equal to twice the peak-to-peak fluctuations of the background signal) was 0.002 $\mu g\ ml^{-1}$ in aqueous solution, for a 1-s time constant. This is an improvement of one order of magnitude over the best flame fluorescence value previously reported[10,11] (Browner *et al.*[10] quoted a detection limit of 0.01 $\mu g\ ml^{-1}$ on the basis of a signal-to-noise ratio of 1). This detection limit was obtained with a 40-mA primary discharge current and a 300-mA current for the supplementary discharge of the boosted-output hollow-cathode lamp. A one-third reduction in the detection limit was obtained either by employing a 3-s time constant or by running the lamp at higher currents (60 mA + 400 mA). The combination of these factors made a detection limit of 0.001 $\mu g\ ml^{-1}$ a reality. The high primary current of 60 mA, however, leads to a decrease in cathode life and was not used for the analytical measurements.

The 405.8-nm lead line gave the best signal-to-noise ratio. The fluorescence signal was somewhat smaller and the noise larger for the 283.3-nm line than for the 405.8-nm line, with the result that the resultant signal-to-noise ratio was considerably worse.

The working range was found to be linear from the detection limit up to 40 $\mu g\ ml^{-1}$. Even up to 200 $\mu g\ ml^{-1}$, where the slope decreased by 50%, the working curve was still usable. The range is large because the 405.8-nm analytical line is only very slightly prone to self-absorption as it is not a resonance line.

Sample preparation

After the blood had been drawn, it was immediately diluted (1 in 20) with

doubly distilled deionized water which caused haemolysis and obviated the need for an anticoagulant. However, should the analysis not be done within 12 h, heparin should be added to prevent agglutination[13]. The sample was placed in a plastic container directly after dilution in order to eliminate adsorption of lead onto the container walls.

Chemical interferences

It appears from the extensive investigations of Browner *et al.*[10] into interference effects that sodium is the only element present in blood at concentrations high enough to cause chemical interference. The sodium concentration of normal serum ranges from 3000 to 3300 μg ml^{-1} (ref. 13, p. 499). Because of the permeability of the blood corpuscle membranes, this value may be used for whole blood[14]. This means that the concentration in 20 × diluted blood samples varies between 150 and 165 μg ml^{-1}. An investigation of the effect of sodium on the lead fluorescence signal showed that, at concentrations of 0.01, 0.02 and 0.04 μg Pb ml^{-1}, the effect of 160 μg Na ml^{-1} was a signal enhancement of 18%. (The expected lead concentration in the diluted blood samples is 0.01–0.04 μg ml^{-1}.) The variation of this effect was negligible for sodium concentrations between 150 and 170 μg ml^{-1}, so that it was only necessary to add a constant amount of sodium (160 μg ml^{-1}) to the standards to correct for the interference.

The absence of other chemical interferences was proved by the fact that, within experimental error, the value obtained for a specific sample by means of calibration standards with added sodium corresponded to that obtained by the addition method.

Light scattering

When the diluted blood solutions were nebulized, scattering of the incident radiation from the primary source by unevaporated particles in the flame resulted in an error in the analytical signal. The existence of a false fluorescence signal was verified by using an aluminium cathode in the lamp and measuring at 396.1-nm the signal reflected when a blood sample was aspirated into the flame. The magnitude of the reflection signal at 405.8-nm could be estimated by comparing the intensities of the 396.1-nm Al and 405.8-nm Pb lines. It caused a false fluorescence signal equivalent to that given by 0.0026 ($\pm$0.0004) μg Pb ml^{-1}. In concentration units, this signal remained the same as long as flame conditions and the blood dilution factor remained constant. It was insensitive to changes in lamp intensity, because both the fluorescence signal and the reflection signal are directly proportional to the primary source line intensity. It was therefore easy to correct for the false signal. In the present case, the value of 0.0026 μg ml^{-1} was subtracted from all the values obtained.

A more elegant and efficient method of eliminating the problem of scatter is to use a filter in the irradiating beam which absorbs radiation at 405.8 nm but transmits below 300.0 nm. Practically all the radiation appearing as fluorescence at 405.8-nm is due to direct line fluorescence, *i.e.* absorption takes place only at the 283.3-nm resonance line. Amos *et al.*[7] used a UG-5 filter for this purpose. From the work of Kasha[15] it appeared that a simple solution filter would also solve the problem. A 10-mm thick cell was made and filled with a 500 g l^{-1} solution of nickel sulphate hexahydrate. This cell absorbed completely at 405.8 nm but trans-

mitted 81% of the light at 283.3 nm. With this filter in the path of the irradiating beam, the fluorescence signal dropped to 76% of its original value. The signal was restored to more than 100% of its original value by back reflection and focussing in the flame with a spherical mirror (the effect was a 50% increase in signal). Since the filter absorbed completely at 405.8 nm, the reflection from the environment with the mirror in position no longer presented a problem.

The reflection from unevaporated particles in the flame was eliminated by the use of this filter, and with the use of the mirror the same signal strength could be recovered with the result that the detection limit was not affected. The use of such a cheap and simple filter is strongly advised for lead fluorescence measurements.

Determination of lead in blood

Figure 2 shows recorder tracings of the fluorescence signals obtained. Figure 2(a) shows a typical measurement of two standards containing 0.01 and 0.02 μg Pb ml^{-1} (both with 160 μg Na ml^{-1}) and three measurements of the signal obtained with a 20× diluted blood sample; Fig. 2(b) shows two sets of signals obtained with the method of standard additions for the same blood sample. The values of 11 fluorescence signals of the 20× diluted blood sample yielded a mean value of 0.011 μg Pb ml^{-1} with a standard deviation of 0.0004 μg ml^{-1}, or a relative standard deviation of 3.7%. These measurements were taken over a period of 45 min and the standard deviation calculated includes drift over this period. Therefore, if the measurements are done in this way, which is equivalent to using a time constant of 3 s and integrating for a period of about 1 min, the detection limit of lead in blood is 0.0012 μg ml^{-1} (no blood without lead being available, 3× the standard deviation of background plus signal was used as criterion).

The lead concentrations of two blood samples were found to be 0.20 and 0.22 μg ml^{-1}. The same diluted blood samples were analysed by the carbon rod atomic absorption technique. The same values were obtained within the experimental

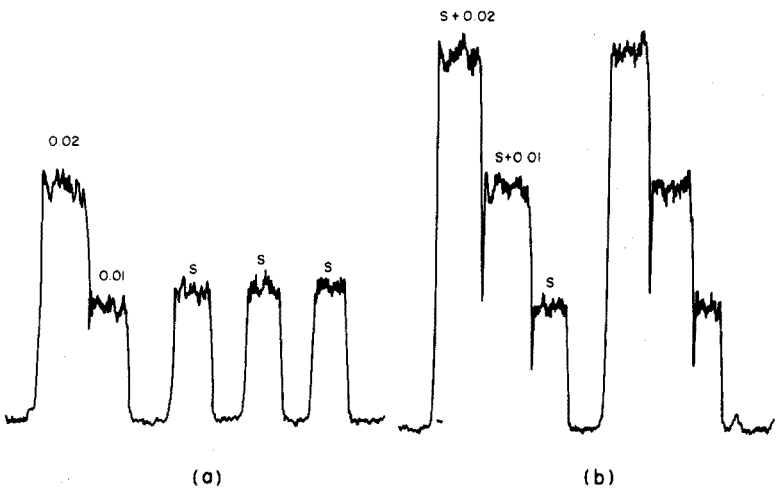

Fig. 2. Recorder tracings of fluorescence signals. (a) Standards of 0.02 and 0.01 μg ml^{-1}, and three runs of a 20× diluted blood sample. (b) Two sets of signals for the same sample with standard additions of 0.02 and 0.01 μg ml^{-1}. Time scale *ca.* 1 min per run. Time constant of measuring apparatus 3 s.

error. The variation of the peak absorbance signal with the latter method was 11.6% and the limit of detection was 0.003 μg ml^{-1}.

Comparison of the flame atomic fluorescence technique and the carbon rod atomic absorption method

Sensitivity is approximately the same for the two methods, but flame atomic fluorescence has the following advantages.

Because of the linearity of the atomic fluorescence calibration curve which passes through the origin, a blank and one standard containing approximately the same lead concentration as the samples are sufficient for a determination. The reproducibility of the fluorescence method was better than that obtained with the carbon rod technique, resulting in a lower limit of detection and more precise results.

The problems associated with loss of lead during the ashing step with the rod were absent with the fluorescence method.

Volumetric metering errors are much reduced as more blood is measured. However, because of the high dilution, relatively small quantities of blood will suffice when necessary, and the method remains a micro method. (Theoretically, a minimum sample quantity of 100 μl is required.)

A disadvantage of the fluorescence technique is that the primary source lamp must be continuously pumped and needs constant and careful control in contrast to the atomic absorption set-up with a standard hollow-cathode lamp.

SUMMARY

The use of atomic flame fluorescence for the direct determination of lead in diluted blood is described. The method is sensitive enough to determine the lead concentration in 20× diluted blood accurately and with a precision of better than 4% at a lead concentration level of 0.20 μg ml^{-1}. A special design of hollow-cathode lamp is used, with an argon–hydrogen–oxygen flame. Sodium interference is compensated by addition to standards, and light scatter effects are eliminated by a simple filter. Linear response to lead concentration is obtained in the range 0–40 μg ml^{-1}.

REFERENCES

1 H. T. Delves, *Analyst (London)*, 95 (1970) 431.
2 T. R. Hauser, T. A. Hinners and J. L. Kent, *Anal. Chem.*, 44 (1972) 1819.
3 J. Y. Hwang, P. A. Ullucci, S. B. Smith and A. L. Malenfant, *Anal. Chem.*, 43 (1971) 1319.
4 J. Y. Hwang, P. A. Ullucci and C. J. Mokeler, *Anal. Chem.*, 45 (1973) 795.
5 E. Norval and L. R. P. Butler, *Anal. Chim. Acta*, 58 (1972) 47.
6 J. F. Rosen, *J. Lab. Clin. Med.*, October 1972, 567.
7 M. D. Amos, P. A. Bennett, K. G. Brodie, P. W. Y. Lung and J. P. Matousek, *Anal. Chem.*, 43 (1971) 211.
8 R. M. Lowe, *Spectrochim. Acta, Part B*, 26 (1971) 201.
9 R. M. Lowe, *IXth Australian Spectroscopy Conference*, Canberra, Australia, 1973.
10 R. F. Browner, R. M. Dagnall and T. S. West, *Anal. Chim. Acta*, 50 (1970) 375.
11 V. Sychra and J. Matousek, *Talanta*, 17 (1970) 363.
12 W. Snelleman, Thesis, Utrecht, 1965.

13 P. B. Hawk, B. L. Oser and W. H. Summerson, *Practical Physiological Chemistry*, McGraw-Hill, New York, 13th edn., 1954, p. 468.
14 J. P. du Plessis, Medical Research Council (South Africa), personal communication.
15 M. Kasha, *J. Opt. Soc. Amer.*, 38 (1948) 929.

Analytica Chimica Acta, 73(1974) 81–85

ATOMIC ABSORPTION SPECTROMETRIC DETERMINATION OF CADMIUM AND LEAD IN DENTAL MATERIAL BY ATOMIZATION DIRECTLY FROM THE SOLID STATE

F. J. LANGMYHR and A. SUNDLI
Department of Chemistry, University of Oslo, Oslo 3 (Norway)
J. JONSEN
Department of Microbiology, University of Oslo, Oslo 3 (Norway)
(Received 18th April 1974)

During recent years, universal interest in the trace elements has stimulated a number of studies of their concentration and distribution in the human body, with the purpose of establishing the normal values and to detect illnesses, occupational diseases and toxic effects. As a contribution to the UNESCO research program "Man and the Biosphere", a study of trace element concentrations in human organs is in progress in Norway; the present work was carried out as a subproject under the national program.

The present paper describes the determination of cadmium and lead in dental material; the two metals are atomized directly from the solid state in the graphite furnace of an atomic absorption spectrometer. The feasibility of this technique was demonstrated by analyzing 14 whole erupted or unerupted human teeth. To the authors' best knowledge, the direct-atomization technique has not been employed previously in the analysis of dental material.

The main component of teeth is hydroxyapatite; minor constituents are proteins, amino acids and other organic compounds. The concentrations of lead in human teeth may range from about 1 p.p.m. up to about 100 p.p.m.

EXPERIMENTAL

Apparatus

The measurements were made with a Perkin-Elmer 303 atomic absorption spectrophotometer equipped with an arc source deuterium lamp for background correction. The construction of the graphite furnace (heated by a high-frequency induction generator) has been described elsewhere[1]. The signals from the photometric detector were registered with a 2-channel recorder; one of the channels plotted the peak (in percent absorption) and the other transformed the detector signal into absorbance and gave the integrated peak area.

The teeth were crushed manually in an agate mortar and pestle; pulverizations were made either manually or automatically in equipment of the same material. To prevent losses, the mortar was partly covered during crushing and pulverization.

Weighings were made with semi-micro or micro balances. Nylon-meshed sieves were employed.

The measurements were made at the following wavelengths: cadmium at 228.8 nm and lead at 283.3 nm.

Reagents and standard solutions

Hydroxyapatite for column chromatography (BioGel HTP, Bio-Rad Labs., U.S.A.) was employed as the solid standard. Before use the reagent was finely pulverized in an agate mortar.

Metal standard solutions were prepared from cadmium sheet or lead wire (both from Koch-Light and of purity 99.999%).

The acids were of "Suprapur" quality from E. Merck. The furnace was purged with argon (purity 99.9% by volume).

Separate primary standard solutions (1000 p.p.m. of the element) of cadmium and lead were prepared by dissolving 1 g of metal in 15 ml of nitric acid (1 + 1) and diluting the solutions to 1 l. Secondary standard solutions containing 500 p.p.b. of cadmium or 30 p.p.m. of lead, both 3% in nitric acid, were also prepared.

From the latter solution, a series of six 250-ml solutions, 3% in nitric acid, and covering the concentration range 0.15–0.90 p.p.m. lead was prepared. From the 500 p.p.b. cadmium solution, a similar series, also 3% in nitric acid, and covering the range 10–50 p.p.b. was prepared.

Samples

The teeth were cleaned carefully by scraping (with equipment made of plastic material) and brushing. The samples were then pulverized to pass a 100-mesh (149 μm) sieve; from this portion smaller amounts were ground to pass a 270-mesh (53 μm) sieve. The samples were stored in glass sample bottles.

Investigations of the hydroxyapatite

The original plan was to use hydroxyapatite as a matrix in the preparation of solid synthetic standards. The purity of the reagent was established by emission spectrography which gave the following results: lead 1 p.p.m.; copper 10 p.p.m.; manganese < 10 p.p.m.; silver < 1 p.p.m. The following elements were sought, but were found to be below the detection limits (given in p.p.m.): chromium (1); nickel (1); and cadmium (100).

The contents of cadmium and lead in the hydroxyapatite were also established by stripping voltammetry. Three 250-mg portions were analyzed by the standard addition technique and the concentrations of the two metals were found to be: cadmium, 0.29 p.p.m. ($s = 0.042$ p.p.m.; $s_r = 14\%$); and lead, 2.8 p.p.m. ($s = 1.00$ p.p.m.; $s_r = 35\%$).

As is apparent from the above preliminary analyses, the concentration of lead (and presumably also of cadmium) is about the same as in teeth; it was therefore decided to employ the hydroxyapatite as the solid standard, and to establish the contents of the two metals by analyzing solutions in the graphite furnace according to the standard addition technique. These analyses were made as follows: 1.3 g of hydroxyapatite was dissolved in 3.0 ml of nitric acid (1 + 1), and the solution was diluted to 25 ml with water. From this solution, five 1.00-ml portions were transferred into five of a series of six small sample bottles. From four different lead standard solutions 1.00 ml was added to four bottles, and to the fifth bottle 1.00

ml of 3% nitric acid was added; the sixth bottle contained a blank of 3% nitric acid.

For the determination of cadmium, a corresponding series of solutions and a blank were prepared.

From all solutions, 25 μl was transferred by syringe to the furnace, and water was removed by 60-s evaporation at about 100°C. Cadmium was determined by 60-s ashing at 300°C, and atomization at 1000°C for 30 s; the tube was then cleaned by 60-s heating at 1950°C. Lead was determined by ashing at 450°C, and atomizations were made by 30-s heating at 1200°C, followed by a final cleaning step as for cadmium. The present atomization temperatures are considerably lower than those recommended by other authors[2]. The low atomization temperatures have the important advantage of volatilizing the elements before any appreciable amounts of smoke are evolved from the matrix. The evolution of smoke becomes marked when the temperature reaches 1400°C.

The positions of the two standard addition curves were established by the method of least squares. The contents of cadmium and lead in the hydroxyapatite were calculated to be: cadmium 0.35 p.p.m. ($s=0.026$ p.p.m.; $s_r=7.0\%$), lead 2.4 p.p.m. ($s=0.19$ p.p.m.; $s_r=8.0\%$).

Determinations in duplicate of the content of water in the hydroxyapatite were made by drying for 2 h at 105–110°C (2 h was sufficent to obtain constant mass). The average was found to be 2.3%

Procedure

Before the start of the measurements, the hollow-cathode and deuterium lamps were heated for about 1 h. The flow of argon was adjusted to 6 ml s^{-1}, and 0.5–3.0 mg of the solid sample or standard were weighed in a small tantalum scoop and placed in the middle of the preheated graphite tube by means of a specially constructed adjustable inserting device (the tantalum scoops and the inserting device are produced by Perkin-Elmer). The scoops were reweighed and the furnace was moved into its preadjusted position.

Five portions of the sample and four portions of the standard were dried, ashed and atomized as follows. For cadmium, drying was done at about 150°C for 60 s, ashing at 350°C for 60 s, atomization at 1400°C for 30 s, and cleaning of the tube at 1950°C for 60 s. For lead, drying and ashing were done as for cadmium, atomization at 1600°C, and cleaning as for cadmium. The amounts of the standard were varied to obtain a calibration curve from the integrated peak areas recorded. Some typical absorption signals are reproduced in Fig. 1.

RESULTS

Analytical data from determinations of cadmium and lead in 14 whole erupted or unerupted human teeth are listed in Table I; the contents of water are also listed. The latter determinations were made as described above for the analysis of hydroxyapatite.

The main advantages of the present technique, compared to other methods for trace metal analysis of dental materials, such as stripping voltammetry, are that the decomposition step is omitted, that no reagents are added, and that only small sample amounts are required.

TABLE I

ANALYTICAL RESULTS FOR CADMIUM AND LEAD

Sample designation	*Cadmium*				*Lead*				*Content of water (%)*
	n[a]	$\bar{x}$ *(p.p.m.)*	s	s_r	n	$\bar{x}$ *(p.p.m.)*	s	s_r	
2	5	0.09	0.033	37	5	2.2	0.18	8	5.2
6	5	0.23	0.054	23	5	1.1	0.12	11	3.5
7	4	0.21	0.082	39	5	2.2	0.20	9	4.4
9b(r)[b]	5	2.2	0.16	7	5	1.5	0.19	13	5.2
12	5	0.87	0.13	15	5	4.9	0.68	14	4.4
16(r)	4	0.56	0.060	11	5	1.6	0.24	15	3.8
17(r)	5	0.07	0.011	16	5	3.1	0.32	10	5.9
19	5	1.0	0.12	12	5	2.4	0.20	8	4.5
20	5	0.49	0.12	24	5	2.3	0.24	10	4.3
23(r)	4	0.49	0.15	31	5	1.4	0.24	17	3.7
28	5	0.15	0.013	9	5	1.4	0.24	17	4.2
29	5	0.20	0.036	18	5	1.9	0.17	9	4.6
37(r)	4	1.6	0.25	16	5	6.4	0.50	8	5.1
41(r)	4	1.2	0.33	28	5	1.1	0.12	11	3.3

[a] n, Number of analyses; $\bar{x}$, average; s, standard deviation; s_r, relative standard deviation.
[b] (r) = Unerupted.

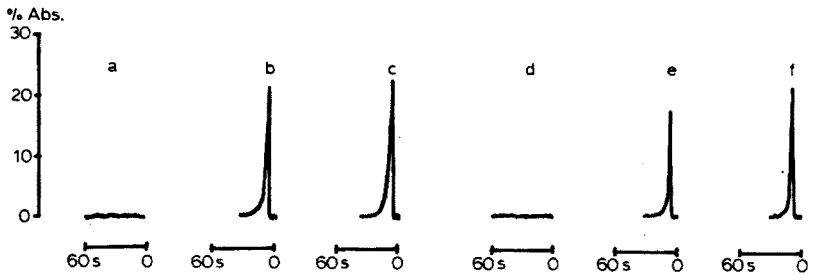

Fig. 1. Typical signals obtained for cadmium from: (a) the empty furnace, (b) $4.40 \cdot 10^{-10}$ g of cadmium in 1.272 mg of hydroxyapatite, (c) $5.00 \cdot 10^{-10}$ g of cadmium in 1.028 mg of a tooth; and for lead from: (d) the empty furnace, (e) $5.50 \cdot 10^{-9}$ g of lead in 2.306 mg of hydroxyapatite, (f) $7.36 \cdot 10^{-9}$ g lead in 3.202 mg of a tooth.

The disadvantages are that the method is destructive, and that only one element can be determined at a time. The evaporation of the matrix may introduce systematic errors, but the good agreement obtained between the voltammetric results and the spectrometric results for hydroxyapatite indicates that such errors should not be serious.

SUMMARY

The direct-atomization technique of atomic absorption spectrometry was applied to the determination of cadmium and lead in 14 whole erupted or unerupted human teeth. Pulverized samples of 0.5–3 mg were dried, ashed and atomized in a graphite furnace; hydroxyapatite was used as the solid standard. The method is simple, rapid and sensitive, and no reagents are added to the samples.

REFERENCES

1 F. J. Langmyhr and Y. Thomassen, *Z. Anal. Chem.*, 264 (1973) 122.
2 See *e.g.* B. V. L'vov, *Spectrochim. Acta, Part B*, 24 (1969) 53.

Analytica Chimica Acta, 73 (1974) 87–95

ATOMIC ABSORPTION SPECTROMETRY OF THE LANTHANIDES IN MINERALS AND ORES

W. OOGHE and F. VERBEEK

Laboratory of Analytical Chemistry, University of Ghent, J. Plateaustraat 22, B-9000 Ghent (Belgium)

(Received 17th April 1974)

Fundamental research and many applications based on the physical properties of the lanthanides, require pure products or at least products of known composition. Even small impurities can influence these properties. The lanthanides are also a very important group of elements for geochemists and geophysicists. Their geochemical coherence in ores is so pronounced that only drastic geological changes will cause fractionation of the original composition. This phenomenon is considered to be a source of information about geological processes. Many methods and techniques are available for the determination of the lanthanides[1,2]. Today it is necessary to have available rapid analytical methods with low detection limits, which combine accuracy and precision. Most of the existing methods are industrially applicable only with difficulty because of the sophisticated instrumentation necessary, or because of lack of sensitivity for trace analysis, or because they are too time-consuming.

Atomic absorption spectrometry (a.a.s.) can offer a solution to these problems. The nitrous oxide—acetylene flame has proved to be very useful for the analysis of refractory metals, and a.a.s. can be considered a rapid, simple, sensitive and accurate method of determining lanthanides, relatively free of interferences. However, so far practically no quantitative analysis for lanthanides has been carried out in the presence of a complex matrix[3–18]. The purpose of this investigation was to examine the possibilities of a.a.s. as a quantitative method of determining lanthanides in a complex matrix, even when they are present in trace amounts.

EXPERIMENTAL

Instrumentation

An atomic absorption spectrophotometer (Perkin-Elmer 303) fitted with a laminar nitrous oxide–acetylene burner (5-cm slot, high sampling type), Intensitron hollow-cathode lamps and an adjustable corrosion-resistant tantalum nebulizer were used.

Reagents

All chemicals were reagent grade and were used without further purification. The lanthanide standard solutions were prepared by dissolution of the lanthanide oxides (Trona and Fluka, >99.9% purity) in 6 *M* hydrochloric acid; before being weighed the oxides were heated in a furnace at 900°C. After removal of the solvent by means of an i.r. lamp the chlorides obtained were redissolved in slightly

acidic demineralized water to obtain lanthanide concentrations of 1 or 10 g l^{-1}.

Buffer solutions of potassium chloride or sodium chloride (20 g l^{-1}) were used to prevent ionization interferences and to improve sensitivity.

Optimal working conditions

Instrumental parameters. All instrumental parameters were adjusted to obtain a straight working curve through the origin with as high a slope as possible.

Sensitivity enhancement. Because of the high energy of the nitrous oxide–acetylene flame, 35–80% of the lanthanide atoms are ionized[10]. These ions are lost to the determination, which causes a decrease in sensitivity. The addition of a material with a lower ionization potential (such as alkali metals) represses the ionization of the element of interest by the increased electron density in the flame[19]. The addition of potassium or sodium ions thus enhances the sensitivity because of the higher proportion of absorbing atoms present. The increase in sensitivity as a function of the potassium concentration is presented in Fig. 1.

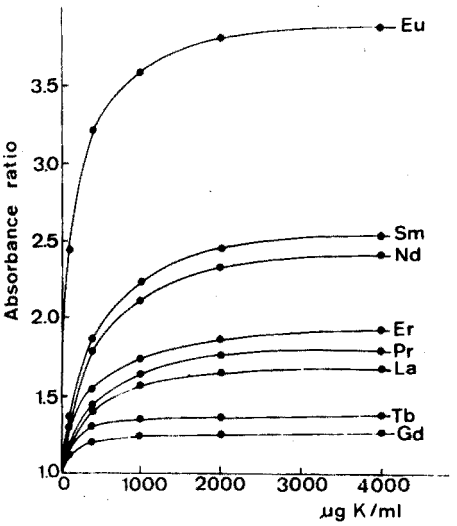

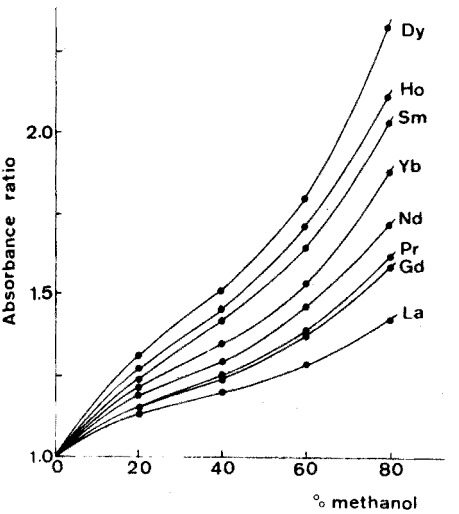

Fig. 1. Increase of the absorbance ratio as a function of the concentration of potassium ions.

Fig. 2. Increase of the absorbance ratio as a function of the percentage of methanol.

Organic solvents that are miscible with water, such as methanol, also increase the sensitivity because of the more efficient atomization, the lower surface tension and the less endothermic nature of the solvent[12,19]. Figure 2 shows the effect of the methanol content on the absorbance.

Working curves. Because the amount of sample is limited by the use of the nitrous oxide burner, and because some lanthanides are present only in trace concentrations, determinations must be carried out in the absorption region up to 25% absorbed light. It was shown for all lanthanides that in this region the working curves are straight lines in a solution of 80% methanol buffered with potassium or sodium ions.

Sensitivity and detection limits. From the analytical sensitivity, determined in

TABLE I

OPTIMAL WORKING CONDITIONS AND SENSITIVITY FOR THE LANTHANIDES

Element	*Wavelength (nm)*	*Spectral width (nm)*	*Lamp current (mA)*	*Burner height (m)*	*Ratio C_2H_2/N_2O*	*Sensitivity ($\mu g\ ml^{-1} \cdot 1\%$)*	*Detection limit ($\mu g\ ml^{-1}$)*
La	550.13	0.136	30	10–11.5	6.4/7.5	14.8	2.5
Pr	495.14	0.136	30	10	6.3/7.5	12.7	5.0
Nd	492.45	0.136	30	10–11.5	6.3/7.5	3.2	0.7
	463.42	0.136	30	10–11.5	6.3/7.5	4.6	1.0
Sm	429.67 (u.v.)	0.235	30	10	6.3/7.5	2.5	0.8
Eu	459.40	0.470	20–25	7–8.5	6.0/7.5	0.17	0.05
Gd	407.87	0.068	30	11.5–13	6.4/7.5	9.3	3.0
Tb	432.65	0.136	20	11.5	6.5/7.5	6.6	2.0
Dy	421.17 (u.v.)	0.068	20	10	6.4/7.5	0.60	0.3
Ho	410.38	0.235	20	10–11.5	6.5/7.5	0.54	0.1
Er	400.80	0.235	20	10	6.4/7.5	0.41	0.1
Tm	371.79	0.235	20	8.5–10	6.4/7.5	0.27	0.1
Yb	398.80	0.235	20–25	7	6.0/7.5	0.090	0.02

the presence of a lanthanide matrix, the approximate detection limit was obtained, taking into account the background signal. Table I summarizes the optimal working conditions and the analytical sensitivities and detection limits for the lanthanides studied.

Accuracy and precision

The accuracy of the a.a.s. determination for several lanthanides was checked by analysing synthetic lanthanide mixtures of known composition. Table II shows good agreement between the found and the added values for europium and holmium. Europium was also determined in some commercial lanthanide oxides of high purity both by a.a.s. and by an independent method, pulse polarography[20]. The agreement between the results obtained (Table III) indicates the good accuracy of the method. This was also confirmed by means of parallel flame emission spectrometric determinations of lanthanides in ores[21].

TABLE II

DETERMINATION OF EUROPIUM AND HOLMIUM IN A SYNTHETIC MATRIX OF LANTHANI

(360 μg ml^{-1} La, Nd, Gd; 90 μg ml^{-1} Dy, Er, Yb)

	Added (μg ml^{-1})	*Found* (μg ml^{-1})						*Mean* (μg ml^{-1})	*s* (%)
Eu	1.80	1.79	1.81	1.81	1.81	1.82	1.83	1.81	0.73
Ho	4.50	4.47	4.48	4.52	4.53	4.55	4.57	4.52	0.84

TABLE III

DETERMINATION OF EUROPIUM IN GADOLINIUM AND SAMARIUM OXIDES BY A.A.S. AND PULSE POLAROGRAPHY

Product	*A.a.s.* (*p.p.m. Eu*)	*Pulse polarography* (*p.p.m. Eu*)
Gd_2O_3 (Fluka 99.9%)	16±1	16.4±0.8
Gd_2O_3 (Trona 99.9%)	304±6	297±10
Sm_2O_3 (Fluka 99.9%)	72±2	71.5±4

Spectral interference

An examination for spectral interferences demonstrated that only the 492.453-nm neodymium line is unsuitable for neodymium determinations in the presence of praseodymium[21]. Because praseodymium and neodymium are adjacent in the periodic system and both belong to the group of the light lanthanides, they usually occur together in minerals and ores.

The neodymium determinations must be carried out either at the 492.453-nm line after separation of praseodymium, or at the less sensitive but interference-free 463.42-nm line.

Procedure

The mineral or ore is mechanically ground to powder in an agate mortar in order to obtain a homogeneous sample. The amount of sample, limited on one side by homogeneity requirements and on the other side by the use of the nitrous oxide burner, is situated between 0.5 and 1.5 g in 50 ml of solution. This can give some problems for the less sensitive lanthanides and especially for those which are present in trace amounts. The ore is quantitatively dissolved in 20 ml of hydrochloric acid (bastnasite and gadolinite) or perchloric acid (monazite), together with a few drops of an oxidant such as hydrogen peroxide or nitric acid. After dissolution by heating, the solution is evaporated to dryness. The silicic acid present is dehydrated by heating for 1–2 h at 115°C. The residue is redissolved in hydrochloric acid and filtered after heating and dilution. The filtrate is reduced to about 8 ml by evaporation and then diluted to 50 ml with 2 ml of the alkali buffer solution and methanol.

To check this procedure, some lanthanides were redetermined by dissolving the ore in a mixture of 20% sulphuric acid in hydrofluoric acid[2, 22]. The sulphates obtained were treated with sodium hydroxide to precipitate the rare earths as their hydroxides. This precipitate was filtered off and redissolved in hydrochloric acid after washing. The standard addition technique was applied to eliminate chemical, ionization and matrix interferences. The final concentrations of the additions were C, $2C$ and $3C$ selected in such a way that the solution with a concentration $3C$ absorbed about 20% of light; the unknown concentration is made to approach C by varying the amount of sample solution.

Because the standard addition technique is time-consuming, a procedure with a comparison standard was developed. For samples of about the same origin and composition, the following equation can be applied

$$A_x/A_s = C_x/C_s$$

where A_x and A_s, respectively, are the absorbances of an arbitrary lanthanide in the unknown and in the comparison standard, and C_x and C_s are the corresponding concentrations.

If the same amounts of sample are weighed the equation can be formulated as

$$P_x = A_x P_s / A_s$$

where P_x and P_s, respectively, are the percentages of an arbitrary lanthanide oxide in the unknown and in the comparison standard.

From the measured absorbances (A_x and A_s), P_x can be calculated when P_s is known and when the measured absorbance values are situated in the linear part of the working curve. P_s can be determined by means of the standard addition technique.

RESULTS

Bastnasite and monazite, two industrially important minerals, were analysed for the 12 considered lanthanides and yttrium, by the standard addition technique. Also the total rare earth oxides[22, 23] and the cerium content[23] were, respectively,

determined gravimetrically and titrimetrically. Because of a shortage of sample, the gadolinite analysis was limited to the heavier lanthanides (samarium–ytterbium).

The results presented in Table IV are the average oxide values of at least three determinations, which in all cases agreed within a few percent. Both bastnasite samples originated from Burundi. The monazite sample was mineral 71aG of the Bureau of Analysed Samples Ltd (England). The gadolinite originated from Iveland (Norway).

TABLE IV

DETERMINATION OF THE LANTHANIDES AND YTTRIUM IN BASTNASITE (TWO DIFFERENT SAMPLES), MONAZITE AND GADOLINITE

Lanthanide oxide	*Bastnasite A (%)*	*Bastnasite B (%)*	*Monazite (%)*	*Gadolinite (%)*
La_2O_3	16.5	16.8	12.6	—[c]
CeO_2[a]	31.9	32.4	27.4	—[c]
Pr_6O_{11}	2.68	2.75	3.19	—[c]
Nd_2O_3	9.04	9.21	11.4	—[c]
Sm_2O_3	1.27	1.33	2.21	1.92
Eu_2O_3	0.192	0.203	0.0359	0.00266
Gd_2O_3	0.280	0.300	1.025	2.73
Tb_4O_7	0.032	0.033	0.112	0.715
Dy_2O_3	0.0487	0.0508	0.384	4.50
Ho_2O_3	0.0064	0.0065	0.0496	0.767
Er_2O_3	0.0085	0.0089	0.0691	1.95
Tm_2O_3	0.0007	0.0008	0.0064	0.312
Yb_2O_3	0.0018	0.0019	0.0236	2.05
Y_2O_3	0.166	0.170	1.11	—[c]
$\Sigma Ln_2O_3 + Y_2O_3$	62.2	63.3	59.6	—[c]
$\Sigma Ln_2O_3 + Y_2O_3 + Sc_2O_3 + ThO_2$ (gravimetry)	64.4	65.5	67.0[b]	—[c]

[a] Titrimetric determination of cerium(IV) with iron(II).
[b] The percentage of ThO_2 amounts to 6.5%.
[c] Not determined.

Table V shows the results obtained for the determination of europium in 7 different bastnasite samples by the procedure with a comparison standard. The agreement between the two techniques is very satisfactory.

The results in Tables II–V show that a.a.s. is very suitable for the direct analysis of minerals, ores and various lanthanide compounds. In minerals and ores the less sensitive light lanthanides are generally present in a larger amount than the more sensitive heavy lanthanides. This results in a satisfactory a.a.s. sensitivity for such analyses.

By plotting the lanthanide content in bastnasite and monazite versus the atomic number Z on semilogarithmic paper[25], a typical lanthanide pattern is obtained with an alternation in abundance between the adjacent even-Z and odd-Z elements (Figs. 3 and 4). This is a classic example of the Oddo–Harkins rule. By dividing each distribution, element by element, by the known distribution

TABLE V

DETERMINATION OF EUROPIUM IN BASTNASITE BY THE STANDARD ADDITION AND COMPARISON STANDARD TECHNIQUES

Sample	*Stand. addition*	*Comparison standard*	
	Eu_2O_3 (%)	A_x	Eu_2O_3 (P_x in %)
1[a]	0.216	0.1160	0.213
2	0.185	0.1029	0.189
3	0.147	0.0822	0.151
4	0.212	0.1148	0.211
5	0.255	0.1412	0.259
6	0.199	0.1062	0.195
7	0.176	0.0964	0.177
8 (stand.)	0.184 (P_s)	0.1002 (A_s)	—

[a] Results obtained by neutron activation analysis[24]: 0.2% Eu_2O_3 and 0.3% Gd_2O_3. Samples 1–5 contain respectively: 0.315, 0.410, 0.352, 0.552, and 0.519% Gd_2O_3 (a.a.s.).

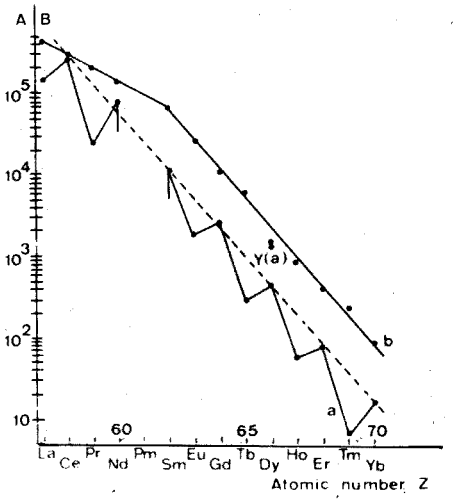

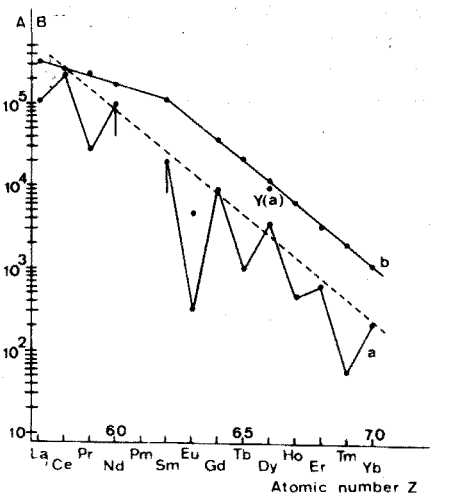

Fig. 3. Concentration of lanthanides and yttrium in bastnasite as a function of the atomic number Z. Curve a: ordinate values A are p.p.m. of lanthanides as determined by a.a.s. Curve b: ordinate values B give the ratios *vs.* the chondritic standard: p.p.m. of lanthanides in bastnasite/p.p.m. of lanthanides in the chondritic standard.

Fig. 4. Concentration of lanthanides and yttrium in monazite as a function of the atomic number Z. Curve a: ordinate values A are p.p.m. of lanthanides as determined by a.a.s. Curve b: ordinate values B give the ratios *vs.* the chondritic standard: p.p.m. of lanthanides in monazite/p.p.m. of lanthanides in the chondritic standard.

of a standard, here the average composition of 20 chondrites[26], a broken line is obtained as shown in Figs. 3 and 4.

For bastnasite and monazite, the proposition of Semenov[27,28] can be confirmed. This author showed that in minerals, selective for the light rare earths,

the logarithm of the abundances of the even-Z (or odd-Z) elements decreases approximately linearly with increasing atomic number. Because Masuda[29] has shown that the reciprocals of the ionic radii are linear functions of the atomic number, this behaviour can be attributed to a strict requirement for similarity of ionic radii between the principal lattice cation and the cations being admitted. In this way a.a.s. has proved to be a useful method for the geochemical study of the lanthanides.

The authors thank Dr. H. Deelstra and Mr. B. M. Aderca for providing the bastnasite samples.

SUMMARY

A method is described for a rapid, sensitive, accurate and precise determination of 12 lanthanides and yttrium by a.a.s. In most analyses the standard addition technique was used to eliminate chemical, ionization and matrix interferences. For samples of similar origin, a procedure with a comparison standard was developed; this proved to be very suitable for routine analyses. The lanthanides and yttrium were determined in bastnasite, monazite and gadolinite. The analyses were performed on solutions containing a maximum sample concentration of 30 g l^{-1} in 80% of methanol and buffered with alkali ions. The accuracy of the method was checked by independent procedures such as gravimetry, pulse polarography and flame emission spectrophotometry.

REFERENCES

1 F. H. Spedding and A. H. Daane, *The Rare Earths*, Wiley, New York, 1961, Chs. 23, 24.
2 R. C. Vickery, *Analytical Chemistry of the Rare Earths*, Pergamon, Oxford, 1961.
3 L. S. Nelson and N. A. Kuebler, *Spectrochim. Acta*, 19 (1963) 781.
4 R. K. Skogerboe and R. A. Woodriff, *Anal. Chem.*, 35 (1963) 1977.
5 V. G. Mosotti and V. A. Fassel, *Spectrochim. Acta*, 20 (1964) 1117.
6 M. D. Amos and J. B. Willis, *Spectrochim. Acta*, 22 (1966) 1325.
7 V. A. Fassel, V. G. Mosotti, W. E. L. Grossman and R. N. Kniseley, *Spectrochim. Acta*, 22 (1966) 347.
8 K. E. Friend and A. J. Diefenderfer, *Anal. Chem.*, 38 (1966) 1763.
9 H. L. Kahn, *J. Chem. Educ.*, 43 (1966) XXV.
10 D. C. Manning, *At. Absorption Newslett.*, 5 (1966) 63, 127.
11 W. Slavin, *Appl. Spectrosc.*, 20 (1966) 281.
12 R. J. Jaworowski, R. P. Weberling and D. J. Bracco, *Anal. Chim. Acta*, 37 (1967) 284.
13 J. Kinnunen and O. Lindsjö, *Chem. Anal.*, 56 (1967) 25, 76.
14 F. Fernandez and D. C. Manning, *At. Absorption Newslett.*, 7 (1968) 57.
15 W. Slavin, *Atomic Absorption Spectroscopy*, Interscience, New York, 1968.
16 J. C. Van Loon, H. M. Aarden and J. H. Galbraight, *Analyst (London)*, 96 (1971) 47.
17 R. L. Scott, *At. Absorption Newslett.*, 9 (1970) 46.
18 T. Ishizuka and H. Sunahara, *Anal. Chim. Acta*, 66 (1973) 343.
19 C. D. Christian and F. J. Feldman, *Atomic Absorption Spectroscopy*, Wiley–Interscience, New York, 1970.
20 P. Vermeiren, doctoral dissertation, University of Ghent, 1973.
21 W. Ooghe, to be published.
22 W. R. Schoeller and A. R. Powell, *The Analysis of Minerals and Ores of the Rarer Elements*, Griffin, London, 1940.

23 C. L. Wilson and D. W. Wilson, *Comprehensive Analytical Chemistry*, Vol. 1 C, Elsevier, Amsterdam, 1962.
24 B. M. Aderca, personal communication.
25 L. A. Haskin, F. A. Frey, R. A. Schmitt and R. H. Smith, *Physics and Chemistry of the Earth*, 7 (1966) 167.
26 L. A. Haskin, T. R. Wildeman and M. A. Haskin, *J. Radioanal. Chem.*, 1 (1968) 337.
27 E. I. Semenov, *Geochem.*, 7 (1957) 735.
28 E. I. Semenov, *Geochem.*, 5 (1958) 574.
29 A. Masuda, *Inst. Nucl. Study, Tokyo, INSJ-54*, 1963.

Analytica Chimica Acta, 73 (1974) 97–106

THE BEHAVIOUR OF METAL TETRAMETHYLENEDITHIOCARBAMATES IN THE GRAPHITE-TUBE FURNACE FOR ATOMIC ABSORPTION SPECTROMETRY

S. GOMIŠČEK, Z. LENGAR, J. ČERNETIČ and V. HUDNIK

Department of Chemistry and Chemical Institute "Boris Kidrič", University of Ljubljana (Yugoslavia)

(Received 25th March 1974)

The role of organic reagents and solvents in flame atomic absorption spectrometry has been known for a long time. Their use is interesting from the points of view of enhancement of sensitivity of measurement, and the possibilities for preconcentration and separation from interfering elements[1–3].

In atomic absorption spectrometry, metals are often determined after they have been extracted in the form of metal tetramethylenedithiocarbamates (MeTMDTC); either the organic solutions are directly sprayed into the flame, or they are atomized in a graphite-tube furnace[4–7]. There are no detailed data about the behaviour of metal chelates in flameless atomic absorption spectrometry to be found in the literature. The only exception is the work of Aggett and West[8], who studied the behaviour of trace metals extracted from aqueous solutions into organic solvents, in the carbon filament atom reservoir for atomic absorption and atomic fluorescence spectrometry.

The present paper deals with the results of an investigation in which some phenomena during the atomization of MeTMDTC in the graphite-tube furnace were observed. Attempts to explain these observations were made by studying the behaviour of MeTMDTC in argon and oxygen at high temperatures.

EXPERIMENTAL

Apparatus

The measurements were made with a Perkin-Elmer graphite-tube furnace, HGA 70, in conjunction with a Jarrell-Ash atomic absorption spectrophotometer model 82–500. The graphite-tube furnace replaced the normal burner. The apparatus has a 0.5-m Ebert monochromator with gratings blazed for 180 nm and 500 nm (1180 grooves/mm) and continuously adjustable curved slits. The reciprocal linear dispersion in the first order is 1.6 nm mm^{-1} and the resolution is 0.02 nm. Westinghouse hollow-cathode lamps were used; the light was modulated with a mechanical chopper (150 Hz), and a Hamamatsu photomultiplier R 213 was used for detection of radiation. A Bristol recorder was used at a chart speed of 20 mm min^{-1}, and peak heights were measured. The temperature in the graphite-tube was 60°C or 100°C (T_1) in the drying stage, 230°C, 330°C, 490°C, 750°C, or 1100°C (T_2) during the destruction of organic substance, and 1600–2700°C (T_3) in the atomization stage. The conditions for measurement of individual elements are shown in Table I.

TABLE I

MEASUREMENT CONDITIONS

(In all cases, the drying temperature was 100°C for 20 s, except in procedure a, where the drying time was 25 s. The destruction time and the atomization times were 30 s and 20 s, respectively.)

Element	*Line (nm)*	*Lamp current (mA)*	*Destruction temp. (°C)*	*Atomization temp. (°C)*
				2450[a]
Cd	229	10	330[b]	1600[c]
Co	241	18	1100[b]	2450
Cu	325	10	1100[b]	2450
Fe	248	10	1100[b]	2450
Ni	232	22	1100[b]	2450
Pb	283	5	490[b]	2450
V	318	20	1100[b]	2450

[a] Procedure a.
[b] Only for procedure b; for procedure a, variable 60–1100°C.
[c] Procedure b.

Reagents

Ammonium tetramethylenedithiocarbamate (NH_4TMDTC), synthesized by the method of Schöffmann and Malissa[9], was used as an aqueous 2% (w/v) solution. Sodium tetramethylenedithiocarbamate (NaTMDTC; p.a. Merck) was used as an aqueous 0.5% (w/v) solution.

All organic solvents were A.R. quality, and were not specially purified or dried. Redistilled water from a Heraeus quartz apparatus was used.

Preparation of organic MeTMDTC solutions

The experiments in the graphite-tube furnace were performed with organic solutions of MeTMDTC, which were obtained by precipitation, filtration and dissolution of the metal carbamate in the organic solvent (procedure a), or with organic solutions after the extraction of the metal carbamate (procedure b).

Procedure a: MeTMDTC were prepared by the addition of 0.2 ml of NaTMDTC or NH_4TMDTC solution to 0.5 ml of a standard metal ion solution (100 $\mu g\ ml^{-1}$). The precipitate was filtered, dried at *ca.* 80°C, and dissolved in organic solvent, and the solution was diluted to a concentration of 0.4 $\mu g\ ml^{-1}$, 2.0 $\mu g\ ml^{-1}$, and 0.2 $\mu g\ ml^{-1}$ for nickel, vanadium and the other metals investigated, respectively. An aliquot (10 μl) of the solution was transferred to the graphite-tube furnace with an Eppendorf micropipette, and the absorption at the resonance spectral line of the element considered was then measured.

An aqueous solution of the examined metal was measured for comparison; its concentration was the same as in the case of a particular MeTMDTC organic solution.

Procedure b: A solution of the MeTMDTC was prepared by pouring 5 ml of redistilled water and the standard metal solution into a separating funnel, adjusting the pH to 2–3, and precipitating the metal ions with a 2% (w/v) solution

of NH_4TMDTC. The metal chelate obtained was extracted with 25 ml of organic solvent (in 10+10+5-ml portions). Before the first and the second extractions, 1 ml of a 2% solution of NH_4TMDTC was added, and 0.5 ml of the same solution was added before the last extraction; every successive extraction was preceded by adjustment of the pH to 2–3. All three extracts were collected in a 25-ml measuring flask, and then the solvent was added to dilute the solution to the mark. Aliquots (5 μl) of the solution were transferred to the graphite-tube furnace. The absorption was measured at the resonance spectral line of the element investigated.

RESULTS

The results of the experiments where MeTMDTC were precipitated, filtered,

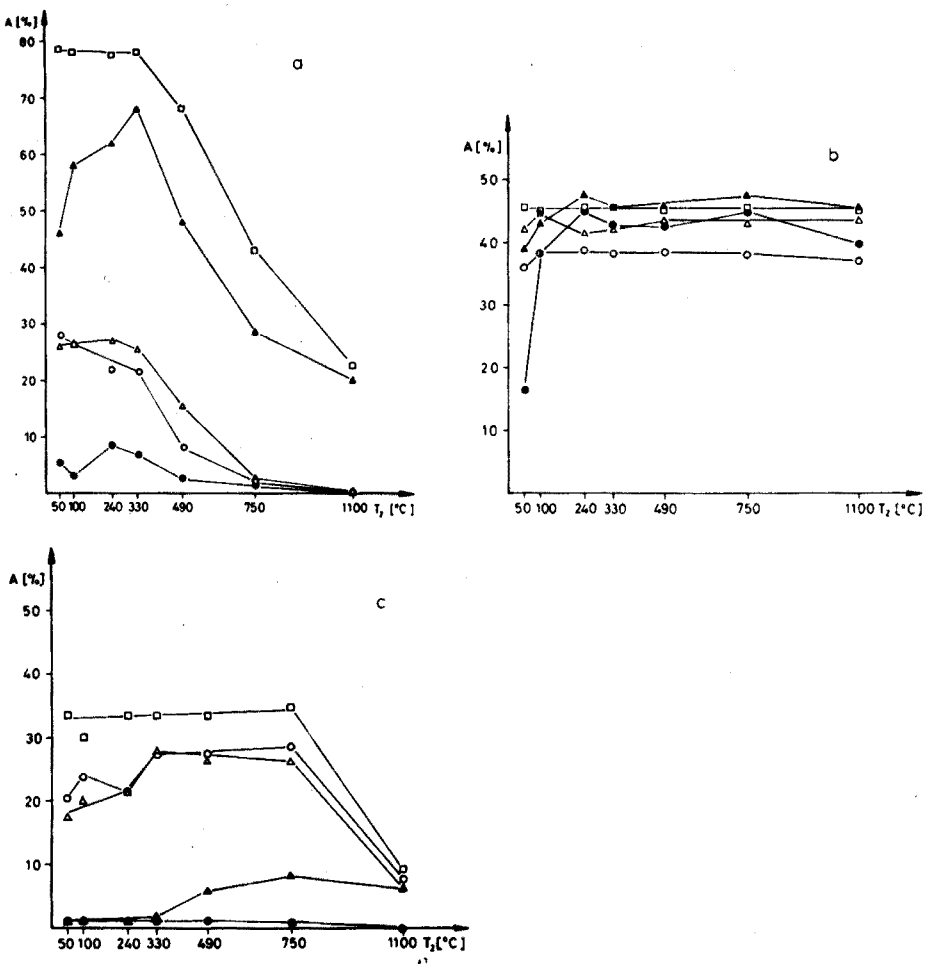

Fig. 1. The influence of the destruction temperature on the absorption of cadmium (Fig. 1a), copper (Fig. 1b), and lead (Fig. 1c). MeTMDTC in the various solvents; 0.2 μg Me ml^{-1}; other conditions as in Table I. (□) Water, (○) MIBK, (△) ethyl acetate, (●) carbon tetrachloride, (▲) chloroform.

and then dissolved in an organic solvent (procedure a), are shown in Fig. 1 for cadmium, copper and lead; the solvents used were methyl isobutyl ketone (MIBK), ethyl acetate, chloroform and carbon tetrachloride. The curves show the dependence of the absorption peaks on the destruction temperature; the temperatures 60°C and 100°C, which are normally applied only in the drying stage, are also included.

The form of the curves indicates some of the characteristics which must be attributed to the properties of individual metals or their compounds, to the solvents used, and to the quantity of solution taken. The general form of the curves, which is valid for most of the elements, is similar to that for CuTMDTC (Fig. 1b). The curves are characterized by tendencies towards decreased absorption signals for the temperatures 60°C and 100°C, and by the relative constancy of the signals for destruction for temperatures from 200°C to 1100°C. Of the MeTMDTC examined (Cu, Cd, Ni, Pb, V, and Fe), cadmium and lad TMDTC deviate from this behaviour.

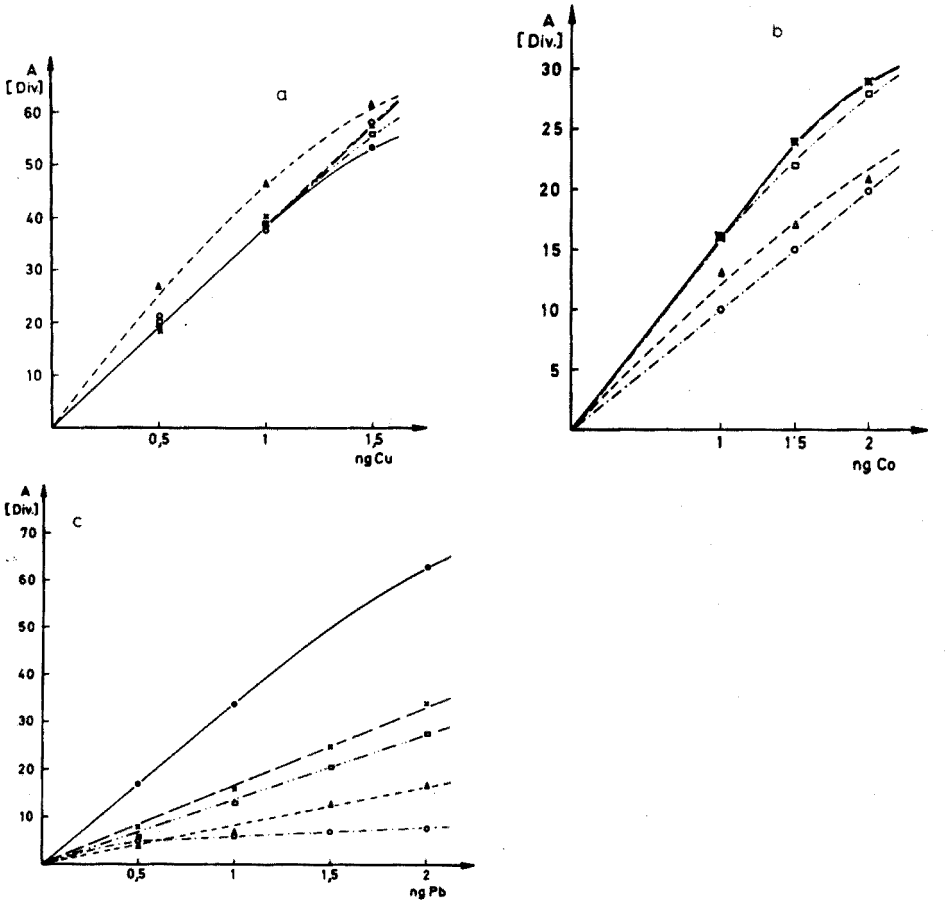

Fig. 2. The absorbance *vs.* concentration curves for CuTMDTC (Fig. 2a), CoTMDTC (Fig. 2b) and PbTMDTC (Fig. 2c). The conditions of measurement are given in Table I. (●) Water, (×) MIBK, (△) chloroform, (○) carbon tetrachloride, (□) ethyl acetate.

They show substantial lowering of the absorption signals at temperatures above 330°C and 750°C, respectively; this tendency is also found to some extent with copper at temperatures above 750°C. For most of these MeTMDTC the curves do not show large deviations for different solvent, except for cadmium and lead TMDTC where the differences are very large.

The results for organic solutions of MeTMDTC prepared by extraction (procedure b), generally show linear relationships between the height of the absorption peak and the concentration of the MeTMDTC. Typical curves for copper, cobalt and lead TMDTC in the solvents chloroform, MIBK, carbon tetrachloride, and ethyl acetate are shown in Fig. 2. The slope of the curve of absorption signal *vs.* concentration is affected by the organic solvent only for cobalt and lead TMDTC; there are no substantial differences with copper, cadmium and nickel TMDTC.

As is apparent from the description of the procedures for the preparation of the organic solutions of MeTMDTC, 10 or 20 μl of the solution were used in the first phase of the investigation. The heights of the absorption peaks measured were often considerably dispersed and the reproducibility was poor. A more detailed investigation showed that this was caused by a phenomenon which does not occur with aqueous solutions of these metal ions at the same concentrations. Under the experimental conditions described, the height of the absorption signal depended

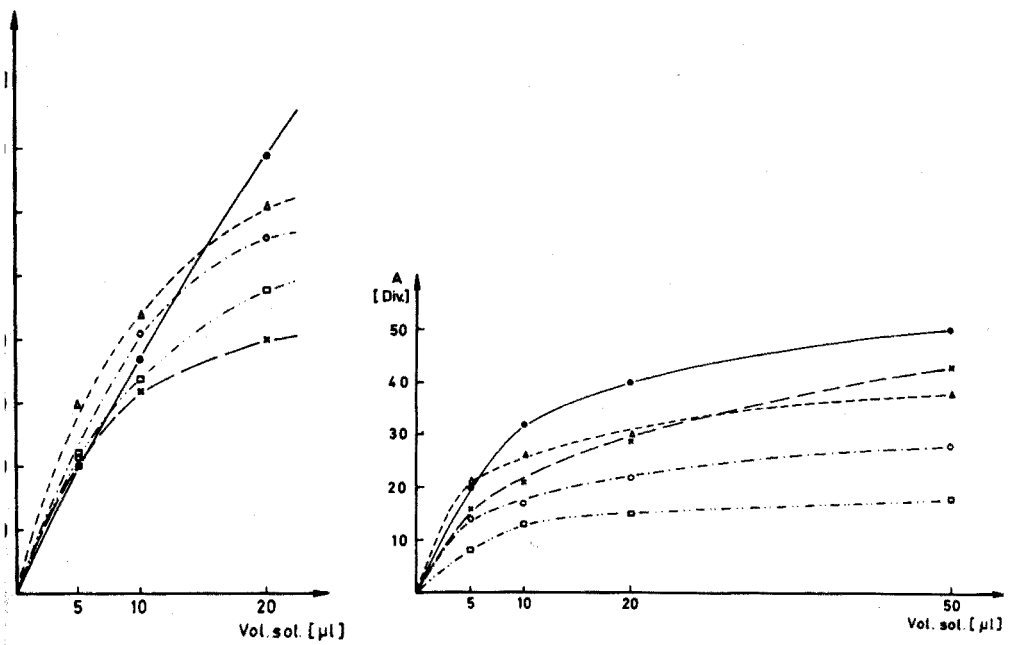

Fig. 3. The influence of volume of the solution, for some organic solvents, on the absorption of copper. 0.1 μg Cu ml^{-1}. (●) Water, (×) MIBK, (△) chloroform, (○) carbon tetrachloride, (□) ethyl acetate.

Fig. 4. The influence of volume of the solution on the absorption for some MeTMDTC in MIBK. (□) Pb (0.1 μg ml^{-1}, (○) Co (0.2 μg ml^{-1}), (△) Cd (0.02 μg ml^{-1}), (×) Ni(0.2 μg ml^{-1}), (●) Cu (0.1 μg ml^{-1}).

on the quantity of the organic solution which was injected into the graphite-tube furnace, dried, ignited, and atomized. Figure 3 shows this dependence of absorption on the volume of the solution for copper TMDTC, and Fig. 4 shows the phenomenon for various MeTMDTC with the solvent MIBK. It is apparent from both Figures that the critical quantity was 10 μl. If 5 μl of the solution were transferred several times in succession, and the solvent was evaporated after every addition, this phenomenon did not occur. This effect was also lessened or eliminated, if the surface of the inner side of the graphite tube was scratched perpendicularly to its axis.

The height of the absorption signal may also depend on the method of decomposition, which is primarily apparent with compounds of easily volatile elements.

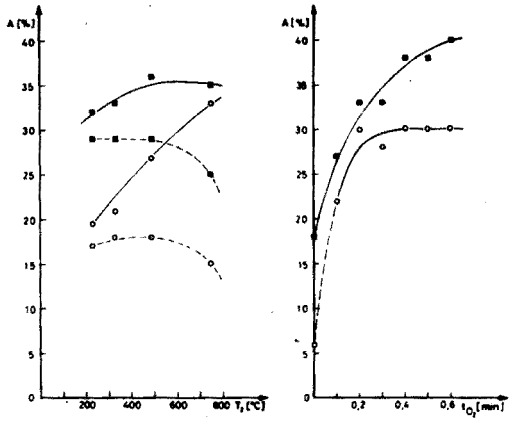

Fig. 5. The influence of oxygen and argon on the destruction of PbTMDTC. (——) O_2 atmosphere (----) Ar atmosphere. (■) Aqueous solution of Pb^{2+}, (○) PbTMDTC in methyl isobutyl ketone. T, temperature; t_{O_2}, time of introduction of oxygen into the furnace.

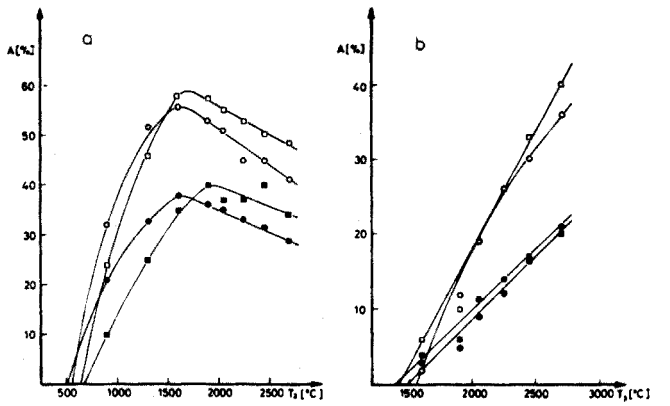

Fig. 6. The influence of the atomization temperature on the absorption of cadmium (a) and copper (b). (a): (■) Aqueous solution (0.1 ng Cd/5 μl), (□) aqueous solution (0.2 ng Cd/5 μl), (●) MIBK solution CdTMDTC (0.1 ng Cu/5 μl), (○) MIBK solution CdTMDTC (0.2 ng Cd/5 μl). (b): (■) Aqueous solution (0.5 ng Cu/5 μl), (□) aqueous solution (1 ng Cu/5 μl), (●) MIBK solution CuTMDTC (0.5 ng Cu/5 μl), (○) MIBK solution CuTMDTC (1 ng Cu/5 μl).

Figure 5 shows an example of this dependence for lead TMDTC with regard to the atmosphere (argon or oxygen) in which the destruction is performed. Decomposition in oxygen produces higher absorption signals and these increase with the temperature of ignition. The dependence of the intensity of the signal on the period of the exposure to oxygen shows that 0.4 min is necessary for lead TMDTC to reach a constant value of absorption.

Finally, the dependence of the absorption peaks on the temperature of atomization was studied. The curves for cadmium and copper TMDTC are shown in Fig. 6. Their forms are similar to those of the curves for aqueous solutions of cadmium and copper(II) ions, respectively.

DISCUSSION

A satisfactory and complete explanation of the behaviour observed is very difficult. In addition to information on the behaviour of MeTMDTC in argon and oxygen at higher temperatures, it is also necessary to consider the phenomena and the reactions at phase boundaries. With the present experimental techniques, however, this is practically impossible, primarily because of the subnanogram quantities of substances involved in possible reactions and processes, and because of the short duration of the atomization. Therefore, these phenomena can only be assessed on the basis of experiments performed in extreme and simulated conditions.

Nevertheless, it is possible, on the basis of the behaviour observed, to indicate the essential processes during the atomization of MeTMDTC in the graphite-tube furnace: at first, the organic solvent in the furnace evaporates, a low temperature of 100°C being sufficient; at the destruction temperature (below 330°C), the organic molecule of MeTMDTC decomposes to an inorganic compound or mixture of compounds, which give free metal atoms at the atomization temperature of 1600–2700°C.

This explanation is supported by the results of an investigation of some physical and chemical properties of MeTMDTC, and by a study of the destruction of MeTMDTC in argon and oxygen at high temperatures. The results of an x-ray diffraction study[10] of the decomposition products at the temperatures 150°C and 300°C, 400°C or 600°C are shown in Table II. It can be seen that in argon, MeTMDTC decompose to metal sulphides, whereas in oxygen, sulphides, oxides or mixtures of sulphides, oxides and sulphur oxy-compounds are formed, depending on the metal. Chemical microanalysis of the decomposition products showed that a considerable amount of carbon remains after the destruction of organic substances in argon, whereas in oxygen the ignition is almost complete.

Table III shows some data obtained by differential thermal analysis (DTA) and thermogravimetric analysis (TGA)[11] for the decomposition of MeTMDTC; it can be seen that they generally decompose between 200°C and 300°C. TGA measurements also showed that MeTMDTC do not sublimate—at least in observable amounts—below the temperature of their decomposition; this justifies the assumption that no losses of metal or MeTMDTC occur during the evaporation of the organic solvents.

Such a simplified scheme of the basic processes which occur during the atomization of MeTMDTC in a graphite-tube furnace can explain most of the experimentally obtained facts, particularly the curves of absorption *vs.* destruction

TABLE II

PRODUCTS OF DESTRUCTION OF SOME MeTMDTC IN ARGON AND OXYGEN

Carbamate	*Temp. (°C)*	*Argon*	*Oxygen*
$Cd(TMDTC)_2$	150	Carbamate	Carbamate
	300	CdS, unknown compound	CdO, CdS
$Co(TMDTC)_2$	150	Carbamate	Carbamate
	600	CoS_{1-y}[a]	Co_3O_4
$Cu(TMDTC)_2$	150	Unknown compound	Cu_2O, Cu_2S
	600	Cu_2S, CuS	CuO, Cu_2S, CuS[b]
$Fe(TMDTC)_3$	150	Unknown compound	Unknown compound
	600	FeS	Fe_2O_3
$Ni(TMDTC)_2$	150	Carbamate, NiS, Ni_7S_6	Carbamate
	600	NiS, Ni_7S_6, Ni_3S_2	NiO, $NiSO_4$
$Pb(TMDTC)_2$	150	Carbamate	Carbamate
	400	PbS	Pb_3O_4, PbO, PbS

[a] $y=0.11$–0.2.
[b] Temp. 400°C.

TABLE III

DECOMPOSITION TEMPERATURES OF SOME MeTMDTC IN ARGON ESTABLISHED BY DTA AND TGA

Carbamate	*DTA (°C)*	*TGA (°C)*
$Cu(TMDTC)_2$	270, 290	200
$Cd(TMDTC)_2$	325, 335	300
$Fe(TMDTC)_3$	260	225
$Ni(TMDTC)_2$	350	290
$Pb(TMDTC)_2$	282	250

temperature shown in Fig. 1. The low temperatures 60°C and 100°C do not suffice for decomposition of the carbamate molecule; therefore, decomposition occurs only at the atomization temperature, so that violent and perhaps also different parallel reactions ensue. Such reactions can cause mechanical escape of some of the metal carbamate from the absorption zone, or diminution in the number of free atoms by binding in undissociated molecules, respectively.

The constancy of the absorption signal for most of the elements at higher destruction temperatures (240–1100°C) can be explained by the formation of stable sulphides from MeTMDTC. Such sulphides do not volatilize in this temperature range. Lead and cadmium, however, represent a group of elements whose inorganic compounds are easily volatile; and this also explains the experimentally obtained diminution of the absorption signal for these higher destruction temperatures. Similar curves were obtained for aqueous solutions of metal ions, as shown in Fig. 7, which supports the above statement.

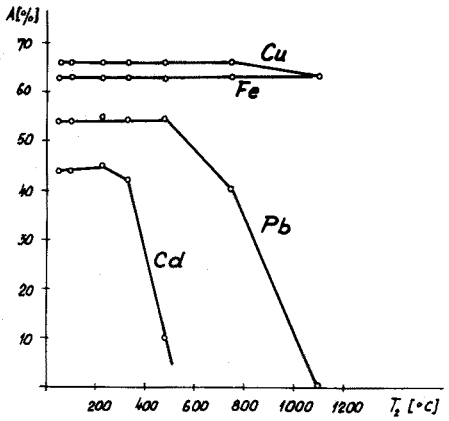

Fig. 7. The influence of the destruction temperature on the absorption of some metals in aqueous solutions.

Oxidative decomposition[12] of the carbamate molecules of easily volatile elements can decrease the losses from volatilization during the decomposition phase, if in the reaction, less volatile oxides and oxy-sulphocompounds are formed. The formation of such compounds is enhanced at higher decomposition temperatures. The experiments confirmed this for lead TMDTC (Fig. 5) and cadmium TMDTC.

The dependence of the height of the absorption peak on the atomization temperature (Fig. 6), which shows only small differences between curves for aqueous solutions of metal ions and organic solutions of MeTMDTC, is in agreement with the above conclusion, as all compounds in the graphite-tube furnace are mineralized in the destruction phase, irrespective of the initial form. For easily volatile cadmium compounds, the maximum at a relatively low temperature of 1600°C is characteristic, whereas with the compounds of higher melting point, absorption increases with the temperature.

It can be concluded that the proposed scheme for the atomization of MeTMDTC in the graphite-tube furnace is valid on the whole. The fundamental relationships can be explained on this basis, but it fails to explain some phenomena: for example, the dependence of the height of the absorption peak on the volume of the solution or the solvent used. The reasons for these phenomena must be sought among the physical properties of solutions influencing the wetting of the tube surface.

Atomization may also be affected by reactions and processes at phase boundaries, whether in the gaseous, liquid or solid state, *e.g.* diffusion of organic solutions or free atoms into the tube walls, or reactions with the carbon from the tube, or with the carbon formed by the destruction of carbamate molecule. These particular phenomena, which would give a more detailed picture of the atomization, have not been investigated yet, but they deserve further attention.

Our thanks are due to Professor L. Golič and Professor J. Šiftar, University of Ljubljana, who provided help and advice in the x-ray diffraction and differential thermal and thermogravimetric investigations. This work was supported by grant 1-104-73 of the Boris Kidrič Foundation, Ljubljana.

SUMMARY

Some phenomena occurring during the atomization of metal tetramethylenedithiocarbamates (MeTMDTC) in the graphite-tube furnace were observed. Explanations based on studies of the behaviour of MeTMDTC in argon and oxygen at higher temperatures, and on the results of x-ray diffraction, differential thermal and thermogravimetric studies, are proposed.

REFERENCES

1 J. E. Allan, *Spectrochim. Acta*, 17 (1961) 467.
2 C. L. Chakrabarti and S. P. Singhal, *Spectrochim. Acta, Part B*, 24 (1969) 663.
3 Yu. A. Zolotov and N. M. Kuzmin, *Zh. Anal. Khim.*, 23 (1967) 773.
4 D. Clark, R. M. Dagnall and T. S. West, *Anal. Chim. Acta*, 63 (1973) 11.
5 M. Yanagisawa and T. Takeuchi, *Anal. Chim. Acta*, 64 (1973) 381.
6 G. D. Renshaw, C. A. Pounds and E. F. Pearson, *At. Absorption Newslett.*, 12 (2) (1973) 55.
7 P. E. Paus, *At. Absorption Newslett.*, 10 (3) (1971) 69.
8 J. Aggett and T. S. West, *Anal. Chim. Acta*, 57 (1971) 15.
9 E. Schöffmann and H. Malissa, *Mikrochim. Acta*, (1961) 319.
10 Z. Lengar, S. Gomišček and L. Golič, to be published.
11 S. Gomišček, P. Bukovec and J. Jernejčič, to be published.
12 S. Gomišček and J. Černetič, to be published.

Analytica Chimica Acta, 73 (1974) 107–119

SYNTHESES AND SPECTROPHOTOMETRIC STUDIES OF 5-(2-PYRIDYLAZO)-2,4-DIAMINOTOLUENE AND ITS DERIVATIVES AS ANALYTICAL REAGENTS

SPECTROPHOTOMETRIC DETERMINATION OF COBALT WITH 5-[(3,5-DICHLORO-2-PYRIDYL)AZO]-2,4-DIAMINOTOLUENE

SHOZO SHIBATA, MASAMICHI FURUKAWA and EIJIRO KAMATA

Government Industrial Research Institute, Nagoya, Hirate-machi, Kita-ku, Nagoya (Japan)

(Received 30th April 1974)

In a search for new sensitive and selective organic reagents[1,2], a thorough study of some of the azo compounds containing diamine groups has been made[3–5]. The authors have already reported on the preparation of 4-(2-pyridylazo)-1,3-diaminobenzene (PADAB, or 4-(2-pyridylazo)-*m*-phenylenediamine) and its halogen substituted compounds[6,7], and the analytical application of these reagents to the determination of cobalt[6] and palladium[8]. These cobalt complexes have extremely high molar absorptivities of the order of 10^5 l mol^{-1} cm^{-1}. The selectivity is also excellent, and these cobalt complexes are very stable between pH 11 and $-H_0$9. Such complexes are very rare in chelate chemistry, and in a previous paper[3] these reaction mechanisms were discussed. Recently, the effectiveness of these reagents for the spectrophotometric determination of cobalt was confirmed by Kiss[9].

Improvements in the molar absorptivity and selectivity of the PADAB derivatives have now been achieved by the introduction of a methyl group into the diamine. The methyl group contributes to increasing the absorption cross-section of the ligand and decreases its reactivity with iron and chromium compared to the PADAB compounds. In the present paper, first, the preparation of seven azo derivatives (compounds I–VII) of 2,4-diaminotoluene (*m*-tolylenediamine) and the color reaction of these reagents with the cobalt ion are reported. Secondly, 5-[(3,5-

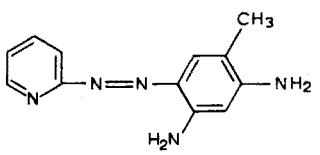

PADAT, I

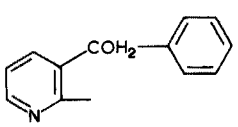

II

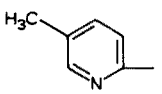

III

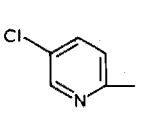

IV

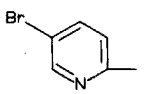
V

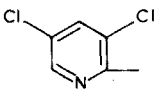
VI

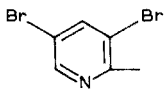
VII

dichloro-2-pyridyl)-azo]-2,4-diaminotoluene (3,5-diCl-PADAT) is used to provide a sensitive and specific method for determining microgram amounts of cobalt in steel and waspaloy.

EXPERIMENTAL

Reagents

Standard metal solutions. The high-purity metal (99.99%) was dissolved in nitric acid (1+1) or hydrochloric acid (1+1), and 10 ml of perchloric acid was added. The mixture was evaporated until fumes of perchloric acid appeared. After cooling, the solution was diluted to 1 l with distilled water, and a 10^{-2} *M* solution was finally prepared.

Buffer solutions. 0.2 *M* Acetic acid–0.2 *M* sodium acetate, 0.2 *M* hydrochloric acid–0.2 *M* potassium chloride and 0.2 *M* disodium hydrogenphosphate–0.1 *M* citric acid were used for pH adjustment.

Reagent solutions, 0.1%. An ethanolic solution was prepared from the pure materials (see below). The solutions were stable for several months if stored in an amber bottle.

Organic solvents were purified by the usual methods. All the other reagents were made from high-purity materials or purified reagents, and all solutions were prepared with redistilled water.

Apparatus

Elemental analyses were done with a Model MT-2 Yanagimoto CHNcorder. Absorbance curves and infrared spectra were measured with a Model 323 Hitachi recording spectrophotometer with 1-cm cells and a Hitachi G-3 infrared recording spectrophotometer. A Hitachi–Horiba M-5 type glass electrode pH meter was used.

Preparation of reagents

The reagents were prepared by coupling 2,4-diaminotoluene with the appropriate diazotate in alcoholic solution under neutral or acidic media. The diazotate was prepared by adding a solution of isopentyl nitrite to a mixture of amine and sodium amide or sodium metal. In the case of 2-aminopyridine and 5-methyl-2-aminopyridine, the diazotization with sodium metal for a long period is preferable.

5-(2-Pyridylazo)-2,4-diaminotoluene (PADAT, I)

To a solution of 1.5 g of clean sodium metal in 25 ml of absolute ethanol, 2-aminopyridine (5.2 g) in 100 ml of anhydrous ether and 8 ml of isopentyl nitrite were added, and the mixture was refluxed for 8 h. To this diazo solution, *m*-tolylenediamine (6 g) in ethanol was added at 0–5°C and hydrochloric acid (1+3) was added dropwise to the mixture until a deep red color appeared. The mixture was allowed to stand overnight. On careful dilution with water, a crude precipitate was formed,

filtered off and washed with water. The crude material was recrystallized from ethanol–water mixture.

Analysis. $C_{12}H_{13}N_5$ requires: 63.42% C, 5.77% H, 30.82% N; found: 63.7% C, 5.3% H, 30.3% N. Red needles (m.p. 188°C).

5-[(3-Benzyloxy-2-pyridyl)azo]-2,4-diaminotoluene (3-Benzyloxy-PADAT, II)

To a solution of 2 g of sodium amide in 20 ml of absolute ethanol plus 40 ml of anhydrous ether, 3-benzyloxy-2-aminopyridine (5 g) in 25 ml of hot ethanol was added, and the mixture was refluxed for 30 min. Then, 3 g of isopentyl nitrite was added to the mixture and refluxing was continued for an additional 5 h. To this diazo solution, *m*-tolylenediamine (3.5 g) in absolute ethanol was added at 0–5°C, and hydrochloric acid (1+3) was added drop wise until the mixture was slightly acidic and the deep red color appeared. The mixture was allowed to stand overnight. Then, after heating on a water bath, 10 g of sodium acetate was added, and the mixture was cooled in a refrigerator. The precipitated light brown crystals were filtered off, and recrystallized from (1+1) aqueous ethanol.

Analysis. $C_{19}H_{19}N_5O$ requires: 68.45% C, 5.74% H, 21.0% N; found: 67.9% C, 5.5% H, 21.3% N. Light brown needles.

5-[(5-Methyl-2-pyridyl)azo]-2,4-diaminotoluene (5-Me-PADAT, III)

To a solution of 1 g of clean sodium metal in 30 ml of absolute ethanol, 5-methyl-2-aminopyridine (5 g) in 50 ml of anhydrous ether was added, and the mixture was refluxed for 30 min. Then 7 ml of isopentyl nitrite was added, and refluxing was continued for an additional 5 h. To this diazo solution, *m*-tolylenediamine (5.6 g) in 50 ml of ethanol was added at 0–5°C, and hydrochloric acid (1+3) was added dropwise until a deep red color appeared. The mixture was allowed to standard overnight. The precipitated inorganic salts were filtered off. On careful dilution of filtrate with water, the reagent separated, as an oily substance. After separation from the solution, and dissolution in ethanol, the reagent was crystallized carefully from aqueous ethanol.

Analysis. $C_{13}H_{15}N_3$ requires: 73.21% C, 7.09% H, 19.70% N; found 72.1% C, 6.7% H, 19.0% N. Reddish brown needles.

5-[(5-Chloro-2-pyridyl)azo]-2,4-diaminotoluene (5-Cl-PADAT, IV)

To a solution of 2.4 g of sodium amide in 60 ml of absolute ethanol, 5-chloro-2-aminopyridine (6 g) was added, and the mixture was refluxed for 30 min. Then, 5.46 g of isopentyl nitrite was added to the mixture and refluxing was continued for an additional 2 h. To this diazo solution, *m*-tolylenediamine (5.7 g) in a mixture of 40-ml of ethanol, 20 ml of water and 7 ml of concentrated hydrochloric acid was added at 0–5°C. The mixture was allowed to stand overnight. Then, 200 ml of water was added and the precipitated orange red crystals were filtered off, and recrystallized from (1+1) aqueous ethanol.

Analysis. $C_{12}H_{12}N_5Cl$ requires: 55.07% C, 4.62% H, 26.76% N; found 55.2% C, 4.5% H, 26.9% N. Orange-red needles (m.p. 219°C).

5-[(5-Bromo-2-pyridyl)azo]-2,4-diaminotoluene (5-Br-PADAT, V)

To a solution of 2 g of sodium amide in 80 ml of absolute ethanol, 5-bromo-2-

aminopyridine (6 g) was added, and the mixture was refluxed for 30 min. Then, 4.1 g of isopentyl nitrite was added to the mixture and refluxing was continued for an additional 2 h. To this diazo solution, *m*-tolyenediamine (4.2 g) in 100 ml of ethanol was added at 0–5°C, and hydrochloric acid (1+3) was added dropwise until a deep red color appeared. The mixture was allowed to stand overnight. Water was added to the mixture and the precipitated crude material was filtered off, and recrystallized from (1+1) aqueous ethanol or ethanol.

Analysis. $C_{12}H_{12}N_5Br$ requires: 47.08% C, 3.95% H, 22.87% N; found: 47.2% C, 4.1% H, 22.6% N. Brown needles (m.p. 216°C).

5-[(3,5-Dichloro-2-pyridyl)azo]-2,4-diaminotoluene (3,5-diCl-PADAT, VI)

To a solution of 1 g of clean sodium metal in 25 ml of absolute ethanol, 3,5-dichloro-2-aminopyridine (4 g) with 50 ml of anhydrous ether was added, and the mixture was refluxed for 30 min. Then, 4 ml of isopentyl nitrite in 50 ml of ether was added, and refluxing was continued for an additional 4 h. To this diazo solution, *m*-tolylenediamine (3 g) in 30 ml of ethanol was added at 0–5°C, and hydrochloric acid (1+3) was added dropwise until a red precipitate appeared. The mixture was allowed to stand overnight, and the precipitated crude material was filtered off, washed with water, dissolved in hot ethanol, and recrystallized from (1+1) aqueous ethanol.

Analysis. $C_{12}H_{11}N_5Cl_2$ requires: 48.67% C, 3.74% H, 23.65% N; found 48.7% C, 3.9% H, 23.3% N. Purplish black lustrous needles (m.p. 183°C).

5-[(3,5-Dibromo-2-pyridyl)azo]-2,4-diaminotoluene (3,5-diBr-PADAT, VII)

To a solution of 2 g of sodium amide in 40 ml of absolute ethanol, 3,5-dibromo-2-aminopyridine (5 g) in 20 ml of anhydrous ether was added, and the mixture was refluxed for 30 min. Then, 5 ml of isopentyl nitrite was added to the mixture and refluxing was continued for 5 h. To this diazo solution, *m*-tolylenediamine (2.5 g) in a mixture of 50 ml of ethanol and 10 ml of (1+1) hydrochloric acid was added. The mixture was allowed to stand overnight, and 60 ml of water was added with stirring. The precipitated crude material was filtered off, washed with water, dissolved in hot ethanol and recrystallized from (1+1) aqueous ethanol.

Analysis. $C_{12}H_{11}N_3Br_2$ requires: 40.37% C, 3.11% H, 11.77% N; found: 40.4% C, 3.0% H, 11.8% N. Purplish lustrous needles (m.p. 230°C).

These reagents have a tendency to sublime, and the values of the melting points depend appreciably on the conditions of recrystallization. For identification of the synthesized materials, the infrared spectra of typical reagents are shown in Fig. 1 (A, B and C).

General properties of cobalt complexes

The general properties of these reagents and their cobalt complexes are almost the same as those of the PADAB analogs. The absorption spectra of the reagents and cobalt complexes are shown in Figs. 2 and 3. With the PADAB and PADAT reagents, highly sensitive and selective determinatons of microgram amounts of cobalt are possible under the optimal conditions. The wavelength of maximum absorbance and the molar absorptivity of each complex are listed in Table I. It can be seen that the values of the molar absorptivities for the complexes listed increase

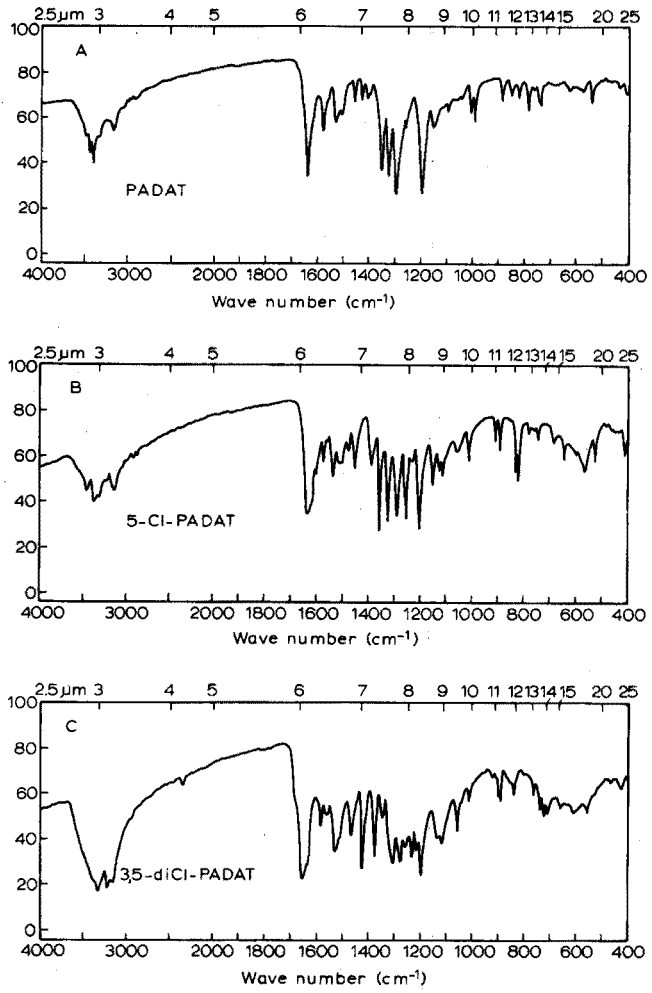

Fig. 1. The infrared spectra of typical reagents. KBr tablet. (A) PADAT, (B) 5-Cl-PADAT, (C) 3,5-diCl-PADAT.

in the order 5-Me-PADAT < 3-Benzyloxy-PADAT < PADAT < 5-Cl-PADAT < 5-Br-PADAT < 3,5-diCl-PADAT < 3,5-diBr-PADAT, and that these values are larger than those of the PADAB analogs.

Although PADAB and PADAT themselves are the most economical reagents, the diazotization and coupling with diamine of the halogen derivatives are very easy compared with the reactions of 2-aminopyridine itself. The preparations of 5-iodo-PADAT and 5-iodo-PADAB are very difficult. The cost of the reagents increased as follows: PADAT < 3,5-diCl-PADAT < 5-Cl-PADAT < 5-Me-PADAT < 3,5-diBr-PADAT < 5-Br-PADAT < 3-Benzyloxy-PADAT, the ratio of the prices being 1:6:8:9:10:13:15, approximately. At the present time, only 5-Cl-PADAB can be purchased commercially (Merck). The best reagent among these derivatives should be selected by comparison of tolerance limits for diverse metals, sensitivity

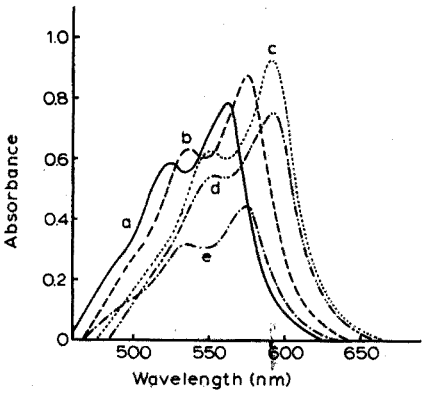

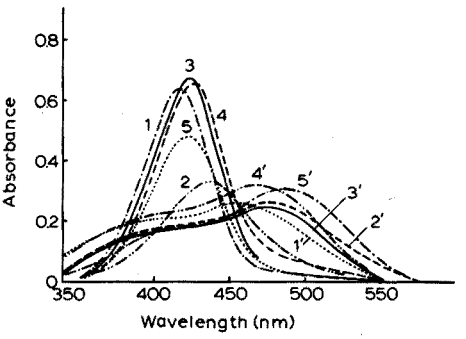

Fig. 2. Absorption spectra of cobalt complexes. (a) 3-Benzyloxy-PADAT, (b) PADAT, (c) 5-Cl-PADAT, (d) 5-Br-PADAT, (e) 3,5-diCl-PADAT; (c) 5 μg Co/ml, others 10 μg Co/25 ml. Reagent: 0.5 ml of 0.1% ethanolic solution, 2.4 *M* HCl, *versus* reagent blank.

Fig. 3. Absorption spectra of reagents. (1), (1′) PADAT; (2), (2′) 3-Benzyloxy-PADAT; (3), (3′) 5-Cl-PADAT; (4), (4′) 5-Br-PADAT; (5), (5′) 3,5-diCl-PADAT. 1–5, 2.4 *M* HCl solution; 1′–5′, aqueous pH 10.0 solution.

TABLE I

MOLAR ABSORPTIVITIES OF COBALT COMPLEXES

Reagents	ε $(\cdot 10^5$ $l\ mol^{-1}\ cm^{-1})$	λ_{max} *(nm)*	*Reagents*	ε $(\cdot 10^5$ $l\ mol^{-1}\ cm^{-1})$	λ_{max} *(nm)*
PADAB	1.07	559	5-Me-PADAT	1.07	563.5
5-Cl-PADAB	1.12	570	3-Benzyloxy-PADAT	1.10	591
5-Br-PADAB	1.17	573	PADAT	1.16	561
5-I-PADAB[9]	1.18	580	5-Cl-PADAT	1.26	573
3,5-diCl-PADAB	1.19	585	5-Br-PADAT	1.30	574
3,5-diBr-PADAB	1.22	590	3,5-diCl-PADAT	1.38	590
			3,5-diBr-PADAT	1.42	591

and economic factors, etc. In any event, it is not too much to say that the PADAB and PADAT groups provide the most advanced reagents for determinations of microgram amounts of cobalt. In this report, 3,5-diCl-PADAT was chosen as the most promising reagent for detailed study because of its moderate cost and high sensitivity.

Recommended procedure for the spectrophotometric determination of cobalt

Into a 25-ml volumetric flask, transfer a suitable aliquot of sample solution containing up to 10 μg of cobalt, and add 1 ml of ethanolic 0.1% reagent solution. Adjust to pH 3–5 with 5 ml of buffer solution (sodium acetate–acetic acid) and mix. In the presence of any other foreign ions, add McIlvaine buffer (disodium hydrogenphosphate–citric acid, pH 3–4) to the sample solution before the addition

of reagent solution. Then add 5 ml of hydrochloric acid (1+1) or sulfuric acid (1+1), dilute to volume and mix. Measure the absorbance of the cobalt complex at 590 nm against a reagent blank or water. Obtain the concentration of cobalt from a standard calibration curve obtained under identical conditions.

RESULTS AND DISCUSSION

Color reaction with metal ions

Ions that do not give a detectable color at room temperature include silver, aluminum, arsenic, boron, barium, beryllium, bismuth, calcium, cadmium, chromium(III, VI), iron(II, III), gallium, germanium, hafnium, indium, iridium, lanthanides, magnesium, manganese, molybdenum, niobium, osmium, lead, platinum, rhodium, ruthenium, antimony(III), scandium, tin(II), strontium, thorium, tantalum, titanium, uranium(VI), vanadium(IV), tungsten, yttrium, and zirconium. The ions that gave a color or precipitate with the reagent are listed in Table II. The tests were made by adding one or two drops of 10^{-3} *M* reagent solution in ethanol to the metal solution (1 mg ml^{-1}). In hydrochloric acid, only cobalt and palladium complexes are stable, therefore this reagent is extremely selective to cobalt in practice. Yet, the color reactions of gold, palladium, and thallium are also of interest for analytical purposes.

TABLE II

COLOR REACTIONS OF METALS WITH 3,5-diCl-PADAT

Metals	*pH 3*	*pH 6–8*	*Acid added*	
			2.4 M HCl	*6.4 M H_2SO_4*
Au^{3+}	Red purple	Red purple	[a]	Dark red purple
Co^{2+}	Red purple	Brown	Purple	Purple
Cu^{2+}	Red purple	Red purple	[a]	[a]
Hg^{2+}	[a]	Red purple	[a]	[a]
Ni^{2+}	[a]	Red purple	[a]	[a]
Pd^{2+}	Violet	Purple	Purplish violet	Purplish violet
Tl^{+}	Red purple	Red purple	[a]	[a]
Zn^{2+}	[a]	Red	[a]	[a]

[a] No color reaction or decomposed to the yellow color of reagent.

The reaction of cobalt with the reagent

Cobalt(II) reacts with the reagent from about pH 1–2 upwards, the absorbance of the complex being constant in the pH range 3–11 (initial pH). Above pH 4 the absorption maximum shifts to shorter wavelength with decreasing molar absorptivity: above pH 5 a definite complex (complex I, see below) is formed finally. Cobalt and the reagent in acidic solution below pH 1 do not form any complex. However, once the complex has been formed, it can be changed into another deeply colored stable species (complex III) via an intermediate (complex II), which possesses increased absorptivity, by addition of a mineral acid, such as hydrochloric, nitric, perchloric or sulfuric acid. Complex III is the most suitable for

analytical purposes. It can also be changed into a final yellowish form (complex IV) by addition of concentrated sulfuric acid.

Absorbance curve

The absorbance curves of the reagent and its cobalt complex in 2.4 *M* hydrochloric acid are shown in Fig. 4. The curves for the complex show two absorption maxima at 548 and 590 nm, respectively.

Optimal pH

The effect of initial pH on color development was studied by preparing a series of solutions varying from pH 1 to 11. The absorbance increased steeply in the pH range 2–3, but no change in absorbance was observed over the pH range 3–10.

For these studies, the initial pH was as stated, but the absorbance was measured finally in 2.4 *M* hydrochloric acid. In order to establish the analytical conditions, acetate buffer was used. However, disodium hydrogenphosphate–citric acid buffer is very useful for practical analysis, owing to its complexing ability for many foreign metal ions.

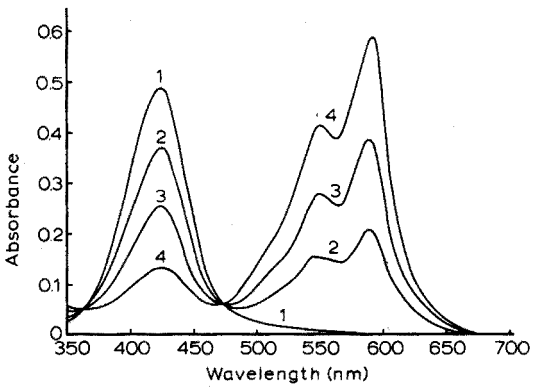

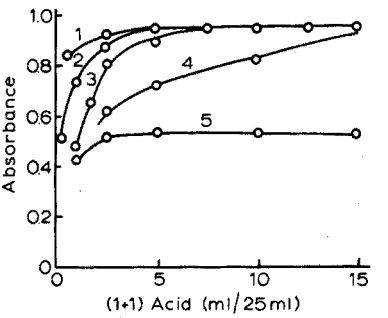

Fig. 4. Absorbance curves of 3,5-diCl-PADAT and its cobalt complex in 2.4 *M* hydrochloric acid solution with $1.37 \cdot 10^{-5}$ *M* 3,5-diCl-PADAT. Amount of Co present: (1) nil (2) $2.7 \cdot 10^{-6}$ (3) $5.4 \cdot 10^{-6}$ (4) $7.1 \cdot 10^{-6}$. 1-cm cell, *versus* water blank.

Fig. 5. Effect of final acid concentration on color development of the cobalt-3,5-diCl-PADAT complex at 590 nm, 10 μg of Co per 25 ml. (1) H_2SO_4 (2) HCl, HNO_3 (3) $HClO_4$ (4) H_3PO_4 (5) CH_3COOH. Each (1+1) acid solution was made from the following analytical-grade reagent: H_2SO_4, 95%; HCl, 35%; HNO_3, 60~62%; $HClO_4$, 60%; H_3PO_4, $d=1.8$; CH_3COOH, 99.0%.

Acid concentration

The effects of acidity and the type of acid used on the color development were studied by preparing a series of solutions varying in final acidity but for which the color had been developed initially at pH 5. The results (Fig. 5) show that hydrochloric, sulfuric, nitric or perchloric acid can be used. Accordingly, the most suitable acid can be selected for particular samples.

Reagent concentration

The absorbances of series of solutions containing 10 μg of cobalt and 0.05–1 ml

of 0.1% dye solution were measured. It was found that 0.2 ml of this dye solution sufficed to complex 10 μg of cobalt; with higher reagent concentrations the absorbance was essentially constant.

Color development, stability and effect of temperature

The minimal time for complete color development of the complex was found to be 1–2 min at room temperature. The absorbance was then stable for at least 1 day. In the presence of large amounts of complexing agent, such as citric acid or tartaric acid, the minimal time for full color development was 10–15 min.

Beer's law and sensitivity

The calibration graph proved to be linear over the range 0.01–0.4 p.p.m. of cobalt. The effective molar absorptivity for the cobalt complex was $1.38 \cdot 10^5$ l mol^{-1} cm^{-1} at 590 nm. The sensitivity of the reaction as calculated from Beer's law was 0.42 ng Co cm^{-2} at 590 nm for log $I_0/I = 0.001$.

Effect of foreign ions

Numerous cations and anions were examined by applying the method to fixed amounts of cobalt. The general character of the reactions with the diverse ions was almost the same as with the PADAB analogs. However, with the proposed reagent, large amounts of iron (*ca.* 50 mg) and chromium did not interfere. The following ions (in 1–5-mg amounts) did not interfere: aluminium, arsenic, boron, barium, bismuth, calcium, cadmium, chromium, gallium, germanium, hafnium, indium, iridium, lanthanides, magnesium, manganese, molybdenum, niobium, osmium, lead, platinum, rhodium, ruthenium, antimony, scandium, tin, strontium, thorium, tantalum, titanium, uranium, vanadium, tungsten, yttrium and zirconium. Gold, copper and thallium(I) in 2–3-fold amounts (w/w) did not interfere. Among the cations, interference was caused only by palladium. Sodium fluoride, sodium sulfate, potassium nitrate, potassium chloride, potassium bromide, sodium perchlorate, sodium chloride, ammonium hydrogenphosphate, tartaric acid, citric acid and urea (each in 1-g amounts) did not interfere. Among the complexing agents, interference was caused by potassium cyanate and EDTA.

Determination of cobalt in steel and waspaloy

Weigh a 0.1-g sample into a conical beaker and dissolve in 20 ml of hydrochloric acid (1+1), which contains suitable amounts of hydrogen peroxide, on a hot plate. Add 5 ml of concentrated perchloric acid and evaporate until fumes of perchloric acid appear. Cool to room temperature, transfer to a 100 or 250-ml volumetric flask, and dilute with water to the mark. Transfer an aliquot of this solution corresponding to 0.2–10 μg of cobalt to a 25-ml volumetric flask. Add 5 ml of pH 3 McIlvaine buffer and 1 ml of ethanolic 0.1% 3,5-diCl-PADAT solution, mix thoroughly, and stand for 15 min. Then, add 10 ml of (1+1) hydrochloric or sulfuric acid. Dilute to the mark with water and measure the absorbance in a 1-cm cell at 590 nm against a reagent blank or water.

Typical results are shown in Table III.

Acid dissociation constant of reagent

The reagent is almost insoluble in water, but soluble in various organic

TABLE III

DETERMINATION OF COBALT IN STEEL AND WASPALOY

Standard sample	*Amounts (%)*	*Co found (%)*
Waspaloy	C, 0.08; Mo, 4.04; Al, 1.23;	14.00
N.B.S. 349[a]	Co, 13.95; Ti, 3.05; B, 0.0046	13.98
	Nb, 0.01; Si, 0.29; Mn, 0.43	13.92
	P, 0.002; Ni, 57.15; Cr, 19.50	
	W, 0.01; Cu, 0.006; Ta, 0.01	13.9 Av.
	Fe, 0.13; Zr, 0.08	
Carbon steel	C, 0.004; Mo, 0.16; V, 0.10	0.058
J.S.I.S. 160-2[b]	Co, 0.061; Ti, 0.093; Al, 0.006	0.059
	As, 0.051; Sn, 0.061; B, 0.0062	0.059
	Pb, 0.002; Nb, 0.11; Fe, balance	
		0.059 Av.

[a] National Bureau of Standards.
[b] Japanese Standard of Iron and Steel.

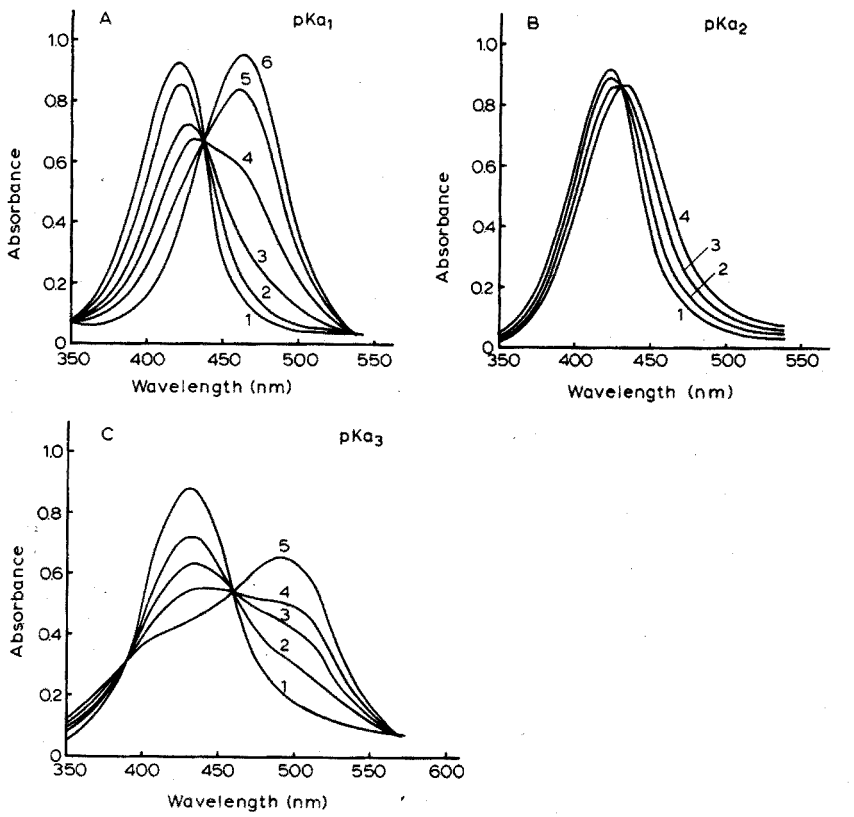

Fig. 6. Absorption spectra of 3,5-diCl-PADAT in aqueous solutions. $2.7 \cdot 10^{-5}$ *M*, 1-cm cell, 20°C. A. $-H_0$ (1) 1.0, (2) 4.4, (3) 4.8, (4) 5.2, (5) 7.5, (6) 8.7. B. (1) $-H_0$, 1.0; (2) pH 0.1; (3) pH 0.5; (4) pH 1.5. C. In 20% ethanolic solution, $\mu = 0.2$ (KCl). pH: (1) 1.5; (2) 4.0, (3) 5.0, (4) 6.7.

solvents including ethanol, acetone, ether and tributyl phosphate as well as in strongly acidic aqueous solution. Four species of reagent, H_3L^{3+}, H_2L^{2+}, HL^+ and L are involved in the acid dissociation behavior. It may be assumed that the values of pK_{a1} correspond to the protonation of the pyridine nitrogen, and the values of pK_{a2} and pK_{a3} to the protonation of the two amino groups. The equilibria are marked by isobestic points on the absorption spectra of the reagent (Fig. 6). In Fig. 7 are shown the plots of absorbance *versus* pH for the calculation of the dissociation constants. The pK_a values obtained are listed in Table IV.

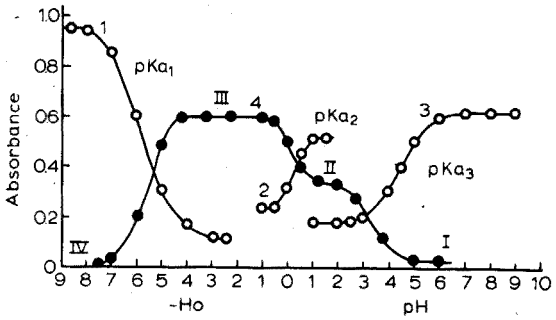

Fig. 7. Absorbance *vs.* pH curves for 3,5-diCl-PADAT and its cobalt complexes in aqueous solution, 1-cm cell, 20°C. Reagent $2.7 \cdot 10^{-5}$ *M*, at (1) 460 nm, (2) 460 nm, (3) 490 nm, (4) 590 nm (reagent and cobalt: $1.37 \cdot 10^{-5}$ *M*).

TABLE IV

ACID DISSOCIATION AND PROTONATION CONSTANTS OF REAGENT AND ITS COBALT COMPLEX

pK	*Reagent*	*Cobalt complex*
pK_{a1}	5.5[a]	5.6[a]
pK_{a2}	0.25	0.2
pK_{a3}	4.6[b]	3.3

[a] Hammett's acidity function in sulfuric acid.
[b] 20% ethanolic aqueous solution, 20°C, $\mu = 0.2$.

Nature of the cobalt complex

As mentioned above, although cobalt ions react with the reagent to form several different complexes, the metal : ligand ratios of these complexes are all the same, *i.e.* Co : L = 1 : 2. The results obtained by Job's method in acidic solution are shown in Fig. 8; precisely the same shape of curve was obtained at pH 8.5 for 500 nm. The explanation of this phenomenon probably lies in the formation of some protonated cobalt complexes which have high stability in acidic solution. Therefore, the following protonation steps are proposed for each equilibrium (charge for cobalt omitted).

$$\underset{(I)}{CoL_2} \underset{pK_{a3}}{\overset{H^+}{\rightleftarrows}} \underset{(II)}{CoL_2H^+} \underset{pK_{a2}}{\overset{H^+}{\rightleftarrows}} \underset{(III)}{CoL_2H_2^{2+}} \underset{pK_{a1}}{\overset{H^+}{\rightleftarrows}} \underset{(IV)}{CoL_2H_3^{3+}}$$

In Fig. 7 are shown the plots of absorbance *versus* pH for the calculation of each protonation constant. The equilibria are marked by the isosbestic points on the absorption spectra of each cobalt complex (see Fig. 9). The optical characteristics of the complexes, with the isosbestic points, are shown in Table V. The calculated protonation constants pK_a are listed in Table IV. In other respects, the cobalt complexes are almost the same as those obtained with the PADAB analogs[1].

TABLE V

ABSORPTION MAXIMA, MOLAR ABSORPTIVITIES AND ISOSBESTIC POINTS OF REAGENT AND ITS COBALT COMPLEXES[a]

Form	*3,5-diCl-PADAT*		*Form*	*Cobalt complexes*	
	λ_{max}	ε		λ_{max}	ε
H_3L^{3+}	462	3.59	CoL_2	488	5.23
				515	5.71
	(436)			(505)	
H_2L^{2+}	422	3.41	CoL_2H^+	535	7.29
				581	8.22
	(430)			(534)	
HL	432	3.18	CoL_2H^{2+}	548	9.73
				590	13.8
	(460)			(490)	
L	490	2.41	CoL_2H^{3+} [b]	250	3.90
				267	4.91
				284	4.28

[a] λ_{max} and isosbestic points (in parentheses) are given in nm. All molar absorptivities (ε) are given as $\cdot 10^4$ l mol^{-1} cm^{-1}.
[b] See ref. 1.

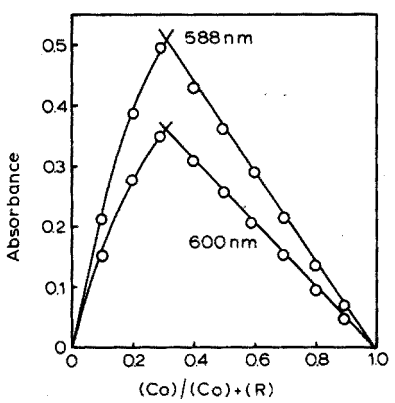

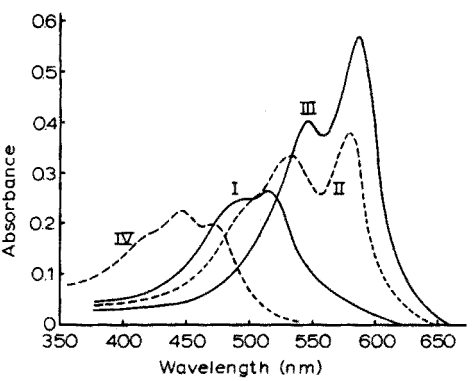

Fig. 8. Composition of cobalt complex by Job's method. [Co] + [3.5-diCl-PADAT] = $1.38 \cdot 10^{-5}$ *M*, 2.4 *M* HCl solution.

Fig. 9. Absorption spectra of 3,5-diCl-PADAT–cobalt complexes in aqueous solution. $1.37 \cdot 10^{-5}$ *M* reagent and cobalt, water as blank, 1-cm cell, 20°C. Initial pH for full color development pH 5.0.

SUMMARY

Seven pyridylazo dyes containing the *m*-tolylenediamine group were synthesized and their analytical potential for the determination of cobalt was studied spectrophotometrically. The molar absorptivities and selectivity of these reagents increased compared with those of PADAB. Cobalt(II) and 3,5-diCl-PADAT (5-[(3,5-dichloro-2-pyridyl)azo]-2,4-diaminotoluene) at pH 3 form a complex which is very stable even in the presence of strong mineral acids. The complex has two absorption maxima at 548 and 590 nm in hydrochloric acid (2.4 *M*) solution. The color is very stable and the system conforms to Beer's law; the optimal range for measurement in a 1-cm cell is 0.01–0.4 p.p.m. cobalt. In practice, this color reaction is specific. The molar absorptivity is $1.38 \cdot 10^5$ l mol^{-1} cm^{-1} at 590 nm. The sensitivity is 0.00042 μg Co cm^{-2} at 590 nm for log $I_0/I = 0.001$. The method was applied to the determination of cobalt in steel and waspaloy.

REFERENCES

1 S. Shibata, M. Furukawa and K. Toei, *Anal. Chim. Acta*, 66 (1973) 397.
2 S. Shibata, M. Furukawa and Y. Ishiguro, *Mikrochim. Acta*, (1972) 721.
3 S. Shibata, M. Furukawa and K. Goto, *Anal. Chim. Acta*, in press.
4 S. Shibata, M. Furukawa and K. Goto, *Talanta*, 20 (1973) 426.
5 S. Shibata and M. Furukawa, *Bunseki Kagaku*, 22 (1973) 1077.
6 S. Shibata, M. Furukawa and Y. Ishiguro, *Anal. Chim. Acta*, 55 (1971).
7 S. Shibata, *Bunseki Kagaku*, 21 (1972) 397.
8 S. Shibata, Y. Ishiguro and R. Nakashima, *Anal. Chim. Acta*, 64 (1973).
9 E. Kiss, *Anal. Chim. Acta*, 66 (1973) 385.

Analytica Chimica Acta, 73 (1974) 121–127

ÉTUDE PAR SPECTROPHOTOMÉTRIE D'ABSORPTION DES PROPRIÉTÉS CHIMIQUES DU PLUTONIUM DANS L'EUTECTIQUE LiCl–KCl FONDU

G. LANDRESSE* et G. DUYCKAERTS

Laboratoire de Chimie Analytique et Nucléaire, Université de Liège au Sart Tilman, B-4000 Liège (Belgique)

(Reçu le 18 avril 1974)

La spectrophotométrie d'absorption visible et proche i.r. est souvent une méthode de choix pour l'étude des réactions chimiques en sels fondus.

Nous avons examiné plus particulièrement le comportement chimique du plutonium dans l'eutectique LiCl–KCl fondu et cette étude nous a permis de préciser certains détails pour plusieurs réactions déjà décrites dans la littérature[1,2].

En solution dans les chlorures fondus, le plutonium peut se trouver aux états d'oxydation III, IV, V et VI, et bien que ces ions s'y trouvent sous forme solvatée, nous les représenterons, pour faciliter l'écriture, par Pu(III), Pu(IV), PuO_2(V) et PuO_2(VI).

Toutes ces espèces présentent des bandes d'absorption caractéristiques dans le domaine de longueur d'onde considéré (400 à 2500 nm).

PARTIE EXPÉRIMENTALE

Appareillages

Le dispositif expérimental (fours, boîtes à gants, spectrophotomètre Cary 14 H) ainsi que les différentes manipulations ont été décrits précédemment[3]. Une modification importante est toutefois intervenue dans le dispositif expérimental: au lieu de soumettre les solutions fondues à l'action de gaz réactionnels stagnants, on fait barboter dans la solution un mélange de gaz (N_2, O_2, HCl ou Cl_2) réalisé dans une rampe appropriée. La connaissance des pressions partielles des constituants résulte de la mesure du débit de chacun d'eux. Les cellules spectrophotométriques en Infrasil soudé (trajet optique = 1,00 cm) sont fournies par Quadrant (Harlow, Angleterre); elles sont soudées à un tube en quartz de 23 mm de diamètre extérieure, pourvu d'un rodage B19 en quartz sur lequel est montée une tête de cellule en pyrex comprenant le capillaire de barbotage central. Les gaz débouchent dans la solution au-dessus du trajet optique, ce qui permet de continuer les barbotages pendant l'enregistrement des spectres. Environ 15 min sont requises pour atteindre l'équilibre entre le gaz et le bain fondu.

Réactifs

Le composé de plutonium utilisé pour préparer les solutions est Cs_2PuCl_6.

* Chargé de Recherches du Fonds National Belge de la Recherche Scientifique.

Ce choix a été dicté par la stabilité remarquable de ce composé et la facilité avec laquelle on peut le préparer dans un état de grande pureté. La méthode de synthèse du Cs_2PuCl_6 adoptée dans notre laboratoire[4] est dérivée de celle de Kooi *et al.*[5]. La pureté du produit est contrôlée par diffraction aux rayons x et par spectroscopie d'absorption en milieu HCl 0,5 *M*. La vérification de la stoechiométrie du composé s'effectue par titrage potentiométrique des chlorures au moyen d'une solution étalonnée de $AgNO_3$.

La préparation et la purification de l'eutectique LiCl–KCl a déjà été décrite[3].

ÉTUDE DES SPECTRES

La Figure 1 montre le spectre d'absorption de Pu(III) dans l'eutectique LiCl–KCl à 450°C. Les maxima d'absorption sont situés à 565, 673, 801, 904, 1038, 1096, 1407 et 1547 nm. Il est à remarquer que le spectre d'absorption du plutonium trivalent varie très peu avec le solvant; ainsi, on retrouve les mêmes bandes dans $HClO_4$ *M* à 25°C[6], dans l'acide acétique anhydre à 25°C[7], dans HCl 11,6 *M* à 25°C[9], dans HNO_3 0,48 et 4,38 *M* à 25°C[8] ainsi que dans des milieux fondus tels l'eutectique LiCl–KCl à 400°C[9], l'eutectique LiCl–CsCl à 400°C[1] et dans LiF–BeF_2–ThF_4 (72–16–12% mol) à 575°C[10]. On peut en conclure que l'environnement n'exerce qu'un effet minime sur les spectres du Pu(III).

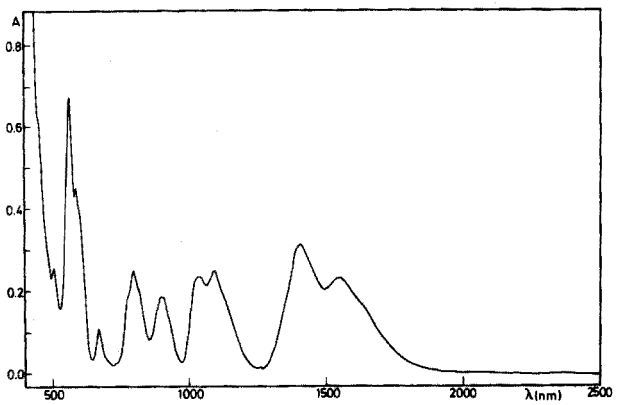

Fig. 1. Spectre d'absorption de Pu(III) dans l'eutectique LiCl–KCl à 450°C ([Pu(III)]=4,46·10^{-2} *M*. Trajet optique 1 cm).

La Figure 2 montre, en trait plein, le spectre d'un mélange de Pu(III)–Pu(IV) dans l'eutectique LiCl–KCl à 450°C sous une atmosphère de chlore, et en traits interrompus, le spectre de Pu(IV) obtenu en soustrayant la contribution de Pu(III). Les maxima d'absorption du plutonium tétravalent sont situés vers 640, 695, 740, 835, 905, 1125 et 1940 nm. Contrairement au cas du Pu(III), les spectres de Pu(IV) sont fortement influencés par le milieu: ainsi, le spectre de Pu(IV) dans LiCl–KCl fondu ne ressemble guère, d'une part, à ceux obtenus dans les milieux aqueux habituels (HNO_3[8], HCl dilué[9], $HClO_4$[6]) ni, d'autre part, au spectre du $PuCl_4$ en phase vapeur à 928°C[11]; par contre, ainsi qu'il ressort de la comparaison de la Fig. 4 (spectres 1 et 2), il est très proche de celui de $[(C_2H_5)_4N]_2PuCl_6$ dans

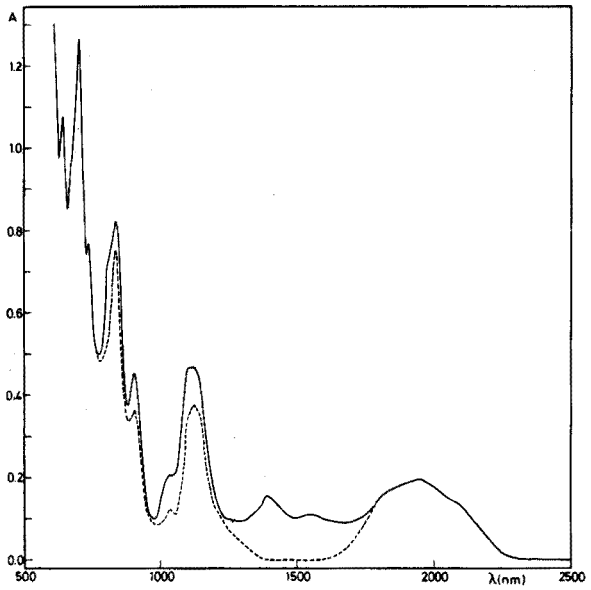

Fig. 2. Trait plein: spectre d'absorption d'un mélange Pu(III)–Pu(IV) dans l'eutectique LiCl–KCl à 450°C sous une atmosphère de chlore ($c_{tot} = 4{,}46 \cdot 10^{-2}$ *M*. Trajet optique 1 cm). Traits interrompus: spectre de Pu(IV) dans l'eutectique LiCl–KCl à 450°C obtenu en soustrayant la contribution de Pu(III) ($1{,}81 \cdot 10^{-2}$ *M*) ([Pu(IV)] = $2{,}65 \cdot 10^{-2}$ *M*).

le nitrométhane à 25°C. Ce dernier spectre, obtenu par Ryan[12], étant caractéristique de l'espèce $PuCl_6^{2-}$, on peut en conclure que dans l'eutectique LiCl–KCl le plutonium se trouve principalement sous forme du $PuCl_6^{2-}$. On trouve d'ailleurs une situation analogue dans le cas de l'uranium[13] et du neptunium[14] stabilisés partiellement sous forme de MCl_6^{2-} dans les chlorures fondus.

La Figure 3, enfin, montre le spectre d'absorption d'un mélange PuO_2(V)–PuO_2(VI) dans l'eutectique LiCl–KCl à 450°C. Les bandes principales dues à PuO_2(VI) sont marquées d'une flèche. Il ne nous a pas été possible d'obtenir l'un

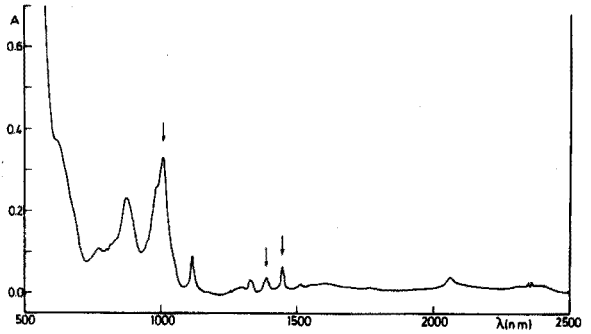

Fig. 3. Spectre d'absorption d'un mélange PuO_2(V)–PuO_2(VI) dans l'eutectique LiCl–KCl à 450°C (c_{tot} = moins de $4{,}46 \cdot 10^{-2}$ *M*; spectre obtenu en présence d'un précipité de PuO_2. Trajet optique 1 cm). Les bandes principales de PuO_2(VI) sont marquées d'une flèche.

de ces deux états d'oxydation à l'état pur, non plus d'ailleurs qu'en l'absence d'un précipité de PuO_2. Les bandes principales de $PuO_2(V)$ sont situées à 770, 780, 875, 990, 1122, 1300 et 2070 nm et celles de $PuO_2(VI)$ à 1012, 1390 et 1448 nm. Le spectre de $PuO_2(V)$ dans LiCl–KCl fondu est assez semblable à celui obtenu dans $HClO_4$ 0,2 *M* à 25°C[6]; par contre, celui de $PuO_2(VI)$ est totalement différent du spectre obtenu dans $HClO_4$ *M* à 25°C[6]. On ne retrouve pas en particulier la bande intense à 830 nm. Cependant, ainsi qu'il ressort de la Fig. 4 (spectres 3 et 4), le spectre de $PuO_2(VI)$ dans LiCl–KCl fondu est très semblable au spectre de $[(C_2H_5)_3NH]_2PuO_2Cl_4$ dans le nitrométhane à 25°C obtenu par Ryan[15] et caractéristique de l'ion $PuO_2Cl_4^{2-}$. Cette ressemblance permet de conclure à la présence de $PuO_2Cl_4^{2-}$ dans l'eutectique LiCl–KCl fondu.

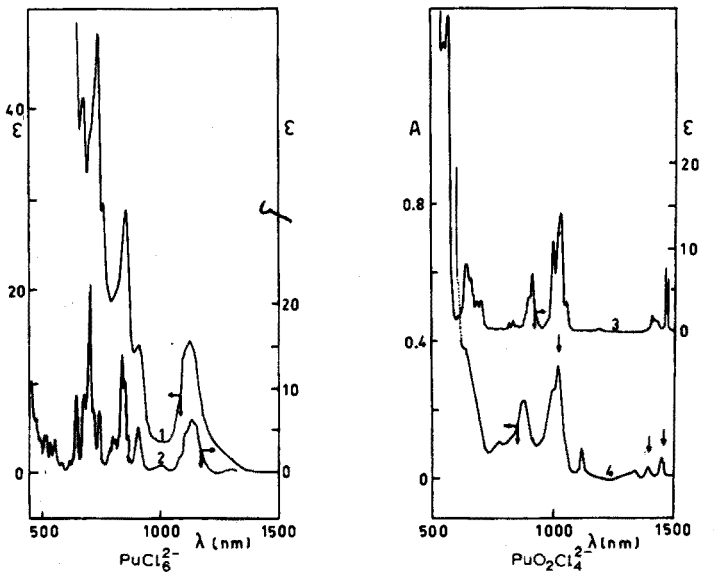

Fig. 4. Indentification des espèces $PuCl_6^{2-}$ et $PuO_2Cl_4^{2-}$. (1) Spectre de Pu(IV) dans l'eutectique LiCl–KCl à 450°C; (2) spectre de $[(C_2H_5)_4N]_2PuCl_6$ dans le nitrométhane à 25°C (d'après[12]); (3) spectre de $[(C_2H_5)_3NH]_2PuO_2Cl_4$ dans le nitrométhane à 25°C (d'après[15]); (4) spectre de $PuO_2(VI)$ dans l'eutectique LiCl–KCl à 450°C (bandes marquées d'une flèche).

ÉTUDE DES RÉACTIONS CHIMIQUES ENTRE 400 ET 550°C

Dès la fusion, un bain de Cs_2PuCl_6 dans LiCl–KCl fournit le spectre de Pu(III) avec quelques bandes d'absorption très peu intenses de Pu(IV). Ces bandes disparaissent d'ailleurs si l'on fait le vide au-dessus du bain ou sous barbotage de HCl et l'on obtient alors le spectre de la Fig. 1. En faisant passer du chlore dans la solution, on reforme partiellement Pu(IV). On obtient à ce moment le spectre en trait plein de la Fig. 2. La réaction peut s'écrire:

$$Pu^{4+} + Cl^- \rightleftharpoons Pu^{3+} + \tfrac{1}{2}Cl_2 \qquad (1)$$

L'étude quantitative de cet équilibre et la détermination du potentiel normal du couple Pu^{4+}/Pu^{3+} feront l'objet d'une publication ultérieure[16].

L'oxydation d'un bain de Pu(III) par l'oxygène pur conduit tout d'abord à la formation partielle de Pu(IV), lequel précipite finalement sous forme de PuO_2 identifié par radiocristallographie.

Si on oxyde par contre Pu(III) ou Pu(IV) par un mélange O_2–Cl_2, ou si on traite par un mélange N_2–Cl_2 un bain de Pu(III)–Pu(IV) contenant des ions oxydes, on obtient le spectre de la Fig. 3 représentatif d'un mélange PuO_2(VI)–PuO_2(V)–PuO_2. Les ions plutonyles (V et VI) sont cependant instables dans le bain, ils se transforment progressivement en précipité de PuO_2; en effet, si on suit l'évolution d'un maximum d'absorption de PuO_2(V) ou de PuO_2(VI) en fonction du temps par voie spectrophotométrique au départ d'un bain de Pu(III)–Pu(IV) traité par un mélange O_2–Cl_2 (33–67%), on observe d'abord une augmentation puis une diminution qui conduit finalement à une absorbance très faible de PuO_2(VI) et PuO_2(V) et à un important précipité noir de PuO_2. Si, au moment où les concentrations en PuO_2(VI) et PuO_2(V) sont maximales, on traite ce bain par un mélange N_2–Cl_2, on observe que les bandes d'absorption de PuO_2(V) augmentent légèrement au détriment de celles de PuO_2(VI) lorsque la proportion d'azote augmente et inversément. Ceci permet d'ailleurs de faire les attributions des bandes observées à PuO_2(V) ou à PuO_2(VI).

Les observations peuvent s'interpréter sur la base des réactions chimiques suivantes:

$$2\,Pu^{3+} + \tfrac{1}{2}O_2 \rightarrow 2\,Pu^{4+} + O^{2-} \quad (2)$$

$$Pu^{4+} + 2\,O^{2-} \rightarrow PuO_2\downarrow \quad (3)$$

$$Pu^{4+} + O_2 + 2\,Cl^- \rightarrow PuO_2^{2+} + Cl_2 \quad (4)$$

$$PuO_2^{2+} + Cl^- \rightleftharpoons PuO_2^{+} + \tfrac{1}{2}Cl_2 \quad (5)$$

$$PuO_2^{+} + Cl^- \rightleftharpoons PuO_2\downarrow + \tfrac{1}{2}Cl_2 \quad (6)$$

Nous avons essayé, sur la base des équilibres (5) et (6), de dissoudre PuO_2 dans LiCl–KCl fondu par un barbotage de chlore pur; dans ces conditions, on observe effectivement une remise en solution très partielle de PuO_2; les absorbances à 1012 nm (PuO_2(VI)) et à 1122 nm (PuO_2(V)) ne dépassant cependant pas 0,04 et 0,01 respectivement. Cette très faible remise en solution signifie que le potentiel normal du couple PuO_2^+/PuO_2 est supérieur à celui du couple Cl_2/Cl^-. D'autre part, le potentiel normal du couple PuO_2^{2+}/PuO_2^+ doit être assez voisin de celui du couple PuO_2^+/PuO_2 puisque les trois espèces PuO_2(VI), PuO_2(V) et $PuO_2\downarrow$ sont toujours présentes simultanément en milieu oxydant.

Un barbotage d'acide chlorhydrique gazeux a pour effet de transformer toutes les espèces en Pu(III) et notamment de dissoudre très lentement PuO_2.

Établissement du diagramme potentiel/pO^{2-} du plutonium dans l'eutectique LiCl–KCl à 400°C

Les diagrammes d'équilibre potentiel rédox/pO^{2-} (où $pO^{2-} = -\log[O^{2-}]$) pour l'uranium[17], le plutonium[18] et le neptunium[19] ont été établis dans notre laboratoire. Le diagramme du plutonium doit être modifié; en effet, il n'y est pas fait mention des états d'oxydation (V) et (VI) d'une part, et d'autre part, la valeur du potentiel normal du couple Pu^{4+}/Pu^{3+} (−1,649 V) déterminée par mesure de

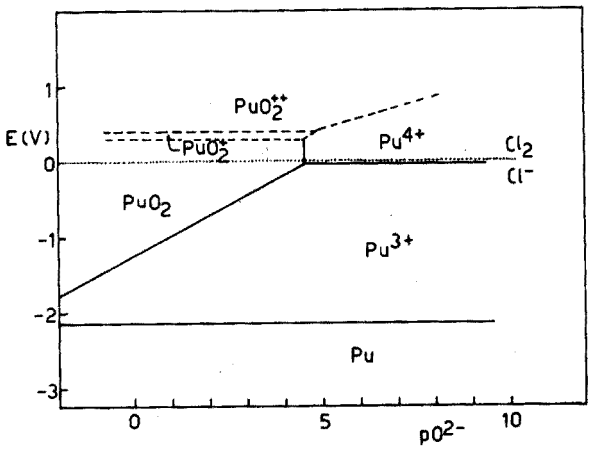

Fig. 5. Diagramme potentiel/pO^{2-} du plutonium dans l'eutectique LiCl–KCl à 400°C. (Traits interrompus: partie du diagramme estimée sur la base des réactions chimiques observées).

potentiel statique est entachée d'une erreur importante due à la réduction spontanée de Pu(IV) en Pu(III). Nous avons redéterminé la valeur du potential normal du couple Pu^{4+}/Pu^{3+} par spectrophotométrie d'absorption et obtenu $E^0 = -0{,}050 \pm 0{,}006$ V à 400°C[16] par rapport à l'électrode normale à chlore. La valeur du potentiel d'équilibre faisant intervenir PuO_2(V) et PuO_2(VI) est basée sur les réactions chimiques observées (Fig. 5).

Ce diagramme montre, contrairement à ce qui a été écrit précédemment[18], que la zone de stabilité de l'état trois augmente en passant du neptunium au plutonium.

Nous remercions vivement le Fonds National de la Recherche Scientifique et l'Institut Interuniversitaire des Sciences Nucléaires pour l'intérêt constant apporté à nos travaux et le soutien financier accordé à notre laboratoire.

RÉSUMÉ

La spectrophotométrie d'absorption visible et proche i.r. a permis d'observer un certain nombre de réactions chimiques du plutonium dans l'eutectique LiCl–KCl fondu avec des réactifs gazeux tels Cl_2, HCl et O_2. La comparaison des spectres obtenus avec ceux d'espèces connues permet d'identifier $PuCl_6^{2-}$ et $PuO_2Cl_4^{2-}$ dans le bain. On présente un nouveau diagramme potentiel/pO^{2-} qui permet d'interpréter les réactions chimiques observées.

SUMMARY

Visible and near-infrared absorption spectrophotometry provides a satisfactory method for the study of the chemical reactions of plutonium in fused LiCl–KCl eutectic with Cl_2, HCl or O_2. Comparison of the spectra obtained with those of known species leads to the identification of $PuCl_6^{2-}$ and $PuO_2Cl_4^{2-}$ in the melt. A new potential/pO^{2-} diagram is presented; this allows interpretation of the various observed chemical reactions.

BIBLIOGRAPHIE

1 J. L. Swanson, *J. Phys. Chem.*, 68 (1964) 438.
2 P. Speeckaert, *Thermodyn. Nucl. Mater., Proc. Symp. Vienna*, (1967) 195.
3 G. Landresse, *Anal. Chim. Acta*, 56 (1971) 29.
4 L. Martinot, *Bull. Soc. Chim. Belg.*, 82 (1973) 327.
5 J. Kooi, E. Weisskopf et D. M. Gruen, *J. Inorg. Nucl. Chem.*, 13 (1960) 310.
6 D. Cohen, *J. Inorg. Nucl. Chem.*, 18 (1961) 211.
7 M. Alei Jr., Q. C. Johnson, H. D. Cowan et J. F. Lemons, *J. Inorg. Nucl. Chem.*, 29 (1967) 2327.
8 A. Schmieder, E. Kuhn et W. Ochsenfeld, *KFK-1306*, 1970.
9 D. M. Gruen, R. L. McBeth, J. Kooi et W. T. Carnall, *Ann. N.Y. Acad. Sci.*, 79 (1960) 941.
10 C. E. Bamberger, R. G. Ross, C. F. Baes Jr. et J. P. Young, *J. Inorg. Nucl. Chem.*, 33 (1971) 3591.
11 D. M. Gruen et C. W. Dekock, *J. Inorg. Nucl. Chem.*, 29 (1967) 2569.
12 J. L. Ryan, *J. Phys. Chem.*, 65 (1961) 1856.
13 J. R. Morrey, *Inorg. Chem.*, 2 (1963) 163.
14 D. M. Gruen, P. Graf, S. Fried et R. L. McBeth, *Proc. 2nd Int. Conf. Peaceful Use At. En., Geneva P/940*, 28 (1958) 112.
15 J. L. Ryan, *Inorg. Chem.*, 2 (1963) 348.
16 G. Landresse et G. Duyckaerts, *Inorg. Nucl. Chem. Lett.*, 10 (1974) 675.
17 G. Landresse et G. Duyckaerts, *Anal. Chim. Acta*, 65 (1973) 245.
18 L. Martinot et G. Duyckaerts, *Anal. Chim. Acta*, 66 (1973) 474.
19 R. Lysy, G. Landresse et G. Duyckaerts, *Anal. Chim. Acta*,

Analytica Chimica Acta, 73 (1974) 129–139

SPECTROPHOTOMETRIC TITRATIONS OF NITRILOTRIACETIC ACID WITH COPPER(II) AS MONOLIGAND AND BILIGAND CHELATES

LEO HARJU and ROLF SARA
Department of Chemistry, Åbo Akademi, Åbo (Finland)
(Received 17th April 1974)

Recently[1], the equilibrium constants of mononuclear copper(II)–nitrilotriacetic acid (NTA) chelates have been determined by a method based on simultaneous pH and pCu measurements. The constants $K_{CuL}^{Cu.L} = 10^{13.3}$ and $K_{Cu(OH)L}^{OH.CuL} = 10^{4.6}$ were reported (L denotes NTA). Potentiometric titrations of copper with NTA as 1:1 chelate were carried out.

According to Ringbom[2], NTA also forms biligand chelates with copper and the value $K_{CuL_2}^{CuL.L} = 10^{3.6}$ is given in his monograph. From pH titrations, Anderegg[3] found this constant to be $10^{4.47}$, whereas Jokl[4], by electrophoretic measurements, obtained the value $10^{3.3}$.

The analytical determination and the complex equilibria of NTA are nowadays of considerable interest, because this reagent can replace phosphates in detergents. A visual titration of NTA in detergent formulations with copper(II) solution to chrome azurol S end-point has been described by Clinckemaille[5].

The present paper describes a study of the formation of monoligand and biligand chelates by spectrophotometric titrations without use of indicators. Spectrophotometric methods where the absorbances depend linearly on the concentrations of the components in the system, are especially useful when very weak chelates are formed.

CONDITIONAL CONSTANTS FOR TITRATIONS AS MONOLIGAND (1:1) AND BILIGAND (1:2) METAL CHELATES

The concept of conditional constants, developed by Ringbom[2], is very useful when choosing appropriate conditions for complexiметric analysis. In two recent papers[6,7], Harju and Ringbom showed how conditional constants can be calculated for cases where mononuclear and binuclear chelates are formed. A thorough explanation of the concepts of conditional constants and α-coefficients can be found in Ringbom's monograph[2].

The titration to the biligand (1:2) chelate can be considered by the reaction (charges are omitted for simplicity):

$$(ML)' + L' = (ML_2)'$$

The conditional constant of the reaction is

$$K_{(ML_2)}^{(ML)'L'} = \frac{[(ML_2)']}{[(ML)'][L']} = \frac{\alpha_{ML_2}}{\alpha_{ML}\alpha_L} K_{ML_2}^{ML.L} \qquad (1)$$

where the α-coefficients have their usual meaning as given by the equations

$$\alpha_L = \alpha_{L(H)} + \alpha_{L(N)} - 1 \quad (2)$$

$$\alpha_{ML} = \alpha_{ML(H)} + \alpha_{ML(OH)} + \alpha_{ML(diss)} - 2 \quad (3)$$

$$\alpha_{ML_2} = \alpha_{ML_2} \quad + \alpha_{ML_2(OH)} - 1 \quad (4)$$

In eqn. (2), $\alpha_{L(N)}$ represents the interference of another metal ion N. $\alpha_{ML(diss)}$ accounts for the dissociation of the 1:1 chelate and is defined by

$$\alpha_{ML(diss)} = \frac{[ML]+[M']}{[ML]} = 1 + 1/[L]K_{ML}^{M'L} \quad (5)$$

where [L] varies during the titration. $\alpha_{ML(diss)}$ can be obtained by iterative calculations, but it very seldom differs from unity.

At the 1:2 equivalence point, the concentration of metal ions not bound to the ligand is very small and the approximation $[L']=[(ML)']$ can be made. The concentration of these components is given by

$$[L'] = [(ML)'] = ([(ML_2)']/K_{(ML_2)'}^{(ML)'L'})^{\frac{1}{2}} \quad (6)$$

$$\approx (c_M/K_{(ML_2)'}^{(ML)'L'})^{\frac{1}{2}} \quad (7)$$

The free metal concentration at the 1:2 equivalence point is approximately given by

$$[M] = 1/K_{(ML)'}^{M,L'} \quad (8)$$

$\alpha_{L(ML)}$ defined by eqn. (10) should not be considered in the conditional constant in eqns. (6)–(8).

The case where the formation of 1:1 chelates represents the main reaction and where biligand chelates are also formed has been thoroughly treated by Ringbom[2]. The conditional constant for the titration to the 1:1 chelate is

$$K_{(ML)'}^{M'L'} = \frac{[(ML)']}{[M'][L']} = \frac{\alpha_{ML}}{\alpha_M \alpha_L} K_{ML}^{M,L} \quad (9)$$

The formation of biligand chelates is taken into consideration by the coefficient

$$\alpha_{L(ML)} = 1 + \frac{[(ML)']K_{ML_2}^{ML,L}\alpha_{ML_2}}{\alpha_{ML}} \quad (10)$$

EXPERIMENTAL

Nitrilotriacetic acid (E. Merck, Darmstadt) was used for most experiments. The following logarithmic protonation constants (mixed)[1,8,9] were used in the calculations: 9.95, 2.57, 1.97, 1.18. For conversion of concentration constants to mixed constants, a modified form of Kielland's table was used[10].

The titrations and pH measurements were performed in a thermostated titration cell. Titrant was added by a Metrohm E 457 microburet. For pH measurements an Orion 801 pH/mV meter was used. The simultaneously performed spectrophotometric measurements were made with a Coleman model 46 UV-VIS Spectrophotometer equipped with a quartz flow cell. The optical path length was 0.5 cm.

When absorptivities were calculated from Beer's law:

$$a = A/bc \tag{11}$$

the sample path length b was taken as unity, in order to simplify calculations. The factor 0.5 need not be repeated in all calculations, but this means that the calculated values of absorptivities are half the true values.

For all calculations a programmable Monroe 1860–44 calculator was used. The program capacity of the calculator was 2048 steps, but less than half the capacity was needed here.

DETERMINATION OF THE STABILITY CONSTANT OF THE BILIGAND COPPER–NTA CHELATE

In order to choose appropriate wavelengths for the spectrophotometric studies, absorbance curves were recorded for 1:1 and 1:2 copper–NTA mixtures at pH 9.00 (Fig. 1).

Both curves show an absorption peak at 700–800 nm, the absorptivities of the monoligand and biligand chelates being quite low and of about the same magnitude. At wavelengths below 380 nm, copper–NTA chelates absorb radiation very strongly, hence absorbance can be measured in both the visible and ultraviolet regions.

The equilibrium constant $K_{CuL_2}^{CuL,L}$ was determined as suggested by Ringbom and Lundqvist[11]. Absorbances of the Cu–NTA chelates were measured as a function of pH in the presence of an excess of ligand (Fig. 2). It can be seen that monoligand chelates predominate below pH 6 and biligand chelates at pH 7–10. From these regions, the absorptivities $a_{CuL} = 6.2$ and $a_{CuL_2} = 111.3$ at 360 nm were calculated. The calculation of the concentrations $[CuL_2]$, $[CuL]$ and $[L']$ is based on the following equations

$$A = a_{CuL}[CuL] + a_{CuL_2}[CuL_2] \tag{12}$$

$$c_{Cu} = [CuL] + [CuL_2] + [Cu'] \tag{13}$$

$$c_L = [CuL] + 2[CuL_2] + [L'] \tag{14}$$

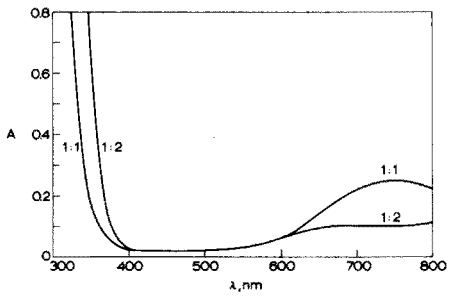

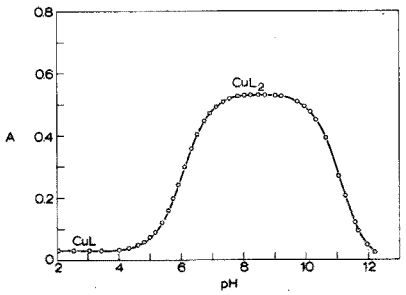

Fig. 1. Absorbance curves for copper(II)–NTA chelates. pH = 9.00, $c_{NTA} = 10^{-2.30}$ M. Metal to ligand ratios are 1:1 and 1:2 (as denoted in the figure).

Fig. 2. The absorbance for a solution containing copper(II) and NTA in the molar ratio of 1:8, as function of pH. $c_{Cu} = 10^{-2.30}$ M, $\lambda = 360$ nm, $V_0 = 50.0$ ml, $\mu \approx 0.1$, 25°C.

TABLE I

DETERMINATION OF THE EQUILIBRIUM CONSTANT $K_{CuL_2}^{CuL,L}$ FROM SPECTROPHOTOMETRIC DATA

($\lambda = 360$ nm, $V_0 = 50.0$ ml, $c_{Cu} = 0.005$ M, $c_{NTA} = 0.04$ M, $\mu \approx 0.1$ (KNO_3), 25°C.)

pH	*A*	*V*	$-log\ [CuL_2]$	$-log\ [CuL]$	$-log\ [L']$	$log\ \alpha_{L(H)}$	$log\ K_{CuL_2}^{CuL,L}$
6.17	0.089	51.76	3.25	2.37	1.48	3.78	4.378
6.39	0.120_5	51.80	3.06	2.40	1.48	3.56	4.380
6.59	0.160	51.84	2.91	2.45	1.49	3.36	4.387
6.74	0.195	51.88	2.80	2.49	1.49	3.21	4.388
6.92	0.242_5	51.92	2.69	2.55	1.50	3.03	4.390
7.12	0.299	51.96	2.59	2.65	1.51	2.83	4.394
7.34	0.356	52.00	2.51	2.77	1.52	2.61	4.387
7.53	0.402	52.04	2.45	2.90	1.52	2.42	4.391
7.77	0.446	52.08	2.40	3.08	1.53	2.18	4.384
7.95	0.471	52.12	2.38	3.23	1.53	2.00	4.382

The concentration of copper ions not bound to the ligand, [Cu'], is very low in the pH region studied and can be omitted. The results of the determination of $K_{CuL_2}^{CuL,L}$ by using eqn. (1) are given in Table I. Because the pH was adjusted with potassium hydroxide solution, a volume correction must be applied to the total concentrations of ligand and metal ion. For $K_{CuL_2}^{CuL,L}$, the value $10^{4.39}$ is obtained, which is in good agreement with the value given by Anderegg[3].

At pH values above 12 the absorbance values in Fig. 2 decrease, indicating the formation of hydroxo monoligand chelates ($Cu(OH)_nL$). From this part of the curve, $K_{Cu(OH)L}^{OH} = 10^{4.6}$ was calculated.

TITRATIONS AS MONOLIGAND (1:1) CHELATES

In Fig. 3, the conditional constants $K_{(CuL)'}^{Cu'L'}$ and $K_{CuL_2}^{(CuL)'L'}$ are plotted as a function of pH. The values of the conditional 1:1 constants are high, and even at pH 2, $K_{(CuL)'}^{Cu'L'}$ equals $10^{4.7}$. The formation of biligand chelates interferes with the spectrophotometric titration to the 1:1 chelate chiefly in the pH range

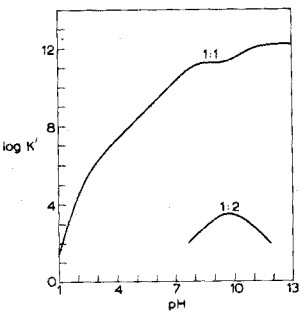

Fig. 3. Conditional constants as functions of pH in titrations of NTA with copper(II) as monoligand (1:1) and biligand (1:2) chelates. c_{NTA} is assumed equal to 10^{-3} M.

8–11. This interference naturally also depends on the total concentration of the ligand or metal ion.

Figures 4 and 5 show some spectrophotometric titrations of NTA with copper(II) solution at different pH in the ultraviolet region. At pH 4.5 (acetate buffer, Fig. 4), where the calculated conditional constant according to Fig. 3 is $10^{7.8}$, the titration consists, as expected, of two almost straight lines. In this case and at higher pH values, it is easy to locate the 1:1 end-point as the intersection of the two branches of the curve.

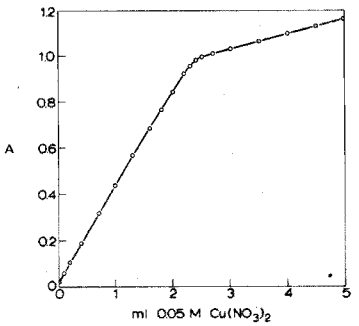

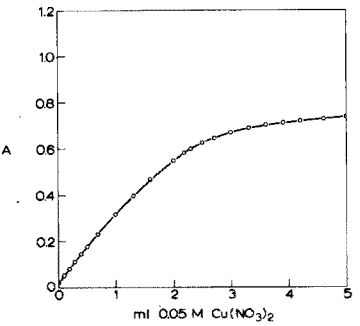

Fig. 4. Spectrophotometric titration of NTA with copper(II) at pH 4.5 ($c_{Ac} = 0.1$ M) without indicator. $\lambda = 280$ nm, $V_0 = 100$ ml. Theoretical consumption 2.320 ml (1:1 chelate); obtained consumption 2.320 ml.

Fig. 5. Spectrophotometric titration of NTA with copper(II) at pH 1.62 without indicator. $\lambda = 280$ nm, $V_0 = 101.2$ ml, $\mu \approx 0.1$ ($NaClO_4$). Theoretical consumption 2.320 ml (1:1 chelate); obtained consumption 2.317 ml.

If the titrations are carried out at low pH, the interference of several metals can be eliminated. Figure 5 presents a titration of NTA at pH 1.62, where the reaction does not proceed quantitatively and the curve is thus rounded in the vicinity of the 1:1 equivalence point. Most methods for the evaluation of the equivalence point from this type of curve[2,12], are based on graphical determination from a "normalized" titration curve, *i.e.* a curve where the absorbance values have been corrected for dilution. If this is done, and the linear portions near the ends of the corrected curve are extrapolated, surprisingly good results can be obtained, probably because of compensation of errors.

Treatment of titration data

In this paper, a new method is described for the determination of the equivalence point for titrations carried out without an indicator. In this method, the conditional stability constant of the reaction is taken into consideration. When the constant is low, *i.e.*, when the titration curve is strongly rounded at the equivalence point, the new method is superior to the graphical one.

For spectrophotometric titrations of L with M where 1:1 metal chelates are formed the following equations are valid:

$$K^{M'L'}_{(ML)'} = \frac{[(ML)']}{[M'][L']} \tag{15}$$

$$c_M = [(ML)'] + [M'] \tag{16}$$

$$c_L = [(ML)'] + [L'] \tag{17}$$

$$A = a_{(ML)'}[(ML)'] + a_{M'}[M'] + a_{L'}[L'] \tag{18}$$

where

$$c_L = \frac{V_{eq} c_t}{V_0 + V} \tag{19}$$

$$c_M = \frac{V c_t}{V_0 + V} \tag{20}$$

V_0 being the initial volume, V the added volume of titrant, V_{eq} the equivalence volume, c_t the molarity of the titrant, A the measured absorbance, and $a_{(ML)'}$, $a_{M'}$ and $a_{L'}$ the absorptivities for the respective components.

An iterative technique is then used to find the values of V_{eq}, $K^{M;L'}_{(ML)'}$ and $a_{(ML)'}$ best satisfying the experimental data. The basic principle is that each of the unknowns is calculated from the optimal part of the spectrophotometric titration curve.

An approximate value for V_{eq} is first determined by fitting straight lines to the linear parts at the beginning and end of the titration curve by the method of least squares and then taking the intersection point as equivalence point. A first approximate value for $a_{(ML)'}$ is calculated from the absorbance at the equivalence point. The iteration is started by calculating the conditional stability constant. For the calculation of $K^{M;L'}_{(ML)'}$ the optimal part of the titration curve lies near the equivalence point because the dissociation of the metal chelate is there maximal. The mean value of the constants calculated for some points around the equivalence point is taken as the value for the conditional constant in the next step of the iteration.

Values of $a_{(ML)'}$ are calculated from the beginning of the titration curve, where the excess of the ligand is greatest and the ratio $[(ML)']/[M']$ is thus maximal. The concentrations of the different components are calculated from eqns. (15)–(17) and the values are inserted in eqn. (18). It is not advisable to calculate the arithmetic mean of the absorptivities thus obtained for the different titration points. Relative errors in measurements of absorbances would have too large an influence on $a_{(ML)'}$ calculated for the first titration points, and would thus also strongly influence the mean. This difficulty can be overcome as follows. The absorptivities are multiplied by the corresponding total metal concentration corrected to the initial volume. A straight line is fitted to the points obtained in this way by the method of least squares. The slope of the line gives a new value for $a_{(ML)'}$. This value is a weighted mean of the absorptivities obtained from eqn. (18).

V_{eq} is calculated from the end of the titration curve, where there is an excess of metal ion and the ratio $[(ML)']/[L']$ is greatest. The concentrations of the different components are calculated from eqns. (15), (16) and (18). The total concentration of the ligand, c_L, is obtained from eqn. (17) and the equivalence volume V_{eq} from eqn. (20). The arithmetic mean of the equivalence volumes is taken as a new value for V_{eq}. The arithmetic mean is satisfactory because the measured absorbances for titration points in the end of the curve are of the same magnitude.

The iteration is continued by repeated calculations of the conditional constant, $a_{(ML)'}$ and V_{eq}. The rate of convergence depends chiefly on the magnitude of the conditional constant of the reaction; the number of titration points used also affects the convergence in some degree. A similar treatment is of course valid for titrations in the reverse direction. The mathematical treatment is the same in both cases. Only c_L and c_M are interchanged in eqns. (19) and (20).

The above principles were first applied to the titration of NTA at pH 1.62 (Fig. 5), where the curve is strongly rounded. Graphical extrapolation from the absorbance curve corrected for dilution gave the consumption 2.14 ml, which corresponds to a titration error of -7.8%. When the new approach was used, the equivalence volume 2.317 ml was computed, which is in good agreement with the theoretical value of 2.32 ml.

To illustrate the method better, the data for titration at pH 1.62 are presented in Table II. The first two columns give the experimental data; the remaining columns present the values $K^{Cu,L'}_{(CuL)'}$, $a_{(CuL)'}$ and V_{eq} obtained after about 10 iterations. The Table shows that the equivalence volume can be computed with good accuracy. The variations of the values of V_{eq} correspond to an error of ± 0.001 units in the measurements of the absorbance.

TABLE II

SPECTROPHOTOMETRIC TITRATION OF NTA WITH COPPER(II) SOLUTION WITHOUT INDICATOR

($\lambda = 280$ nm, $V_0 = 101.2$ ml, pH = 1.62, $\mu \approx 0.1$; theoretical equivalence volume 2.320 ml.)

ml 0.05 M Cu(II)	*A*		$a_{(CuL)'}$	V_{eq}
0	0.017			
0.101	0.0485	—	683.8	—
0.200	0.0785	—	677.4	—
0.300	0.110	—	686.3	—
0.400	0.1415	—	692.8	—
0.500	0.173	—	698.4	—
0.700	0.230	—	689.7	—
1.000	0.316	—	—	—
1.600	0.4655	—	—	—
2.000	0.5455	—	—	—
2.200	0.5795	3.972	—	—
2.300	0.5945	3.974	—	—
2.500	0.621	3.977	—	—
2.700	0.642	3.974	—	—
3.000	0.667	—	—	—
3.300	0.687	—	—	—
3.600	0.701	—	—	2.316
3.900	0.712	—	—	2.316
4.200	0.720	—	—	2.318
4.600	0.7275	—	—	2.319
5.000	0.7335	—	—	2.318
		$K^{Cu,L'}_{(CuL)'} = 10^{3.974}$	$\bar{a}_{(CuL)'} = 693.1$	$\bar{V}_{eq} = 2.317$

This approach can also be used as an exact method for the determination of stability constants. For the case presented in Table II, the conditional equilibrium constant $K^{Cu,L'}_{(CuL)'}$ equals $10^{3.97}$. The values calculated for four titration points in the vicinity of the equivalence point vary only in the third decimal place. If $\alpha_{L(H)}$ is inserted in the constant, $K^{Cu,L}_{(CuL)'} = 10^{13.80}$ is obtained. This high value for the 1:1 constant implies that protonated chelates are formed. If the stability (non-conditional) constant $K^{Cu,L}_{CuL}$ is taken as $10^{13.3}$ (ref. 1), the value $10^{1.95}$ is obtained for K_{CuHL}.

For further illustration, the variations of the concentrations of the different components are shown as a function of ml of titrant added in Fig. 6. It can be seen that about 70% of the ligand has reacted at the 1:1 equivalence point.

The titrations of NTA at pH 4.55, where only a slight curvature can be observed, were also treated by the proposed method. The values $V_{eq} = 2.320$ ml, $K^{Cu;L'}_{(CuL)'} = 10^{6.0}$ and $a_{(CuL)'} = 857$ were computed. The simple graphical extrapolation method gave a result of 2.28 ml, corresponding to an error of -2%. The computed conditional constant is surprisingly low compared to the value given in Fig. 3, because of the side reaction between copper and acetate ions. It may be pointed out that if the reaction is almost complete, the determination of the conditional equilibrium constant is more uncertain. The relatively steep rise in the titration curve after the 1:1 equivalence point is caused by the formation of acetato–copper complexes. The value 857 for $a_{(CuL)'}$ in this case is considerably higher than the values obtained in absence of buffer. This again indicates the formation of mixed ligand chelates of the type $Cu(Ac)_nNTA$, which is very probable because the quadridentate ligand hardly can satisfy the coordination tendencies of the copper(II) ions.

Figure 7 shows a spectrophotometric titration of $1.62 \cdot 10^{-5}$ *M* NTA solution at pH 4.55 (acetate). Iterative calculations gave the equivalence volume 1.65 ml, which is in fair agreement with the theoretical value 1.62 ml. In this titration the scale readings were amplified to give the absorbances to four decimal places. Better accuracy might be attained if the titration were performed at somewhat higher pH.

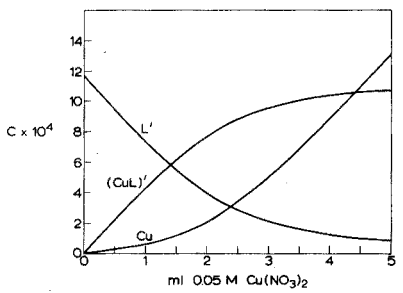

Fig. 6. The concentrations of the components L', (ML)' and *M'* for the titration given in Fig. 5 as a function of ml of copper(II) solution added.

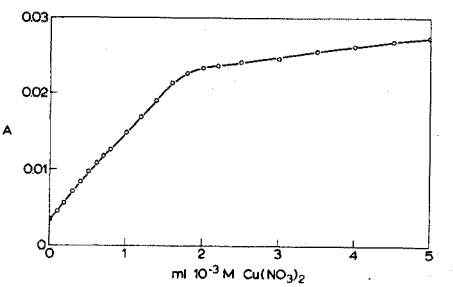

Fig. 7. Spectrophotometric titration of $1.62 \cdot 10^{-5}$ *M* NTA with copper(II) at pH 4.6 ($c_{Ac} = 0.01$ *M*) without indicator. $\lambda = 270$ nm, $V_0 = 100$ ml. Theoretical consumption 1.62 ml (1:1 chelate); obtained consumption 1.65 ml.

TITRATIONS AS BILIGAND (1:2) CHELATES

For titrations as biligand copper–NTA chelates (M:L = 1:2) the optimal pH range is 9–10, where $K_{CuL_2}^{(CuL)'L'}$ attains its maximal value, $10^{3.5}$ (Fig. 3). Some spectrophotometric titrations of NTA with copper(II) solution were performed in this pH region; in order to avoid interference from buffers, the pH was kept automatically constant by addition of potassium hydroxide with a Radiometer TTT 1 titrator.

Figure 8 shows a titration of 0.005 *M* NTA at pH 9.00 with measurement at 340 nm. The angle formed by the extrapolated lines at the 1:2 equivalence point is very favourable for determination of this end-point. However, in this case the determination of the 1:2 equivalence point is of minor practical interest because the ligand can be determined accurately as the 1:1 chelate.

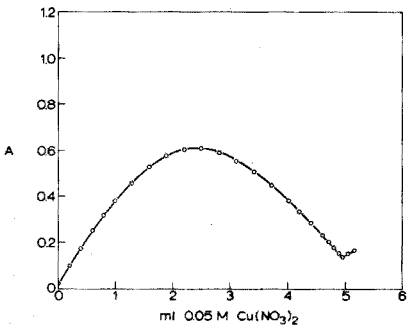

Fig. 8. Spectrophotometric titration of NTA with copper(II) at pH 9.00. $V_0 = 50$ ml, $\mu \approx 0.1$ ($NaClO_4$), $\lambda = 340$ nm. Theoretical consumptions 2.49 ml (1:2 chelate) and 4.97 ml (1:1 chelate); obtained consumption 4.97 (1:1 chelate).

Since the spectrophotometric curve (Fig. 8) is rounded at the 1:2 equivalence point, the conditional constant for the formation of the biligand chelate can be calculated from the curve by the following equations:

$$K_{CuL_2}^{(CuL)'L'} = \frac{[CuL_2]}{[(CuL)'][L']} \tag{21}$$

$$c_L = 2[CuL_2] + [(CuL)'] + [L'] \tag{22}$$

$$c_{Cu} = [CuL_2] + [(CuL)'] + [Cu'] \tag{23}$$

$$A = a_{CuL_2}[CuL_2] + a_{(CuL)'}[(CuL)'] + a_{L'}[L'] + a_{Cu'}[Cu'] \tag{24}$$

Before the 1:1 equivalence point, the concentration of copper(II) is very small, and the terms including [Cu'] can be neglected. The absorptivities of L' and (CuL)' can be obtained from the initial part of the titration curve and from the 1:1 equivalence point, respectively.

An iterative procedure is used for the calculation of $K_{CuL_2}^{(CuL)'L'}$. First a value is assumed for $K_{CuL_2}^{(CuL)'L'}$ and the concentrations of the components CuL_2, (CuL)' and L' are calculated from eqns. (21)–(23); a_{CuL_2} is obtained from the beginning

of the titration curve by eqn. (24) with a procedure similar to that described previously for the calculation of $a_{(CuL)'}$. From this value for a_{CuL_2} and from the measured absorbance value in the 1:2 equivalence point, a new value for $K_{CuL_2}^{(CuL)'L'}$ can be computed from eqns. (21), (22) and (24). After a few iterations, the value $10^{2.9}$ was obtained. For the non-conditional constant we have

$$K_{CuL_2}^{CuL,L} = K_{CuL_2}^{(CuL)'L'} \alpha_{CuL(OH)} \alpha_{L(H)} = \quad (25)$$
$$= 10^{2.95}\ 10^{0.15}\ 10^{1.00} = 10^{4.10}$$

This value is somewhat low compared to the earlier obtained constant $10^{4.38}$, probably because the ionic strength and pH were adjusted with sodium salts, and sodium ions form relatively stable complexes with the ligand.

DISCUSSION

Titrations of NTA with copper(II) solution—or in the reverse direction—can best be performed to the 1:1 chelate. The conditional 1:1 constant is sufficiently high in almost the entire pH region to allow an accurate determination. For titrations of NTA at pH 4.5 (acetate buffer) or at higher pH, a sharp break is obtained at the 1:1 equivalence point. Even at pH values below 2, where the titration curves are very rounded, the end-point can be detected with good accuracy.

This was made possible especially by the development of a new method for the exact determination of the equivalence volume. For cases where the conditional constants are low and the titration curves are rounded, this approach was superior to the graphical method based on linear extrapolation of the two branches of a volume-corrected curve. The performance of titrations as well as the treatment of data can easily be automated. The conditional constant of the reaction can be obtained simultaneously; calculations for the titration at pH 1.62 showed that the constant can be obtained with good accuracy.

The use of the ultraviolet spectral region allows titrations of dilute NTA solutions. About 10^{-5} M solutions were titrated with satisfactory accuracy. Even more dilute solutions could be titrated if some factors affecting the accuracy were optimized, *e.g.* by using longer path lengths, scale expansion, and filtration of solutions.

The formation of the biligand chelate does not usually affect the equilibrium situation in the copper(II)–NTA system. Only when titrations are made to the 1:1 chelate in the pH region 8–11 at sufficiently high ligand concentration, need the formation of biligand chelates be considered.

If spectrophotometric and potentiometric titrations are compared, one can generally say that the latter perhaps are simpler and faster. Especially when the conditional 1:1 constant is sufficiently high, a potentiometric titration with a copper(II)-selective electrode as indicator electrode, is probably the more accurate. However, if the conditional constant for the reaction is low, or if very dilute solutions are to be titrated, the spectrophotometric method may be more advantageous.

We thank Prof. E. Wänninen for reading and commenting on the manuscript, and Mr. M. Pickering for revising the English text of this paper.

SUMMARY

NTA was determined at different concentrations and at different pH values by spectrophotometric titration with copper(II) solution as titrant without an indicator. A method was developed for the exact determination of the equivalence volume for such titrations. The conditional constant for the reaction was simultaneously computed. The method is especially advantageous if the spectrophotometric titration curve is very rounded, *i.e.* the reaction does not proceed quantitatively. The equilibrium constant $K_{CuL_2}^{CuL,L} = 10^{4.39}$ was determined for the formation of biligand copper–NTA chelates. For basic and protonated mononuclear chelates, $K_{Cu(OH)L}^{CuL,OH} = 10^{4.6}$ and $K_{CuHL}^{CuL,H} = 10^{1.95}$ were obtained.

REFERENCES

1 L. Harju, *Suom. Kemistilehti, B*, 46 (1973) 199.
2 A. Ringbom, *Complexation in Analytical Chemistry*, Wiley–Interscience, New York, 1963.
3 G. Anderegg, *Essays in Coordination Chemistry*, Birkhäuser Verlag, Basel, 1963.
4 V. Jokl, *J. Chromatogr.*, 14 (1964) 71.
5 G. G. Clinckemaille, *Anal. Chim. Acta*, 43 (1968) 520.
6 L. Harju and A. Ringbom, *Anal. Chim. Acta*, 49 (1970) 205.
7 L. Harju and A. Ringbom, *Anal. Chim. Acta*, 49 (1970) 221.
8 G. Schwarzenbach and E. Freitag, *Helv. Chim. Acta*, 34 (1951) 1492.
9 G. Anderegg, *Helv. Chim. Acta*, 50 (1967) 2333.
10 I. M. Kolthoff and P. J. Elving, *Treatise on Analytical Chemistry, Part I. Theory and Practise*, Vol. I, Interscience—Wiley, New York, 1959.
11 A. Ringbom and G. Lundqvist, unpublished results.
12 R. F. Goddu and D. N. Hume, *Anal. Chem.*, 26 (1954) 1740.

Analytica Chimica Acta, 73 (1974) 141–148

ANION-EXCHANGE ISOLATION OF RARE-EARTH ELEMENTS FROM APATITE MINERALS IN METHANOL–NITRIC ACID MEDIUM

I. ROELANDTS* and G. DUYCKAERTS**

University of Liège, B-4000 Sart-Tilman by Liège 1 (Belgium)

A. O. BRUNFELT

Mineralogical-Geological Museum, University of Oslo, Sarsgate, 1, Oslo (Norway)

(Received 1st May 1974)

Radiochemical procedures for the isolation of rare-earth elements (REE) from various matrices are abundant in the literature. Most of these methods are based on ion-exchange chromatography, with complexing organic acids, *e.g.* citric acid[1], lactic acid[2], α-hydroxyisobutyric acid (α-HIBA)[3], ethylenediaminetetraacetic acid (EDTA)[4], N-hydroxyethylethylenediaminetriacetic acid (HEDTA)[5]. More recently, the suitability of inorganic filters such as calcium fluoride has been investigated for this purpose[6–8].

In apatite minerals, $Ca_5(PO_4)_3(OH, F, Cl)$, with generally high contents of REE (of the order of tenths of a percent or higher), different methods have been proposed: *e.g.* liquid–liquid extraction with tri-n-butyl phosphate (TBP)–nitric acid[9,10] and bis-(2-ethylhexyl)phosphoric acid (HDEHP)–cyclohexane–perchloric acid[11], or extraction chromatography with tri-n-butyl phosphate (TBP)–nitric acid[12].

In pure aqueous nitric acid solutions, no significant adsorption of REE on strongly basic anion-exchange resins has been observed at any acid concentration[13–15]. However, during the last decade, mineral acid–miscible organic solvent mixtures have been widely studied by Korkisch and his co-workers[16–28] and other authors[29–41], who have demonstrated an enhanced sorption of these elements by the resin from such media. A general survey of analytical applications of ion-exchange in mixed and nonaqueous media has been published by Korkisch[28]. Several investigators have reported on the anion-exchange behaviour of REE from nitric–methanol medium[16–18,28,30,34,35,37,39,40]. Korkisch and Tera[16] found that the REE and thorium were adsorbed strongly from nitric acid–methanol and thus separated from many other elements. Faris and Warton[34] studied the adsorption of REE, yttrium and scandium from nitric acid–methanol mixtures on to strongly basic anion-exchange resins, *e.g.* Dowex 1-X4, 200–400 mesh.

The aim of the present research was to extend previous studies on nitric acid–methanol mixtures to a wider range of concentrations (ranging from 5% (v/v) 7 *M* nitric acid–95% methanol to 50% 7 *M* nitric acid–50% methanol) and to determine, radiochemically, the distribution coefficients, K_d, for REE as well for

* Geology, Petrology and Geochemistry.

** Analytical Chemistry.

other elements under these various conditions by a batch equilibrium method, in order to obtain the fundamental information needed to facilitate the prediction of column separation possibilities for analytical purposes. On the basis of these data, a mixed solvent anion-exchange method has been developed for separation of REE from calcium and other common elements in apatites.

EXPERIMENTAL

Chemicals and equipment

Ion-exchange resin. A 8% cross-linked 100–200 mesh Dowex 1 strongly basic anion-exchange resin of the quaternary amine type, in chloride form, was suspended in water and colloïdal particles were removed by several decantations. The rest was transferred to a large preparative column and converted to the nitrate form by sequential treatment with 1 *M* to 7 *M* nitric acid until no chloride ion was detectable in the effluent. The resin was further rinsed with methanol. Then it was left to dry overnight, exposed to the air, afterwards placed in an oven at 70°C for 3 h, and finally stored in a screwcap bottle.

Nitric acid–methanol mixtures. Stock solutions were prepared for all the experiments by mixing the required volumes of methanol, nitric acid and water.

Tracers. The radioisotopes used were obtained by irradiation of spectrographically pure rare-earth oxides with a neutron flux of about $2.8 \cdot 10^{11}$ n cm^{-2} s^{-1} in the BR-1 reactor, CEN, Mol (Belgium) for 1–5 days. The lanthanide nitrate stock solutions were prepared by dissolving the irradiated oxides in nitric acid with the addition of a few drops of hydrogen peroxide to speed up dissolution, evaporating nearly to dryness on a hot plate, taking up in very dilute nitric acid, and filtering off.

Counting Equipment. A $3 \times 3''$ NaI(Tl) well-type scintillation detector and a 400-channel pulse-height analyser were used for the radioassay of REE and scandium. For the other elements, the measurements were performed with an atomic absorption spectrophotometer (Perkin-Elmer, model 290B).

Determination of batch distribution coefficients

The batch distribution coefficient, K_d, of a specific element is defined as the concentration of element per gram of dry resin divided by the concentration of element per ml of solution. As the concentration may be considered directly proportional to the radioactive counting rates, the distribution coefficient can be calculated by using the formula:

$$K_d = (A_O - A_E)V/A_E W$$

where A_E is the measured activity in an aliquot of solution after equilibration, A_0 is the initial activity in the same volume, V is the volume of solution (10 ml), and W is the weight of dry resin (0.5 g).

Procedure. Volumes of 10 ml containing a nitric acid–methanol mixture of a given composition and the tracer of interest were introduced in 50-ml round-bottom Pyrex centrifuge tubes, together with an accurately weighed amount of about 0.5 g of dry resin. The stoppered tubes were mixed mechanically on a home-made rotator machine for 18 h. After equilibration, the resin was allowed

to settle for 30 min. Exactly 5-ml aliquots of solution were pipetted carefully in order to avoid transferring any resin particles and transferred to polypropylene tubes for the γ-activity measurements. The activity was compared with that of a reference solution. All the experiments were carried out at room temperature.

According to Stewart *et al.*[35], in a nitric acid–organic solvent system, equilibrium is reached after a mixing period of less than 1 h. To ensure complete attainment of equilibrium, all data in this work were obtained after rotating for 18 h.

Because of the relatively short half-life for ^{165}Dy ($t_{\frac{1}{2}}=2.35$ h), the K_d values for dysprosium were determined by atomic absorption spectrometry.

RESULTS AND DISCUSSION

Table I presents the distribution coefficients for Na, Mg, Al, K, Ca, Sc, Mn, Fe and REE obtained from a series of experiments carried out with varying compositions of nitric acid–methanol mixtures. From these data, it can be seen that

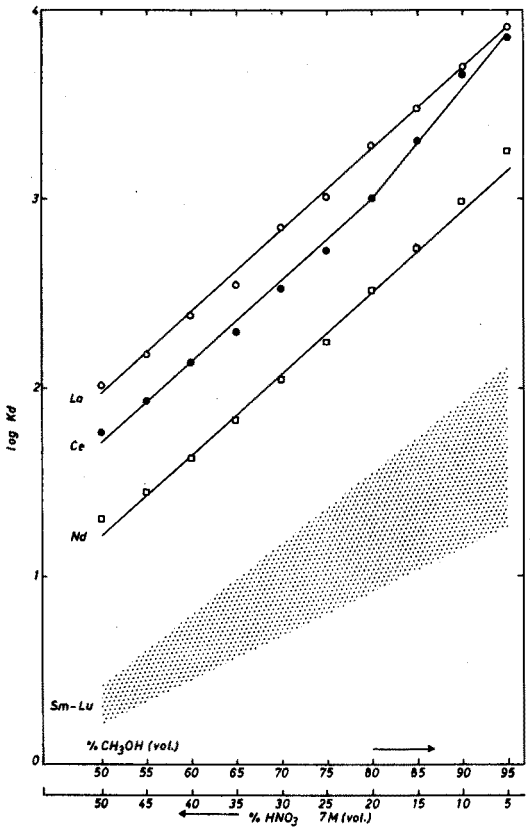

Fig. 1. Variation of distribution coefficient, K_d, with the solvent concentration and acidity. Dowex 1–×8, 100–200 mesh.

all the common cations in the apatite have, in general, distribution coefficients below those of the REE. The results clearly indicate that, in all cases, the adsorption of these elements on the resin from these mixed solvent solutions is

TABLE I

DISTRIBUTION COEFFICIENTS IN 7 *M* NITRIC ACID–METHANOL MIXTURES

	5% 7 M HNO_3 95% CH_3OH	*10% 7 M HNO_3 90% CH_3OH*	*15% 7 M HNO_3 85% CH_3OH*	*20% 7 M HNO_3 80% CH_3OH*	*25% 7 M H 75% CH_3O*
Na^+	<1	<1	<1	<1	<1
Mg^{2+}	<1	<1	<1	<1	<1
Al^{3+}	<1	<1	<1	<1	<1
K^+	<1	<1	<1	<1	<1
Ca^{2+}	3.9	3.3	1.8	<1	<1
Sc^{3+}	<1	<1	<1	<1	<1
Mn^{7+}	<1	<1	<1	<1	<1
Fe^{3+}	<1	<1	<1	<1	<1
La^{3+}	8000	5000	3000	1929	1028
Ce^{3+}	7100	4500	2000	995	522
Nd^{3+}	1763	954	535	314	173
Sm^{3+}	113	72	43	26	17
Eu^{3+}	126	60	33	20	14
Gd^{3+}	69	52	29	23	14
Tb^{3+}	63	42	28	20	12
Dy^{3+}	52	40	30	21	15
Ho^{3+}	28	22	17	13	10
Tm^{3+}	25	22	19	13	10
Yb^{3+}	19	14	12	10	7.9
Lu^{3+}	25	18	15	12	8.8

	30% 7M HNO_3 70% CH_3OH	*35% 7 M HNO_3 65% CH_3OH*	*40% 7 M HNO_3 60% CH_3OH*	*45% 7 M HNO_3 55% CH_3OH*	*50% 7 50% C*
Na^+	<1	<1	<1	<1	<1
Mg^{2+}	<1	<1	<1	<1	<1
Al^{3+}	<1	<1	<1	<1	<1
K^+	<1	<1	<1	<1	<1
Ca^{2+}	<1	<1	<1	<1	<1
Sc^{3+}	<1	<1	<1	<1	<1
Mn^{7+}	<1	<1	<1	<1	<1
Fe^{3+}	<1	<1	<1	<1	<1
La^{3+}	692	351	238	152	104
Ce^{3+}	332	196	135	84	57
Nd^{3+}	111	67	42	28	20
Sm^{3+}	12	6.9	4.9	3.4	2.0
Eu^{3+}	8.5	5.7	4.3	2.8	1.8
Gd^{3+}	12	7.9	4.6	3.9	2.1
Tb^{3+}	8.8	6.0	4.8	3.0	2.0
Dy^{3+}	11	8.2	6.4	4.6	2.5
Ho^{3+}	6.6	4.8	3.2	2.6	2.1
Tm^{3+}	7.8	5.5	4.7	3.6	2.6
Yb^{3+}	6.0	4.0	3.7	2.8	1.8
Lu^{3+}	6.2	5.0	3.5	2.7	2.2

substantially higher at low nitric acid content and decreases as the percentage of methanol in the solutions decreases, as may be seen from Fig. 1.

The calculated separation factors, α, relative to calcium, listed in Table II, are defined as

$$\alpha_{\text{element/calcium}} = \frac{(K_d)\,\text{element}}{(K_d)\,\text{calcium}}$$

Under the present conditions, the separation factors are roughly constant for an individual REE; therefore, an average value is given for each REE.

TABLE II

AVERAGE VALUES FOR SEPARATION FACTORS, α, EXPRESSED RELATIVE TO CALCIUM, IN THE RANGE 95% CH_3OH–5% 7 *M* HNO_3 TO 85% CH_3OH–15% 7 *M* HNO_3

La	*Ce*	*Nd*	*Sm*	*Eu*	*Gd*	*Tb*	*Dy*	*Ho→Lu*
$1.7 \cdot 10^3$	$1.4 \cdot 10^3$	$3.5 \cdot 10^2$	25	23	17	15	14	<10

On the basis of literature data, it is now well known that ion exchange with a mixed solvent very often shows distribution coefficients higher, by several orders of magnitude, than those obtained in pure aqueous systems. In order to attempt to explain this sorption mechanism, it is necessary to consider that the introduction, in an anion-exchange system, of organic solvents such as aliphatic alcohols (with lower polarity and smaller dielectric constant than water: $\varepsilon_{H_2O} = 78.54$; $\varepsilon_{CH_3OH} = 32.6$ at 25°C) generally decreases the degree of dissociation of a metallic salt and greatly intensifies the formation of negatively charged species[42].

The variation of log K_d with the REE ionic radii, under the present working conditions, is illustrated in Fig. 2. The distribution coefficients increase with increasing ionic radii, and the higher REE are more strongly retained by the resin than the heavier ones, for which the K_d values vary very little from one to another. This evolution is in agreement with the trend previously mentioned for aqueous 8 *M* nitric acid by Ichikawa[15] and in mixed solvent systems by *e.g.* Faris and Warton[34], Korkisch *et al.*[18], Alstad and Brunfelt[38]. It is interesting to note that, in all cases, the shape of the curves is roughly divided into two distinct zones: the "cerium" group (La–Sm) and the "yttrium" group (Eu–Lu).

This system offers an attractive way for separating light from heavy REE. It has been applied by Edge[30] for isolating milligram amounts of La, Ce, Pr, Nd as a group from the heavy REE. A chromatographic anion-exchange separation of Sc, Y, Sm and La has been described by Desai *et al.*[37]. The Ce and Eu as well as the Lu, Yb, Tb content of some standard rocks has been determined by Brunfelt and Steinnes[39] using a similar procedure. In neutron activation analysis of REE in ultramafic rocks, Brunfelt *et al.*[40] have recently used a nitric acid–methanol medium to elute the REE into three fractions: Lu and Yb (15% 7.8 *M* HNO_3–85% methanol); Tb, Gd, Eu, Sm (45% 7.8 *M* HNO_3–55% methanol); Nd, Ce, La (water).

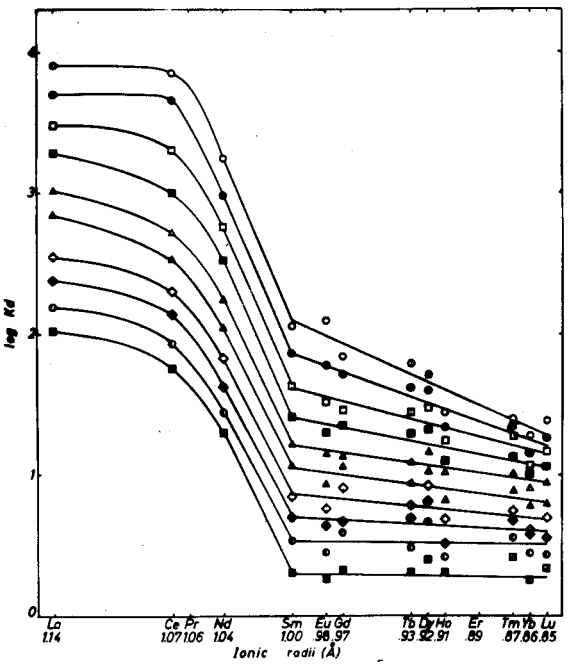

Fig. 2. Variation of distribution coefficient, K_d, with REE ionic radii. (○) 95% (v/v) CH_3OH–5% 7 *M* NHO_3, (●) 90% CH_3OH–10% 7 *M* HNO_3, (□) 85% CH_3OH–15% 7 *M* HNO_3, (■) 80% CH_3OH–20% 7 *M* HNO_3, (△) 75% CH_3OH–25% 7 *M* HNO_3, (▲) 70% CH_3OH–30% 7 *M* HNO_3, (◇) 65% CH_3OH–35% 7 *M* HNO_3, (◆) 60% CH_3OH–40% 7 *M* HNO_3, (◑) 55% CH_3OH–45% 7 *M* HNO_3, (◪) 50% CH_3OH–50% 7 *M* HNO_3.

The results presented in Tables I and II suggest that a similar method would be satisfactory for quick and effective separation of REE from apatites.

The following tracer experiments were carried out: ^{140}La, ^{153}Sm and ^{177}Lu were added to an inactive apatite mineral. After a nitric acid attack of the phosphate matrix and evaporation to dryness on a water bath, the residue was taken up in 50 ml of a 5% 7 *M* nitric acid–95% methanol mixture. This solution was passed through a pretreated 140-mm column of Dowex 1–X8, 100–200 mesh, diameter 10 mm, at a flow rate of about 0.8 ml min^{-1}. Under these conditions, no REE were eluted, while Na, Mg, Al, K, Sc, Mn, Fe passed into the effluent ($K_d < 1$) with the major part of calcium and other anions such as phosphates. After this sorption step, the complete elution of calcium was obtained by washing with another 50 ml of 5% 7 *M* nitric acid–95% methanol mixture. The heavier REE (^{177}Lu and ^{153}Sm) could then be desorbed from the resin by means of 200 ml of a mixture of 45% 7 *M* nitric acid–55% methanol[40]. Finally a very pure fraction of ^{140}La was eluted by treating the resin with 100 ml of water.

In conclusion, the method developed should be suitable for preparing light and heavy concentrates from mixtures of REE from apatite minerals.

We are indebted to Professor J. Govaerts, Laboratoire d'Application des Radioéléments, University of Liège, for laboratory facilities.

SUMMARY

Batch distribution coefficients, K_d, of rare-earth elements (REE) and other elements were determined radiochemically for a strongly basic nitrate anion-exchange resin Dowex 1–X8 100–200 mesh, in nitric acid–methanol media of varying composition. This method was developed for the separate recovery of REE from apatite minerals. Calcium and other common elements of the apatite are eluted by a 5% (v/v) 7 *M* nitric acid–95% methanol mixture, while the REE are retained. The REE are recovered and separated into two fractions; the heavier REE by elution with a 45% nitric acid–55% methanol mixture, and a very clean fraction of La, Ce, Pr, Nd by elution with water.

REFERENCES

1 E. R. Tompkins and S. W. Mayer, *J. Amer. Chem. Soc.*, 69 (1947) 2859.
2 W. E. Nervik, *J. Phys. Chem.*, 59 (1955) 690.
3 G. R. Choppin and R. J. Silva, *J. Inorg. Nucl. Chem.*, 3 (1956) 153.
4 J. Fuger, Thesis, University of Liège, 1959.
5 E. Merciny, Thesis, University of Liège, 1968.
6 F. Guichard, H. Jaffrezic, N. Descamps and M. Treuil, *Radiochem. Radioanal. Lett.*, 9 (1972) 35.
7 I. Roelandts, *Radiochem. Radioanal. Lett.*, 12 (1972) 89.
8 M. Treuil, H. Jaffrezic, N. Descamps, C. Derre, F. Guichard, J. L. Joron, B. Pelletier and S. Novotny, *Modern Trends in Activation Analysis, Paris, 1972*, to be published.
9 G. Werner, J. Pritzkow, O. Wildner and H. Holzapfel, *J. Less-Common Metals*, 10 (1966) 323.
10 G. Werner, H. Giseke and H. Holzapfel, *J. Less-Common Metals*, 11 (1966) 209.
11 I. Roelandts and G. Duyckaerts, *Anal. Chim. Acta*, 68 (1974) 131.
12 A. O. Brunfelt, *Separ. Sci.*, 8 (1973) 633.
13 J. Danon, *J. Inorg. Nucl. Chem.*, 5 (1958) 237.
14 L. R. Bunney, N. E. Ballou, J. Pascual and S. Foti, *Anal. Chem.*, 31 (1959) 324.
15 F. Ichikawa, *Bull. Chem. Soc. Jap.*, 34 (1961) 183.
16 J. Korkisch and F. Tera, *Anal. Chem.*, 33 (1961) 1264.
17 J. Korkisch and G. E. Janauer, *Talanta*, 9 (1962) 957.
18 J. Korkisch, I. Hazan and G. Arrhenius, *Talanta*, 10 (1963) 865.
19 J. Korkisch and I. Hazan, *Talanta*, 11 (1964) 1157; *Anal. Chem.*, 37 (1965) 707.
20 J. Korkisch and F. Feik, *Anal. Chem.*, 36 (1964) 1793; 37 (1965) 757.
21 J. Korkisch, *Mikrochim. Acta*, (1964) 816; *Separ. Sci.*, 1 (1966) 159.
22 I. Hazan, S. S. Ahluwalia and J. Korkisch, *Z. Anal. Chem.*, 206 (1964) 324.
23 J. Korkisch and S. S. Ahluwalia, *Anal. Chim. Acta*, 31 (1964) 552; *J. Inorg. Nucl. Chem.*, 28 (1966) 264.
24 F. Feik and J. Korkisch, *Talanta*, 11 (1964) 1585.
25 T. F. Cummings and J. Korkisch, *Anal. Chim. Acta*, 40 (1968) 520.
26 E. Klakl and J. Korkisch, *Talanta*, 16 (1969) 1177.
27 C. W. Walter and J. Korkisch, *Mikrochim. Acta*, (1971) 81, 137, 158, 194.
28 J. Korkisch in *Progress in Nuclear Energy, Series IX, Analytical Chemistry*, Vol. 6, Pergamon, Oxford, 1966, pp. 1–94.
29 R. A. Edge, *J. Chromatogr.*, 5 (1961) 526, 539; 6 (1961) 452.
30 R. A. Edge, *J. Chromatogr.*, 8 (1962) 419; *Anal. Chim. Acta*, 29 (1963) 321.
31 J. S. Fritz and D. J. Pietrzyk, *Talanta*, 8 (1961) 143.
32 J. S. Fritz and R. G. Greene, *Anal. Chem.*, 36 (1964) 1095.
33 D. H. Wilkins and G. E. Smith, *Talanta*, 8 (1961) 138.
34 J. P. Faris and J. W. Warton, *Anal. Chem.*, 34 (1962) 1077.
35 D. C. Stewart, C. A. A. Bloomquist and J. P. Faris, *USAEC Report ANL – 6999*, 1965.
36 L. W. Marple, *J. Inorg. Nucl. Chem.*, 26 (1964) 859.

37 H. B. Desai, R. K. Lyer and M. Sankar, *Talanta*, 11 (1964) 1249.
38 J. Alstad and A. O. Brunfelt, *Anal. Chim. Acta*, 38 (1967) 185.
39 A. O. Brunfelt and E. Steinnes, *Chem. Geol.*, 2 (1967) 199; *Analyst (London)*, 94 (1969) 979.
40 A. O. Brunfelt, I. Roelandts and E. Steinnes, *Analyst (London)* in press.
41 J. M. Peters and G. del Fiore, to be published.
42 B. Trémillon, *Les séparations par les résines échangeuses d'ions*, Gauthier-Villars, Paris, 1965, p. 129.

Analytica Chimica Acta, 73 (1974) 149–155

THE DETERMINATION OF CHLORINE IN ORGANIC MATERIALS BY COMBUSTION AND MICROCOULOMETRY

J. SOLOMON and J. F. UTHE*

Environment Canada, Fisheries and Marine Service, Freshwater Institute, 501 University Crescent, Winnipeg, Manitoba R3T 2N6 (Canada)

(Received 12th March 1974)

Various complex analytical procedures have been developed to enable the analyst to determine the amounts of man-made compounds containing covalently bound chlorine that are presently being found in a large variety of environmental materials[1,2]. Many government and private agencies are currently using such procedures to monitor the environment so that changes in the level of such compounds can be noticed as soon as possible. It would seem feasible and economic to determine the amount of covalently bound chlorine in chloride-free extracts of samples before detailed analyses. If such a determination indicated insignificant levels or changes in levels, often analyses could be terminated at this point. Such a procedure has been used with hexane extracts of water samples by Greve and Haring[3] to determine levels of organic chlorine.

Another advantage to determining the organochlorine content of a sample is that a simple calculation could then be made to determine if detailed compound analysis of the sample had accounted for the covalently bound chlorine as determined by organochlorine analysis. Had such a procedure been routine a number of years ago, the presence of polychlorinated biphenyls and other material in samples being analyzed for organochlorine pesticides might have been suspected much earlier.

Obviously, a cheap and fast method of determining the organochlorine content of a material is desirable. Techniques based on combustion, followed by chlorine determination are the most appropriate methods for low cost and speed. The combustion method of Gouverneur *et al.*[4] is fast and efficient but is limited to liquid samples. In this paper a similar combustion system is described for solid and liquid samples. Disposable volatilization inserts are employed to eliminate any possibility of cross contamination between samples.

EXPERIMENTAL

A schematic diagram of the combustion apparatus is shown in Fig. 1. The sample was volatilized in an inert (helium) atmosphere and the vapors then combusted in humid oxygen to yield hydrogen chloride which was in turn collected and determined by microcoulometry.

* Present address: Environment Canada, Fisheries and Marine Service, Halifax Laboratory, P.O. Box 429, Halifax, Nova Scotia B3J 2R3.

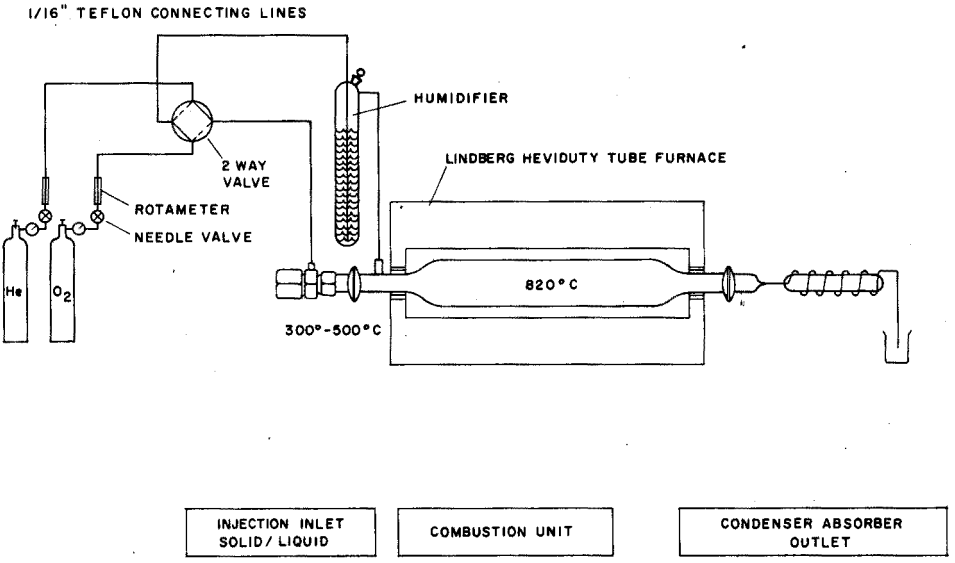

Fig. 1. Schematic diagram of the microcombustion unit. All gas connections from tank pressure reducing valves were made with 2 mm i.d. Teflon spaghetti tubing.

Gas cylinder flow pressures were regulated to 5 p.s.i.g. and flow control was maintained through needle valves and rotameters. The helium flow was set at 10 ml min^{-1} and the oxygen flow at 200 ml min^{-1}. Oxygen was humidified by bubbling through a "cold finger" type humidifier (24 cm long $\times$2.5 cm i.d. with a 1-mm i.d. bubbler tube and fitted with a small glass port for addition of makeup water) maintained at 90°C in a water bath. This level of humidification was found to yield about 0.25 ml of effluent condensate in 10 min. Humidification was necessary to supply the required hydrogen for conversion of chlorine to hydrogen chloride. Water also acted as an absorber for hydrogen chloride in the condenser and aided in washing the system between combustions. Before humidification, a two-way valve was used to interchange gas flows between sample tube and combustion chambers. In this way the sample was volatilized and pyrolysed in helium and following this the gas flows were interchanged so that oxygen was used to burn residues in the sample tube. Direct volatilization and combustion in oxygen led to incomplete oxidation and carbonization of the sample as well as injection needle damage.

Injector inlet

An exploded view of the injector inlet is shown in Fig. 2 and consisted of a standard brass reducing union (Swagelok B-600-604) fitted with an injection port and was coupled into the combustion tube by means of a ball and socket joint. The septum nut (B) (Swagelok B-602-1) was fitted with a 0.125-in. thick aluminum disk (A) machined to press-fit into the nut. A 0.0625-in. diameter hole was drilled through the center of the disk to act as a needle guide. A standard 0.5-in. silicone rubber septum (C) was used. The reducing union (E) was modified by redrilling the inside hole large enough to admit loosely the 6-mm o.d. Pyrex

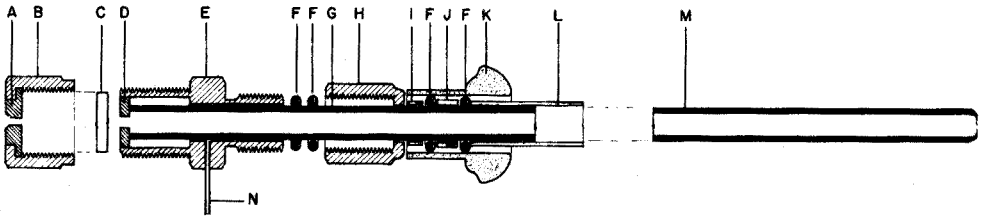

Fig. 2. Blowup of the injector inlet showing construction details. A, Brass washer with 0.0625-in. center hole; B, septum nut (Swagelok B-602-1); C, 0.5-in diameter silicone septum; D, brass sealing disk (0.125-in. thick) center hole (0.125-in. diam.); E, male reducing union, 0.500 in. × 0.375-in. (Swagelok B-600-6-4); F, silicone rubber O-rings 0.375-in. diameter; G, Pyrex glass tube (6 mm o.d. × 4 mm i.d. × 3 in. long); H, 0.25-in. tube nut (Swagelok B-402-1); I, Teflon spacer (0.25-in. long × 0.25-in. i.d.); J, Pyrex glass spacer (0.625-in. long × 88-mm o.d. × 6-mm i.d.); K, ball joint (quartz ₹ 18/9 × 1.125-in. long); L, Teflon connecting sleeve (0.25-in. o.d. × 1.25-in. long); M, sample tube (Pyrex glass, 3.75-in. long × 6-mm o.d. × 4-mm i.d.); N, gas inlet (0.0625-in. o.d. stainless steel tubing).

glass tube (G). The large end of the union was permanently sealed off by a brass disk 0.125-in. thick with a 0.125-in. diameter center hole (D). Grooves (0.0625-in. deep and 0.0625-in. wide) were machined on one side of the disk to provide for gas passage into the Pyrex glass tube (G). A 0.0625-in. hole was drilled through the middle of one of the wrench pads on the reducing union through to the inside. A small piece of 0.0625-in. o.d. stainless steel tubing was silver-soldered into this hole to make a gas fitting (N). Gas-tight fitting between the Pyrex glass tube (G) and the reducing union was made in the usual way with a Swagelok nut, and two silicone O-rings. A ball joint (K) was positioned as shown to form a gas-tight seal on the Pyrex glass tube (G) by means of a Teflon spacer (I), a Pyrex spacer (J) and two silicone O-rings (F). A Teflon connecting sleeve (L) extended about 0.3-in. over the Pyrex glass tube (G) and served to butt-join the sample tube (M) in position. The whole unit was held firmly in place on the quartz combustion tube by means of a ball and socket joint spring clamp.

Sample tubes (M) were constructed from 6-mm o.d. Pyrex tubing fire-polished at one end and slightly constricted at the other. A 1-cm plug of Pyrex glass wool was placed inside the tube against the constriction. Solid samples were weighed directly into these tubes and the sample was held in place with a small bit of glass wool.

The quartz combustion tube

The quartz combustion tube (Fig. 3) is similar to that described by Gouverneur *et al.*[4]. The enlarged portion of the tube was of a length sufficient to utilize all the available space within the tube furnace. The tube was positioned within the furnace by simply wrapping the smaller tube ends with 1-in. wide asbestos cloth to the diameter of the furnace openings so that the combustion tube was solidly held in place when the furnace door was latched.

Condenser–absorber unit

The tube section of the ball and socket joint to fit the discharge of the

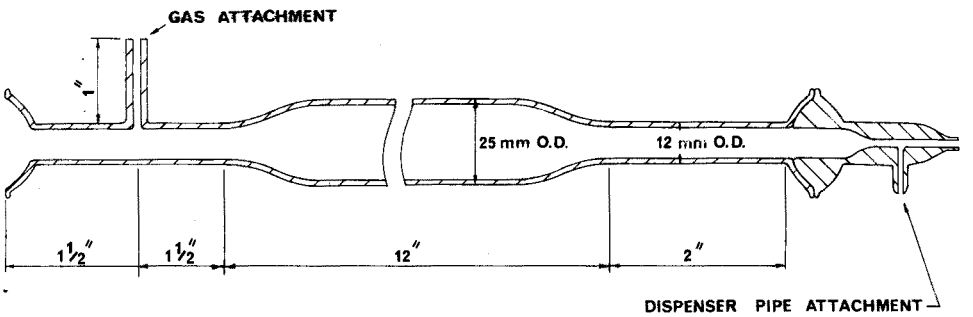

Fig. 3. Quartz combustion tube and condenser attachment adaptor with attachment for dispenser pipet.

combustion tube was drawn to a fine capillary (1 mm i.d.) and a similar side arm was attached as shown (Fig. 3). The ends of the capillary tube and the side arm were drawn out to allow attachment of 2-mm i.d. Teflon spaghetti tubing. The side-arm tubing was attached to a dispensing pipet. The end of the capillary tubing was attached to the Teflon condenser–absorber unit (Fig. 1). The condenser–absorber unit was made from 450 cm of 2-mm i.d. Teflon spaghetti tubing, closely wound around a 2.5-cm o.d. glass mandrel. The tubing was securely fastened at each end of the mandrel. One end was connected to the effluent tube from the combustion tube and the other exited into a titration vial.

Other equipment. A Lindberg Heviduty Tube Furnace type 55035-A was operated at 820–900°C. For the microcoulometric chloride determination, an Aminco Clinical Chloride Titrator (American Instrument) was used throughout.

Procedures

Liquid sample injection. A 10-μl syringe, fitted with a 11.5-cm needle was used for liquid injections. The temperature of vaporization was controlled by the depth of needle insertion. A slow, smooth rate of injection (1/2 μl/5 s) was used to avoid oxygen depletion. Injections were made with helium flowing through the sample tube. After injection the two-way valve was positioned to flush the sample tube with oxygen to burn out the residue. In general, the depth of injection was such that the end of the needle was at a temperature of 300–500°C (9–11 cm).

Solid sample combustion. The sample tube containing the weighed sample was positioned in the unit as described above, and the unit clamped into the combustion tube. Vaporization and pyrolysis of the sample proceeded slowly as the sample tube heated up (1–2 min), the final temperature depending upon the spacing of the sample within the sample tube. The sample end of the sample tube approached the operating temperature of the oven while the end coupled to the injector unit remained cool enough to handle. After operating temperature was reached, oxygen was used, as above, to burn residues within the tube.

Chloride determination. The condensates from the condenser–absorber unit were collected directly in Aminco titration vials. Collection was carried out for 5 min after injection and at the end of this time the unit was flushed with 3 ml of the acetic–nitric acid titration reagent by means of the dispenser pipet. After addition of 3 drops of gelatin solution, titration was carried out in the usual way. The

titration was standardized with either standard sodium chloride solutions pipetted directly into titration vials, or with standard hydrochloric acid solutions injected as liquid samples, with no difference in results.

The chlorine content of a sample was determined as follows:

$$\%\text{Cl} = \frac{K\,(\text{mg Cl}^-/\text{s titrated}) \times \text{Net seconds (sample-blank)} \times 100}{\text{Sample weight (mg)}}$$

Analysis of a liquid sample took about 15–20 min to complete. Solid samples requiring weighing and some minor disassembly took somewhat longer.

RESULTS AND DISCUSSION

Chloride recoveries obtained from combustion of either pure compounds (liquids) or solutions of pure (solid) compounds in hexane are shown in Table I. Excellent chlorine recoveries were found for all compounds, showing that quantitative conversion of chlorine to hydrogen chloride had occurred. No noticeable difference was found between relatively easily combustible materials (chlorobenzene) and relatively difficult materials (carbon tetrachloride, polychlorinated biphenyl). The presence of material with a high oxygen demand (hexane) also did not affect recoveries.

Two samples of Orzan A (a commercial sulfolignin preparation) were analyzed by three laboratories using three different methods (Table II). One was a sample of Orzan A as received; the other was dialyzed overnight against tap water to yield

TABLE I

PERCENT RECOVERY OF CHLORINE FROM COMBUSTION OF PURE COMPOUNDS OR PURE COMPOUNDS IN SOLUTION IN HEXANE

(In all cases, 10 μl was injected.)

Compound	*Percent recovery*	*Compound*	*Percent recovery*
Chlorobenzene	99.9±0.94	Chloroform	99.3±1.5
p-Dichlorobenzene		Carbon tetrachloride	100.3±1.28
(128.04 mg/ml)	99.4±0.70	Aldrin (2.138 mg ml^{-1})	105.6±3.7
Ethylene chloride	100.4±0.51		
Methylene chloride	99.9±0.54		

TABLE II

ANALYSIS FOR CHLORINE IN DIALYZED AND NON-DIALYZED ORZAN A BY DIFFERENT METHODS

	Present method (%)	*Combustion (Parr bomb–potentiometric) (%)*	*Ignition–turbidity*
Dialyzed	0.017	0.010	—[a]
Non-dialyzed	0.024	0.010	0.020

[a] Sample lost.

a high-molecular-weight fraction. Reasonably similar results were obtained, but the microcombustion–microcoulometric method gave slightly higher results.

To test the new method further polychlorinated biphenyl standards were burned in the presence or absence of cod-liver oil (Table III). Again no effect on recoveries was found, and combustion proceeded smoothly and good recoveries were found.

The major problem associated with determination of organochlorine by this method is the presence of inorganic chloride ion in samples before combustion, and this must be corrected for, either by removal of chloride ion or its determination in unburned samples. Common inorganic chlorides such as sodium and potassium chlorides (Table IV) did not yield hydrochloric acid in the combustion, but ammonium chloride and cysteine hydrochloride gave 100% conversion.

TABLE III

ANALYSIS OF POLYCHLORINATED BIPHENYL (AROCHLOR 1254) WITH AND WITHOUT 50% (v/v) COD-LIVER OIL IN HEXANE

	Chlorine content (mg/ml)
1 Polychlorinated biphenyl in hexane (1 mg ml^{-1})	0.548 ± 0.013
2 Polychlorinated biphenyl in hexane (1 mg ml^{-1}) with 50% cod-liver oil	0.561 ± 0.011
3 50% Cod-liver oil in hexane	0.014 ± 0.019
Difference between 2 and 3	0.547

TABLE IV

ANALYSIS OF AQUEOUS CHLORIDE SOLUTIONS (1 *M*)

Salt	*Boiling point (°C)*	*Injection depth (cm)*	*(%) Recovery*
NaCl	1413	11.5	0
KCl	1500	11.5	0
NH_4Cl	335 (subl.)	11.5	92
$CaCl_2$	1600	11.5	13
		10.5	0
Cysteine hydrochloride		10	101
Cysteine hydrochloride + $CaCl_2$		9	102.9

Calcium chloride showed slight conversion to hydrochloric acid when injected at the same temperature as the above salts. Injection at slightly less depth (lower temperature) gave no hydrochloric acid formation but injection of calcium chloride (the highest boiling of all chlorides tested) along with an amino acid (cysteine hydrochloride) gave conversion of all of the chloride present in both the amino acid salt and the calcium chloride to hydrochloric acid, showing the potential for conversion of any inorganic chloride to hydrochloric acid when burnt with organic material. Gouverneur *et al.*[4] found that high-boiling inorganic chlorides are not recovered when burned with kerosine and isopropanol.

In many of the analytical procedures for organochlorine pesticides, polychlorinated biphenyls and other organochlorine residues, owing to the hydrophobic nature of these materials, the initial extracts are often in hexane. Model studies showed that no detectable chloride could be extracted by hexane from 1 *M* solutions of NaCl, KCl, NH_4Cl or $CaCl_2$ in the absence or presence of homogenized fish tissue. These results suggest that interference by inorganic chloride may not be too great. In any case, correction by determination of free chloride ion in unburnt samples is not difficult unless the amount of sample is limited (often a problem in environmental samples). Greve and Haring[3] washed their hexane extracts with water to remove any inorganic chloride. Microcoulometry as used in this study is neither the most selective nor the most sensitive method of determining chloride, but was used because of the ease and speed of analysis, and instrument availability.

CONCLUSIONS

The new microcombustion apparatus has been shown to yield total conversion of covalently bound chlorine to hydrogen chloride. Instrumental and operational costs are low and the time of analysis short. Solid and liquid samples are readily handled. The use of low gas pressures eliminates leak problems, and the gentle burning of samples is controlled by injection in inert helium; vaporization and then combustion eliminates explosion dangers. The use of simple disposable sample tubes should eliminate any problems caused by carryover from one analysis to the next.

SUMMARY

A combustion apparatus capable of burning both solid and liquid samples is described. The samples were vaporized in helium and then burned in humid oxygen. Oxygen was then used to burn non-volatile residues within the vaporization chamber. The use of cheap, disposable vaporization chambers eliminated carryover from one analysis to the next. The application of this instrument to the determination of organochlorine-containing samples is described. The moist effluent hydrogen chloride from the combustion was condensed and the chloride content was determined by microcoulometry. Pure solutions of high-boiling inorganic chlorides did not evolve chloride but the addition of an amino acid resulted in evolution of all of the chloride present.

REFERENCES

1 L. Fishbein, *J. Chromatogr.*, 68 (1972) 345.
2 J. A. Burke, J. E. Gaul and P. E. Corneliussen (Eds.), *Pesticide Analytical Manual*, U.S. Dept. of Health, Education and Welfare, Food and Drug Administration, Washington, D.C., 1971.
3 P. A. Greve and B. J. A. Haring, *Schriftenr. Ver. Wasser-, Boden-, Lufthyg., Berlin-Dahlem*, 37 (1972) 59.
4 W. Lädrach, F. Van de Craats and P. Gouverneur, *Anal. Chim. Acta*, 50 (1970) 219.

Analytica Chimica Acta, 73 (1974) 157–166

THE EFFECT OF SOLUTION ACIDITY ON THE RESPONSE OF THE LANTHANUM TRIFLUORIDE SINGLE-CRYSTAL ELECTRODE

JOSEF VESELÝ and KAREL ŠTULÍK

Geological Survey, Malostranské nám. 19, 118 21 Prague 1; Department of Analytical Chemistry, Charles University, Albertov 2030, 128 40 Prague 2 (Czechoslovakia)

(Received 9th May 1974)

The behaviour of the lanthanum trifluoride electrode with a single-crystal membrane differs in certain respects from that of other crystal electrodes designed during the last decade. For example, the time dependence of its response in alkaline media[1,2] and its response to non-ionic fluorine in *p*-fluorodinitrobenzene[3] are atypical. There are doubts concerning the role of the lanthanum trifluoride crystal solubility during measurement of very low fluoride activities, and even the LaF_3 solubility product itself is not known with certainty[2,4,5].

The present paper is a contribution to the study of these aspects of the electrode behaviour. The *E vs.* pH dependences were monitored in solutions containing fluoride and lanthanum(III) ions and the effect of the solution on the LaF_3 single crystal was studied by means of x-ray powder patterns, infrared spectroscopy and radioactivity measurements in systems labelled with tritium. Laboratory electrodes with various crystal membranes have been constructed.

EXPERIMENTAL

Reagents, apparatus and procedures

All reagents employed were of p.a. purity (Lachema, Czechoslovakia and Fluka, Switzerland). Nitric acid was distilled before use and potassium nitrate was purified by zone-refining, thus decreasing the amount of impurities below one tenth of the original value. A 0.3 *M* lanthanum nitrate solution was prepared by dissolving lanthanum hydroxide in nitric acid, evaporating the acid and dissolving the residue in water; the solution was standardized complexometrically. The ionic strength (μ) of the studied solution was adjusted to 0.1 with potassium nitrate (the 0.1 *M* lanthanum nitrate solution had an ionic strength of 0.6). The acidity of solutions within the pH range 3–9 was adjusted by additions of very small volumes of 1 *M* nitric acid or 1 *M* potassium hydroxide and the solutions were not used for more than three measurements; the solutions with pH values greater than 9 and smaller than 3 were prepared before each measurement.

The potential values were measured with the PHM 52 pH-meter (Radiometer, Denmark) coupled with the Servogor 2s recorder (Goerz Electro, Austria), using the Orion 94-09A fluoride electrode and the 90-02 double-junction silver chloride reference electrode (Orion Research, USA) without a liquid bridge. The 0.1 *M* KCl internal solution in the reference electrode was saturated with silver chloride

at an elevated temperature, During measurement of the *E vs.* pH dependences in solutions of lanthanum(III) ions and of the *E vs.* pF dependences given in Fig. 3, the K 401 saturated calomel reference electrode (Radiometer, Denmark) was employed.

The laboratory lanthanum trifluoride electrodes were prepared from cylindrical crystalline elements (produced by Monokrystaly, Turnov, Czechoslovakia), 5.6–5.8 mm in diameter and 2–60 mm long. The circular surfaces of the cylinders were polished with fine emery paper (4/0, SIA, Switzerland) and an alumina suspension (No. 2, Greiz-Dölau, G.D.R.). The crystals were cemented in glass tubes with polysulphide cement or with Alkapren 50 cement (Matador, Czechoslovakia) with a silicone rubber base. Silver chloride (0.1 *M* NaF + 0.1 *M* KCl) internal reference electrodes were used.

All measurements were carried out in 100-cm^3 polyethylene vessels in solutions stirred with Teflon-coated bars; all the potential values reported were obtained by measurement in stirred solutions. For pH measurement the glass electrode (GK 2301C, Radiometer, Denmark) was employed; this yields reliable results in the presence of hydrogen fluoride up to a concentration of about $5 \cdot 10^{-3}$ *M* (see Warren[6]).

The surface properties of the lanthanum fluoride crystal were followed by means of x-ray powder patterns (Micrometa instrument, Chirana, Czechoslovakia) and infrared spectra. The transmittance spectra were measured with the UR-20 instrument (C. Zeiss, G.D.R.) in nujol mulls and KBr pellets, and the frustrated multiple internal reflectance (f.m.i.r.) spectra on the Perkin-Elmer 225 instrument on a KBr crystal. For these measurements a lanthanum fluoride crystal was crushed to obtain a powder with a grain size $\leqslant$ 170 mesh. The same amount of this powder was immersed in solutions of various acidities for several days, then decanted, dried thoroughly at laboratory temperature and measured. Most of the measurements were performed in duplicate, the powder being washed with distilled water before drying in one experiment and dried unwashed in the other. Radioactivity measurements were carried out with LaF_3 cylindrical crystals, which were immersed in 2 ml of solutions containing various concentrations of potassium hydroxide and potassium fluoride with potassium nitrate to adjust the ionic strength to 0.1. The solutions contained water labelled with ^3H, the resulting specific activity being 200 μCi ml^{-1}. After several days the crystals were taken out, the liquid was gently absorbed from the surface with a piece of filter paper (without wiping), and the crystals were immediately transferred to cuvettes containing 0.5 ml of distilled water and 5 ml of liquid scintillator. Only one crystal was washed with distilled water and wiped dry before being transferred to the cuvette. The β- activity was measured with the Packard Tri-Carb spectrometer, model 3003 (U.S.A.).

The solutions were thermostatted with the U 10 thermostat (Prüfgeräte, G.D.R.).

RESULTS

The E vs. pH dependences in fluoride solutions

The dependences of *E* on the pH, measured for several fluoride molalities

and in 0.1 *M* KNO_3 at 25°C, are shown in Fig. 1. Since the electrode potential did not stabilize even after several hours at fluoride molalities below 10^{-6}, the values were read 60 min after immersion of the electrode into the solution or after a change in the solution pH. In the pH range 3–9, the *E vs.* pH dependences at individual fluoride molalities differed greatly for different directions of pH change. When the pH was varied from alkaline values to acidic, the upper curves in Fig. 1 were obtained; the lower curves resulted from pH variation in the opposite direction. These curves enclose regions of various size, which may be called hysteresis regions. The fluoride electrode may attain various potential values inside these regions at a given pH and fluoride molality, depending on the electrode history, experimental technique and time. The hysteresis region becomes smaller with increasing fluoride molality in the solution and with increasing time. After several hours or tens of hours, the two curves enclosing the hysteresis region merge into a single curve, passing approximately through the centre of the original region. The steady-state potential values can be obtained relatively more rapidly when the LaF_3 electrode is not immersed in the solution until after the pH adjustment. These values for pH 5.7 ± 0.1 are denoted by crosses in Fig. 1.

A minimum was observed on the lower limit of the hysteresis region between pH 2 and 3, at fluoride molalities below 10^{-6} (see Fig. 1). However, when the pH is further decreased, the electrode potential rapidly increases, owing to a decrease in a_{F^-} caused by the formation of the slightly dissociated species, $[HF]_n$. The potential values below pH 3 have poorer reproducibility.

In the alkaline region the curves for all fluoride molalities merge to practically a single curve, representing the pOH response of the electrode. This response is substantially lower than the Nernstian response at 25°C (about 33 mV/pOH). However, when the potential is read immediately (at most after 60 s), the response equals 55 mV/pOH in the pH region above 7. The very rapid and possibly even Nernstian response to hydroxide, observable up to pOH 8–9, deteriorates with time. A more rapid electrode response to changes in a_{OH^-} than that for a_{F^-} is also indicated by potential changes on adjustment of the initially alkaline solution to a pH within 3–7, when *E* first considerably and rapidly shifts to more positive values and then slowly becomes more negative. For example, when the pH of a 0.1 *m* KNO_3 solution was changed from 12.2 to 1.1, the first potential reading was +570 mV, the potential change, ΔE, being 510 mV. After this abrupt change, the electrode potential slowly shifted not to more positive values as might be expected, but to negative values. When the solution was changed from acidic to alkaline, potential changes in the opposite direction were observed.

Potential shifts between the first and the sixtieth minute are denoted by arrows at some points in Fig. 1. The arrows at the hysteresis region borders are mostly directed into the region at $3 < pH < 9$ (there are two exceptions, which cannot as yet be explained). Above pH 10–11, the potential always shifted to more positive values, irrespective of the electrode history and practically also of the fluoride molality. However, when strongly alkaline solutions were measured several times, the electrode being rinsed with distilled water between measurements, the potential change was smaller during subsequent measurements.

The *E vs.* pH dependence at 60°C is depicted in Fig. 2. The potentials stabilize more rapidly at an elevated temperature and therefore the hysteresis

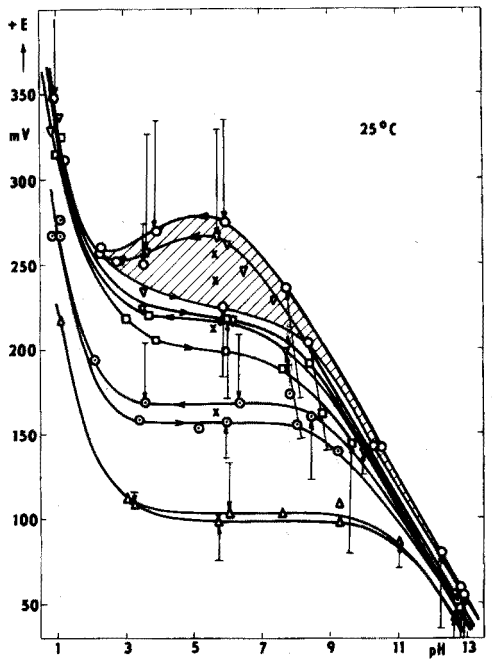

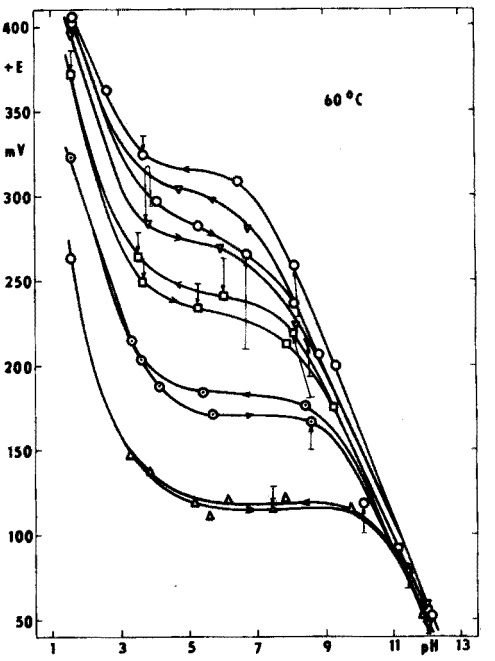

Fig. 1. The *E vs.* pH dependence for various fluoride molalities at 25°C. (○) 0.1 *m* KNO_3, (▽) $3 \cdot 10^{-7}$ *m* F^-, (□) $1 \cdot 10^{-6}$ *m* F^-, (⊙) $1 \cdot 10^{-5}$ *m* F^-, (△) $1 \cdot 10^{-4}$ *m* F^-. The shaded area is the hysteresis region obtained in 0.1 *m* KNO_3. The potentials were read after 60 min; steady-state values are denoted by x. A silver chloride reference electrode was used.

Fig. 2. The *E vs.* pH dependence for various fluoride molalities at 60°C. Symbols as for Fig. 1. The potentials were read after 60 min. A silver chloride reference electrode was used.

regions are smaller. The minimum, observed at 25°C and pH 2–3 with the lowest fluoride molalities, is practically absent here. However, the increase in the electrode sensitivity towards hydroxide from 33 mV/pOH to about 53 mV/pOH (readings taken after 1 h) is noteworthy. Even this slope is lower than the theoretical value (66.10 mV/pOH), but the increase is much larger than that caused by the increase in the factor in the Nernst equation on a temperature change from 25°C to 60°C (+6.94 mV). Potential changes with time are in the same direction as those at 25°C, but they are smaller and there are more exceptions in the direction of the shift in the neutral region.

The Orion fluoride electrode is most sensitive to fluoride at about pH 5.5 and its sensitivity rapidly decreases on both sides of this value (Fig. 1); this holds for both temperatures studied. The hysteresis actually increases the electrode sensitivity at very low fluoride activities, as follows from Figs. 1 and 3. Figure 3 shows that after electrode exposure for 30 min to a $1 \cdot 10^{-3}$ *m* NaF solution, the potential values depart from the theoretical dependence on the activity earlier, apparently because of reversible "poisoning" of the electrode surface by adsorption of fluoride ions (curve 4). Curves 1 and 2 show that exposure of the electrode to potassium hydroxide renders the electrode supersensitive (the local slope is higher than Nernstian). However, this increase is difficult to utilize analytically, since the

E values are non-equilibrium and hence poorly reproducible, similar to the boundaries of the hysteresis regions. For example, when two repeated measurements in $1 \cdot 10^{-6}$ *m* F^- were made, after the electrode had been exposed for 5 min to 0.1 *M* KOH before each measurement, the second potential value was 15 mV more positive than the first one. The *E* values measured in 0.1 *m* KNO_3 (Fig. 3) are determined by impurities in potassium nitrate, complexation equilibria and possibly by liberation of fluoride ions from the membrane. The potential is strongly affected by the electrode history (*e.g.* adsorption on the electrode during previous measurements).

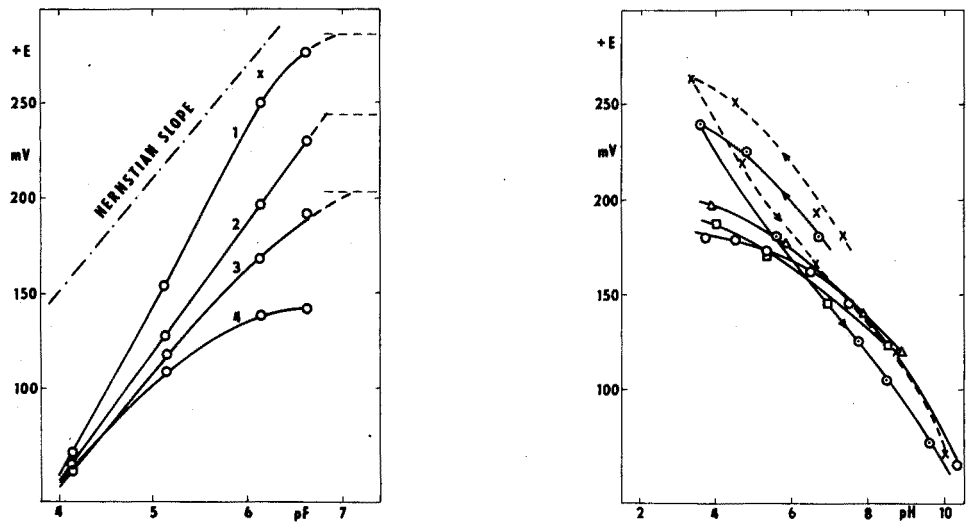

Fig. 3. The *E vs.* pF dependences (25°C). Curve 1, electrode exposed to 0.1 *M* KOH for 5 min before each measurement. Curve 2, electrode exposed to 0.1 *M* KOH for 1 min before each measurement. Curve 3, electrode not exposed to hydroxide. Curve 4, electrode exposed to $1 \cdot 10^{-3}$ *m* NaF for 30 min. (×) Repeated measurement in $1 \cdot 10^{-6}$ *m* F^- with 5 min exposure to 0.1 *M* KOH. (——) Buffered solution. (-----) Potentials measured in 0.1 *m* KNO_3 only. All measurements at pH 5.7±0.1. Potentials were read after 5 min against a saturated calomel reference electrode.

Fig. 4. The *E vs.* pH dependences in lanthanum(III) nitrate solutions (25°C). (×) $1 \cdot 10^{-5}$ *M* La^{3+}, (⊙) $1 \cdot 10^{-4}$ *M* La^{3+}, (□) $1 \cdot 10^{-3}$ *M* La^{3+}, (△) $1 \cdot 10^{-2}$ *M* La^{3+}, (○) $1 \cdot 10^{-1}$ *M* La^{3+}. Potentials read after 30 min against a saturated calomel reference electrode.

Figure 3 also indicates that fluoride activities can be measured in unbuffered solutions down to pF 7. However, expecially pure chemicals would have to be used, as is shown by the distortion of the *E vs.* pF dependence which is probably caused by the presence of complex-forming metals.

The E vs. pH dependences in solutions of lanthanum(III) ions

The experiments were conducted similarly as in the above section, but the potentials were read after 30 min. It is evident from Fig. 4 that the Orion fluoride electrode does not respond to lanthanum(III) activities at 25°C, at least in the absence of lanthanum fluoride precipitate with a large surface area (see

Ross[4]), but rather to changes in pOH. The E values obtained in concentrated lanthanum(III) solutions at pH 5–7 are similar to those obtained in the potassium nitrate base electrolyte.

The response to hydroxide ions is poorer in lanthanum(III) solutions than in solutions of fluoride. The slope equals about 25 mV/pOH in 10^{-4}–10^{-5} M La^{3+} solutions. However, the potential reproducibility is very poor. Hysteresis, similar to that observed for fluoride is also evident, but to a lesser degree. The precipitation of lanthanum(III) hydroxide is apparently a complex, slow and irreversible process; a turbidity, once formed, persists in solution for a long time, even at pH values at which no hydroxide is formed.

The study of surface changes of LaF_3 crystals

The systems studied by x-ray powder patterns and i.r. spectroscopy are surveyed in Table 1. The x-ray powder patterns showed no changes in the crystalline structure under any conditions. The i.r. spectra in nujol and KBr were in all cases identical with the spectra of untreated lanthanum fluoride, except for sample 2b, the spectra of which exhibited characteristic CO_3^{2-} absorptions (840 cm^{-1}, out-of-plane vibration; 1410 cm^{-1}, degenerate stretching), absorption of water or possibly OH^- strongly hydrogen-bonded (1640 and 1660 cm^{-1}, bending), and absorption of hydroxyl (3460 cm^{-1}, vibration). All these absorptions disappeared when the sample was rinsed with water. The f.m.i.r. spectra did not change, presumably because any adsorbed material (sample 2b) was removed during sample pretreatment before the spectra were taken (evaporation with carbon tetrachloride).

TABLE I

SYSTEMS STUDIED BY X-RAY PATTERNS AND I.R.-SPECTROMETRY

(Crystalline powder, $\leq$ 170 mesh, immersed in the given solutions for several days).

Number	*Solution composition*	*Sample treatment*
1a	0.1 M HNO_3	Sample rinsed twice with H_2O before drying
1b	0.1 M HNO_3	Sample not rinsed before drying
2a	0.1 M KOH	Sample rinsed twice with H_2O before drying
2b	0.1 M KOH	Sample not rinsed before drying
3	Distilled water	Sample dried
4	Untreated crystalline powder	—

A titrimetric determination of the concentration of hydroxide ions adsorbed on the crystalline powder was attempted. Changes in the pH were monitored when 1 g of LaF_3 powder, 60–170 mesh, was introduced into 10 ml of distilled water, with pH adjusted to 5–9. In weakly alkaline solutions, the pH decreased rapidly and reproducibly by 0.1–0.3 pH units. When the original pH was 5–6, an increase in the pH occurred, but it was slower and smaller. In both samples, the fluoride activity (measured by the fluoride electrode) strongly increased to a value of $5 \cdot 10^{-5}$–$1 \cdot 10^{-4}$ M. The amount of fluoride liberated in the solution was about

one half of the above value when the same LaF_3 sample was used for a second time after drying.

At about pH 9 and 10^{-6} *m* fluoride, thorough wiping of the fluoride electrode crystal with filter paper caused a change in the potential values lasting 5–10 min. After the electrode had been wiped, the potential (compared to the steady-state value) in an alkaline solution shifted from positive to negative values, passed through a minimum within several seconds and then more slowly shifted again to positive values. Hence wiping the electrode has an effect similar to changing the pH. This phenomenon diminished with decreasing pH values and in unstirred solutions. Prolonged washing of LaF_3 powder with distilled water (8 h) led to formation of a macroscopic layer of colourless gel adhering to the vessel walls, although the crystalline powder was initially difficult to wet.

The results obtained during measurements of the β-activity in ^3H-labelled systems are summarized in Table II. The activity of the LaF_3 crystal immersed in the potassium nitrate solution in the absence of potassium hydroxide and sodium fluoride was subtracted as a blank. The values of the hydroxide concentration on the surface, given in the last column of Table II, are definitely higher than the actual concentration, since an electric double-layer is formed at the crystal surface, containing a layer of adsorbed hydroxide or fluoride and a layer of hydrogen ion and oriented water molecules, which are also labelled with ^3H. It is thus impossible to make any quantitative conclusions. Nonetheless, these measurements indicate that both hydroxide and fluoride are strongly adsorbed

TABLE II

RESULTS OF THE MEASUREMENTS IN THE SYSTEMS LABELLED WITH TRITIUM

(μ=0.1 adjusted with KNO_3; specific activity 200 μCi ml^{-1})

Sample No.	*Solution composition*	*β-Activity per cm^2 of crystal corrected for background (c.p.m.)*	*β-Activity per cm^2 after subtraction of sample 1 activity (10^{-8} Ci)*	*Concentration of OH^- corresponding to these activities (mol cm^{-2})*
1	KNO_3 (μ=0.1)	27,050	—	—
2	10^{-1} *M* KOH+KNO_3	239,000	28.35	$1.6 \cdot 10^{-4}$
3	10^{-2} *M* KOH+KNO_3	88,400	8.22	$4.7 \cdot 10^{-5}$
4	10^{-3} *M* KOH+KNO_3	106,000	10.56	$6.0 \cdot 10^{-5}$
5	10^{-2} *M* NaF+KNO_3	100,800	9.87	$5.6 \cdot 10^{-5}$
6	10^{-1} *M* KOH+10^{-2} *M* NaF+KNO_3	183,800	20.95	$1.2 \cdot 10^{-4}$
7	10^{-2} *M* KOH+10^{-2} *M* NaF+KNO_3	39,500	1.67	$9.5 \cdot 10^{-6}$
8	10^{-3} *M* KOH+10^{-2} *M* NaF+KNO_3	143,300	15.57	$8.9 \cdot 10^{-5}$
9	10^{-1} *M* KOH+KNO_3 (Rinsed with water and wiped dry before measurement)	222	—	—

on the crystal surface and that they are removed by rinsing and wiping the crystal.

Preparation of laboratory LaF_3 electrode

Laboratory electrodes were prepared from LaF_3 crystals differing in the rare earths used for their activation (0.01–0.1 mole% of Eu, Sm, Pr, Ho, and Nd) and in their crystallographic properties (from single crystals to cylinders formed by up to three differently oriented crystals). The performance of these electrodes was compared over several months at pH 5.7 ± 0.1 with the Orion electrode. It was found that the character of the crystal had no marked effect on the electrode performance, but that cementing was very important. In general, the sensitivity of the prepared electrodes was poorer than that of the Orion electrode; in a few cases, electrodes with the same, or even slightly better, sensitivity than that of the Orion electrode were prepared, but the sensitivity deteriorated when the crystal was cemented into another body, although the cements used are usually satisfactory in preparation of ion-selective electrodes.

DISCUSSION

On the basis of present knowledge, it can be considered that the potential formation at the lanthanum trifluoride electrode arises from a reversible ion exchange at the interface and mobile Schottky defects inside the crystal. In the hexagonal lanthanum trifluoride, fluorine ions form undulating layers on both sides of a central layer containing La^{3+} and F^- ions[7]; there are several non-equivalent fluoride ion positions. The electric conductivity is based on the combination of molecular holes $[LaF_3]$ (their amount being about 0.1% at 27°C (ref. 8)) with LaF_3 formula units,

$$[LaF_3] + LaF_3 \rightleftharpoons LaF_2^+ + F^- \qquad (1)$$

while each LaF_2^+ and F^- ion occupies the same volume as LaF_3 in the crystal. The fluoride ions move from LaF_3 units to neighbouring LaF_2^+ ions (Schottky defects), leading to a relatively high conductivity[7] of about 10^{-7} Ω^{-1} cm^{-1}. It has been found that charged lattice defects form an internal electric double-layer in many solid electrolytes (*e.g.* AgI)[9–12] and take part in charge transport between the solid and liquid phases. The original electric charge on the crystal surface (unaffected by sorption) is formed because of a higher concentration of defects in the area adjacent to the interface, since the conditions here favour defect formation[13,14].

The above-mentioned processes play a role in the LaF_3 electrode potential formation but the decisive effect is that of processes on the crystal surface where a hydrophilic film is formed in contact with solution, as was shown by Brand and Rechnitz on the basis of impedance measurements[15]. According to these authors, the structure of the film differs from that on glass electrodes.

The results obtained in this paper support the assumption of the existence of a surface film. The x-ray, i.r., and radioactivity measurements show that in no case is the crystal lattice itself attacked by solution components and that the layer in which potential-determining changes take place is removed simply by

rinsing and wiping the crystal (see also refs.[5,16,17]). It seems that the species which may be contained in this film, depending on the solution composition (H_2O, OH^-, F^-, FHF^-, $[HF]_n$, *etc.*), are chiefly adsorbed physically and that the resulting composition of the film is the result of competition of these particles for active surface sites. This concept also explains why the electrode is not irreversibly poisoned even after prolonged exposure to 0.1 *M* potassium hydroxide. It can be assumed that LaF_3 functions as an inorganic ion-exchanger, on which F^- and OH^- ions are strongly adsorbed, perhaps with participation of hydrogen bonds or hydroxyl bridges[18].

For the long-term potential changes observed after a change in the solution pH to the alkaline region, two explanations may be offered.

(a) In solutions with $a_{OH^-} \gg a_{F^-}$, fast hydroxyl adsorption on the electrode occurs, accompanied by a rapid shift of the potential towards negative values. During this process a certain amount of adsorbed fluoride ions is displaced from the surface; these ions, however, remain in the hydrophilic film, increase a_{F^-} at the electrode surface and only slowly are transported into the bulk of the solution.

(b) Hydroxyl ions are rapidly adsorbed on the crystal surface, but the adsorption is a non-equilibrium process; then slow formation of energetically more favourable bonds occurs.

After neutralization of alkaline solutions, fluoride ions at the electrode may be temporarily depleted, since they replace the hydroxide ions adsorbed on the crystal. In acidic solutions, where $a_{[HF]_n} \gg a_{F^-}$, $[HF]_n$ (for the existence of $[HF]_2$, see Warren[6]) may be adsorbed on the electrode surface by hydrogen bonds. When the pH is increased, $[HF]_n$ desorbs and dissociates, giving rise to a temporary excess of fluoride ions at the electrode surface and consequently to the observed potential changes. The formation of the minima on the curves in Fig. 1 may be explained by the fact that the potential stabilization after a change in pH is faster at pH 2–3 than at pH 5 and that a_{F^-} decreases owing to the formation of $[HF]_n$. At an elevated temperature the potential stabilization proceeds even faster and the minimum disappears. The dependence of the properties of the hydrophilic film on pH requires that analytical measurements be carried out at a constant pH (5–6), the pH adjustment being made before the electrode is immersed in the solution, in order that potential stabilization may be more rapid.

A frequently discussed question is the degree to which the electrode potential is affected by fluoride ions liberated from the membrane at low a_{F^-}. Very different values have been published for the solubility product of crystalline LaF_3 (from 10^{-20} to 10^{-30})[2,5], and an attempt to calculate the K_s value from thermodynamic data has led[19] to an even lower value of $10^{-50.7}$. The present experiments agree well with the value, $K_s \leqslant 10^{-30}$, published recently by Buffle *et al.*[5]. These authors point out that the minimum determinable concentration is limited chiefly by "self-poisoning" of the electrode by adsorption of fluoride (this is similar to chalcogenide electrodes). The LaF_3 solubility product definitely does not play such an important role as, for example, that of silver chloride with the chloride electrode, since the fluoride electrode is almost insensitive to lanthanum(III) ions. As has been shown by Ross[4], the concentration of lanthanum(III) ions can be measured in the presence of a fine LaF_3 precipitate in the solution, where the equilibria are established much more rapidly.

The experiments with laboratory-prepared electrodes showed that the properties of the crystals play a negligible role compared to the quality of cementing the crystal in the electrode body; this has already been observed[4]. The deterioration of the electrode performance over a period of several months can be explained only by the appearance of minute crevices around the crystal, the formation of which may be enhanced by a possible tendency of the material to form gels (*cf.* the gel formed during prolonged shaking of crystalline LaF_3 powder with water). The possible effect of the properties of the crystals on the electrode performance[20] can be studied only when the effects of the electrode construction are eliminated.

We would like to thank Drs. A. Čajková, J. Loub, M. Matucha, J. Moravec and B. Strauch for their assistance during various stages of the work.

SUMMARY

The response of the lanthanum trifluoride electrode in solutions of various acidities, and the surface properties of the LaF_3 crystals in these solutions, have been studied potentiometrically and with the help of x-ray powder patterns, infrared spectrometry and measurement of the β-activity in ^3H-labelled systems. It is concluded that the electrode behaviour is determined by competitive adsorption of hydroxyl and fluoride ions and of various fluoride-containing species in the hydrophilic film formed on the electrode; the crystal itself is not attacked by the solution components. The long-term changes in the electrode potential are described and discussed on the basis of this concept. Several LaF_3 electrodes were prepared in the laboratory, and the effect of crystal-cementing on their performance is discussed.

REFERENCES

1 R. Block and S. Strecker, *Z. Anal. Chem.*, 235 (1968) 322.
2 J. N. Butler in R. A. Durst (Ed.), *Ion-Selective Electrodes*, NBS 314, Washington, 1969, p. 161.
3 H. Zentner, *Chem. Ind. (London)*, (1973) 480.
4 J. W. Ross in R. A. Dunst (Ed.), *Ion-Selective Electrodes*, NBS 314, Washington, 1969, pp. 76, 417, 420.
5 J. Buffle, N. Parthasarathy and W. Haerdi, *Anal. Chim. Acta*, 68 (1974) 253.
6 L. J. Warren, *Anal. Chim. Acta*, 53 (1971) 199.
7 A. Sher, R. Solomon, K. Lee and M. W. Muller, *Phys. Rev.*, 144 (1966) 593.
8 J. Kummer and M. E. Milberg, *Chem. Eng. News*, 47 (1969) 90.
9 E. P. Honig, *Nature (London)*, 225 (1970) 537.
10 E. P. Honig, *Trans. Faraday Soc.*, 65 (1969) 2248.
11 T. B. Grimley and N. F. Mott, *Discuss. Faraday Soc.*, 1 (1947) 3.
12 T. B. Grimley, *Proc. Roy. Soc. Sec. A*, 201 (1950) 40.
13 K. Lehovec, *J. Chem. Phys.*, 21 (1953) 1123.
14 K. L. Klilever, *J. Phys. Chem. Solids*, 27 (1966) 705.
15 M. J. D. Brand and G. A. Rechnitz, *Anal. Chem.*, 42 (1970) 478.
16 J. A. W. Dalziel and A. V. Dangi, *Euroanalysis Conf.*, 1972, Heidelberg.
17 G. J. Moody and J. D. R. Thomas, *Proc. Soc. Anal. Chem.*, 8 (1971) 84.
18 J. Veselý, *J. Electroanal. Chem. Interfacial Electrochem.*, 41 (1973) 134.
19 J. J. R. Frausto da Silva and M. M. Queimado, private communication.
20 J. Veselý, *Chem. Listy*, 65 (1971) 86.

Analytica Chimica Acta, 73 (1974) 167–172

DETERMINATION OF DIGITOXIN IN PHARMACEUTICAL ORAL DOSAGES BY AUTOMATIC DISCRETE-SAMPLE ANALYSIS

J. RAMÍREZ-MUÑOZ
Beckman Instruments, Inc., Irvine, California 92664 (U.S.A.)
(Received 18th April 1974)

Digitoxin, one of the glycosides used as cardiotonic in pharmaceutical preparations, has been studied by pharmaceutical analytical chemists in two aspects[1]: (a) separation of digitoxin from various naturally occurring glycosides, and (b) determination of digitoxin in separated and/or purified fractions, or in manufacturing processes, as the main analyte in intermediate or final pharmaceutical preparations.

Glycosides can be determined by various analytical approaches. Color reactions based on the chromogenic reactions of the α, β-unsaturated lactone substituent have been used, *e.g.* reaction with picric acid and alkalis (readings at 525 nm)[2,3], reaction with 3,5-dinitrobenzoic acid and alkalis (readings at 535 nm)[4,5], reaction with sodium nitropruside (readings at 470 nm)[6], reaction with sodium β-naphthoquinone sulfonate (readings at 450 nm)[7], and reaction with *m*-dinitrobenzene (readings at 620 nm)[8,9]. Chromogenic and fluorogenic reactions are not necessarily related to the butenolide side chain; for instance, the color and fluorescence produced in the presence of antimony trichloride can be utilized[10,11]. U.v. spectrophotometry, based on the absorption of the α, β- unsaturated group (maxima between 215 and 200 nm)[12] and polarographic procedures[13,14] have also been utilized.

The induced fluorescence caused by hydrogen peroxide in the presence of hydrochloric acid has been accepted as a standard procedure for the determination of digitoxin in tablets[15,16]. This analytical method has been modified to provide an automatic procedure by means of a recently developed automatic analyzer designed to work in a discrete-sample mode[17,18]. The instrumentation used, operating conditions, procedure and setup, and final analytical results are summarized in this paper.

The automatic determination of digitoxin is a typical case of analysis of dosages where the active ingredient is present in submilligram quantities, (0.1–0.2 mg per tablet). The high sensitivity of the reaction compensates for the low concentration of the analyte in the tablets under test.

EXPERIMENTAL

Instrumentation

A Beckman Automated Materials Analyzer (AMA 40) was used for all tests. The unit was equipped with a Beckman Ratio Fluorimeter, a ten-inch potentiometric recorder, and a teletypewriter (via an intercoupler) used as printer and tape puncher.

Reagents

Special care is required in the preparation of reagents. This is particularly true in the case of the hydrogen peroxide solution, where an excess of reagent spoils the fluorescence reaction. Results, therefore, may become too low and inconsistent.

The ascorbic acid and peroxide reagents should be freshly prepared before every run. Deionized–distilled water was used in all preparations.

Solvent. An aqueous 70% solution of ethanol (3A reagent grade) was used.

Alcoholic-acid ascorbic acid reagent. 0.175 g of ascorbic acid was dissolved in 125 ml of reagent-grade methanol. The solution was added to 500 ml of concentrated hydrochloric acid (reagent grade) with continuous stirring.

Hydrogen peroxide reagent. 1 ml of 30% hydrogen peroxide solution (reagent grade) was diluted to 500 ml with water; 50 ml of this solution were diluted to 1 l with water.

Standards

Stock solution. 20 mg of U.S.P. Digitoxin Reference Standard were dissolved to 500 ml with 70% ethanol.

Working standards for content uniformity and assay tests. 8.5, 10.0 and 11.5 ml of stock solution were diluted to 100 ml with 70% ethanol. Working standards prepared in this way correspond to 85, 100 and 115% potency. Other standards for linearity tests are described later.

Ethanol (70%) was used as the blank.

Operating conditions

Operating conditions are summarized in Table I. Because of the highly concentrated acid solutions, metal tips should be avoided in all probes. Instead of metal tips, short plastic tips (polypropylene) were used in the reagent pump probes, and long plastic tips (also polypropylene) in the pipetter–diluter probe and in the sampling probe.

Procedure

The analytical setup for the AMA 40 system, shown in Fig. 1, was prepared for the analysis of dosages containing 0.1 or 0.2 mg digitoxin. For higher contents, the pipetter–diluter setting can be varied to pipet smaller aliquots of the solution obtained by disruption of the tablet.

To adjust the temperature of the alcoholic solvent for the disrupter pump, the temperature of the external thermostatic bath, used to heat the solvent, is slowly increased until the boiling point is reached. Then, the temperature is lowered 4–5°C. The setting can vary from one to another location (as a function of location altitude). When the temperature is stabilized, the pump can be primed with the hot solvent to heat the glass pump and the run should be started at once.

Data evaluation

Data were evaluated by computer techniques. Numerical data collected on punched tape were processed with the help of a time-shared terminal (IBM 370 System).

TABLE I

DIGITOXIN OPERATING CONDITIONS

Disruption	Yes
Disruption speed	Position 40
Disruption time	120 s
Incubation	No
Filter Tubes	Yes
Filter vacuum	15 in
Analysis rate	*ca.* 17/h
Excitation radiation	395 nm
Fluorescence radiation	580 nm
Fluorimeter operation	
Attenuator	Adjusted
Filters	
primary	Corning 7-59 or Corning 7-51
secondary	Corning 3-69 or Corning 3-68 and Corning 4-95
Sleeve	360 nm
Zero adjustment	Adjusted to maximum suppression
100% adjusted	High or maximum scale expansion
Bar	No. 4
Sample volume	6 ml
Recorder chart speed	5 in/min^{-1}
Recorder span setting	100 mV
Solvent pump	50 ml of 70% ethanol (heated to near boiling point)
Sample vacuum	15 in
Sequence	2 Blanks, 3 standards, 15 samples, 3 standards, 15 samples, and 2 blanks (standards in reference tubes).

RESULTS

Repeatability

Repeatability was tested at standard level (100% potency standard) and at blank level (Table II).

Linearity

The correlation between relative fluorescence intensity and concentration was tested under the operating conditions given in Table I for several scale expansions. The series of standards for these tests were automatically prepared, by diluting an original standard of 0.2 mg of digitoxin per 50 ml ($4 \cdot 10^{-3}$ mg ml^{-1}) by means of the pipetter–diluter, as shown in Table III.

The results of linear and quadratic fit[5] of one of the series measured are shown in Fig. 2. The calibration plot shows a slight curvature, and a quadratic fitting and interpolation (on the basis of the quadratic fitting) is recommended. The working curve might be considered as a straight line in the narrow interval used in content uniformity and assay tests. However, better accuracy will be obtained if quadratic fitting is used.

Net fluorescence readings are calculated by subtracting the readings of blanks from the readings of standards. Net values may vary according to the scale expansion used in the instrument. Small variations in these relative fluorescence

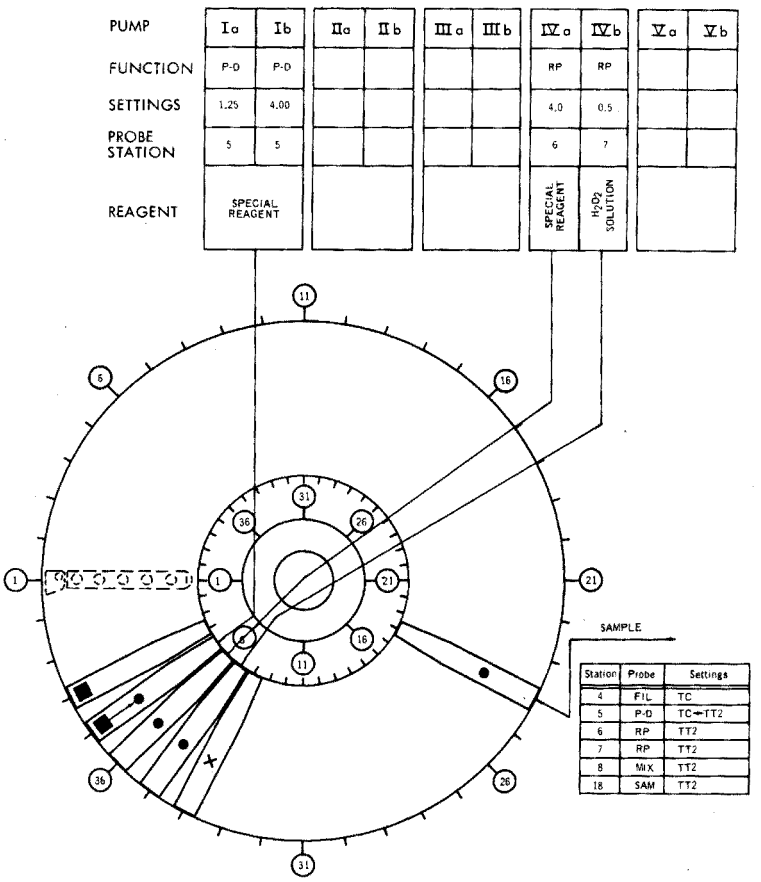

Fig. 1. Analytical setup for automatic determination of digitoxin. P-D = pipetter–diluter, RP = reagent pump, SAM = sample probe, FIL = filter, MIX = mixer, TC = T-Cup, TT = T-Tube.

LINEAR FIT. SLOPE = 0.704661

PAIR	X VALUES	Y VALUES	Y CALCD.	DIFFERENCE	% ERROR
1	11.4400	9.0000	8.0613	-0.9387	-10.4297
2	22.2000	16.9000	15.6435	-1.2565	-7.4350
3	32.4400	24.3000	22.8592	-1.4408	-5.9292
4	42.0000	29.0000	29.5958	0.5958	2.0544
5	51.2000	34.9000	36.0787	1.1787	3.3773

QUADRATIC FIT. COEFFICIENTS:

T1 = 0.829628

T2 = -0.002971

PAIR	X VALUES	Y VALUES	Y CALCD.	DIFFERENCE	% ERROR
1	11.4400	9.0000	9.1021	0.1021	1.1342
2	22.2000	16.9000	16.9534	0.0534	0.3157
3	32.4400	24.3000	23.7863	-0.5137	-2.1140
4	42.0000	29.0000	29.6030	0.6030	2.0795
5	51.2000	34.9000	34.6879	-0.2121	-0.6076

Fig. 2. Linearity tests. The concentration range tested was 11.44–51.20 μg ml^{-1}.

TABLE II

REPEATABILITY TESTS

Level tested	*Average reading*[a]	*Relative standard deviation*[b] *(%)*
100% Potency standard (0.2 mg)	79.0	2.17
Blank	31.2	3.05

[a] Readings in relative fluorescence intensity (scale 0–100, maximum scale expansion).
[b] For five determinations.

TABLE III

PREPARATION OF STANDARDS FOR LINEARITY TESTS

(4.00 ml of diluent and 4.50 ml of total reagents added. Initial digitoxin standard contained $4 \cdot 10^{-3}$ mg ml^{-1})

Standard added (ml)	0.25	0.50	0.75	1.00	1.25
Final volume (ml)	8.75	9.00	9.25	9.50	9.75
Final digitoxin concn. ($\cdot 10^{-4}$ mg ml^{-1})	1.14	2.22	3.24	4.23	5.12

intensity readings, from run to run, will not significantly affect the results in precision and/or accuracy, as long as the scale expansion setting is kept constant in each individual run.

Tablet analysis

Sets of five tablets were examined. Tablets containing 0.1 and 0.2 mg of digitoxin were assayed. Assay limits established for digitoxin are 90 and 110% potency[16]. Results for one of the sets examined (0.1 mg of digitoxin) were as follows: individual tablet potencies were 102.6, 110.8, 112.0, 111.2 and 101.3, the average potency being 107.6. All the tablets were thus acceptable for content uniformity (their potencies were inside the range 85–115% potency) and for assay (their average was inside the range 90–110% potency). Another set of five tablets of the same brand and batch gave an average of 108.9% potency, quite close to the previous 107.6% average.

DISCUSSION

The automatic fluorimetric procedure described above is appropriate for content uniformity and assay test in digitoxin tablets. The precision achieved is acceptable (see Table II). Low relative standard deviation values were obtained even with low contents of analyte (0.1 and 0.2 mg of digitoxin per tablet).

Aliquots pipetted from disrupted and filtered solutions can be varied easily of other tablets of a different potency are to be tested. Only a pump setting needs to be varied.

Tablets can be analyzed in a single run. Net fluorescence readings are calculated by means of common blanks measured in the same run. The solvent pump will handle, without difficulty, the hot alcoholic solution used in the disruption stage. Thirty tablets can be analyzed in each run at the rate of 17 readings per hour.

SUMMARY

An automatic procedure for determination of digitoxin in pharmaceutical oral dosages is described. The procedure is based on the fluorimetric determination of digitoxin in hydrochloric acid media in the presence of hydrogen peroxide. Operational conditions and analytical setup are detailed. Results for repeatability, linearity, and tablet analysis are given. The procedure can be used for analysis of sets of up to 30 tablets at the rate of 17 readings per hour. Contents as low as 0.1 mg of digitoxin can be determined.

REFERENCES

1 T. Higuchi and E. Brochmann-Hanssen (Eds.), *Pharmaceutical Analysis*, Interscience, New York, 1961, p. 49.
2 F. K. Bell and J. C. Krantz, Jr., *J. Pharmacol.*, 83 (1945) 213.
3 F. K. Bell and J. C. Krantz, Jr., *J. Amer. Pharm. Ass., Sci. Ed.*, 38 (1949) 107.
4 E. L. Pratt, *Anal. Chem.*, 24 (1952) 1324.
5 D. H. E. Tattje, *J. Pharm. Pharmacol.*, 9 (1957) 29.
6 L. F. Fisher and M. Fisher, *Steroids*, Rheinhold, New York, 1959.
7 A. T. Warren, F. O. Howland and L. W. Green, *J. Amer. Pharm. Ass., Sci. Ed.*, 37 (1948) 186.
8 S. Baar, *Biochem. J.*, 58 (1954) 175.
9 D. Banes, *J. Amer. Pharm. Assoc., Sci. Ed.*, 42 (1953) 674.
10 F. Jaminet, *J. Pharm. Belg.*, (1950) 297.
11 D. Lawday, *Nature (London)* 170 (1952) 415.
12 T. Canbäck, *J. Pharm. Pharmacol.*, 1 (1949) 201.
13 J. G. Hilton, *Science*, 110 (1949) 526.
14 J. G. Hilton, *J. Pharmacol. Exp. Ther.*, 100 (1950) 258.
15 K. B. Jensen, *Acta Pharmacol. Tox. Kbh.*, 10 (1954) 69.
16 *U.S. Pharmacopeia XVIII*, U.S. Pharmacopeia Convention, Inc., Bethesda, Maryland, 1970.
17 J. Ramírez-Muñoz, *AMA-40 Chemical Manual, Industrial Technical Report TR-581*, Beckman Instruments, Inc., 1973.
18 J. Rohrbaugh and J. Ramírez-Muñoz, *Anal. Chim. Acta*, in press.

Analytica Chimica Acta, 73 (1974) 173–176

SHORT COMMUNICATION

The determination of cadmium in sea water by radioactivation

H. V. WEISS
Naval Undersea Center, San Diego, California 92132 (U.S.A.)
K. CHEW, M. GUTTMAN and A. HOST
San Diego State University, San Diego, California 92115 (U.S.A.)
(Received 25th March 1974)

A procedure exists for the determination of cadmium in sea water that is based on ion-exchange separation of cadmium from sea salts and subsequent determination by atomic absorption spectrometry[1]. It nonetheless seemed desirable to develop a neutron activation analysis technique, which provides the basis for unequivocal identification and is at the same time inherently sensitive.

This report describes a method of isolating cadmium from sea water by co-crystallization with 8-hydroxyquinoline (oxine), the radiochemical purification scheme in the determination of radio-induced ^{115}Cd–^{115}In, and the results of replicate analyses of two different volumes of a stock sea-water sample. Also several analyses were performed to demonstrate that cadmium and mercury are determinable on the same sample of sea water.

Experimental

Chemicals. A solution was prepared to contain 10% (w/v) oxine in ethanol.

Potassium and sodium chloride used as holdback carriers in the radiochemical purification process were added as solid (about 10 mg each).

Cadmium, iron, and copper carrier solutions were made to contain 10 mg of the respective cation per ml in distilled water. Cadmium and copper were prepared from nitrates and iron from the chloride.

Comparator solution consisted of a standardized cadmium solution diluted to a concentration of 10 μg ml^{-1}. Its volume was adjusted to the same as that of the sample with concentrated nitric acid.

Other chemicals used were of reagent grade quality.

Isolation of cadmium from sea water. Cadmium probably exists in the oceans at concentrations that are considerably less than a part per billion. At such concentrations neutron irradiation of the unfractionated sea-water sample is impractical since the level of induced radioactivity from ^{24}Na and ^{38}Cl is objectionable in view of the magnitude of sample volume that would be required to provide the requisite sensitivity. Accordingly, cadmium was isolated from the bulk of sea salts by co-crystallization with oxine.

Sea water was acidified with concentrated nitric acid to 0.16 *M*. Aliquots

(1 l) were transferred to containers to which were added a known quantity of ^{109}Cd activity and 10 ml of oxine solution. Ammonia solution was added until the pH of the solution attained a value of 7–8. Crystallization was encouraged by agitation or sonic shock. After the solution had stood for about 1 h, the resultant crystals were collected on sintered glass (coarse porosity). The crystals, including those which adhered to the walls of the container, were dissolved in concentrated nitric acid, and the γ-ray activity of this extract was measured with a NaI(Tl) detector. The results indicated that $100.0 \pm 1.1\%$ of the cadmium activity was recovered by the co-crystallization process.

Treatment of sea-water sample. Sea water was collected at a depth of 20 ft off the end of the pier at the Scripps Institution of Oceanography, La Jolla, California. Upon collection, the sample was acidified with concentrated nitric acid (10 ml l^{-1} of sea water) and filtered through a Millipore filter membrane (0.45 μm). Aliquots of 0.5 or 1 l were transferred to beakers, and cadmium was co-crystallized from solution by the procedure described above. (Only 5 ml of oxine solution was added to the aliquots of lesser volume.)

Upon dissolution of crystallized oxine, the sample was adjusted to a volume of 15 or 30 ml with concentrated nitric acid for the 0.5- and 1-l aliquots, respectively. The solutions were placed in polyethylene snap-top vials in preparation for irradiation.

Blanks. Twenty ml each of the oxine solution, nitric acid and ammonia used in the pre-irradiation treatment served as blanks.

Irradiation. Samples, comparators, and blanks were irradiated for 1 h in a flux of $2 \cdot 10^{12}$ n cm^{-2} s^{-1} in a rotating sample container (1 rev min^{-1}) at Gulf Energy and Environment Services, San Diego, California.

Radiochemical separations and measurements. After irradiation the sample or blank was quantitatively transferred to a vessel that contained 2 ml of cadmium carrier, 1 drop of phosphoric acid and about 10 mg each of potassium and sodium chloride. Samples and blanks were evaporated to a volume of 1–2 ml, and diluted with about 50 ml of water, and cadmium sulfide was precipitated by passing hydrogen sulfide gas through the solution. (Subsequent sulfide precipitations were effected in the same manner.) The precipitate was collected by filtration, and the small quantity of coprecipitated oxine was eliminated by ashing with 3 ml of concentrated sulfuric acid and 5 ml of concentrated nitric acid. Upon appearance of sulfur trioxide fumes, another volume of nitric acid was added if the solution was not clear. The solution was heated to dryness, the residue dissolved in 2.5 ml of concentrated hydrochloric acid, and the solution diluted to 30 ml with water and heated to expel the hydrogen sulfide. Copper (5 mg) was added and copper sulfide was precipitated. The precipitate was separated and discarded and after a further heating copper carrier was again added and reprecipitated. Iron carrier (5 mg) was added to the filtrate, which was made ammoniacal. Iron(III) hydroxide was coagulated by heating and removed by filtration. The filtrate was reduced to a volume of about 10 ml to evolve excess ammonia, and then diluted to 30 ml with water, and sodium hydroxide pellets were added until cadmium hydroxide formed. The precipitate was separated by filtration, and dissolved in 10 drops of concentrated hydrochloric acid, and the solution was diluted to 30 ml with water. Potassium and sodium chloride and 1 drop of phosphoric acid were added and then cadmium

sulfide was precipitated. The precipitate was collected on a Millipore membrane filter and mounted on a brass planchet.

Comparators were carried through the radiochemical separation procedure, starting with the iron(III) hydroxide scavenging step, after first adding cadmium carrier and evolving most of the nitric acid.

Measurement. The β-ray activity measurements of ^{115}Cd–^{115}In were started one day after the radiochemical separation to allow time for growth of the indium daughter. The measurements were usually carried out several times a day for a period of 5–6 days in an automatic Beckman Wide-Beta counter equipped with a sample changer.

Carrier yield determination. The processed cadmium samples as well as cadmium standards (4 mg) were re-irradiated for 30 s in a flux of about $3 \cdot 10^{12}$ n cm^{-2} s^{-1} for 30 s. After 24 h, the γ-rays of ^{115}Cd–^{115}In were measured with a NaI(Tl) detector coupled to a pulse-height analyzer. Through comparison—with standards—of the activity value of the samples, comparators and blanks, the carrier yield was computed and the count rate in the original irradiation was corrected for this factor.

Results and discussion

A typical β-decay curve of ^{115}Cd–^{115}In appears in Fig. 1. The growth of the ^{115}In daughter is apparent in the earliest measurements. From 47 h to about 143 h after irradiation, the decay is linear with a half-life of 53.5 h. Beyond this time, the decay rate deviates from this half-life owing to the ever-increasing relative contribution of 44.1-d ^{115m}Cd.

The results of the assay of cadmium in sea water are as follows. Eight

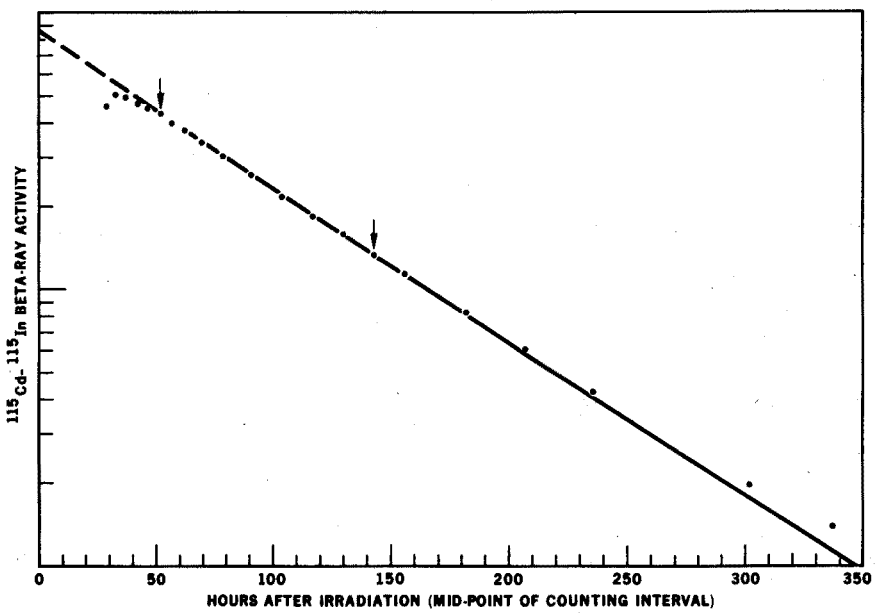

Fig. 1. β-Ray decay curve of ^{115}Cd–^{115}In.

analyses of 0.5-l samples and five of 1-l samples averaged 0.737 ± 0.041 and 1.451 ± 0.044 μg, respectively. The overall standard deviation is 4.7%. Further, the average cadmium concentrations for the two sets of aliquots are in favorable agreement when normalized for volume.

Occasionally, low-level ^{64}Cu contaminant was present over the first to second day after radiochemical purification. By the third day the β-decay followed the half-life of ^{115}Cd. This interference could probably be eliminated completely by the introduction of an additional copper sulfide decontamination step.

The analysis of the comparators indicated that 1 count min^{-1} of ^{115}Cd–^{115}In per nanogram of cadmium was realized at the end of the irradiation. Thus with an instrumental background of 0.4 counts min^{-1}, a background counting interval of 200 min, an average carrier yield of 50% and sensitivity defined by a count rate in excess of 3 standard deviations from the background, the limit of sensitivity three days after the irradiation is below 1 ng.

In subsequent work the oxine crystallized from sea water was dissolved in 2 *M* rather than in concentrated nitric acid and in the same volumes described above. Use of the more dilute acid offers advantage by way of avoiding the generation of oxides of nitrogen that occurs when concentrated acid interacts with oxine at the usual nuclear reactor temperature (about 30°C).

A method reported previously for the determination of mercury in sea water[2] is inherently compatible with the analytical scheme described here. In the mercury analysis, the initial step depends upon its quantitative coprecipitation with copper sulfide; cadmium remains in solution. Thus upon separation of phases, the filtrate is susceptible to cadmium assay. Analyses have been performed on four samples of Arctic Ocean water in which a 1-l aliquot was processed as described in this report and a second aliquot was treated in the manner prescribed for mercury determination. The filtrate of this second aliquot was then analyzed for cadmium. The results of these analyses appear in Table I. These data indicate that mercury and cadmium are reliably determined on a single aliquot.

TABLE I

CADMIUM DETERMINED ON TWO ALIQUOTS OF THE SAME SEA-WATER SAMPLE BY THE DIRECT METHOD AND AFTER PRETREATMENT FOR THE ISOLATION OF MERCURY ($\mu g\ l^{-1}$)

Sample	*Direct method*	*Pretreated for Hg isolation*	*Average*	*Deviation from average (%)*
1	0.273	0.287	0.280	2.5
2	0.367	0.453	0.410	10.5
3	0.277	0.245	0.261	6.1
4	0.415	0.339	0.377	10.1

REFERENCES

1 J. P. Riley and D. Taylor, *Anal. Chim. Acta*, 40 (1968) 479.
2 H. V. Weiss and T. E. Crozier, *Anal. Chim. Acta*, 58 (1972) 231.

Analytica Chimica Acta, 73 (1974) 177–179

SHORT COMMUNICATION

Determination of phenylacetylene by atomic absorption spectrometry

ROBERT V. SMITH and DONOVAN L. BAILEY

Division of Medicinal Chemistry and Natural Products, College of Pharmacy, The University of Iowa, Iowa City, IA 52242 (U.S.A.)

(Received 18th March 1974)

Monosubstituted acetylenes react with silver nitrate to form silver acetylides plus an equivalent of hydrogen ions[1]. This reaction has been used in a variety of indirect titrimetric procedures[2–7]. Measurement of the silver adduct or excess of silver nitrate is not as readily utilized since silver nitrate–silver acetylide complexes with variable stoichiometries tend to form under neutral or acidic conditions[1]. In the presence of ammonia, however, the reaction is straightforward:

$$R\text{–}C{\equiv}C\text{–}H + Ag(NH_3)_2^+ + OH^- \rightarrow R\text{–}C{\equiv}C\text{–}Ag\downarrow + H_2O + 2NH_3$$

This reaction has recently been employed by Rizk *et al.*[8] for an indirect assay of acetylenic steroids based on spectrophotometric measurement of excess of silver ion as its dithizone complex. While this method is reported to possess a high degree of accuracy and precision, it involves several solvent partitioning steps that appear to be time-consuming. It was expected that the reaction of ammoniacal silver nitrate with acetylenic compounds might be conveniently measured by atomic absorption spectrometry (a.a.s.). Phenylacetylene was used as a model compound in the development of the direct and indirect a.a.s. procedures which are described in this communication.

Reagents and apparatus

Chloride-free water. Water distilled from 1% sodium hydroxide was used throughout.

Ammoniacal silver nitrate reagent. Dissolve 787 mg of silver nitrate in enough diluted (1+49) ammonia liquor to make 100 ml. These and all other silver-containing solutions were prepared and maintained in Ray-Sorb (Kimax) glassware.

Phenylacetylene solution. Dissolve 100 mg of phenylacetylene (Aldrich Chemical Co.) in enough tetrahydrofuran to make 100 ml.

Silver phenylacetylide. React phenylacetylene with an equivalent of ammoniacal silver nitrate solution (0.7 g silver nitrate/ml in dilute (1+4) ammonia liquor) at room temperature. Collection of the precipitate, followed by washing with acetone, gives a nearly quantitative yield of silver phenylacetylide. Recrystallization from piperidine–methanol gives white crystals, m.p. 100°C (decomp.; lit. 100°C, decomp.[1]). Store in a light-resistant container.

Silver phenylacetylide working standards. In a 100-ml volumetric flask, dissolve 3.88 mg of silver phenylacetylide in a minimum of piperidine; dilute to volume with *N*,*N*-dimethylformamide (DMF). Dilute 5, 10, and 15-ml aliquots of this stock solution to 100 ml with DMF in volumetric flasks (1, 2 and 4 p.p.m. silver).

Silver nitrate working standards. Dilute 1 ml of ammoniacal silver nitrate reagent (5 mg of silver) to 100 ml with water. Dilute 5, 10 and 15-ml aliquots of this solution to 100 ml in volumetric flasks (2.5, 5.0 and 7.5 p.p.m. silver).

A Jarrell-Ash 82-270 Atomsorb atomic absorption spectrophotometer, equipped with a single-slot burner head (10-cm pathlength) and silver hollow-cathode lamp, was used throughout. Silver was measured at 328.1 nm with the instrumental parameters described previously[9].

Procedures

Direct method. React 2 ml of phenylacetylene solution (2 mg of phenylacetylene) with 1 ml of ammoniacal silver nitrate reagent at room temperature for 5 min in a 12-ml centrifuge tube. Centrifuge the mixture at 2000 *g* for 5 min. Discard the supernate and wash the precipitate with three separate 5-ml portions of water. Dissolve the washed precipitate in a minimum of piperidine and dilute to 100 ml with DMF; dilute a 10-ml aliquot of this solution to 100 ml with DMF. Optimize the a.a.s. settings while aspirating the 2 p.p.m. silver acetylide working standard solution. Aspirate standard and unknown solutions; prepare a calibration graph and determine the amount of phenylacetylene in the sample.

Indirect method. React 2 ml of phenylacetylene solution (2 mg phenylacetylene) with 1 ml of ammoniacal silver nitrate reagent at room temperature for 5 min in a graduated 12-ml centrifuge tube. Dilute the reaction mixture to 5 ml with water and centrifuge for 5 min at 2000 *g*. Dilute 1 ml of the supernate to 100 ml with water. Optimize the a.a.s. settings while aspirating the silver nitrate working standard solution containing 7.5 p.p.m. of silver. Aspirate standard and unknown solutions; prepare a calibration curve and determine the amount of phenylacetylene in the sample.

Results and discussion

Direct method. Silver phenylacetylide, like the majority of alkynyl silver compounds, is insoluble in most solvents; this is apparently due to formation of coordinate polymers[1]. Many alkynyl silver compounds, however, can be dissolved in simple amines, presumably because amines form soluble complexes[1]. Piperidine was therefore used to solubilize the silver phenylacetylide; the initial solution could then be suitably diluted with DMF. Calibration curves were consistently linear over the range 1.0–4.0 p.p.m. (silver) with typical absorbance readings of approximately 0.06–0.24. An estimate of the accuracy and precision of this method was ascertained from the results for fifteen samples containing 2 mg of phenylacetylene. These samples gave a mean percent recovery of 100.4% with a relative standard deviation of 6.5%.

Indirect method. With this method, calibration curves were consistently linear over the range 2.5–7.5 p.p.m. (silver) with usual absorbance readings of about

0.08 to 0.24. Thus, in comparison to the direct method, there is a decrease in sensitivity by a factor of about two; this is likely to be a solvent effect. The accuracy and precision of the indirect method were evaluated with fourteen samples containing 2 mg of phenylacetylene. Analysis of these samples yielded a mean recovery of 100.3% with a relative standard deviation of 2.9%.

Comparing the two methods, equivalent accuracy is attained with each, while the precision of the indirect procedure is superior to that of the direct method. The indirect procedure is more quickly performed since it obviates the wash step that is incorporated in the direct method.

The a.a.s. methods presented herein are convenient and selective procedures for the determination of phenylacetylene. It is believed that these techniques might be readily adapted to the analysis of other compounds containing monosubstituted acetylenic functions (*e.g.* 17 α-ethinylsteroids).

Financial support from the Division of Undergraduate Education in Science, National Science Foundation (Grant GY 8734) is gratefully acknowledged.

REFERENCES

1 C. D. M. Beverwijk, G. J. M. Van Der Kerk, A. J. Leusink and J. G. Noltes, *Organometal. Chem. Rev., Sect. A*, 5 (1970) 215.
2 L. Barnes, Jr. and L. J. Molinini, *Anal. Chem.*, 27 (1955) 1025.
3 M. Miocque and J. A. Gautier, *Bull. Soc. Chim. Fr.*, (1958) 467.
4 N. D. Cheronis and T. S. Ma, *Organic Functional Group Analysis*, Wiley–Interscience, New York, 1964, p. 385.
5 S. Gorog, *Acta Chim. Acad. Sci. Hung.*, 47 (1966) 1.
6 *British Pharmacopeia*, 1968, pp. 390–391.
7 *National Formulary*, XIII, 1970, pp. 290–292.
8 M. Rizk, J. J. Vallon and A. Badinand, *Anal. Chim. Acta*, 65 (1973) 220.
9 R. V. Smith and M. A. Nessen, *J. Pharm. Sci.*, 60 (1971) 907.

Analytica Chimica Acta, 73 (1974) 180–184

SHORT COMMUNICATION

Determination of lead in 'instant' coffee and tea powders by carbon filament atomic absorption spectrometry

J. K. KAPUR and T. S. WEST
Chemistry Department, Imperial College, London SW7 2AY (England)
(Received 10th March 1974)

Recent years have seen a tremendous growth in the development[1] and application of atomic absorption spectrometry in analyses for trace metals, particularly by "non-flame" techniques, but little has been published on the determination of lead in water-soluble foods by "non-flame" methods; only two papers have described the determination of the heavy metal contents of fruit juices[2] and the determination of lead in milk[3] by conventional (flame) atomic-absorption spectrometry. In the present work on soluble coffees and teas, an "Alder–West type" carbon filament atom reservoir was used, because of its ease of application and very low cost per analysis. The determination of lead by carbon-filament atomic-absorption spectrometry has been described previously[4].

Usually, lead is determined in such products by absorption spectrophotometry with dithizone; the disadvantages of this procedure are well known. Conventional atomic absorption lacks sufficient sensitivity for the analysis of foodstuffs. The permitted level for "instant" coffee and tea powders is $\leqslant 2$ p.p.m. Pb.

Experimental

Apparatus. A Varian Techtron AA4 atomic-absorption spectrophotometer was used with a Pye–Unicam hollow-cathode lamp operated in the d.c. mode. The silica cover-slip over the monochromator slit mechanism was removed to improve transmission into the monochromator housing. The standard photomultiplier (Hamamatsu Model R213) of the AA4 was replaced by a RCA 213A tube which gave a better response at the lead resonance line at 217 nm. The signal was taken directly from the photomultiplier and amplified by means of the type K amplifier of a Telequipment storage oscilloscope, type TD51. A 50.000 pF damping capacitor was placed across the input terminals of the oscilloscope.

The carbon filament unit used was of the Alder–West[5] variety, suitably modified to take bigger samples[6]. The filament was 3.2 mm in diameter with an effective length of 1 cm, and had a notch 2 mm by 1 mm deep filed into it to accommodate a 5-μl sample drop. The entire filament unit was enclosed by a glass cell which had a removable lid to allow easy application of sample, and silica windows to allow passage of u.v. radiation between the lamp and the monochromator. The sample was vaporized from the filament by connecting the

water-cooled electrodes to a 1.2-kW step-down transformer (20:1), powered from the mains via a "Variac" transformer, so that the voltage could be varied between 0 and 12 V; the maximum current drawn was 70 A.

Light from the hollow-cathode lamp was focused by a 25-mm diameter fused silica lens (62.5-mm focal length) into the filament notch. This beam was re-focused onto the entrance slit of the monochromator by means of a similar lens.

Reagents. Stock solutions containing 10,000 p.p.m. of lead were prepared by dissolution of analytical reagent-grade lead nitrate in deionized water. The ammonia solution, 35%, was lead-free, and the citric acid was also low in lead.

Procedure. The lamp current, E.H.T. and monochromator slit-width were adjusted for the optimal signal: noise ratio. The flow-rate of shielding gas (nitrogen) was not very critical in the range 3–5 l min^{-1} but was optimal at 4.5 l min^{-1}. The height of incidence of the light beam above the filament was investigated with a travelling microscope (Fig. 1a); grazing incidence was used for maximal sensitivity. The absorbance increased steeply with increasing atomization voltage from 7 to 7.8 V and decreased gradually above 8 V; 8 V was therefore used.

Under these conditions, the sensitivity of the two main lead lines 283.31 nm and 217.00 nm was investigated with 5-μl samples. The solvent was dried with 0.5 V for 10 s before atomization. The sensitivities and detection limits are shown in Table I.

A calibration graph for lead (in aqueous solution) at 217 nm (Fig. 1b). prepared by dilution of a stock lead solution, was linear up to 0.2 p.p.m. and could be used up to 0.4–0.6 p.p.m. with reasonable precision.

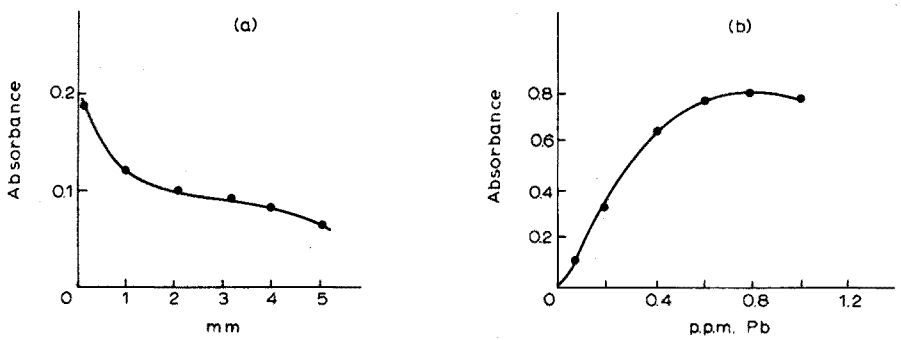

Fig. 1. Optimisation of parameters of the analytical procedure. (a) Absorbance *vs.* height above filament for Pb at 217 nm; (b) absorbance *vs.* conc. for Pb at 217 nm.

TABLE I

SENSITIVITY AND DETECTION LIMIT DATA FOR LEAD IN PURE SOLUTION

Wavelength	*Sensitivity, g (for 1% absorption)*	*Detection limit, g (S:N = 2)*
217.0 nm	$3 \cdot 10^{-11}$	$2.5 \cdot 10^{-11}$
283.31 nm	$2.5 \cdot 10^{-10}$	$1 \cdot 10^{-10}$

Direct analysis of coffee extract powder

In pure aqueous solutions lead was completely atomized at 8 V, but lead-free coffee powder solutions gave scatter signals from the matrix even at higher voltages. When standard lead solutions were added to a 5% coffee solution, *ca.* 50% recoveries were obtained even after an initial pyrolysis at *ca.* 2 V to smoke off most of the volatile organic material.

Several methods were investigated to improve the pyrolysis process. Application of 5 μl of concentrated mineral acids, 10% trichloracetic acid or varying strengths of hydrogen peroxide, after the initial evaporation of solvent, was unsuccessful; matrix effects were still observed. Since a true solution of the sample was not being obtained, the use of basic solvents was examined, *e.g.* KOH, NaOH, NH_3, and these ensured complete dissolution of the coffee extract; no matrix effects were observed but the lead was hydrolysed. The use of ammonium citrate (50% (w/v) citric acid solution adjusted to pH 9 with ammonia) was then examined; this not only solubilized the matrix, but retained the lead in solution as a complex. The optimal pH was established as 8.7–9.3; at lower pH values (8–8.5) the coffee matrix was not completely dissolved whilst at pH 9.5–10 lower signals were observed, probably because of hydrolysis of the lead ions.

Method of analysis. Coffee extract powder (5 g) was dissolved in hot deionized water, 20 ml of the ammonium citrate solution were added, and the mixture was diluted to 100 ml. Similarly, a "lead-free" coffee blank solution was prepared. The following voltage sequence was applied: 0.5 V—10 s (drying); 2.0 V—10 s (pyrolysis); 8 V—atomization. An interval of 45 s was allowed between the drying and pyrolysis, and 60 s between the pyrolysis and atomization, so that the rod could reach an equilibrium temperature. These precautions considerably improved the precision of measurement. Each result required about 5 min.

A standard addition method was used and a blank was subtracted to account for the lead content of the reagents. The relative standard deviation was 5%.

Instant tea samples were analysed in exactly the same way. The relative standard deviation was 6%, the lowest concentration of lead that could be detected in the solid was 0.2 p.p.m., and up to 50 determinations could be done with one rod. Typical results are shown in Table II.

Analysis based on extraction

Lower limits than the 0.2 p.p.m. provided by the above direct method were desirable, and a concentration method based on extraction of lead as its ion-association iodide complex into methyl isobutyl ketone[7] was therefore examined.

The efficiency of the extraction system was investigated. A series of solutions was made which contained 2.5 μg of lead, 4 ml of a saturated solution of potassium iodide (AnalaR) and 1 ml of concentrated hydrochloric acid (AnalaR) diluted to 25 ml. The iodide solution was made lead-free by acidifying with hydrochloric acid and extraction with MIBK immediately before use. A blank solution containing no added lead was also prepared. Lead was extracted with 2.5, 5 or 10 ml of MIBK, previously equilibrated with 5% hydrochloric acid, and the lead concentration was determined with 5-μl samples of the organic

BLE II

TERMINATION OF LEAD IN COFFEE EXTRACT POWDER AND INSTANT TEA POWDER

ıple	*Direct a.a.s. (p.p.m.)*	*Independent dithizone procedure (p.p.m.)*	*Sample*	*Extraction a.a.s. (p.p.m.)*	*Independent dithizone procedure (p.p.m.)*
	1.1±0.06	1	8	1.65±0.08	1.75
	0.65±0.05	0.7	9	0.65±0.03	0.6
	0.62±0.06	0.6	10	0.45±0.04	0.4
	0.64±0.03	0.7	11	1.1±0.02	1.0
	1.6±0.06	1.75	12	0.56±0.02	0.6
	0.5±0.03[a]	0.4[a]	13	0.6±0.03	0.7
	0.5±0.03[a]	0.4[a]			

:a.

layer. By this method 96% of lead was extracted into 2.5 ml of MIBK in a single pass. Ammonium citrate did not interfere with the extraction; the ammonium citrate was made lead-free, similarly to the potassium iodide.

Analysis of coffee extract powder. The coffee samples were analysed by standard addition. The above 5% coffee solution in ammonium citrate medium (5 ml), 5 ml of concentrated hydrochloric acid, and 5 ml of purified iodide solution were diluted to 25 ml. Lead was extracted with MIBK (2.5 ml), previously equilibrated as described above. The organic layer, containing a small amount of sediment, was centrifuged or allowed to stand for 5 min, and the clear solution was then analysed. The following voltage sequences were used with similar intervals between pyrolysis and drying as before: 0.5 V—5 s (drying); 3 V—6 s (pyrolysis); 8 V—atomization.

The linear range of the calibration curve for this procedure was $2 \cdot 10^{-3}$–$1 \cdot 10^{-1}$ p.p.m. Pb in the sample solution. A lower limit could be obtained for lead in the coffee powder by using a larger volume of the 5% coffee solution, with the same volumes of reagents.

The available coffee samples of known lead content contained more lead than could conveniently be handled by this extraction procedure at the most sensitive line (217 nm), hence the 283.3-nm line was used. Typical results are shown in Table II. Approximately 80 analyses could be done on each carbon filament. The relative standard deviation at 283.3 nm was 5%.

The lowest possible concentration of lead in the solid coffee powder that could be determined by this procedure would be 0.02 p.p.m., if a 20-ml sample of 5% coffee solution was used with measurement at 217 nm.

Conclusion

The direct analysis procedure for lead in coffee extract powder is simple and rapid; only dissolution of the sample in ammonium citrate is needed before the measurement at 217 nm. Coffee powders containing down to 0.2 p.p.m. Pb can be analysed, and it takes only about 5 min to obtain an answer. The extraction technique takes considerably longer, *ca.* 1–1.5 h, but offers equally good precision, 6%, and permits samples to be analysed for lead contents down to 0.02 p.p.m. (w/w).

We thank the British Food Manufacturing Industries Research Association and their related industries for the provision of a research grant and for their interest and support. We are also particularly indebted to Messrs. J. Lyons (Cadby Hall, London) for the supply of samples.

REFERENCES

1 J. W. Robinson and P. J. Slevin, *Int. Lab.*, (1973) 10.
2 J. C. Meranger, *Bull. Environ. Contam. Toxikol.*, 5 (3) (1970) 271.
3 I. Brooks, C. Luster and D. Easterly, *At. Absorption Newslett.*, 93 (1970) 93.
4 R. G. Anderson, H. N. Johnson and T. S. West, *Anal. Chim. Acta*, 57 (1971) 281.
5 J. F. Alder and T. S. West, *Anal. Chim. Acta*, 51 (1970) 363.
6 A. C. Oborne and T. S. West, *Proc. Soc. Anal. Chem.*, 9 (1972) 19.
7 P. W. West and J. K. Carlton, *Anal. Chim. Acta*, 6 (1953) 604.

Analytica Chimica Acta, 73 (1974) 185–190

SHORT COMMUNICATION

Spectrometric evidence for *d*-orbital participation in the lowest excited singlet states of naphthalenethiols

A. C. CAPOMACCHIA and S. G. SCHULMAN
College of Pharmacy, University of Florida, Gainesville, Florida 32610 (U.S.A.)
(Received 8th April 1974)

The acid–base properties of the naphthols have been extensively studied[1–4]. It is generally recognized that in the lowest excited singlet state, these substances are some 6–10 orders of magnitude more acidic than in the ground electronic state. Little information exists, however, about the electronic absorption or fluorescence spectra or about the prototropic properties in ground or excited states of the naphthalenethiols. Since the latter compounds are periodic congeners of the naphthols it appeared to be of fundamental chemical interest to study the electronic spectra and acid–base chemistry of these substances. Moreover, from the analytical point of view, the reaction of many transition metal ions with sulfhydryl compounds suggests that the knowledge of the fluorescent properties of aromatic mercaptans might be useful in the evolution of fluorimetric analyses.

Experimental

1-Naphthalenethiol and its 2-isomer (Eastern Organic Chemicals, Inc., Rochester) were purified, respectively, by vacuum distillation and by recrystallization from ethanol. These compounds were very sparingly soluble in water (especially the uncharged molecules). Spectra were taken on solutions $1 \cdot 10^{-5}$ *M* in the appropriate mercaptonaphthalene. Solutions for spectrometric titrations were prepared by pipetting 100 μl of $1 \cdot 10^{-3}$ *M* stock solution of naphthalenethiol in ethanol into a 10-ml volumetric flask and diluting to volume, adjusting the pH with dilute sulfuric acid and sodium hydroxide.

Absorption spectra were taken on a Beckman DB-GT spectrophotometer. Fluorescence spectra were taken on a Perkin-Elmer MPF-2A fluorescence spectrophotometer whose monochromators were calibrated against the xenon line emission spectrum and whose output was corrected for instrumental response by means of a rhodamine-B quantum counter. pH measurements were made on an Orion model 801 pH meter with a Corning silver/silver chloride–glass combination pH electrode. Fluorescence lifetimes were measured with a TRW nanosecond decay time fluorimeter and a Tektronix model 556 dual-beam oscilloscope interfaced with two 1A1 plug-in dual channel amplifiers. Lifetimes as low as 1.6 ns could be measured with this apparatus.

Results and discussion

The absorption and fluorescence maxima as well as the fluorescence lifetimes of the neutral molecules and anions derived from the naphthalenethiols, in aqueous solutions, are presented in Table I. The absorption spectra of the neutral molecules and anions (Fig. 1A) are very close in appearance to those of their

TABLE I

ABSORPTION ($\bar{\nu}1_{L_a}$ AND $\bar{\nu}1_{L_b}$) AND FLUORESCENCE ($\bar{\nu}_f$) SPECTRAL FEATURES OF THE NEU MOLECULES AND ANIONS DERIVED FROM 1- AND 2-NAPHTHALENETHIOL IN AQUEOUS M

	$\bar{\nu}1_{L_a}$ $(\cdot 10^4\ cm^{-1})$	$log\ \varepsilon 1_{L_a}$	$\bar{\nu}1_{L_b}$ $(\cdot 10^4\ cm^{-1})$	$log\ \varepsilon 1_{L_b}$	$\bar{\nu}_f$ $(\cdot 10^4\ cm^{-1})$	τ_f $(10^{-9}$
1-Naphthalenethiol						
Neutral molecule ($H_0 - 1.6$)	3.36	3.74	3.10	3.26	2.76	5.8
Anion (pH 10.0)	3.00	3.85	—[a]	—	2.13	3.9
2-Naphthalenethiol						
Neutral molecule ($H_0 - 1.6$)	3.56	3.36	3.00	2.69	2.79	2.5
Anion (pH 10.0)	3.41	3.68	2.88	2.96	2.15	1.8

[a] The 1_{L_b} band of the 1-naphthalenethiolate anion is hidden under the more intense 1_{L_a} band.

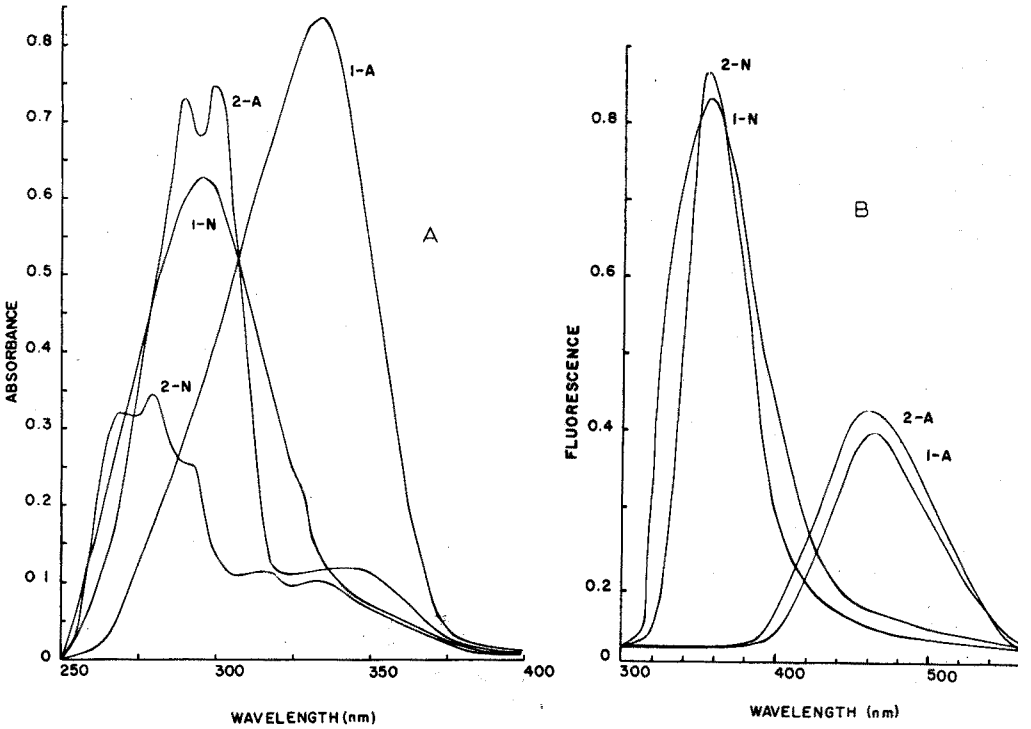

Fig. 1. Electronic absorption spectra (A) and fluorescence spectra (B) of the 1- and 2-naphthalenethiols (1N and 2N) and of their conjugate anions (1A and 2A) in water. (For fluorescence, $\lambda_{exc} = 309$ nm for the 1-isomer and 323 nm for the 2-isomer.)

oxygen counterparts, the naphthols and naphtholates[1], but their main features lie at slightly lower energies. The latter observation is attributable to the higher energy of the sulfur 3*p*-orbital relative to that of the oxygen 2*p*-orbital and thus to the smaller energy gap in the sulfur derivatives, between the lone-pair orbital and the lowest vacant π^* orbital of the aromatic ring.

The fluorescence spectra (Fig. 1 B) of the naphthalenethiolate anions are also shifted to lower frequencies compared to the naphtholate anions. However, unexpectedly, the fluorescence peak of the uncharged 1-naphthalenethiol is shifted to higher frequency than that of 1-naphthol, while that of 2-naphthalenethiol is only slightly lower in frequency than the fluorescence maximum of 2-naphthol[4]. This cannot be attributed to a solvation phenomenon since in n-hexane, chloroform, 1,4-dioxane, acetonitrile, and ethanol, the fluorescence maxima of both mercaptonaphthalene isomers lie at shorter wavelengths than in water. Another example of anomalous behavior in the naphthalenethiols was observed in the pH dependence of the fluorescence spectra (Fig. 2) of both isomers and their conjugate

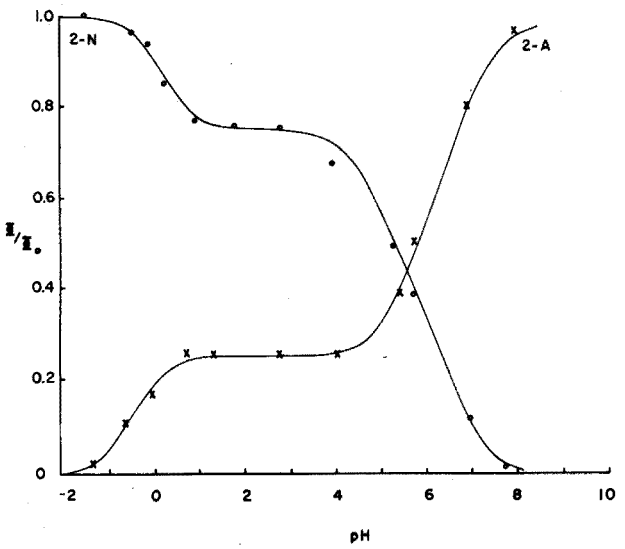

Fig. 2. Variation of the relative quantum yield of fluorescence (Φ/Φ_0) of 2-naphthalenethiol and of its anion, with pH.

anions. The conversions of the fluorescences of the anions to those of the neutral molecules, with decreasing pH, are similar to the fluorimetric titration behavior of the naphthols[1,3] and reflect the similarities between the rates of fluorescence and excited singlet state proton exchange in these excited species. Weller[1] has shown that under these circumstances the relative quantum yields of fluorescence of the conjugate acids (Φ/Φ_0) and those of the conjugate bases (Φ'/Φ'_0) are given, respectively, by

$$\frac{\Phi}{\Phi_0} = \frac{1+\tilde{k}\tau'_0[\mathrm{H}^+]}{1+\vec{k}\tau_0+\bar{k}\tau'_0[\mathrm{H}^+]} \tag{1}$$

and

$$\frac{\Phi'}{\Phi'_0} = \frac{\vec{k}\tau_0}{1+\vec{k}\tau_0+\overleftarrow{k}\tau'_0[H^+]} \tag{2}$$

where $\vec{k}$ and $\overleftarrow{k}$ are the rate constants for dissociation and protonation, respectively, in the lowest excited singlet state, τ_0 and τ'_0 are the lifetimes of excited acid and conjugate base, respectively, in the absence of bimolecular deactivating processes (*i.e.*, at very low pH and at very high pH, respectively), and $[H^+]$ is the hydrogen ion activity as given by antilog $(-H_0)$ in concentrated acid. Above pH 3, $\overleftarrow{k}\tau'_0[H^+]$ invariably becomes smaller than 1 so that eqns. (1) and (2) reduce to

$$\frac{\Phi}{\Phi_{0\,\mathrm{const}}} = \frac{1}{1+\vec{k}\tau_0} \tag{3}$$

and

$$\frac{\Phi'}{\Phi'_{0\,\mathrm{const}}} = \frac{\vec{k}\tau_0}{1+\vec{k}\tau_0} \tag{4}$$

which are independent of pH and therefore represent the flat regions of the fluorimetric titration curves in Fig. 2. From eqn. (3) or (4), $\vec{k}$ may be immediately calculated if τ_0 is known. Then, with knowledge of $\vec{k}$, τ_0 and τ'_0 several points in the low pH inflection region (Fig. 2) in the plot of Φ/Φ_0 or Φ'/Φ'_0 *vs.* pH may be used to calculate $\overleftarrow{k}$. Moreover, from the kinetic definition of equilibrium we have

$$\frac{\vec{k}}{\overleftarrow{k}} = K_a^* \tag{5}$$

or

$$-\log\frac{\vec{k}}{\overleftarrow{k}} = pK_a^* \tag{6}$$

The pK_a^* values of the naphthalenethiols determined from the fluorimetric titrations are similar to those of the naphthols and are considerably less negative than expected on the basis of the lower electronegativity of sulfur relative to oxygen which should result in greater charge transfer from the sulfur atom to the aromatic ring than from the oxygen atom to the aromatic ring, upon excitation. This hypothesis is supported by Förster cycle[5] calculations employing the ground-state pK_a values of the naphthalenethiols and the shifts in absorption and fluorescence spectra accompanying dissociation. These calculations indicate that the naphthalenethiols should be some 8–11 orders of magnitude more acidic in the excited state than in the ground state (Table II) rather than 5 orders of magnitude more acidic in the excited state as indicated by the fluorometric titrations. Large discrepancies between pK_a^* values obtained by fluorimetric titrimetry and by calculations based upon spectral shifts accompanying dissociation are usually the result of inadequacy of the calculation based upon spectral shifts, arising from lack of thermal[6] or electronic[4,7] correspondence between the species involved in each electronic transition.

These observations suggest the following explanation for the anomalously

TABLE II

DISSOCIATION ($\vec{k}$) AND PROTONATION ($\overleftarrow{k}$) RATE CONSTANTS OF THE EXCITED NAPHTHALENETHIOLS AND THEIR ANIONS AND EQUILIBRIUM CONSTANTS OF THE CORRESPONDING EQUILIBRIA

(Equilibrium constants calculated from the rate constants (pK^*_{kin}), the shifts of the absorption spectra (pK^*_{abs}), the shifts of the fluorescence spectra (pK^*_{flu}) and the shifts in the averages of absorption and fluorescence spectra (pK^*_{av})).

	pK_a	$\vec{k}(s^{-1})$	$\overleftarrow{k}(M^{-1}\,s^{-1})$	pK^*_{kin}	pK^*_{abs}	pK^*_{flu}	pK^*_{av}
1-Naphthalenethiol	6.51	$4.9 \cdot 10^7$	$6.5 \cdot 10^8$	1.1	−1.1	−6.7	−3.9
2-Naphthalenethiol	6.23	$1.2 \cdot 10^8$	$1.8 \cdot 10^9$	1.2	3.7	−7.2	−1.8

high frequencies of fluorescence of the uncharged naphthalenethiols and their small excited state dissociation constants. After promotion of a $3p$-electron from sulfur to the lowest unoccupied π^*-orbital of the aromatic ring, in the uncharged naphthalenethiols, the –SH group rehybridizes from the ground-state sp^3 configuration to the excited state sp^2 configuration providing optimal geometry for overlap of the $3pz$ donor orbital of the sulfur atom with the π-system of the aromatic ring. However, in this configuration the $3dz^2$-orbital of sulfur which is an acceptor orbital, also has optimal geometry to withdraw charge from the aromatic system. The tendency of the $3dz^2$-orbital of sulfur to withdraw charge from the aromatic system depends upon the degree of positive charge at the sulfur atom. In the uncharged, excited thiol the combination of the presence of the proton on the mercapto group and the loss of charge from the $3pz$-orbital resulting from excitation likely provides the driving force for the withdrawal of charge into the $3dz$-orbital of sulfur. Clearly this phenomenon is less probable in the thiolate anions because of the absence of the positively polarizing proton. The withdrawal of charge by the $3dz^2$-orbital of the excited thiol partially offsets the donation of charge from the $3pz$-orbital reducing the charge-transfer quality of the lowest excited singlet state and thereby shifting the emission from the latter state to higher energy. In the naphthols no such back-donation is possible because of the absence of low-lying d-orbitals on oxygen, hence only the donation from the $2pz$-orbital of oxygen affects the spectra of these compounds. Back donation of charge to the $3dz$-orbital also diminishes the excited state acidities of the naphthalenethiols because of the increased charge density in the region of the S–H bond. However, in the anions this effect is not prevalent and the proton affinities of the excited anions would be expected to be lower than in the corresponding naphtholate anions because of the lower electronegativity of sulfur. This is borne out in the rate constants of excited state dissociation of the neutral naphthalenethiols which are comparable to those of the excited naphthols and in the rate constants of protonation of the excited naphthalenethiolate anions which are substantially lower than those of the corresponding rate constants for the excited naphtholate anions.

REFERENCES

1 A. Weller, *Z. Elektrochem.*, 56 (1952) 662.

2 N. Trieff and B. Sundheim, *J. Phys. Chem.*, 69 (1969) 2044.
3 J. L. Rosenberg and I. Brinn, *J. Phys. Chem.*, 76 (1972) 3558.
4 S. G. Schulman, *Spectrosc. Lett.*, 6 (1973) 197.
5 T. Förster, *Z. Elektrochem.*, 54 (1950) 42.
6 P. J. Kovi and S. G. Schulman, *Anal. Chim. Acta*, 63 (1973) 39.

Analytica Chimica Acta, 73 (1974) 191–193

SHORT COMMUNICATION

Fluorescence reactions of eriochrome red B with metals

Part I. Detection of Be, Mg, Al, In, Ga and Zn*

C. PÉREZ CONDE, J. A. PÉREZ-BUSTAMANTE and F. BURRIEL MARTÍ

Departamento de Química Analítica, Facultad de Ciencias y C.S.I.C., Universidad Complutense, Ciudad Universitaria, Madrid-3 (Spain)

(Received 25th March 1974)

Eriochrome red B, the sodium salt of 3-hydroxy-4-[(5-hydroxy-3-methyl-1-phenyl-4-pyrazolyl)-azo]-naphthalene-1-sulfonic acid, has found few analytical applications; cobalt can be determined spectrophotometrically[1], aluminium fluorimetrically[2] and fluoride by indirect fluorimetry[3,4]. In a search for possible new fluorescence reagents among a considerable number of azo dyestuffs, eriochrome red B was found to be useful for the sensitive identification of several elements. In this communication, some preliminary results are reported.

Experimental

Reagents and apparatus. Eriochrome red B solutions (0.1% w/v) were prepared by dissolving the dye (Schuchardt) in (1 + 1) water–ethanol. These solutions remained stable for a few months, and then precipitated in a gelatinous form with decolorization. Stock 0.01 *M* metal solutions were prepared from the corresponding nitrates (p.a. Merck or C. Erba).

"Schleicher & Schüll" Nr. 589 blue-ribbon filter paper was found to possess the lowest blank fluorescence of the papers tested. Self-filling micropipettes (5–50 μl, "ring-oven" type) were prepared from 0.1–0.25 mm internal diameter glass rods.

Procedure. One drop of buffer, acid or base solution was placed at the center of a filter paper followed by one drop each of eriochrome red B reagent and the particular metal cation. The filter paper was then dried with a hot hairdrier and immediately observed under a u.v. lamp (Mineralight UVSL 15). The papers were observed at intervals (1–5, 24, 48 h) so as to detect any fluorescence variations, delayed fluorescence phenomena, etc. Initially, 0.01 *M* metal ion solutions were used; if positive fluorescence (immediate and/or delayed) reactions were obtained, limits of detection were established by dilution in the usual way.

The reaction media tested were 1 *M* hydrochloric acid, 1 *M* sodium hydroxide, 2.5 *M* hexamine (pH 8–9) and acetic acid–sodium acetate buffer (pH 5), so that the effect of pH on the selectivity of the fluorescence could be studied.

* Communication presented at the XVI Biennial Meeting of the Spanish Royal Chemical Society, Oviedo, September, 1973.

TABLE I

FLUORESCENCE REACTIONS OF ERIOCHROME RED B WITH METAL IONS

Metal ion	*Hexamine (pH 8–9)*		*Acetate (pH ~ 5)*		*1 M HCl*		*1 M NaOH*	
	Colour	*Limit*[a]	*Colour*	*Limit*	*Colour*	*Limit*	*Colour*	*Limit*
Be(II)	light yellow	0.09	—	—	—	—	—	—
Mg(II)	yellow	0.03	yellow	1.2[b]	—	—	yellow	0.06
Al(III)	orange	0.07	orange	0.3[b]	—	—[b]	orange	—
Ga(III)	red	5.0[c]	orange	~1	orange	1.3[b]	orange	—
In(III)	orange	5.0[c]	yellow	1.3	orange	0.6[b]	yellow	—
Zn(II)	red	0.02	yellow	(±)[d]	orange	—[b]	orange	0.03

[a] The absolute limit of detection expressed in μg is given in all cases.
[b] Delayed fluorescence phenomena were observed (⩾24 h); the widely variable characteristics made it difficult or impossible to estimate sensitivity.
[c] A very drastic decrease of the otherwise excellent fluorescence characteristics was observed on moderate dilution of the 10^{-2} *M* metal ion solutions.
[d] Strong instantaneous fluorescence was observed for 10^{-2} *M* Zn(II) solutions; the fluorescence reaction was delayed as the metal concentration was decreased. With 10^{-3}–10^{-4} *M* solutions, the fluorescence intensity increased continuously with time.

Results and discussion

Of the many elements tested, only Be, Mg, Al, In, Ga and Zn produced satisfactory fluorescence phenomena. The results obtained are summarized in Table I, where media, fluorescence colours, absolute detection limits and some particular features of certain reactions are given. Neither thallium(I) nor thallium(III) gave any fluorescence in any of the media investigated.

The hexamine medium provided the least selectivity, but usually the best sensitivity, of all the investigated media. Curiously, Ga(III) and In(III) gave excellent fluorescence reactions at high concentration levels (10^{-2} *M*), but suddenly on moderate dilution failed to give any fluorescence at all. The detection limits for these reactions are thus poorer by factors of 50–150 than the remaining limits. In acetate medium (pH 5), Be(II) showed no fluorescence reaction, while the reactions of Mg(II) and Al(III) were considerably less sensitive than in hexamine buffer. However, In(III) and Ga(III) gave more sensitive reactions (by a factor of about 5) than in hexamine.

In 1 *M* hydrochloric acid medium, the fluorescent reaction was selective for In(III) and Ga(III), the sensitivity being similar to that in the acetate medium. In 1 *M* sodium hydroxide, only Mg(II) and Zn(II) fluoresced, the sensitivities being similar to those in hexamine buffer. Beryllium(II) provided a fluorescent reaction only in hexamine medium. On the basis of these results, eriochrome red B appears promising for qualitative identification and possibly for some sensitive determinations. Preliminary attempts to improve the selectivity of the Al(III), Be(II) and Mg(II) reactions in hexamine medium by masking agents (EDTA, tartaric acid, triethanolamine, sulfosalicylic acid and fluoride) have proved unsatisfactory. Extractive separation processes are now being studied in order to work out suitable fluorimetric methods of determination for these elements.

REFERENCES

1 *Fluka Katalog*, (1973) 9, Fluka A.G., Buchs, Switzerland.
2 G. Hocman, *Acta Fac. Rerum Natur. Univ. Comeniane, Chim.*, 13 (1968) 75.
3 G. Hocman, L. Lacko and L. Hegedus, *Acta Fac. Rerum Natur. Univ. Comeniane, Chim.*, 13 (1968) 71.
4 W. A. Powell and J. H. Saylor, *Anal. Chem.*, 25 (1953) 960.

Analytica Chimica Acta, 73 (1974) 194–197

SHORT COMMUNICATION

High-pressure liquid chromatography for monitoring benzo(a)pyrene contents of cigerette smoke condensate fractions*

D. B. WALTERS, W. J. CHAMBERLAIN, M. E. SNOOK and O. T. CHORTYK
Richard B. Russell Agricultural Research Center, ARS, USDA, Athens, Georgia 30604 (U.S.A.)
(Received 14th March 1974)

Use of high-speed liquid chromatography (h.p.l.c.) and spectrophotofluorimetry has, for the first time, made possible the direct determination of benzo(a)pyrene in separate cigarette smoke condensate (CSC) fractions.

This method has several advantages over existing methods[1–5] for benzo(a)pyrene: it is faster (2 h) than other procedures (about 8 h for the standard t.l.c. procedure[1]); h.p.l.c. separates benzo(a)pyrene from extraneous material in the sample, eliminating cleanup procedures, and provides good resolution between benzo(a)pyrene and the benzo(e)pyrene isomer, a serious problem with other methods; the fluorimetric detection system is inherently more sensitive than the u.v. detector system in the h.p.l.c. and improves the lower limits for the method by a factor of 10 or better[6]; recovery is good (91%), compared with 60% recovery by the standard t.l.c. method; this method is simple, routine, and nondestructive.

This method for benzo(a)pyrene determination resulted from this laboratory's interest in the biological activities of fractions of CSC[7]. The CSC fractionation scheme used by this laboratory (Fig. 1) has evolved over the last 8 years in an effort to isolate and identify active CSC constituents. The determination of benzo(a)pyrene contents of CSC fractions has been used to follow the distribution of total polycyclic aromatic hydrocarbons in CSC fractions. The procedure described here provides a simple determination of benzo(a)pyrene in each fraction and, hence, substantiates the efficiency and completeness of the fractionation scheme.

Experimental

Cigarette smoke condensate (1.0-kg quantities) was prepared, fractionated and subjected to bioassay studies under conditions previously described[7].

A DuPont Model 820 liquid chromatograph equipped with a u.v. detector (254 nm) and a DuPont ODS (octadecylsilane) column (2 mm × 1 m) were used at 60°C. The liquid phase was degassed methanol–water (60–40 v/v) pumped at 1.0 ml min^{-1}, with a pressure of 1500 p.s.i. An Aminco Bowman ratio spectrophotofluorimeter was used to measure the emission maxima (405 nm) of benzo(a)pyrene with an excitation wavelength of 294 nm.

* Presented in part at the 25th Southeast Regional American Chemical Society Meeting, Charleston, S.C., November 1973.

Methanol, benzene (Mallinckrodt-nanograde), and water (glass-distilled) were used. Reagent-grade benzo(a)pyrene (K and K) was sublimed before use.

Samples (1 g) were dissolved in 1 ml of benzene and 5-μl aliquots were injected into the liquid chromatograph. Because of different relative concentrations of benzo(a)pyrene in different samples, different numbers of injections were needed to collect sufficient material for analysis. Cigarette smoke condensate solutions were injected 5 times; TN, 3 times; F-20 and F-55, once each. For each sample, the effluent corresponding to the retention time of benzo(a)pyrene was collected. The solvent was removed on a rotary evaporator and the benzo(a)pyrene-enriched sample was redissolved in 50 μl of benzene. The enriched samples (5 μl) were reinjected into the chromatograph, the corresponding effluent was collected, and the benzo(a)pyrene concentration was determined by standard fluorimetric procedures, from calibration curves prepared from standard benzo(a)pyrene solutions (0.04–0.70 μg benzo(a)-pyrene ml^{-1} solution).

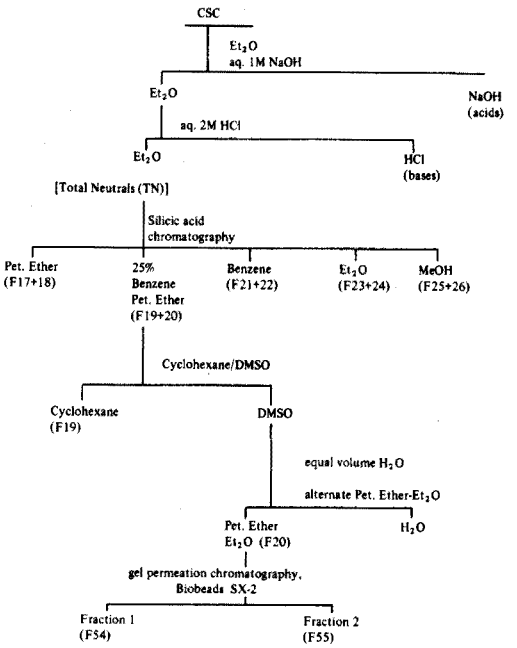

Fig. 1. Fractionation of cigarette smoke condensate.

Results and discussion

The CSC fractionation scheme (Fig. 1) has been previously described[7,8]. Several of the carcinogenic polycyclic aromatic hydrocarbons, including benzo(a)-pyrene, are known constituents of CSC[9]. It was shown that polycyclic aromatic hydrocarbons are concentrated in the following fractions: CSC, TN, F-20 and F-55[10]. Their distribution in the fractionation scheme can be correlated to that of benzo(a)pyrene, a representative compound.

Figure 2 shows the h.p.l.c.-results from a 5-μl injection of a saturated solution (60–40 v/v methanol–water) of benzo(a)pyrene; under the conditions described,

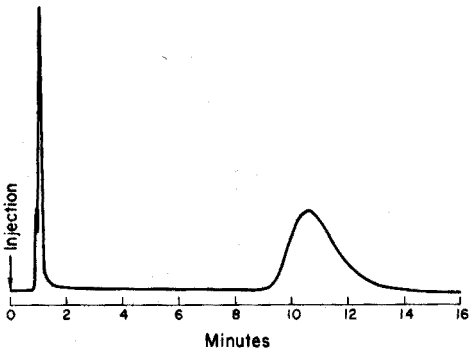

Fig. 2. High-pressure liquid chromatogram of benzo(a)pyrene standard (5 μl).

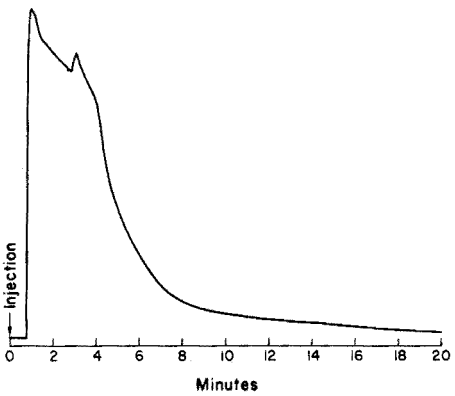

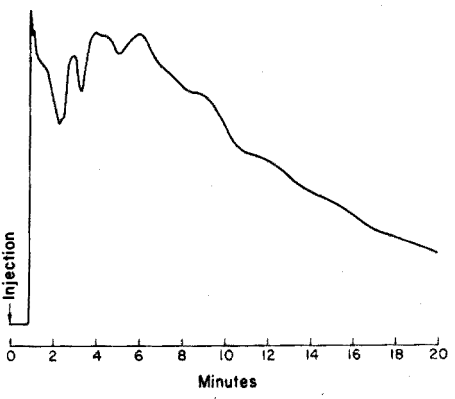

Fig. 3. High-pressure liquid chromatogram of cigarette smoke condensate (5 μl).
Fig. 4. High-pressure liquid chromatogram of fraction F-55 (5 μl).

benzo(a)pyrene has a retention time of 9–13 min. Figures 3 and 4 show chromatograms resulting from the direct injection of CSC and F-55, respectively. Similar chromatograms resulted for all fractions studied. Effluents were collected for the benzo(a)pyrene retention-time interval and analyzed by fluorimetry.

TABLE I

BENZO(A)PYRENE FOUND IN CIGARETTE SMOKE CONDENSATE FRACTIONS

Sample	*BaP found*[a] *(mg)*	*% of Total BaP*
CSC	3.50	100.0
TN	3.44	98.3
F-19	0.04	1.1
F-20	3.41	97.5
F-21+22	0.04	1.1
F-54	0.07	2.0
F-55	3.19	91.2

[a] Average of three determinations.

Table I shows the concentration of benzo(a)pyrene determined. As expected from a scheme based on liquid–liquid extraction and column chromatography, the quantities of benzo(a)pyrene found in adjacent fractions (F-19, F-21 + 22, and F-54) were insignificant. Initially, 3.50 mg (3.5 p.p.m.) of benzo(a)pyrene per kg of CSC was found in the original condensate. After fractionation, 3.19 mg (23.6 p.p.m.) was found in F-55 (0.135 g), which shows a recovery of 91% of the initial benzo(a)pyrene and accomplishes the primary objective of this scheme, *i.e.*, considerable concentration in a single fraction.

The amount of benzo(a)pyrene (3.50 mg) found in this sample of CSC is in good agreement with literature values[1]. Reproducibility of the method, based on triplicate determinations, was within 5%. Percentage recovery, based on samples spiked with known amounts of benzo(a)pyrene, ranged from 93 to 101%. Future plans include direct interfacing of the h.p.l.c. with the fluorimeter by means of a microflow cell.

The authors thank Mr. Howard K. Davenport for technical assistance.

REFERENCES

1 I. Schmeltz, R. L. Stedman and W. J. Chamberlain, *Anal. Chem.*, 36 (1964) 2499.
2 H. Markemeyer, *Beitr. Tabakforsch.*, 1 (1962) 325.
3 D. Hoffman and E. L. Wynder, *Anal. Chem.*, 32 (1960) 295.
4 R. L. Cooper, *Analyst (London)*, 79 (1954) 573.
5 E. Sawicki, *Chemist-Analyst*, 53 (1964) 24.
6 D. A. Skoog and D. M. West, *Principles of Instrumental Analysis*, Holt, Reinhart and Winston, New York, 1971, p. 222.
7 A. P. Swain, J. E. Cooper and R. L. Stedman, *Cancer Res.*, 29 (1969) 579.
8 A. P. Swain, F. G. Bock, J. E. Cooper, W. J. Chamberlain, E. D. Strange, L. Lakritz, R. L. Stedman and I. Schmeltz, *Beitr. Tabakforsch.*, 7 (1973) 1.
9 R. L. Stedman, *Chem. Rev.*, 68 (1968) 153.
10 W. J. Chamberlain, manuscript in preparation.

Analytica Chimica Acta, 73 (1974) 198–203

SHORT COMMUNICATION

The determination of water in a strong base anion-exchange resin by Karl Fischer titration

P. VAN ACKER*, F. DE CORTE** and J. HOSTE

Institute for Nuclear Sciences, Rijksuniversiteit Gent, Proeftuinstraat 86, B-9000 Gent (Belgium)

(Received 18th April 1974)

Little attention seems to have been paid to the accurate determination of the water content in anion-exchange resins by Karl Fischer titration, although this information is certainly important for the study of anion exchange in non-aqueous media. In the direct Karl Fischer titration of the water present in a strong base anion-exchange resin in the chloride form (RCl), which is suspended in methanol, there is interference from the exchange between the chloride and the iodide, formed by the reaction of water with the Karl Fischer reagent. Because of the greater affinity of the iodide for the functional groups of the resin, the latter is transformed into the iodide-form (RI). Furthermore, the resin can then take up several iodine molecules[1]. These interferences can be written as:

$$I_2+SO_2+H_2O \rightarrow 2\,HI+SO_3;\ RCl+HI \rightarrow RI+HCl;\ RI+nI_2 \rightarrow RI_{2n+1} \quad (1)$$

As a result of these reactions no stable endpoint can be reached, and an accurate direct titration is impossible.

This paper describes a method for the determination of water in Dowex 1-X8 (chloride form), based on the water distribution between the resin and a water–acetic acid mixture of known composition.

On the basis of these distribution data, with the aid of the solvent uptake properties of the exchanger, a simple Karl Fischer titration of the water–acetic acid mixture, equilibrated with the resin and after separation from it, is sufficient to calculate the water content of the exchanger.

Expression for the calculation of the water content

When an amount (g' in g) of wet resin, with an unknown water content x (% H_2O as referred to the dry weight g) is equilibrated with a volume V (ml) of an acetic acid–water mixture, having an initial water concentration of C_0 (μg ml^{-1}), the total quantity of water (expressed in g) introduced in the system can be written as:

$$10^{-6}C_0V + \frac{xg'}{(100+x)} \quad (2)$$

* Research associate of the I.I.K.W.

** Research associate of the N.F.W.O.

After equilibration, this quantity can be expressed as:

$$10^{-6} C_e \left[V + \frac{xg'}{(100+x)d_{H_2O}} - \frac{\beta g' 100}{d_i(100+x)} \right] + C_i 10^{-6} \frac{\beta g'}{d_i} \frac{100}{(100+x)} \quad (3)$$

where

C_e = water content of the external solution at equilibrium (μg ml^{-1}),
C_i = water concentration inside the resin beads at equilibrium (μg ml^{-1}),
d_{H_2O} = density of water (g ml^{-1}),
d_i = density of the internal acetic acid–water mixture, sorbed by the resin beads (g ml^{-1}),
β = solvent uptake by the resin in the given experimental conditions (g solvent/g dry resin)

$$= \beta' \left(1 + \frac{x}{100} \right) \text{ with } \beta' = \text{g solvent/g wet resin.}$$

In eqn. (3) the first term stands for the amount of water present in the external solution, and the second term for that present inside the resin beads.

As the expressions from eqns. (2) and (3) are equal, one obtains after rearrangement:

$$x = \frac{10^{-4} C_e [V(1 - C_0/C_e) + \beta g'/d_i (C_i/C_e - 1)]}{g'(1 - 10^{-6} C_e/d_{H_2O}) + 10^{-6} C_e V (C_0/C_e - 1)} \quad (4)$$

From eqn. (4) it follows that the water content x of the resin can be calculated from C_0 and C_e (obtained by titration of the acetic acid–water mixture before and after equilibration with the resin), i the following quantities are known: (1) C_i/C_e, *i.e.* the ratio of internal to external water concentration as a function of C_e; and (2) the solvent uptake β or β/d_i (ml solvent/g dry resin). These parameters can be calculated from the experimentally accessible value of β' (solvent uptake per g of wet resin), only if the water content of the resin, x, and the C_i/C_e values are known. It will thus only be possible to determine β or β/d_i by an iteration method.

Determination of C_i/C_e and β

The internal density (d_i) of the sorbed acetic acid–water mixture, can be found if the internal composition, C_i, of the sorbed solution is known. C_e being determined by Karl Fischer titration, this problem can thus be converted to the determination of C_i/C_e.

It should be mentioned that as an approximation in this reasoning, the sorbed solution is considered as being uniform, and that electrostriction phenomena from hydration and solvation effects are not taken into account.

The C_i/C_e values can be determined by acetic acid titration before and after equilibration with the resin, as described earlier for a resin in the acetate form[2]. The internal and external acetic acid molarities obtained can easily be converted into C_i and C_e values, respectively. However, because of the conversion of molarities to water concentrations, this method can only give accurate results for water–acetic acid mixtures down to *ca.* 10% water ($C_e = 10^5$ μg H_2O ml^{-1}).

For lower C_e values, a method of successive approximations was used.

If for low C_e values (where V is kept relatively high), the right term

$$\left[\frac{\beta g'}{d_i}(C_i/C_e - 1)\right]$$

of the denominator in eqn. (4) is neglected, a first approximation of x values (x_1) is obtained. For the other C_e values, the corresponding $(C_i/C_e)_1$ values can be calculated from:

$$\frac{C_i}{C_e} = 1 + \frac{d_i}{\beta}\left[\frac{V}{g'}\left(\frac{C_0}{C_e} - 1\right)\left(1 + \frac{x}{100}\right) + \frac{x}{100}\left(\frac{10^6}{C_e} - \frac{1}{d_{H_2O}}\right)\right] \quad (5)$$

where $\beta_1 = \beta'(1 + x_1/100)$ and $(d_i)_1$ is replaced by d_e, the density of the external acetic acid–water mixture, for which the composition is known by determination of C_e. From this $(C_i/C_e)_1$ value and the corresponding composition of solvent inside the resin, $(C_i)_1$, a new value of $(d_i)_1$ can be found, thus allowing a second calculation of $(C_i/C_e)_1$ ratios. This procedure can be continued, resulting in converging values of $(C_i/C_e)_1$. From the plot of this series of $(C_i/C_e)_1$ values as a function of C_e, it is possible to find graphically the $(C_i/C_e)_1$ values at the original low C_e values, thus allowing a second approximation of x values (x_2) according to eqn. (4). Thus a new set of $(C_i/C_e)_2$ values can be computed, with allowance for $\beta_2 = \beta'(1 + x_2/100)$, and for conversion of the new $(d_i)_2$ values. This double iteration procedure can be repeated, resulting in converging x_i, $(C_i/C_e)_i$ and β_i values.

Experimental

Apparatus and reagents. A dry-atmosphere glove box (*ca.* 20 mg H_2O m^{-3}), especially designed for the study of ion exchange in non-aqueous media[3], was used, with an automatic Beckmann KF4 aquameter titrator. The Karl-Fischer stabilized single-solution (Beckman aquameter reagent) was standardized with sodium tartrate dihydrate. Methanol and pyridine for Karl Fischer titrations (water contents $\leqslant 0.01\%$) were used.

Acetic acid with a water content $\leqslant 50$ μg ml^{-1} was prepared by refluxing[4] acetic acid (water content = 0.5%), for 5 h with chromium trioxide and acetic acid anhydride, followed by fractional distillation under high-purity nitrogen. The dehydrated acetic acid was pumped, without air contact, from the receiving flask into a storage vessel in the glove box. The minimal water content of the acetic acid was 33 μg ml^{-1}. Acetic acid of higher water content was prepared by addition of known quantities of water to the distilled acetic acid. The water content in acetic acid was determined by Karl Fischer titrations in (1 + 1) methanol–pyridine media.

The resin used was the strong base anion exchanger Dowex 1-X8 (100–200 mesh) in the chloride form. It was purified by column conditioning with sodium hydroxide and hydrochloric acid[5]. The resin bed was finally conditioned with glacial acetic acid, followed by thorough rinsing with hydrochloric acid and water, and drying *in vacuo* over phosphorus pentoxide for 14 days. The dried resin was stored in a stoppered 20-cm^3 glass tube, after shaking so as to obtain a uniform water content. All manipulations with the dried resin, and with the acetic acid solvents of low water content were performed in the glove box.

Procedure for the determination of β and C_i/C_e values as a function of C_e. For the determination of β and C_i/C_e values at $C_e \geq 9\%$, the procedure was analogous to that described earlier[2]; the external and internal acetic acid molarities were converted to water concentrations. Below $C_e = 9\%$, weighed quantities of resin were transferred to 100-ml Erlenmeyer flasks and shaken with known volumes of acetic acid–water mixtures. After equilibration, the resin was filtered off and the solvent uptake (β') was evaluated[2]. The water contents of the original acetic acid–water mixture (C_0) and of the filtrate (C_e) were determined by Karl Fischer titration. Two different resin batches were used, originating from two different conditioning and drying procedures. All experiments were performed at 25°C.

Results and discussion

The results of the determinations of β', C_e and C_0 in Dowex 1-X8, 100–200 mesh, chloride form, are summarized in Table I.

Figures 1 and 2 show the final curves C_i/C_e *versus* C_e, and β *versus* C_e obtained from the double iteration procedure described. The points at C_e values of 139, 158, 224, 268 and 65, 190, 432 μg ml^{-1} were taken as reference for the calculation of the x_1 values. The C_i/C_e values, computed from the internal and external acetic acid molarities, are also presented. Figure 1 shows that the results obtained by acid–base titration are in good agreement with those calculated from the water titrations; and there is no systematic deviation between the results for

TABLE I

EXPERIMENTAL CONDITIONS AND RESULTS

Resin batch	*g' Wet resin weight (g)*	*V Volume HAc–H_2O mixture (ml)*	*β' Solvent uptake (g g^{-1} wet resin)*	*C_0 μg H_2O ml^{-1}*	*C_e μg H_2O ml^{-1}*
1	0.7083	20	0.716	33	268
	0.7841	30	0.716	33	224
	0.5222	40	0.716	33	139
	0.8648	50	0.716	33	158
	0.8480	10	0.716	588	1002
	0.8172	6	0.716	1047	1590
	0.6222	4	0.716	2818	2927
	1.2750	10	0.718	6371	5864
	0.8707	4	0.723	17810	14046
	0.9320	4	0.729	32940	25340
	0.8493	4	0.736	52236	41956
	0.7860	4	0.745	83849	70810
	0.6731	4	0.747	88617	78301
	0.6328	6	0.749	95252	89052
2	0.3284	30	0.716	33	65
	0.5263	30	0.716	139	190
	0.5775	30	0.716	384	432
	0.7018	6	0.717	4991	4355
	0.7695	4	0.721	13690	10730
	1.0028	4	0.727	27296	20029

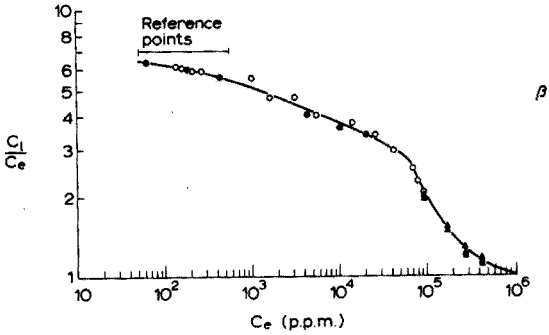

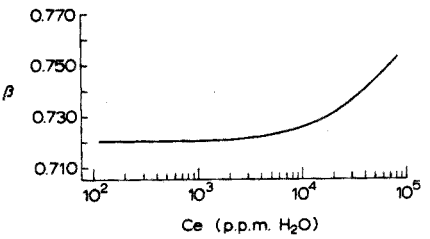

Fig. 1. C_i/C_e as a function of C_e for Dowex 1-X8; (○) Karl Fischer titration ($x=0.80\%$), (●) Karl Fischer titration ($x=0.35\%$), (▲) HAc titration.

Fig. 2. β (g of solvent per g of dry resin) as a function of C_e (Dowex 1-X8).

the two resin batches. The following water contents were found: for resin batch 1, $0.80\pm0.02\%$; for resin batch 2, $0.35\pm0.04\%$ (standard deviation on the mean). These values were obtained after four iteration steps.

The water contents of the two resin batches were also calculated from the data of Table I by converting C_0 to mg of water added per g of wet resin (δ). The apparent x values were then calculated from eqn. (4), with $C_0=0$. The results of this standard addition method are given in Fig. 3, x *versus* δ showing a linear relationship. Regression analysis proved that the slopes had the same value (0.107) for both resin batches. From Fig. 3 the water contents were evaluated (for $\delta=0$) as $0.78\pm0.02\%$ for resin batch 1 and $0.30\pm0.01\%$ for resin batch 2 (standard deviation on the mean). These values are, within experimental error, in good agreement with those obtained from the iteration procedure. It should be mentioned that, as expected from the form of eqn. 4, the results at high C_e ($>10^4$ μg H_2O ml^{-1}) could not be used to calculate the water content, as small errors in one of the parameters of eqn. (4) cause large deviations in x values. This had already been noted during the iteration procedure, where it was found that C_i/C_e at high C_e values did not change appreciably during successive approximations.

In conclusion, the distribution and solvent uptake data of Figs. 1 and 2, and with a knowledge of d_i, make it possible to calculate the water content of the

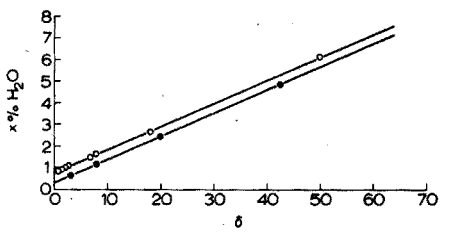

Fig. 3. Determination of x by the standard addition method. $x\%$ H_2O is given per g of dry resin. δ is the amount of water added in mg per g of wet resin. (○) Resin batch 1, $x=0.107$ $\delta+0.78$; (●) Resin batch 2, $x=0.107$ $\delta+0.30$.

strong base anion-exchanger Dowex 1-X8, 100–200 mesh, Cl^- form, from eqn. (4) after a simple Karl Fischer titration of an acetic acid–water mixture before and after equilibration with the resin. Obviously, depending on the expected water content x, determinations should be done under the optimal conditions of C_0, g' and V, so as to obtain the best precision; thus C_0/C_e, C_i/C_e and $10^{-6}\ C_e/d_{H_2O}$ should differ as much as possible from unity, *i.e.* C_e should be low ($<10^4$ μg H_2O ml^{-1}). Finally, if the two addition terms in the nominator and denominator are of opposite sign, care should be taken to ensure a reasonable spread on their respective absolute values.

Grateful acknowledgement is made to the Interuniversitair Instituut voor Kernwetenschappen and the Nationaal Fonds voor Wetenschappelijk Ohderzoek for financial support.

REFERENCES

1 B. Trémillon, *Les séparations par les résines échangeuses d'ions*, Gauthier-Villars, Paris, 1965, p. 116.
2 F. De Corte and J. Hoste, *J. Inorg. Nucl. Chem.*, 35 (1973) 2043.
3 F. De Corte, P. Van Acker and J. Hoste, to be published.
4 I. Gyenes, *Titration in non-aqueous media*, Akademiai Kiado, Budapest, 1967, p. 141.
5 W. Rieman III and H. F. Walton, *Ion exchange in Analytical Chemistry*, Pergamon, Oxford, 1970.

Analytica Chimica Acta, 73 (1974) 204–208

SHORT COMMUNICATION

A rapid and sensitive method for determination of submicrogram amounts of ammonia in fresh and sea waters

KATSUHIKO MATSUNAGA and MASAKICHI NISHIMURA
Department of Chemistry, Faculty of Fisheries, Hokkaido University, Hakodate 040 (Japan)
(Received 12th March 1974)

Although the indophenol method has been widely used for determination of ammonia in natural waters[1–4], the method is time-consuming and the sensitivity is rather low. A more rapid and sensitive method is required for traces of ammonia in natural waters, especially for continuous or automated analysis.

Richards and Kletsch[5] described an oxidation method, in which ammonia is oxidized to nitrite by hypochlorite in the presence of bromide ion, and then the nitrite is determined by spectrophotometry with sulfanilamide and N-1-naphthylethylenediamine. Strickland and Parsons[6], and recently Truesdale[7] reported modifications. Those oxidation methods are the best for sensitivity, but they have a disadvantage that some amino acids are determined together with the ammonia.

In this paper, the authors present a modified Richards and Kletsch method in which the oxidation time is reduced to 1 min from 17 min in Truesdale's method or 3.5 h in Strickland and Parsons' method. Moreover, the shortening of the oxidation time results in the elimination of the interference of coexisting amino acids.

Reagents

Deionized water. Remove the ammonia from distilled water by passing it through cation-exchange resin in the hydrogen form, if necessary.

Potassium bromide, 7% solution. Dissolve 35 g of potassium bromide in 500 ml of 2.5 *M* sodium hydroxide.

Sodium hypochlorite solution, 0.2 M. The concentration was determined by iodimetry. If the solution is stored in an amber bottle, the solution is stable for at least a week at room temperature.

Arsenite solution. Dissolve 1 g of arsenious oxide and 0.5 g of sodium hydroxide in 50 ml of water, and dilute to 500 ml with water.

Sulfanilamide solution. Dissolve 1 g of sulfanilamide in 100 ml of 3.5 *M* hydrochloric acid. This is stable for many months.

N-1-naphthylethylenediamine solution. Dissolve 0.1 g of N-1-naphthylethylenediamine dihydrochloride in 100 ml of water. Store the solution in an amber bottle. It is stable for a month.

Oxidizing solution. Add 5 ml of 0.2 *M* sodium hypochlorite solution to

50 ml of the potassium bromide solution. If the solution is stored in an amber bottle, it is stable for one hour at room temperature.

Procedure

Take 25 ml of a fresh or sea water sample in a 50-ml stoppered Erlenmeyer flask and keep in a water bath at 35°C. Add 2 ml of the oxidizing solution and mix well. After 2 min, add 1 ml of the arsenite solution and 2 ml of the sulfanilamide solution, followed by 1 ml of *N*-1-naphthylethylenediamine solution. After 5 min, measure the absorbance at 543 nm in a 5-cm cell. By the same procedure, measure the blank absorbance using 25 ml of the deionized water.

This method is so sensitive that the analysis should be done in a room which is free from ammonia and nitrogen dioxide gases.

Results and discussion

Effect of concentration of added reagents. Analytical conditions were studied with a solution containing 1 μg-at NH_3–N l^{-1} in an artificial sea water. The concentration of sodium hydroxide had no effect in the range 2–4 *M* but low results were obtained at 1 *M*. The concentration of potassium bromide had no effect in the range 5–10% in the reagent solution; concentrations of only 2% led to slower oxidation. The oxidation reached a maximum in 1 min at concentrations more than 0.15 *M* of sodium hypochlorite (Fig. 1). Truesdale[7] reduced the oxidation time, from 3.5 h in the method of Richards and Kletsch to 17 min, by adding a larger amount of sodium hypochlorite. In this study the oxidation time was shortened to 1 min by using a greater amount of bromide.

Effect of temperature on oxidation time. As is usual in chemical reactions, the oxidation rate increased with increase in temperature (Fig. 2), but variation in temperature from 32 to 40°C had no effect on the oxidation time and a constant absorbance was obtained after 1 min.

Effect of nitrogen-containing compounds. In the previous oxidation

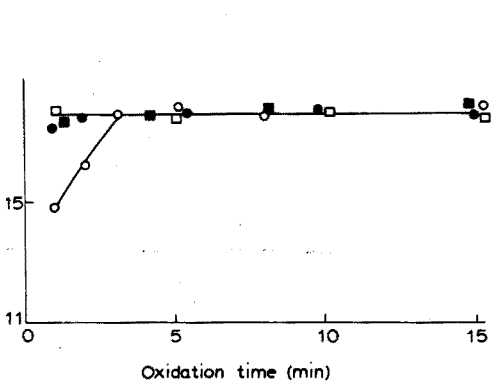

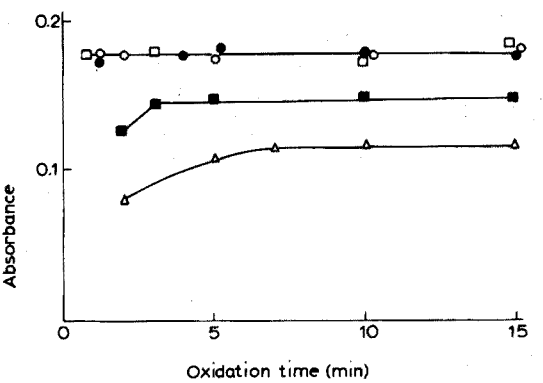

Fig. 1. Effect of sodium hypochlorite concentration. (○) 0.1, (●) 0.15, (□) 0.2, (■) 0.3 *M* NaOCl in the reagent solution.

Fig. 2. Effect of temperature. (○) 40, (●) 35, (□) 32, (■) 25, (△) 15 C.

methods[5–7], considerable portions of amino acids are determined together with ammonia, but in the present method amino acids did not interfere (Table I) because of the shortened oxidation time. Hydroxylamine was completely oxidized to nitrite and gave a positive error, but its existence in natural waters is limited to anaerobic conditions in the sea and lakes[6]. Even in this method, longer oxidation

TABLE I

EFFECT OF NITROGEN-CONTAINING COMPOUNDS

N-containing compound	*μg l⁻¹*	*Oxidation time (min)*	*Absorbance*
None	—	2	0.178[a]
Aspartic acid	200	2	0.177
		5	0.177
		8	0.180
l-Histidine	200	2	0.178
		8	0.182
Glycine	200	2	0.180
		8	0.184
dl-Alanine	100	2	0.173
		8	0.178
	200	2	0.178
		5	0.198
Urea	1000	2	0.175
		8	0.180
NH_2OH	15	2	0.269
		8	0.265

[a] NH_3–N, 1 μg-at l^{-1}.

TABLE II

EFFECT OF OXIDATION TIME FOR COASTAL SEA WATERS

Sample number	*Oxidation time (min)*	*NH_3–N found (μg-at l^{-1})*	*Sample number*	*Oxidation time (min)*	*NH_3–N found (μg-at l^{-1})*
1	2	2.20	4	2	0.39
	5	2.22		5	0.39
	8	2.21		8	0.41
	15	2.74		10	0.44
				15	0.48
2	2	2.96			
	2	3.09	5	2	2.63
	8	3.20		5	2.67
	15	4.20		8	2.80
				15	3.30
3	2	0.70			
	5	0.68			
	8	0.73			
	10	0.84			
	15	1.23			

times gave apparently higher values (Tables I and II), owing to the oxidation of amino acids. If the oxidation time is controlled to 2 min, only ammonia can be determined.

Comparison with the indophenol method. The concentrations of ammonia of coastal sea waters which seem to contain some amino acids were analysed by the indophenol method[3] and by the proposed method. The results are plotted in Fig. 3, which shows a very good correlation.

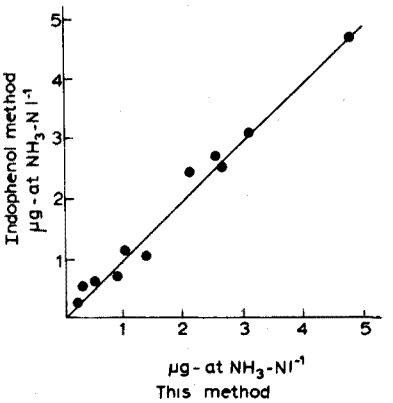

Fig. 3. Comparison with an indophenol method in analysis of various coastal sea waters. The line shows the 1:1 relationship.

Working curve. A working curve was drawn by adding known amounts of ammonia to deionized water, artificial or natural sea water. All the straight lines were parallel to each other. Since the working curve gives the sum of ammonia and nitrite present originally in the sample, the molar concentration of ammonia is given by the difference between the sum and the original nitrite molar concentration determined separately, *e.g.* by Bendschneider and Robinson's method[8]. The original nitrite molar concentration must be subtracted after dividing it by 0.85, because the yield of nitrite produced by the oxidation of ammonia is 85%. The molar concentration of ammonia in the sample is calculated from the following equation:

$$NH_3 \text{ in sample} = NH_3 \text{ from the working curve} - (NO_2^- \text{ in the sample}/0.85)$$

Precision and sensitivity. The relative standard deviation for 5 replicate determinations of ammonia in an artificial sea water was about 4% at the 0.5 μg-at l^{-1} level and 2% at the 2 μg-at l^{-1} level. The accuracy for a sample is also affected by the accuracy of determination of the original nitrite. The sensitivity for 0.001 absorbance in a 1-cm cell is 0.03 μg-at NH_3–N l^{-1}, which is 3–5 times higher than the ordinary indophenol method[1–3].

Conclusion

In this modified Richards and Kletsch method, the oxidation time is only 2 min. The shortening of time of the procedure is very favourable to automated analysis of ammonia, and results in the elimination of interference of amino acids.

REFERENCES

1 T. Sagi, *Oceanographical Magazine*, 18 (1966) 43.
2 B. S. Newell, *J. Mar. Biol. Ass. U. K.*, 47 (1967) 271.
3 L. Solorzano, *Limnol. Oceanogr.*, 14 (1969) 789.
4 K. Matsunaga and M. Nishimura, *Bunseki Kagaku*, 20 (1971) 993.
5 F. A. Richards and R. A. Kletsch, *Recent Researches in the Fields of Hydrosphere, Atmosphere and Nuclear Geochemistry*, Maruzen, Tokyo, 1964, p. 65.
6 J. D. H. Strickland and T. R. Parsons, *Bulletin No. 167*, Fisheries Research Board of Canada, 1968, pp. 81, 93.
7 V. W. Truesdale, *Analyst (London)*, 96 (1971) 584.
8 K. Bendschneider and R. J. Robinson, *J. Mar. Res.*, 11 (1952) 87.

Analytica Chimica Acta, 73 (1974) 209–212

SHORT COMMUNICATION

Microdetermination of metals in organometallic compounds by the oxine method after closed flask combustion

A. B. SAKLA, S. W. BISHARA* and RAMADAN A. HASSAN
Microanalytical Unit, Faculty of Science, Cairo University, Giza (Egypt)
(Received 1st May 1974)

It has been shown that Cd, Mg, U, Zn, Co, Mn, and Ti in metal-containing organic compounds can be determined on the micro scale with 8-hydroxyquinoline (oxine) after closed flask combustion[1,2]. The present communication reports extensions to the determinations of Ca, Cu, Al, Fe, Bi, and Ni. The analysis of metal-organic compounds is important not only for synthetic organic chemistry but also in the pharmaceutical and petroleum industries. Organically-bound calcium is usually determined by an eventual titration with EDTA[3,4]. Copper has been precipitated with 5,7-dibromo-8-hydroxyquinoline after wet oxidation of the sample[5], titrated complexiметrically or iodimetrically on the microscale[6], and determined spectrophotometrically at the submicro level[7]. Gravimetric determination of aluminium as alumina is not reliable; dissolution of the oxide and precipitation of aluminium oxinate gives greater accuracy[8]. Complexiметric[9] and spectrophotometric[10] finishes have also been proposed but most methods depend on titration with EDTA. Iron(III) can be determined spectrophotometrically with 4,7-diphenyl-1,10-phenanthroline[11] or complexiметrically with sulfosalicylic acid as indicator[12]. Gravimetric determination of organically-bound bismuth predominates over other methods; weighing as the sulfide[13] or as the tetraiodobismuthate thiocaprolactam complex[14] have been suggested. Few methods are available for determination of nickel; Janauer and Korkisch[15] employed the nickel–solochrome red ERS complex spectrophotometrically, while Belcher *et al.*[16] recommended the dimethylglyoxime complex. Ni, Cu, Fe, or Bi in organic compounds have been determined by wet combustion and EDTA titrimetry[3].

For Al, Fe, Bi and Ni, all the methods reported have depended on ashing or wet digestion; the closed flask method of decomposition has not been successfully applied previously.

Procedure for closed flask combustion and precipitation of the metal–oxine complex

Calcium. Burn the sample by the standard procedure[3,17] using a platinum gauze sample holder and a 500-ml conical flask charged with 5 ml of *M* hydrochloric

* Present address: Microanalytical Research Laboratories, National Research Centre, Dokki, Cairo, Egypt.

acid. After combustion, leave the flask for 15 min with intermittent shaking. Rinse the holder out with twice-distilled water and evaporate to about 5 ml. Cool and add 1 ml of ethanolic 1% oxine solution. At this stage, the total volume should not exceed 10 ml. Introduce ammonia solution (1+1) dropwise with shaking till a precipitate just appears and add one drop in excess. Shake for a few minutes and leave for 3 h to allow complete precipitation.

Copper, aluminium, iron, bismuth or nickel. For these metals, burn the organic sample using a quartz spiral and a 500-ml conical flask containing 5 ml of 6 *M* hydrochloric acid. (For Al-, Fe- or Bi-containing compounds, mix the solid sample with 5–10 mg of sodium hydrogen sulfite before burning; use 15–20 mg for organo-nickel compounds.) After ignition, shake intermittently for 15 min; then release the stopper and rinse with twice-distilled water. Place the holder at the mouth of the conical flask and boil the absorbent for 3–5 min. Rinse the spiral and evaporate to about 5 ml. (In the case of iron or nickel, add more hydrochloric acid plus a few drops of concentrated nitric acid to dissolve all metal oxides; evaporate to dryness and then add 5 ml of twice-distilled water.) Cool the solution to room temperature.

To the cooled metal ion solution, add 2 ml of 20% (w/v) tartaric acid solution, 2 ml of 20% (w/v) ammonium acetate solution, and 1 ml of 1% (w/v) oxine solution in 1 *M* acetic acid. (For bismuth, heat the solution before adding oxine.) Now, the total volume should not exceed 15 ml. With shaking, introduce ammonia solution (1+1) dropwise until a precipitate appears and then add one more drop. Digest on a water bath at 60–80°C for about 30 min. Allow to cool (about 10 min).

Determination of the metal content

Method I. Filter the metal oxinate through a G4 sintered glass crucible. Wash the calcium precipitate with three 3-ml portions of cold water; for the other metals wash with two 3-ml portions of (1+99) ammonia solution, two 3-ml portions of hot water, and finally two 3-ml portions of cold water. Dry the pricipitate to constant weight at 100°C for Ca, 110°C for Cu, 140°C for Al, 120°C for Fe, 140°C for Bi, and 230°C for Ni[18]. Weigh the metal complexes as CaQ_2, CuQ_2, AlQ_3, FeQ_3, BiQ_3, and NiQ_2, respectively (where Q is the oxine radical).

Method II. After filtration of the metal–oxine complex, collect the filtrate and washings in a 250-ml conical flask. Acidify with 5 ml of 6 *M* hydrochloric acid, and add 1 ml of 10% (w/v) potassium bromide solution followed by a measured excess of standard 0.05 *N* potassium bromate solution. Stopper the flask, shake, and leave in the dark for 15 min. Add 1 ml of 10% (w/v) potassium iodide solution and titrate the liberated iodine with 0.02 *N* sodium thiosulfate to a starch end-point.

Under identical conditions, carry out a blank using 1 ml of 1% oxine solution.

Method III. Dissolve the dried precipitate in 5 ml of 6 *M* hydrochloric acid (for Al, Fe or Bi use hot hydrochloric acid) and proceed exactly as described under Method II. To prevent interaction between iron(III) and potassium iodide[19,20], add 2–3 drops of concentrated phosphoric acid before adding the bromide solution, and then proceed as described above. For copper, determine the released copper(II) iodometrically.

Results and discussion

The general aim of this work was to establish general experimental conditions

for the determination of the greatest possible number of metals. Some modifications were found necessary but those were kept to a minimum. It is unusual for an organic compound to contain more than one metal, hence a selective method or reagent is unnecessary. Oxine is a widely applicable reagent, and has the advantage that the metal–oxine complexes can be analysed by gravimetric, titrimetric, colorimetric or polarographic procedures.

The gravimetric conversion factors for metal oxinates are good, which provides greater accuracy, and the precipitates need only be dried and weighed directly as the anhydrous salts. In most cases, precipitation is quantitative within a few minutes; only with calcium, complete precipitation requires 3 h[21].

The proposed procedure has an advantage in that three results can, if desired, be obtained for every sample weight. After precipitation of the metal oxinate (Method I), the unreacted oxine can be determined titrimetrically (Method II), and the precipitated metal oxinate can be dissolved and the liberated oxine titrated similarly (Method III). The titration of oxine depends on its bromination to yield

BLE I

ALYSIS OF METAL-CONTAINING ORGANIC COMPOUNDS

ipound	*Sample weight (mg)*	*Metal calc. (%)*	*Method I*		*Method II*		*Method III*	
			Metal found (%)	*Error (%)*	*Metal found (%)*	*Error (%)*	*Metal found (%)*	*Error (%)*
ium	5.421	25.34	25.00	−0.34	25.23	−0.11	24.93	−0.41
ate	6.833		25.61	+0.27	25.02	−0.32	25.10	−0.24
	7.290		25.49	+0.15	24.90	−0.44	25.31	−0.03
per	2.770	31.82	31.65	−0.17	32.30	+0.48	31.70	−0.12
ate	5.429		31.73	−0.09	32.40	+0.58	31.98	+0.16
per	2.884	14.09	14.20	+0.11	14.52	+0.43	14.10	+0.01
ipyridine loride	2.770		14.30	+0.21	14.60	+0.51	14.00	−0.09
ninium	7.667	7.03	6.95	−0.08	6.50	−0.53	6.82	−0.21
ate	8.529		7.22	+0.19	7.03	0	7.11	+0.08
	6.819		7.41	+0.38	6.84	−0.19	7.33	+0.30
ninium	3.874	5.87	5.90	+0.03	6.11	+0.24	5.85	−0.02
ate	3.992		6.10	+0.23	5.98	+0.11	6.12	+0.25
	7.403		6.12	+0.25	5.72	−0.15	6.00	+0.13
(II)	4.347	16.67	16.50	−0.17	16.27	−0.40	16.54	−0.13
te	4.662		16.44	−0.23	16.22	−0.45	16.75	+0.08
(III)	5.476	15.95	15.92	−0.03	15.48	−0.47	15.94	−0.01
yl- onate	5.428		15.40	−0.55	15.45	−0.50	15.39	−0.56
nuth	2.062	62.93	62.82	−0.11	63.21	+0.28	62.77	−0.16
gallate	2.457		62.53	−0.40	63.12	+0.19	62.64	−0.29
el	2.623	23.59	24.00	+0.41	24.10	+0.51	23.98	+0.39
ate	2.490		23.89	+0.30	24.01	+0.42	23.83	+0.24
el	2.224	20.31	20.10	−0.21	20.57	+0.26	20.64	+0.33
ethyl- ximate	2.409		19.78	−0.53	20.03	−0.28	19.92	−0.39

the 5,7-dibromo derivative. Every mole of oxine requires 4 equivalents of bromine, thus the oxinates of Ca, Cu, and Ni require 8 equivalents while those of Al, Fe, and Bi require 12 equivalents. Direct titration of oxine with bromate is not usually satisfactory, even on a macro scale[19], hence the back-titration procedure is recommended.

Table I shows the results obtained by the three methods; the average errors are ± 0.24, ± 0.34, and $\pm 0.20\%$ for methods I, II, and III, respectively.

The proposed procedure utilizes closed flask combustion for mineralization of the organic substance. No difficulty was encountered in decomposition of organocalcium compounds even with *M* hydrochloric acid as absorbent[3]. Hydrochloric acid (6 *M*) absorbent and a quartz spiral sample holder gave accurate results for copper. Compounds containing Al, Fe, Bi, or Ni, known to give difficultly soluble oxides after ignition[3], were mixed with nearly double the amount of sodium hydrogensulfite. During ignition, the simultaneous fusion–combustion process prevents the formation of difficultly soluble oxides, especially with Al or Bi. Complete dissolution of the oxides of iron or nickel was accomplished by heating the absorbing medium after adding more hydrochloric acid and a few drops of nitric acid; nitric acid is useful also to ensure quantitative oxidation to iron(III). Consequently, the closed flask method does not seem to offer great advantages over the wet digestion technique for decomposition of organoiron or organonickel compounds, but it is advantageous for the other metals listed.

REFERENCES

1 A. B. Sakla, S. W. Bishara and S. A. Abu-Taleb, *Microchem. J.*, 17 (1972) 436.
2 A. B. Sakla and S. A. Abu-Taleb, *Microchem. J.*, 18 (1973) 502.
3 A. M. G. Macdonald and P. Sirichanya, *Microchem. J.*, 14 (1969) 199; R. Belcher, A. M. G. Macdonald and T. S. West, *Talanta*, 1 (1958) 408.
4 J. Kormicki and E. Mikolajek, *Diss. Pharm. Pharmacol.*, 20 (1968) 87.
5 F. Hecht and R. Reissner, *Mikrochemie*, 17 (1935) 127.
6 T. V. Reznitskaya and E. I. Burtseva, *Zh. Anal. Khim.*, 21 (1966) 1132.
7 R. Belcher, B. Crossland and T. R. W. Fennell, *Talanta*, 17 (1970) 639.
8 G. Ingram, *Methods of Organic Elemental Microanalysis*, Reinhold, New York, 1962, p. 290.
9 L. V. Myshlyaeva and T. G. Maksimova, *Zh. Anal. Khim.*, 23 (1968) 1584.
10 A. P. Terentev, E. A. Bondarevskaya, N. A. Gradskova and E. D. Kropotova, *Zh. Anal. Khim.*, 22 (1967) 454.
11 J. S. Forrester and J. L. Jones, *Anal. Chem.*, 32 (1960) 1443.
12 J. Jenik and F. Renger, *Collect. Czech. Chem. Commun.*, 29 (1964) 2237.
13 C. L. Tseng and L. Wang, *J. Chin. Chem. Soc. (Peiping)*, 5 (1937) 3.
14 H. Sikorska-Tomicka, *Chem. Anal. (Warsaw)*, 13 (1968) 1279.
15 G. E. Janauer and J. Korkisch, *Z. Anal. Chem.*, 179 (1961) 241.
16 R. Belcher, B. Crossland and T. R. F. W. Fennell, *Talanta*, 17 (1970) 112.
17 T. S. Ma, in F. J. Welcher (Ed.), *Standard Methods of Chemical Analysis*, Vol. II, 6th edn., Van Nostrand, Princeton, 1963, p. 392.
18 M. Borrel and R. Paris, *Anal. Chim. Acta*, 4 (1950) 267.
19 L. Kampf, *Ind. Eng. Chem., Anal. Ed.*, 13 (1941) 72.
20 R. G. W. Hollingshead, *Oxine and its Derivatives*, Vol. 1, Butterworths, London, 1954, p. 281.
21 H. F. Walton, *Principles and Methods of Chemical Analysis*, 2nd. edn., Prentice-Hall, New Delhi, 1966, p. 94.

Analytica Chimica Acta, 73 (1974) 213–215

SHORT COMMUNICATION

Microdetermination of lead by a fluorescent ring-oven technique

ZDENKA SKURIĆ, FEDOR VALIĆ and JASNA PRPIĆ-MAREČIĆ
Andrija Štampar School of Public Health, University of Zagreb, Zagreb (Yugoslavia)
(Received 15th February 1974)

The use of the absorption of haloplumbate complexes in the ultraviolet region has been suggested[1] for the determination of micro quantities of lead, and analytical procedures for lead have also been based on the green fluorescence of chloroplumbate ions under u.v. radiation[2,3]. It has also been proved that the tetrachloroplumbate ion $(PbCl_4)^{2-}$ fluoresces much more intensely when adsorbed on cellulose than in the dissolved state[3]. A method has been described for the determination of lead in the form of a chromate ring developed on the ring-oven[4]; the method is based on the relative insolubility of lead sulphate in dilute sulphuric acid to separate lead from other soluble components, and on the selective solubility of lead sulphate in ammonium acetate to separate it from other cations precipitated as sulphates. After lead sulphate has been washed to the ring zone, lead is converted to a lead chromate ring by dipping the filter paper into a chromate solution. The lead concentration is determined by visual colour-matching with standard lead chromate rings in the conventional manner[5].

A combination of the above techniques seemed worthy of study for the determination of lead. The efficacy of the ring-oven technique for separating and concentrating trace amounts of lead, combined with the high fluorescence intensity of the lead chlorocomplex in the adsorbed state, was found to provide a simple, reasonably rapid procedure adaptable for air pollution studies.

Experimental

Apparatus and accessories. A Weisz ring-oven (ROFA) was used with calibrated capillary micropipettes, and Munktell's filter paper No. 00, 5.5 mm diameter. A low-pressure mercury lamp (G.m.b.H. Hanau) was also required.

Procedure. Place the filter paper on the ring-oven maintained at 105–110°C and fix in position with the retainer ring. To the centre of the paper, add one or more 5–10-μl portions of the sample solution, drying the paper almost completely between additions. Then add 4–5 portions of 0.05 *M* sulphuric acid in order to obtain the sulphates of the cations present; the amount of sulphuric acid in each portion should be just sufficient to obtain a wet spot marginally larger than the area of the sample, and the spot should be nearly dry before more acid is added. Place the dried filter paper on the ring and wash the soluble sulphates out to the periphery with several portions of 10^{-4} *M* sulphuric acid until the

whole paper is wet; do not allow the paper to dry between additions of sulphuric acid. If $5 \cdot 10^{-3}$ *M* sulphuric acid is used, as suggested in the lead chromate method[4], some lead is also washed out if less than 1 μg is present, but no losses occur down to 0.05 μg of lead with 10^{-4} *M* sulphuric acid.

Dry the paper completely, centre it again on the ring-oven, and wash lead sulphate to the ring zone with several portions of 0.1 *M* sodium chloride solution, thus obtaining fluorescent rings of sodium tetrachloroplumbate. Match the fluorescence intensity of the ring obtained with the fluorescence of a set of standard lead rings under a low-pressure mercury lamp with maximum emission intensity at 254 nm. The fluorescence of standard rings is not stable for more than 24 h, hence a fresh set of standard rings must be prepared daily.

The method is directly applicable for the determination of lead in airborne particulates collected on the filter paper. Treat the sample with 0.05 *M* sulphuric acid, taking care that the sample stain is wetted, dry the paper, wash soluble sulphates out with 10^{-4} *M* sulphuric acid and, finally, wash lead to the ring zone with 0.1 *M* sodium chloride.

The sensitivity of the method is 0.05 μg and the analytical range is 0.1–5 μg the relative standard deviation being about 20–30%.

Interferences

The procedure suggested by West[6] was used for the study of possible interfering effects of foreign ions. Four rings were prepared from each of the ions studied, one containing only the ion at the level of 1 μg, the second containing 1 μg of the ion and 0.1 μg of lead, the third containing 10 μg of the foreign ion, and the fourth 10 μg of the ion and 1 μg of lead. If the first and the third ring had the same fluorescence intensity as the blank, and the second and the fourth ring showed the same intensity as the corresponding lead standard, the ion was considered as not interfering.

The following 29 foreign ions were studied:

Group I	K^+, Na^+, Cu^{2+}
Group II	Ca^{2+}, Mg^{2+}, Cd^{2+}, Hg^{2+}, Ba^{2+}
Group III	Al^{3+}
Group IV	Sn^{2+}, $C_2H_3O_2^-$, $C_2O_4^{2-}$, CO_3^{2-}
Group V	Bi^{2+}, NO_2^-, PO_4^{3-}, $H_2PO_4^-$
Group VI	WO_4^{2-}, CrO_4^{2-}, MoO_4^{2-}
Group VII	Mn^{2+}, MnO_4^-, I^-, F^-
Group VIII	Fe^{2+}, Fe^{3+}, Co^{2+}

Permanganate appears to exert a positive interference effect at concentrations at least ten times higher than that of lead irrespective of the lead level. Barium and bismuth interfered with the quantitative washing out of the lead chloro-complex into the ring at concentrations three times higher than that of lead at the 1-μg lead level, and at concentrations equal to the lead at the 0.1-μg level.

Discussion

The ring-oven method proposed for the determination of lead in the form of a

fluorescent chlorocomplex is simple and of sufficient sensitivity. Few of the foreign ions likely to occur together with lead interfere.

With regard to the applicability of the proposed determination of lead in air, its sensitivity is quite satisfactory not only for industrial environments but also for outdoor atmospheres. If the very strict Soviet hygienic standard for lead in the outdoor atmosphere (0.7 $\mu g\ m^{-3}$ in a 24-h sample) is taken as the threshold, the sensitivity of the proposed method is sufficient for standard smoke samples[7] collected not only from a 24-h air sample (2 m^3) but also from a 2-h sample, even when the atmospheric lead concentration is below the threshold limit of 0.7 $\mu g\ m^{-3}$. If a less stringent threshold limit for atmospheric lead (10 $\mu g\ m^{-3}$) is considered[8], the sensitivity is sufficient for the determination of lead present at concentrations well below the threshold in a 10-min sample.

REFERENCES

1 C. Merrit, H. M. Herschenson and L. B. Rogers, *Anal. Chem.*, 25 (1953) 572.
2 E. A. Boževol'nov and E. H. Solov'ev, *Zh. Anal. Khim.*, 20 (1965) 1330.
3 K. Weber, Z. Turina and Z. Skurić, *Croat. Chem. Acta*, in press.
4 M. Fugaš and R. Pauković, *Anal. Chim. Acta*, 49 (1970) 356.
5 H. Weisz, *Microanalysis with the Ring Oven*, Pergamon, Oxford, 2nd edn., 1970.
6 P. W. West, *J. Chem. Educ.*, 18 (1941) 528.
7 *The Measurement of Atmospheric Pollution*, Department of Scientific and Industrial Research, H. M. Stationery Office, London, 1957.
8 R. Schwanecke, *Arbeitsschutz (Cologne)*, 11 (1966) 296; R. A. Kehoe, *Atmos. Environ.*, 3 (1969) 87.

Analytica Chimica Acta, 73 (1974) 216–219

SHORT COMMUNICATION

Catalytic-coulometric determination of copper at microgram and nanogram levels*

C. DAVID McGLOTHLIN and WILLIAM C. PURDY

Department of Chemistry, University of Maryland, College Park, Maryland 20742 (U.S.A.)

(Received 11th March 1974)

Copper has been determined by constant-current coulometric titration in the milligram and microgram range by several procedures. Titrants for direct methods include electrogenerated EDTA[1], tin(II)[2], hexacyanoferrate(II)[3], and chromium(II)[4]. Indirect methods have involved precipitation steps, with subsequent coulometric determination of the precipitant[5,6]. The procedures suggest a minimum of several hundred micrograms of copper. Cadersky[7] determined 6–100 μg of copper by an indirect iodimetric technique.

A recent report[8] has shown the feasibility of combining a catalytic reaction with a coulometric titration, producing a very sensitive indirect determination of mercury. Reactions in which copper acts as a catalyst have been summarized by Yatsimirskii[9]. One of the reactions is the decomposition of hydrogen peroxide which has been adapted for a manometric determination of 100–400 μg of copper[10].

The present communication describes the development of a coulometric procedure for copper, based on its activity in the decomposition of hydrogen peroxide. The reactions employed in the procedure are:

$$2\,H_2O_2 \xrightarrow[OH^-]{Cu(II)} 2\,H_2O + O_2 \qquad (1)$$

$$H_2O_2 + 2\,I^- + 2\,H^+ \xrightarrow{Mo(VI)} 2\,H_2O + I_2 \qquad (2)$$

$$I_2 + 2\,S_2O_3^{2-} \rightarrow 2\,I^- + S_4O_6^{2-} \qquad (3)$$

Reactions (2) and (3) are quite fast and proceed to completion in a few seconds. If a known excess of thiosulfate is added in reaction (3), that excess may be titrated with electrogenerated iodine to a biamperometric end-point. The procedure is useful for microgram and nanogram quantities of copper.

Experimental

Apparatus. Coulometric titrations were performed with a constant-current apparatus constructed in this laboratory. The circuitry and mode of operation are described in detail elsewhere[8,11]. Proper choice of resistors allowed the use of a 48.25-mA generating current. The titration cell was a 100-ml beaker equipped with

* Taken in part from the Ph.D. dissertation of C. David McGlothlin, University of Maryland, 1973.

four platinum foil electrodes. The generation cathode was isolated from the bulk of the solution by a chamber made from a 10-cm length of pyrex tubing, fitted with a fine porosity fritted glass disc. A 100-μl Eppendorf pipet and various Hamilton syringes were used to deliver the copper solutions.

Reagents. All chemicals were reagent grade and were used without further purification. Distilled or deionized water was used in the preparation of solutions.

Copper(II) stock solutions were prepared by dissolving 1.596 g of anhydrous copper sulfate (dried overnight at 105°C) in water and diluting to 1 l. This solution contained 63.5 μg Cu/100 μl. Dilutions of 1:1000 to 1:100 provided working standards for the determination of copper in the nanogram range.

Hydrogen peroxide solutions of 1.3 *N* and 0.4 *N* concentrations were prepared by diluting 30% hydrogen peroxide with water. Dilutions of 6.8 ml and 5.7 ml of the 30% peroxide to 100 ml and 250 ml yielded the respective concentrations. These solutions were stored at 4°C and were standardized coulometrically by the procedure of Christian[12] just before use.

A 0.2 *N* sodium thiosulfate solution was prepared by dissolving 49.64 g of sodium thiosulfate pentahydrate in water and diluting to 1 l. Coulometric standardization showed the solution to be stable within 1% of the original concentration for several weeks.

A Clark and Lubs buffer of pH 3.0 was prepared by dissolving 10.21 g of potassium hydrogen phthalate in 223 ml of 0.1 *M* hydrochloric acid and diluting to 1 l with water.

A potassium iodide–ammonium molybdate reagent was prepared by dissolving 166 g of potassium iodide and 1.2 g of $(NH_4)_6Mo_7O_{24}\cdot 4H_2O$ in water and diluting to 1 l.

Procedure for the microgram range. Place 1 ml of 0.2 *M* sodium hydroxide and 0–1000 μl of sample (0–635 μg of copper) in a 100-ml beaker with sufficient water to yield 16.0 ml of solution. Add 4 ml of standardized 1.3 *N* hydrogen peroxide place the beaker immediately in a 50°C water bath and incubate for 15.0 min. Add 5 ml of 2 *M* hydrochloric acid and cool in an ice bath, to quell the catalytic reaction. When the solution has cooled to about room temperature, add 5 ml of the iodide–molybdate reagent. The resultant solution is the post-incubation mixture referred to below.

Add 30 ml of pH 3.0 buffer, 5 ml of iodide–molybdate reagent, and a small unmeasured portion of thiosulfate to the titration cell, and pretitrate with electrogenerated iodine until the current is 2 μA above the base current. Stop the generation; add 500 μl of the post-incubation mixture and 500 μl of standardized 0.2 *N* thiosulfate. Resume generation and continue to the same current value as in the pretitration.

Procedure for the nanogram range. Add 1 ml of 0.2 *M* sodium hydroxide and 0–1000 μl of sample solution (0–635 ng of copper) to a 100-ml beaker, with sufficient water to give 19.0 ml of solution. After addition of 1.00 ml of standardized 0.4 *N* hydrogen peroxide and a 20.0-min incubation at 50°C, add 5 ml of 2 *M* hydrochloric acid. Cool in an ice bath, and then add 3 ml of the iodide–molybdate reagent.

Carry out the coulometric pretitration as in the microgram determination previously described. To the pretitrated solution, add 7.0 ml of the post-incubation

mixture and 750 μl of standardized 0.2 *N* thiosulfate. Electrogenerate iodine until the current reaches the same value as in the pretitration.

Results and discussion

Preliminary investigations in the microgram range showed that the rate of decomposition of hydrogen peroxide (catalytic activity of copper) in reaction (1) increased in a logarithmic manner between 24°C and 50°C (see Fig. 1). A 50°C incubation temperature was chosen since it was easily maintained with available instrumentation and gave more reproducible results.

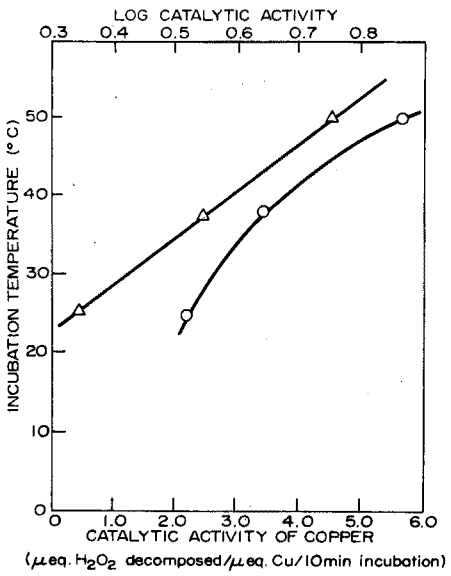

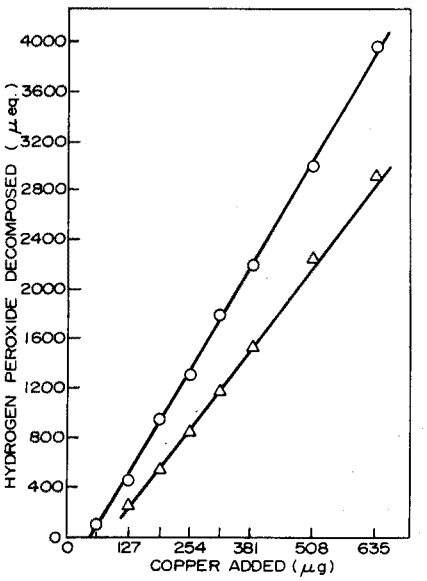

Fig. 1. Effect of variation of incubation temperature on the catalytic activity of copper in the decomposition of hydrogen peroxide. (△) Log scale; (○) linear scale.

Fig. 2. Effect of the time development of copper(II) hydroxide on the activity of copper. (○), Incubation started immediately; (△), $Cu(OH)_2$ developed one hour before the incubation was started.

The catalytic activity of copper decreased with increasing incubation time; however, the linearity of calibration curves relating the quantity of hydrogen peroxide decomposed to the amount of copper added was greatly improved. A 15–20 min incubation time was judged to be optimal.

It was noted that a fine precipitate of copper(II) hydroxide formed in the microgram range investigated. The precipitate, if allowed to remain at room temperature, tended to coagulate, leaving a smaller catalytic surface area available to the solution of hydrogen peroxide. Figure 2 shows the influence of this coagulation on a calibration curve for copper; also shown is a normal calibration curve in which coagulation of the precipitate was not allowed to proceed. No precipitate was formed in the nanogram range.

Reaction (1) occurs so swiftly that the incubation mixture becomes supersaturated with oxygen. The loss of oxygen from a quiescent solution was not as fast

as its catalytic production. This caused the calibration plot to show a negative deviation for determinations of greater than 250 μg of copper. The deviation disappeared when nitrogen was bubbled slowly through the solutions during incubation.

A pH of 10.4 was found to be the most favorable for the catalytic reaction. Carbonate and borax buffers of this pH, however, did not enhance the determination of copper. An impurity level of copper or one of the interfering catalysts (Fe^{3+}, Mn^{2+}, and Pd^{2+}) in the reagent grade buffer salt equivalent to $10^{-4}\%$ was sufficient to swamp the determination of copper in the nanogram range.

Linearity of calibration curves in the microgram range was achieved for 63.5–635 μg of copper. The catalytic activity of copper in this range was 9.1 ± 0.3 μeq of peroxide decomposed per μg of copper. The variation was compiled over a two-week period. In the nanogram range, the range of linear response was 63.5–380 ng of copper (*ca.* 20–280 μeq of peroxide decomposed); the plot then curved gently towards the concentration axis up to 635 ng of copper. The activity of copper calculated from the slope of the linear portion of the curve averaged 821 μeq of peroxide decomposed per μg of copper with a variation of $\pm 1.5\%$. This corresponds to a ninety-fold increase in the activity of copper over the microgram range. Owing to the reaction kinetics, no simple relationship (linear or logarithmic) was found for the region between 0.6 and 60 μg.

REFERENCES

1 C. N. Reilley and W. W. Porterfield, *Anal. Chem.*, 28 (1956) 443.
2 J. J. Lingane, *Anal. Chim. Acta*, 21 (1959) 227.
3 A. Takahashi, *Bunseki Kagaku*, 9 (1960) 565.
4 A. J. Bard and A. G. Petropoulos, *Anal. Chim. Acta*, 27 (1962) 44.
5 L. G. Hargis and D. F. Boltz, *Talanta*, 11 (1964) 57.
6 G. Perraz and O. Delgado, *Rev. Fac. Ing. Quim., Univ. Nac. Litoral*, 29 (1960) 87.
7 I. Cadersky, *Z. Anal. Chem.*, 224 (1969) 122.
8 T. J. Rohm, H. C. Nipper and W. C. Purdy, *Anal. Chem.*, 44 (1972) 869.
9 K. N. Yatsimirskii, *Kinetic Methods of Analysis*, Pergamon, New York, 1966.
10 T. Shiokawa and S. Suzuki, *J. Chem. Soc. Jap., Pure Chem. Sect.*, 72 (1951) 12.
11 J. H. Ladenson and W. C. Purdy, *Clin. Chem.*, 17 (1971) 908.
12 G. D. Christian, *Anal. Chem.*, 37 (1965) 1418.

Analytica Chimica Acta, 73 (1974) 220–223

SHORT COMMUNICATION

A liquid-state perchlorate ion-selective electrode based on Brilliant green perchlorate

A. G. FOGG, A. S. PATHAN and D. THORBURN BURNS
Chemistry Department, University of Technology, Loughborough, Leicestershire (England)
(Received 20th March 1974)

The Orion liquid-state ion-selective electrode for perchlorate has been used by Baczuk and DuBois[1], and by Smith and Manahan[2], for the potentiometric titration of perchlorate with tetraphenylarsonium chloride. Hseu and Rechnitz[3] have evaluated the electrode in detail and have used it to determine solubility products of several perchlorate salts. Other workers have developed other perchlorate electrodes. The electrodes of Ishibashi and Kohara[4] are based on perchlorate salts formed from 1,10-phenanthroline and similar chelating agents, whereas that of Sharp[5] is based on amine salts.

The present authors are investigating water-insoluble basic dye salts as ion-exchangers for use in ion-selective electrodes. Electrodes based on Brilliant green tetrathiocyanatozincate(II) have been described[6]; the liquid-state electrode responded faster than did either the Pungor-type electrode or the carbon paste electrode which were also prepared. In the liquid-state electrode, a natural rubber membrane was saturated with a solution of the basic dye salt in 1,2-dichlorobenzene; electrical contact was made at the back of the membrane by means of a carbon rod. This communication describes the response characteristics of a similar electrode based on Brilliant green perchlorate dissolved in chlorobenzene.

Experimental

Kerr and Gregory[7] have described the preparation of Brilliant green perchlorate as a means of purifying this dye for colorimetric use. A similar procedure was followed here, although a pure sample of Brilliant green (British Pharmacopoeia grade) was used. A slight excess of sodium perchlorate solution was added to an aqueous solution (0.5% w/v) of the Brilliant green at 75°C. After the mixture had been adjusted to pH 1–1.5 with perchloric acid, the mixture was kept at 75°C for 5 min. The precipitated Brilliant green perchlorate was then filtered, washed free of acid and soluble salts with water, recrystallized from ethanol–water (4 + 1) and dried at 45°C under vacuum. A 3% (w/v) solution of the Brilliant green perchlorate in chlorobenzene was used in the preparation of membranes.

Owing to the potentially explosive nature of organic perchlorates, it may be considered preferable not to prepare samples of the dry solid Brilliant green

perchlorate. An alternative method of preparing a solution of Brilliant green perchlorate in chlorobenzene was therefore devised. The precipitated Brilliant green perchlorate was extracted directly into a minimal amount of chlorobenzene without filtration, and the chlorobenzene solution was freed from water droplets by passing it through filter paper. Provided that a sufficiently concentrated solution of Brilliant green perchlorate was used (about 3% w/v), electrodes prepared in this manner behaved as satisfactorily as those prepared from solid Brilliant green perchlorate.

Details of the electrode body used have been given previously[6]. A commercial natural-rubber sheeting was used as the inert membrane; this swelled to twice its original size when immersed in a 3% (w/v) solution of Brilliant green perchlorate in chlorobenzene. After about 6 h of soaking the rubber, the basic dye salt was found to be evenly distributed through it, and the rubber gave a good response when used in a membrane electrode.

Potentiometric measurements were made at 25°C (except for the temperature dependence studies) in a thermostatted cell with a Pye 290 pH meter. An Orion double-junction saturated calomel reference electrode was used with 10% (w/v) ammonium nitrate solution in the outer compartment. The response of the electrode to perchlorate, Brilliant green and potentially interfering ions was studied.

Results

The response of the electrode to perchlorate, Brilliant green and several anions is shown in Fig. 1. A steady potential response was obtained for 10^{-3}–10^{-1} *M* solutions of perchlorate or Brilliant green within 1 min, and after slightly longer periods of time at lower concentrations. At 10^{-2}–10^{-1} *M* concentrations the potential was stable for at least 30 min, but a slight drift was noticed after

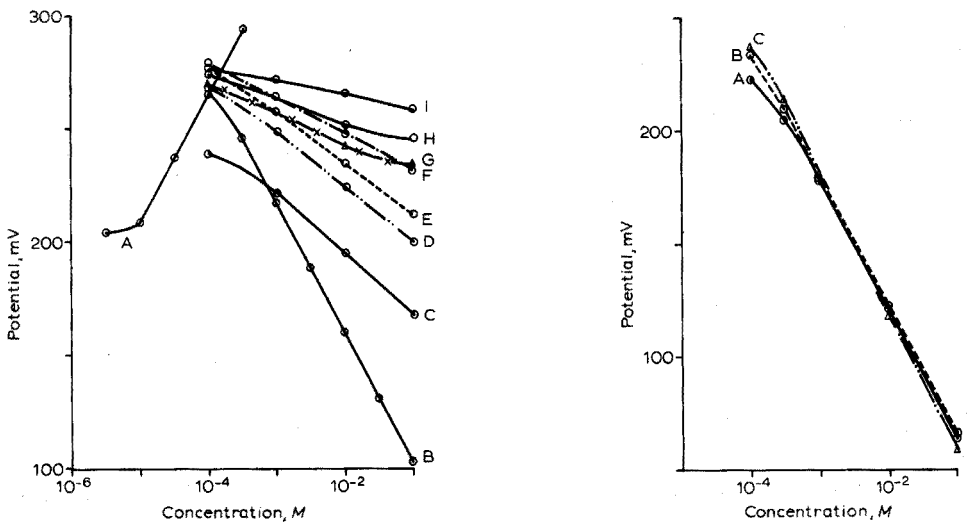

Fig. 1. Electrode response to perchlorate, Brilliant green and several anions. (A) Brilliant green, (B) perchlorate, (C) iodide, (D) hydrogencarbonate, (E) nitrate, (F) bromide, (G) acetate, (H) chloride, (I) fluoride.

Fig. 2. Effect of temperature on electrode response to perchlorate (A) 25°C, (B) 35°C, (C) 45°C.

10 min at lower concentrations. Over the linear portions of the graphs for perchlorate and for Brilliant green (Fig. 1), the slopes are almost Nernstian (57.5 and −57.0 mV per decade change in concentration, respectively). Although the measured potentials of the electrodes in particular solutions drifted, the slope remained Nernstian for at least two weeks.

Selectivity constants are shown in Table I. These were calculated in two ways. First, from the equation

$$\log K_{ClO_4^-/\text{interf.}} = \frac{E_{ClO_4^-} - E_{\text{interf.}}}{2.303\,RT/F}$$

TABLE I

SELECTIVITY CONSTANTS

Interfering ion	*Selectivity constant*	
	Potential difference method	*Constant potential method*
I^-	0.08–0.85	0.09
HCO_3^-	0.02–0.29	0.05
NO_3^-	0.01_3–0.21	0.01_5
Br^-	0.0066–0.16	0.008
CH_3COO^-	0.006–0.21	0.007
Cl^-	0.0037–0.17	0.005
F^-	0.002_3–0.12	0.003

The constants were calculated for minimal and maximal values of $E_{ClO_4^-} - E_{\text{interf.}}$ within the concentration range 10^{-3}–10^{-1} *M*. Secondly the constants were calculated by comparing the concentrations of perchlorate and interfering ion that were required to give the same potential *i.e.* $K_{ClO_4^-/\text{interf.}} = [ClO_4^-]/[\text{interf.}]$.

A brief study was made of the effect of temperature on the response of the electrode. The results shown in Fig. 2 indicate slopes of 57, 57 and 61 mV at 25, 35 and 45°C respectively, compared with the theoretical slopes at these temperatures of 59, 61 and 63 mV.

The effect of the pH of the test solution on the electrode response was studied. Perchlorate is extracted by Brilliant green into benzene[8] from aqueous solutions of pH 4.5–7. The lower pH is that at which the R^+ form of Brilliant green is further protonated to the RH^{2+} form; the upper pH limit corresponds to the conversion of the R^+ form to the carbinol base. The response of the electrode is in accord with these acid–base reactions; a stable constant response was obtained for 10^{-1} *M* perchlorate solutions in the pH range 4.5–8. Below pH 4, the response increases, whereas it decreased above pH 8.

A typical potentiometric titration curve for the titration of perchlorate with tetraphenylarsonium chloride solution using the electrode is shown in Fig. 3.

Discussion

The perchlorate electrode described above has been prepared as a further

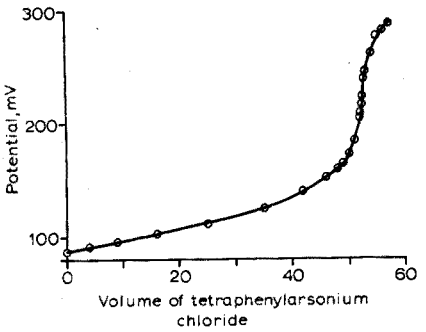

Fig. 3. Potentiometric titration of perchlorate (2.6 mmol) with tetraphenylarsonium chloride solution ($5 \cdot 10^{-2}$ *M*).

example of the use of insoluble basic dye salts as ion-exchangers in selective-ion electrodes. The wide application of photometric extraction methods with basic dyes gives an indication of the great potential of these dyes for use in selective electrode studies. In the present example the selectivity constants obtained for the determination of perchlorate compare very favourably with those obtained for other ion-exchangers.

The authors wish to thank the Harborough Rubber Company for providing rubber sheeting. One of us (A.S.P.) wishes to thank the University of Sind, Pakistan, for financial assistance.

REFERENCES

1 R. J. Baczuk and R. J. DuBois, *Anal. Chem.*, 40 (1968) 685.
2 M. J. Smith and S. E. Manahan, *Anal. Chim. Acta*, 48 (1969) 315.
3 T. M. Hseu and G. A. Rechnitz, *Anal. Lett.*, 1 (1968) 629.
4 N. Ishibashi and H. Kohara, *Anal. Lett.*, 4 (1971) 785.
5 M. Sharp, *Anal. Chim. Acta*, 61 (1972) 99.
6 A. G. Fogg, M. Duzinkewycz and A. S. Pathan, *Anal. Lett.*, 6 (1973) 1101.
7 G. O. Kerr and G. R. E. C. Gregory, *Analyst (London)*, 94 (1969) 1036.
8 A. G. Fogg, C. Burgess and D. T. Burns, *Analyst (London)*, 96 (1971) 854.

Analytica Chimica Acta, 73 (1974) 224–228

SHORT COMMUNICATION

Kinetic determination of thorium, vanadium and iodide with the use of a potentiostat

H. WEISZ, K. ROTHMAIER and H. LUDWIG

Lehrstuhl für Analytische Chemie, Chemisches Laboratorium der Universität Freiburg i. Br. (German Federal Republic)

(Received 19th April 1974)

In an earlier publication from this laboratory, a kinetic determination with the use of a potentiostat has been described[1]. This procedure is a stat method[2] and is an example of an "open system", because during the course of the catalyzed reaction

$$A + B \xrightarrow{K} X + Y$$

the system is influenced by external factors.

For the potentiostatic technique discussed here, a preset electrochemical potential is kept constant by addition of one of the reactants. According to the Nernst equation, the electrochemical potential of a system is defined by the ratio of the activities of the oxidized and reduced forms of the element in question; thus, with the potentiostat, not only the concentration of a reactant or product (*cf.* "pH-stat"[3]), but also the ratio [Ox]/[Red] is kept constant in the system.

This is illustrated here by the example of the thorium–catalyzed oxidation of iodide to iodine by hydrogen peroxide. To the system, containing an excess of hydrogen peroxide and the catalyst, thorium(IV), iodide is added from a buret; thus the iodide consumed by the reaction is always replaced, and the iodide is used to compensate the iodine formed during the reaction, *i.e.* it is used to keep constant the quotient $[I_2]/[I^-]^2$. The rate of addition of the iodide solution depends on the concentration of thorium and can therefore be used as a measure of its concentration. This reaction has already been applied to the determination of molybdenum[1]. Fluoride has been determined by its inhibiting action on the zirconium-catalyzed reaction between perborate and iodide[4].

The present paper describes the determination of thorium, based on its catalytic action on the oxidation of iodide with hydrogen peroxide[5], and the determination of vanadium, based on the oxidation of iodide with bromate[6]. The catalytic action of iodide on the cerium(IV)–arsenic(III) reaction[7] can also be utilized in the proposed technique.

Measuring device

For the determinations, the "Combititrator 3D" (Metrohm AG, Herisau, Switzerland) was used as a potentiostat. Three units are combined in this automatic titrator: a mV/pH meter, a controller ("Impulsomat"), and an automatic buret

connected to a recorder. The potentials were measured by a platinum electrode with a saturated calomel reference electrode. The titration vessel (Metrohm, 50 ml) as well as the delivery tube of the buret were thermostated [see Fig. 1 of ref. (1)].

Determination of thorium by use of the hydrogen peroxide–iodide reaction

The reaction between hydrogen peroxide and iodide is catalyzed by thorium[5]

$$H_2O_2 + 2\,I^- + 2\,H^+ \rightarrow I_2 + 2\,H_2O$$

Procedure. Before the determinations, the Combititrator is adjusted as follows: continuous pulse limit 5 mV, adaption dE/dV 6 units, automatic buret (total volume 10 ml) 4 units, recorder 15 mm min^{-1}. The temperature of the thermostat was 20.6°C. In order to find the best position for the set point potential (about 440 mV), a kinetic run was performed (see below). The set point potential was adjusted so that the continuous pulse was interrupted between 4 and 6 ml (see Fig. 1).

To the reaction vessel, transfer x ml of thorium sample solution, $(24-x)$ ml of twice-distilled water, 20 ml of acetate buffer solution (250 ml of 0.1 *M* sodium acetate and 25 ml of 0.1 *M* acetic acid diluted to 500 ml), and 5 ml of freshly prepared 0.1 *M* hydrogen peroxide solution. Then add 1 ml of freshly prepared $5 \cdot 10^{-4}$ *M* iodine/$1.2 \cdot 10^{-3}$ *M* iodide solution, in order to obtain a defined starting potential (about 500 mV). After 10 min, start the reaction by switching on the measuring unit, thus adding $2 \cdot 10^{-3}$ *M* potassium iodide solution (prepared daily from 0.1 *M* solution) to the thermostated reaction mixture (20.6°C). Between determinations, the platinum indicator electrode is conditioned in a solution which is identical with the reaction mixture except for thorium; this solution is freshly prepared every day.

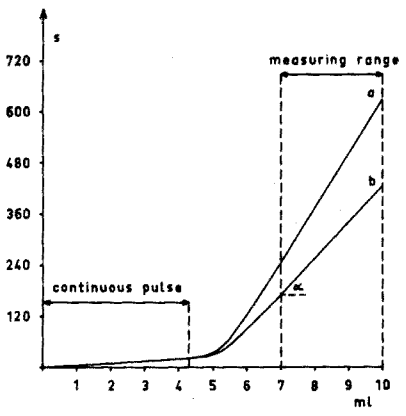

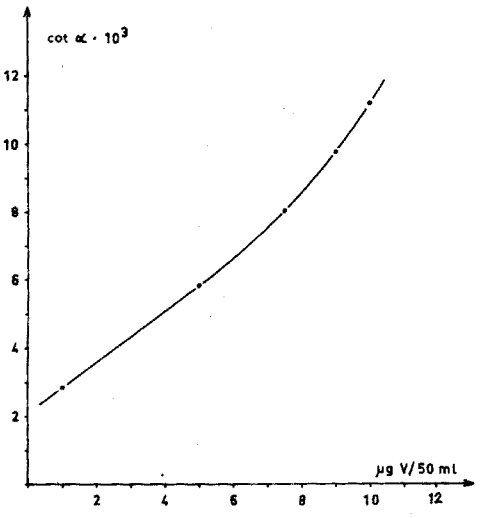

Fig. 1. Recorder graphs; (a) 46.4 µg Th/50 ml, (b) 92.8 µg Th/50 ml.

Fig. 2. Calibration graph for the determination of vanadium.

TABLE I

DETERMINATION OF THORIUM, VANADIUM AND IODIDE

(All results in μg/50 ml).

Thorium			*Vanadium*			*Iodide*		
Given	*Found*	*Rel. error (%)*	*Given*	*Found*	*Rel. error (%)*	*Given*	*Found*	*Rel. error (%)*
37.2	38.0	+2.1	0.90	0.80	−11.1	0.33	0.31	−6.1
66.1	60.2	−8.9	1.21	1.18	−2.5	0.50	0.52	+4.0
69.6	72.2	+3.7	1.73	1.68	−2.9	0.60	0.54	−10.0
92.8	87.3	−5.9	2.44	2.35	−3.7	0.75	0.74	−1.3
116	110	−5.2	4.75	4.70	−1.1	0.94	0.96	+2.1
123	102	−17.1	5.10	5.30	+3.8	1.00	0.95	−5.0
139	134	−3.6	5.10	5.25	+3.8	1.20	1.22	+1.7
142	156	+9.9	6.55	6.90	+5.1	1.40	1.51	+7.9
162	167	+3.1	9.26	9.25	−0.1	2.00	2.06	+3.0
226	188	−16.8	10.05	9.73	−3.2	2.19	2.39	+9.1
						3.00	2.98	−0.7
						3.06	3.14	+2.6

Evaluation and results. For evaluation, the cotangent of the inclination angle α of the line plotted by the recorder is graphically determined for the measuring range between 7.00 and 10.00 ml (Fig. 1). This value is identical with the rate of addition of the iodide solution ($\cot \alpha = 3$ (ml)/t (s)).

In order to prepare the calibration graph, 3 measurements are performed with known thorium concentrations (2.0, 4.0 and 8.0 ml of 10^{-4} *M* thorium solution/50 ml). This linear calibration graph was prepared before each series of measurements.

Some results are listed in Table I.

Determination of vanadium(V) by use of the bromate–iodide reaction

Vanadium acts as a catalyst for the oxidation of iodide by bromate[6].

$$BrO_3^- + 6\,I^- + 6\,H^+ \rightarrow 3\,I_2 + Br^- + 3\,H_2O$$

Procedure. The Combititrator is adjusted as follows: continuous pulse limit 18 mV, adaption dE/dV 7 units, automatic buret (total volume 10 ml) 3 units, recorder 15 mm min^{-1}; the temperature of the thermostat was 35.0°C. The set point potential (about 435 mV) is adjusted so that the continuous pulse is interrupted after the addition of 2–3 ml of iodide solution.

To the reaction vessel, add x ml of vanadium sample solution, $(42.5 - x)$ ml of twice-distilled water, 5 ml of buffer solution (150 ml of 0.1 *M* trisodium citrate and 850 ml of 0.1 *M* hydrochloric acid), 2 ml of 0.2 *M* citric acid, and 0.5 ml of 0.1 *M* bromate solution. Then add 0.1 ml of $5 \cdot 10^{-4}$ *M* iodine/$1.2 \cdot 10^{-3}$ *M* iodide solution (starting potential about 500 mV). After 10 min, start the reaction by switching on the measuring unit, thus adding 10^{-3} *M* potassium iodide solution (prepared daily from 0.1 *M* solution) to the reaction mixture. The platinum electrode is stored between measurements in a solution which is identical with the reaction mixture except for vanadium.

Evaluation and results. Here, the value of cot α is taken from the recorder graph for the measuring range 8.00–10.00 ml.

The calibration graph is prepared with the following vanadium concentrations: 1.0, 5.0, 7.5, 9.0 and 10.0 μg V/50 ml; the standard solution (100 μg V ml^{-1}) is prepared from ammonium vanadate. In this case a nonlinear calibration graph was obtained (Fig. 2); this graph was checked before each series of measurements.

Some results are given in Table I.

Determination of iodide by use of the reaction between cerium(IV) and arsenic(III)

Small traces of iodide accelerate the reaction between cerium(IV) and arsenic(III)[7].

Arsenic(III) solution. 0.2 *M*. Dissolve 9.892 g As_2O_3 in 200 ml of 0.1 *M* sodium hydroxide, add 35 ml of 10 *M* sulphuric acid and dilute to 500 ml with twice-distilled water.

Procedure. The Combititrator is adjusted as follows: continuous pulse limit 5 mV, adaption dE/dV 7 units, automatic buret (total volume 5 ml) 3 units, recorder 15 mm min^{-1}; the temperature of the thermostat was 35.0°C.

To the reaction vessel, add x ml of iodide sample solution, 1 ml of the above arsenic(III) solution, 1 ml of 4 *M* sulphuric acid, and 0.1 ml of 0.1 *M* cerium(III)

sulphate solution in 0.5 *M* sulphuric acid; dilute to 49 ml with twice-distilled water. After the solution has attained 35.0°C, add 1 ml of 10^{-3} *M* cerium(IV)sulphate solution (in 0.5 *M* sulphuric acid). Then, the cerium(IV) in the mixture is consumed by the reaction, until the potential measured in the solution reaches the preset potential of 650 mV (set point potential). This value is kept constant by adding $2 \cdot 10^{-4}$ *M* cerium(IV)sulphate solution in 0.5 *M* sulphuric acid (prepared daily) from the automatic buret. Between measurements the platinum electrode is stored in a 5% (w/v) ascorbic acid solution.

Evaluation and results. For evaluation the value of cot α is taken from the recorder graph for the measuring range 0.50–1.50 ml.

For each series of measurements, a calibration graph is prepared with the following iodide concentrations: 0.30, 0.75, 1.50, 2.50 and 3.00 μg I^-/50 ml; the stock iodide solution contained 1 mg I^- ml^{-1}. The calibration graph obtained was similar to that in Fig. 2.

Results are listed in Table I.

Conclusion

Kinetic–catalytic determination by the potentiostatic method is suitable for thorium in the range 30–250 μg/50 ml, vanadium in the range 1–10 μg/50 ml, and iodide in the range 0.3–3.0 μg/50 ml.

REFERENCES

1 H. Weisz, D. Klockow and H. Ludwig, *Talanta*, 16 (1969) 921.
2 D. Klockow, H. Weisz and K. Rothmaier, *Z. Anal. Chem.*, 264 (1973) 385.
3 C. F. Jacobson, J. Léonis, K. Linderstrøm-Lang and M. Ottesen in D. Glick (Ed.), *Methods of Biochemical Analysis*, Vol. 4, Interscience, New York, 1957, p. 171.
4 D. Klockow, H. Ludwig and M. A. Giraudo, *Anal. Chem.* 42 (1970) 1682.
5 K. B. Yatsimirskii and U. A. Zhukov, *Radiochemistry (U.S.S.R.)*, 3 (1961) 466; ref. in K. B. Yatsimirskii, *Kinetic Methods of Analysis*, Pergamon, Oxford, 1966, p. 89.
6 K. B. Yatsimirskii and V. E. Kalinina, *Zh. Anal. Khim.*, 24 (1969) 390; ref. in *Chem. Abstr.*, 71 (1969) 18588y.
7 E. B. Sandell and I. M. Kolthoff, *J. Amer. Chem. Soc.*, 56 (1934) 1426.

(Continued from page 4 of cover)

Short Communications

VOL. 73 NO. 1 ANALYTICA CHIMICA ACTA NOVEMBER 1974

CONTENTS

(Continued on inside page of cover)